PIPER NIGRUM MEDIATED SILVER OXIDE NANOPARTICLES USING CARDIUM SEASHELL FOR BIO-MEDICAL APPLICATIONS

A project work report submitted to

DEPARTMENT OF PHYSICS

ST. MARY'S COLLEGE (AUTONOMOUS) – THOOTHUKUDI

Affiliated to

MANONMANIAM SUNDARANAR UNIVERSITY,

TIRUNELVELI

In partial fulfillment of requirement for the award of

MASTER OF SCIENCE IN PHYSICS

Submitted by

R.ANJUTHA

Reg. No: 21SPPH01

Under the guidance of

Mrs. P.PADMAVATHI M.Sc., M. Phil., SET

DEPARTMENT OF PHYSICS

ST. MARY'S COLLEGE (AUTONOMOUS), THOOTHUKUDI.

(Re-accredited with 'A+' Grade by NAAC)

(2022 – 2023)

CERTIFICATE

This is to verify that this project work report entitiled **"PIPER NIGRUM MEDIATED SILVER OXIDE NANOPARTICLES USING CARDIUM SEASHELL FOR BIO MEDICAL APPLICATIONS"** submitted to **ST. MARY'S COLLEGE (AUTONOMOUS), THOOTHUKUDI** in partial fulfillment of requirement for the award of **MASTER OF SCIENCE IN PHYSICS** and is a record of work during the academic year **2022 – 2023** by **R.ANJUTHA**(Register No: 21SPPH01)

Signature of the Guide

Signature of the Co-ordinator

Signature of the Director

Director
Self Supporting Courses
St. Mary's College (Autonomous)
Thoothukudi - 628 001.

Lucia Rose

Signature of the principal

Principal
St. Mary's College (Autonomous)
Thoothukudi - 628 001.

12/4/23

Signature of the Examiner

CERTIFICATE

This is to certify that the project work entitled " **PIPER NIGRUM MEDIATED SILVER OXIDE NANOPARTICLES USING CARDIUM SEASHELL FOR BIO MEDICAL APPLICATIONS"** submitted to **St. Mary's College (Autonomous), Thoothukudi** for the award of the **Degree of Master of science in physics** is a bonafide record of project work done by the candidate **R.ANJUTHA (21SPPH01)** during the period **2022-2023** at St. Mary's college, Thoothukudi.

Padmavathi P

INTERNAL GUIDE

Mrs.P.Padmavathi
Assistant Professor
Department of Physics
St. Mary's College (Autonomous)
Thoothukudi - 628001

EXTERNAL GUIDE

Dr.A.Murugeswari
Assistant Professor
Department of Physics
Anna University
Chennai – 600025.

Date : 05.04.2023

DECLARATION

I hereby declare that the project work report entitled **"PIPER NIGRUM MEDIATED SILVER NANOPARTICLES USING CARDIUM SEASHELL FOR BIO-MEDICAL APPLICATION"** is submitted to **ST. MARY'S COLLEGE (AUTONOMOUS), THOOTHUKUDI** affiliated to **MANONMANIUM SUNDARANAR UNIVERSITY , TIRUNELVELI** for the award of the Degree of Master of Science in Physics is my unique work and no part of this project work report has been submitted for any Degree, Diploma or other similar titles.

R. Anjutha.

Signature of the Student

(R.ANJUTHA)

Station: Thoothukudi

Date: 05.04.2023.

ACKNOWLEGEMENT

On the very outset of this report, I feel obliged to our Almighty for his aid in the completion of this project work successfully.

I wish to record our profound gratitude to our principal REV. Dr. Sr .A.S.J. LUCIA ROSE M.Sc., PGDCA., M.Phil., PhD., for her motivation.

I sincerely thank our Director of SSC, Rev.Sr.JOSEPHINE JEYARANI M.A.,M.Phil., for her encouragement and support.

I wish to thank Rev. Sr. JESSIE FERNANDO M.Sc., M.Phil., Ph.D., HOD & Associate professor for her inspirational words to complete this project work.

I owe a great deal to Mrs. P.PADMAVATHI M.Sc., M. Phil., SET., SSC Co-ordinator for her valuable time and guidance provided throughtout for the successful completion of my project.

I express my sincere thanks to Dr. A.MURUGESWARI M.Sc.,Ph.D., for giving valuable guidance to complete my project.

I thank Dr. M.KARUNAKARAN M.Sc.,M.Phil., Ph.D.,for the support and providing the necessary data and information to complete my project successfully.

I wish to thank Mrs.S.IRUDAYA SAHAYA LANCY M.Sc., M.Phil., For her moral support and guidance.

I am deeply greatful to all the staff members of Department of physics (SSC) for supporting me in all aspects.

I acknowledge my deep sense of gratitude to my loving parents and friends for being a constant source of motivation.

ABSTRACT

A simple and efficient method of Piper Nigrum mediated Ag_2O nanoparticles using cardium seashell for bio-medical applications was carried out by co-precipitation method .The resultant product was characterized by X-ray diffraction(XRD), Energy dispersive X-ray(EDAX), Scanning Electron Microscope (SEM). X-ray diffraction confirmed the prepared nanostructured as Ag_2O and the grain size of the Ag_2O nanoparticles is 24nm. SEM images show that the Ag_2O particle. Ag_2O nanoparticles are basically composed of flower like structure and assembled together to yield morphology. EDAX test shows the compounds present in the particles(i.e silver and oxygen).This co-precipitation method gives a large scale production of Ag_2O nanoparticles easily uniqueness of the research in this report is that nanostructures have been formed without any caping agents or surfactants. Two multidrug-resistant bacterial strains were used to determine antimicrobial activity by the well-diffusion method. Thus the synthesized Ag_2O NPs were also used as effective microbicidal agents.

CONTENT

(i) LIST OF FIGURE

(ii) LIST OF TABLES

(iii) LIST OF ABBREVIATION

NPs	Nano particles
Nm	Nanometer
LED	Light Emitting Diode
UV	Ultra Violet
Ag_2O	Silver Oxide
$AgNO_3$	Silver Nitrate
XRD	X-Ray Diffraction
EDAX	Energy Dispersive X-Ray Analysis
SEM	Scanning Electron Microscopy
KeV	Kilo electron Volt

(iv) LIST OF SYMBOLS

℃	Degree Celsius
D	Grain size
λ	X-Ray wavelength
B	Full width half maximum
ϴ	Bragg angle
K	Scherrer constant

CHAPTER I

CHAPTER-I

INTRODUCTION

1.1 Nano science:

"All things are small All things small are beautiful and useful" Nanoparticles (NPs; 1-100 nm in size) have a special place in science and technology, not only because of their particular properties resulting from their reduced dimensions, but also because they are promising building blocks for more complex nanostructures. This chapter gives an overview of NPs and their presence in our daily lives. It provides an example of the use of NPs in nanotechnology to obtain different end-products in different sectors of economic activity. In addition, a classification of NPs based on their dimensions, morphology and chemical composition is presented[1]. The word nanoscience refers to the study of, manipulation and engineering of matter, particles and structures on the nanometer scale (one millionth of millimeter, the scale of atoms and molecules). Nanoscience is a compound word having two parts, nano and science. Although nano is a prefix as in nanometer, nanoampere, nanosecond, etc. referring to 10^{-9}, in nanoscience, it refers specifically to Nanometer. Important properties of materials, such as the electrical, optical, therm al and mechanical properties, are determined by the way molecules and atoms assemble on the nanoscale into larger structures. Moreover, in nanometer size structure these properties often different then on nanoscale, because quantum mechanical effects become important [2]. Nanoscience is the science of objects in the size regime of nanometers

1.2 Nanotechnology:

Nanotechnology is an area of modern science and is defined as the science which deals with the ability to control and manipulate matter at a scale ranging from less than a nanometer up to 100nm. Nanotechnology is very diverse, ranging from extensions of conventional device physics to completely new approaches based upon molecular self-assembly, from developing new materials with dimensions to on to the nanoscale to investigating whether we can directly control matter on the atomic scale. It has the potential to create many new materials and devices with a vast range of applications as shown in figure 1.1.

Nanotechnology is the technology using objects or structures or phenomena at the nanometer scale. Macroscopic matter consisting of elementary units below this dimension is called a nanomaterial.

Nanotechnology is the application of nanoscience leading to the use of new nanomaterials and nano size components in useful products. Nanotechnology will eventually provide us with the ability to design custom-made materials and products with new enhanced properties, new nano electronics components, new types of “smart” medicines and sensors, and even interfaces between electronics and biological systems.

These new born scientific disciplines are studied at the interface between physics, chemistry, materials science, microelectronics, biochemistry, and biotechnology. Control of these disciplines therefore requires an academic and multidisciplinary scientific education [3].

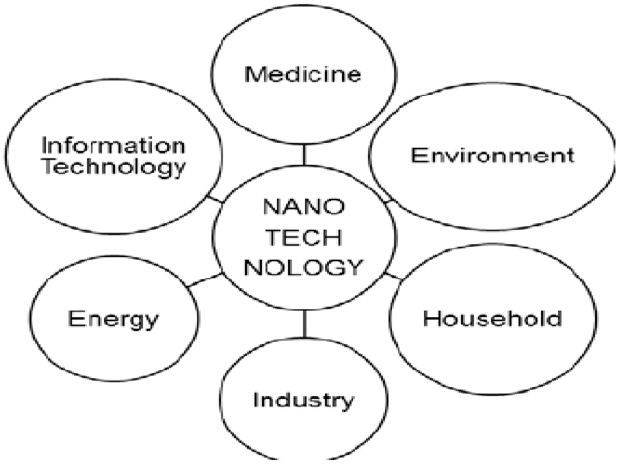

Figure : 1.1(Nanotechnology)

1.3 History of nanotechnology:

Richard Feynmann (American physicist, 1918-1988) was the first scientist who raised the first discussions about nanoscience in 1959, with a speech entitled "**There is a plenty of room at the bottom**". Feynmann highlighted the importance of controlling and manipulating on a small scale. However, Norio Taniguchi (1912-1999) used for the first time the term "Nanotechnology" in 1974 in a technology production paper that created objects and features on nanometer order.

In the 1980s, IBM Zurich scientists invented the tunneling microscope a significant mark in nanotechnology development, which allowed scientists to analyse materials at an unprecedented atomic level and also in 1980s Dr. K. Eric Drexler, promoted the technological significance of nano-scale phenomena and devices.

The term "Nanotechnology" was defined by Norio Taniguchi of the Tokyo Science University in a 1974 paper as follows: "Nanotechnology" mainly consists of the processing of separation, consolidation and deformation of materials by one atom or one molecule. Since that time the definition of nanotechnology has generally been extended to include features as large as 100nm [7].

In 1980s, Dr. K. Eric Drexler, promoted the technological significance of nano-scale phenomena and devices. In 2004 Richard Jones explains what is soft nanotechnology, which is the way forward, to design functional nanodevices that can cope with all the problems at nanoscale. Over the past few years, nanotechnology expenditure on search and development has increased dramatically, science has reached an important place in the society development and many consider that the investment in science may be the only key to a country's future. Nanoscience and nanotechnologies are new approaches to research and development aiming to control the fundamental structure and behaviour of matter at the level of atoms and molecules[1].

1.4 Nanoparticles:

The term "nano particles" is not usually applied to individual molecules, it refers to inorganic material. Nevertheless, there are also thermodynamically stable nanoparticles. This corresponds to particles of specific shapes and structures as in the case of molecular nanoparticles. Nano particles are considered as an invention of modern science because of its recent description. Nano particles are the particles between 1 to 100 nanometer[4]. Nanoparticles have known to the human civilization long ago. Generally, they are considered as an invention of modern science because of its recent description in terms of material science. Nanoparticles or nano crystals derived from metals, semiconductors or oxides are of interest for their mechanical, electrical, magnetic optical, chemical and some other properties in various applications.

Nano particle is the particle described and used in nanotechnology. A particle is defined as a small object behaving as a whole unit in terms of its transport and properties. The particle is classified according to their size as fine and ultrafine particles. Fine particles have got a diameter range of 100-250nm. Ultrafine particles have got a diameter range of 1 and 100nm. Nanoparticles may or may not have size related intense properties. properties of nano particles are different from that of fine particles or bulk materials in a significant way.

Various synthesis of nanoparticle full-fill the following conditions.

- Control of particle size, shape, crystal structure and composition distribution.
- Improvement of the purity of nanoparticles.
- Control of aggregation.
- Stabilization of physical properties, structures and reactants.
- Higher reproducibility.
- Higher mass production, scale up and lower costs[5].

1.4.1 Properties of nanoparticles:

Nanoparticles effectively form a bridge between bulk materials and atomic or molecular structures.

➢ Due to small size of nanoparticles, there are more atoms on the surface compared to the interior of the particles, which leads to large surface to volume ratio.

➢ The optical properties of nanomaterials are different from bulk materials of optical absorption peak of a semiconductor nanoparticle shifts to the short wavelength due to an increased band gap.

➢ Nanoparticles often possess unexpected visible properties because they are small enough to confine their electrons and produce quantum effects. For example, gold nanoparticles appear deep red to black in solution.

➢ Nano-size powder particles are potentially important in ceramics, powder metallurgy, in the achievement of uniform nano porosity and similar applications.
➢ When materials are made into nanoparticles their reactivity increase. These more reactive particles can enter the body through the skin, lungs etc.

➢ In optical properties the absorption occurs because electrons are induced by the photons of the incident light which make transitions between the lower lying occupied levels and higher unoccupied levels of the materials.

➢ Cluster of different sizes will have different electronic structures and different energy level separations[9].

1.5 **Nanostructures**:

The familiar word of microstructures and microelectronics is nanostructure materials in nano dimensions. Nanostructures are structures with the size between 1 and 100 nm. In nanosized materials large number of atoms is on the surface compared to the interior of the particles, which leads to the large surface over volume ratio. Nanostructured materials have remarkable unique mechanical, magnetic and catalytic properties. There are four categories of characteristic modulation dimension in nanostructure as shown in figure1.2 [8].

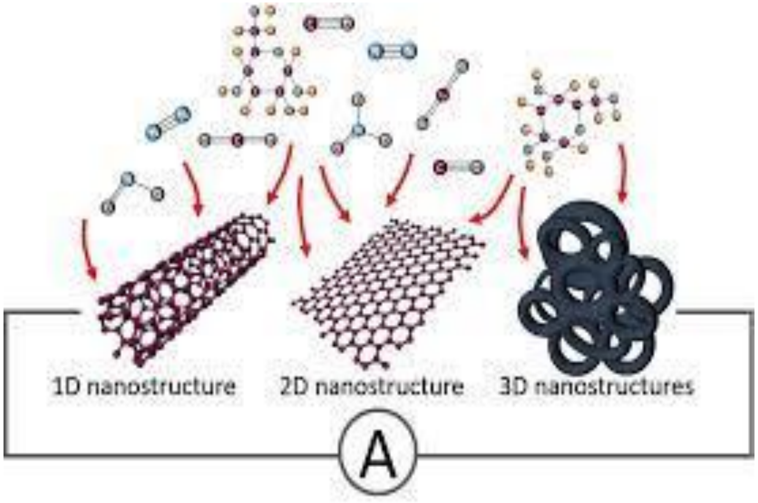

Figure : 1.2(Nanostructure)

1.5.1 Zero dimensional nanostructured materials:

Zero- dimensional nanostructure such as uniform particles arrays (quantum dots) heterogeneous particles array, core shell quantum dots, onions, hollow spheres and nano lenses have been extensively studied in light emitting diodes (LEDs) solar cells, single electron transistors and lasers.

1.5.2 One dimensional nanostructured materials:

One-dimensional nanostructure is nanotube, nanowires, nanorods and nanobelts. Generally, two approaches are adopted to fabricate nanostructures top-down and bottom-up methods. Major advantage of onedimensional nanostructure materials are their extraordinary lengths, flexibility and structure that can allow them to be physically manipulated into various shapes according to the design requirements.

1.5.3 Two dimensional nanostructured materials:

Two-dimensional nanostructures have two-dimension outside of the nanometric size range. In recent years two dimensional nanostructures have become a focal area in materials research, owing to their many low dimensional characteristic different from the bulk properties. Two dimensional nanomaterials are applications in sensors, photocatalysts, nanotainers, nanoreactors. Two dimensional nanostructured materials are nanoflakes, nano discs and nanofilms.

1.5.4 Three dimensional nanostructured materials:

Three-dimensional nanostructure materials are strongly depends on the sizes, shapes, dimensionality and morphologies. Three-dimensional nanostructures are an important material due to its wide range of application in the area of catalysis, magnetic material and electrode material for batteries. Moreover because the nanostructures have higher surface area and supply enough absorption sites for all involved molecules in a small space. Three- dimensional nanostructured materials are nanoballs, nano coils, nano cones, nano fillers and nano flowers[6].

1.6 Nanopowder:

Nano-powders are defined as power materials with individual particles having sizes under 100nm. The particles in nano-powder are smaller than the 8 wavelength of visible light. This means they can be used in applications like sun screens that are clear. The tin size of nano-powders gives them an extremely high surface area to volume ratio that results in extraordinary properties like extreme strength.

1.7 Green nanoscience:

Green chemistry and nano science are both emerging fields that take advantage of molecular-level designing and have enormous potential for advancing our science. Nano science is the study of materials that are on the length scale of 100 nanometers or smaller and have properties that are dependent on their physical size. The principles of green chemistry can guide responsible development of nano science, while the new strategies of nano science can fuel the development of greener products and processes.

Phytochemicals occluded in tea have been extensively used as dietary supplements and as natural pharmaceuticals in the treatment. The parallel development of green chemistry and nano science and the potential synergy of the two fields can lead to more successful and profitable technologies with reduced environmental impacts and improved conservation of resources. In recent years, green synthesis of metal nanoparticles is an interesting issue of the nanoscience[7].

- Green chemistry and health implications of nanoparticles
- Green chemistry and health for the synthesis of nanoparticles

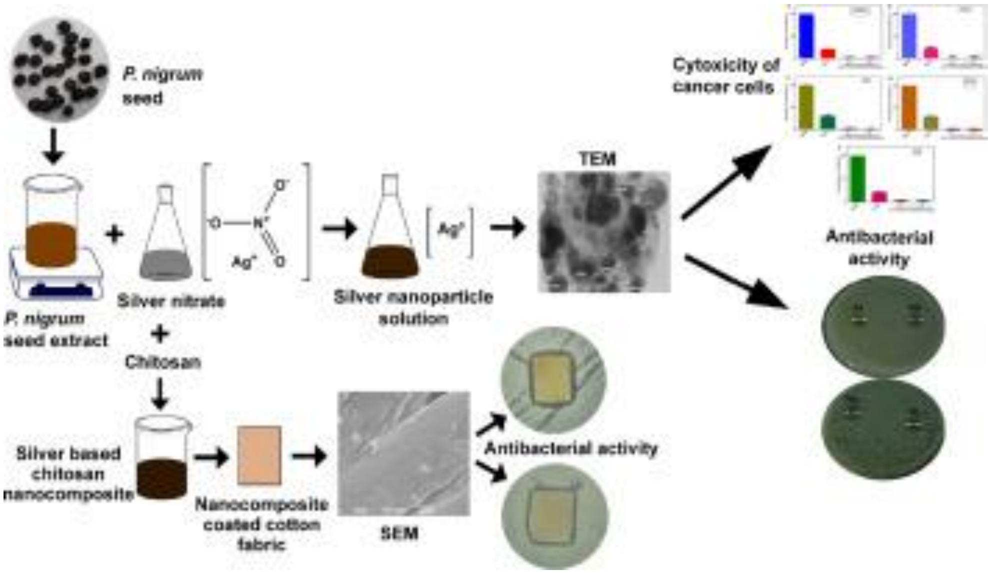

Figure 1.3 Green synthesis of Nanoparticles

1.8 Applications of nanoparticles:

Nanoparticles are used, or being evaluated for use, in many fields. The list below introduces few of the uses under development.

1.8.1 Nanoparticle Applications in Medicine:

The use of polymeric micelle nanoparticles to deliver drugs to tumors. The use of polymer coated iron oxide nanoparticles to break up clusters of bacteria, possibly allowing more effective treatment of chronic bacterial infections. The surface change of protein filled nanoparticles has been shown to affect the ability of the nanoparticle to stimulate immune responses. These nanoparticles may be used in inhalable vaccines. The cerium oxide nanoparticles act as an antioxidant to remove oxygen free radicals that are present in a patient's bloodstream following a traumatic injury. The nanoparticles absorb the oxygen free radicals and then release the oxygen in a less dangerous state, freeing up the nanoparticle to absorb more free radicals. Researchers are developing ways to use carbon nanoparticles called nanodiamonds in medical applications. For example, Nanodiamonds with protein molecules attached can be used to increase bone growth around dental or joint implants. Researchers are testing the use of chemotherapy drugs attached to nano diamonds to treat brain tumors. Other researchers are testing the use of chemotherapy drugs attached to nanodiamonds to treat leukemia.

1.8.2 Nanoparticle Applications in Manufacturing and Materials:

Ceramic silicon carbide nanoparticles dispersed in magnesium produce a strong, lightweight material. A synthetic skin that may be used in prosthetics has been demonstrated with both self-healing capability and the ability to sense pressure. The material is a composite of nickel nanoparticles and a polymer. If the material is held together after the cut it seals together in about 30 minutes giving it a self-healing ability. Also, the electrical resistance of the material changes with pressure, giving it a sense ability like touch. Silicate nanoparticles can be used to provide a barrier to gasses (for example oxygen), or moisture in a plastic film used for packaging. This could slow down the process of spoiling or drying out in food. Zinc oxide nanoparticles can be dispersed in industrial coatings to protect wood, plastic, and textiles from exposure to UV rays. Silicon dioxide crystalline nanoparticles can be used to fill gaps between carbon fibers, thereby strengthening tennis racquets. Silver nanoparticles in fabric are used to kill bacteria, making clothing odour-resistant.

1.8.3 Nanoparticle Applications and the Environment:

Researchers are using photocatalytic copper tungsten oxide nanoparticles to break down oil into biodegradable compounds. The nanoparticles are in a grid that provides high surface area for the reaction, is activated by sunlight and can work in water, making them useful for cleaning up oil spills. Researchers are using gold nanoparticles embedded in a porous manganese oxide as a room temperature catalyst to breakdown 11 volatile organic pollutants in air. Iron nanoparticles are being used to clean up carbon tetrachloride pollution in ground water. Iron oxide nanoparticles are being used to clean arsenic from water wells.

1.8.4 Nanoparticle Applications in Energy and Electronics:

Researchers have used nanoparticles called nano tetra-pods studded with nanoparticles of carbon to develop low- cost electrodes for fuel cells. This electrode may be able to replace the expensive platinum needed for fuel cell catalysts. Researchers at Georgia Tech, the University of Tokyo and Microsoft Research have developed a method to print prototype circuit boards using standard inkjet printers. Silver nanoparticle ink was used to form the conductive lines needed in circuit boards. Combining gold nanoparticles with organic molecules creates a transistor known as a NOMFET (Nanoparticle Organic Memory Field-

Effect Transistor). This transistor is unusual in that it can function in a way similar to synapses in the nervous system. A catalyst using platinum-cobalt nanoparticles is being developed for fuel cells that produces twelve times more catalytic activity than pure platinum. In order to achieve this performance, researchers anneal nanoparticles to form them into a crystalline lattice, reducing the spacing between platinum atoms on the surface and increasing their reactivity. Researchers have demonstrated that sunlight, concentrated on nanoparticles, can produce steam with high energy efficiency. The "solar steam device" is intended to be used in areas of developing countries without electricity for applications such as purifying water or disinfecting dental instruments. A lead free solder reliable enough for space missions and other high stress environments using copper nanoparticles. Silicon nanoparticles coating anodes of lithium-ion batteries can increase battery power and reduce recharge time. Semiconductor nanoparticles are being applied in a low temperature printing process that enables the manufacture of low cost solar cells. A layer of closely spaced palladium nanoparticles is being used in a hydrogen sensor. When hydrogen is absorbed, the palladium nanoparticles swell, causing shorts between nanoparticles. These shorts lower the resistance of the palladium layer.

1.9 Scope of the present work:

Piper Nigrum mediated silver oxide nanoparticle using seashell for bio-medical application.

1.9.1 Objective of the present work:

In the present work, Ag_2O nanoparticles are prepared by green synthesis and their structural and morphology are studied using the following tools.

- To determine the grain size of the pure Ag_2O nanoparticles using X-Ray diffraction analysis.
- To analyse and identify the elemental composition in the material through EDAX study.
- To obtain information about the surface's topography and composition of the pure Ag_2O nanoparticles using SEM studies.

CHAPTER II

CHAPTER 2

2.1 REVIEW OF LITERATURE:

Hussain ***et al*** (2023) [10] reported that Characterization and tribological behaviour of Indian clam seashell-derived hydroxyapatite coating applied on titanium alloy by plasma spray technique. The Various hydroxyapatite (HA) powders synthesized at different temperatures are deposited on titanium alloy by using an atmospheric plasma spray process. These different HA powders were synthesized from Indian clam seashells through the hydrothermal technique at varying temperatures from 700℃ to 1000℃ for a 2 h time duration .The synthesized HA powders are spray-dried to obtain agglomerated powders suitable for spraying during the coating application. Crystallite size, Ca/P ratio, and crystallinity of agglomerated HA powders and their respective coatings are estimated by standard methods. The average surface roughness (Ra) and porosity of the coating are decreased with an increase in the synthesis temperature. The minimum Ra and porosity obtained for the 1000℃ coating sample suggest a high degree of melting of such powder particles. However, the highest adhesion strength noticed in the case of the 900℃ coating sample is due to the high compatibility of such coating material with Ti-alloy substrate in terms of thermal properties. The 900℃ coating sample has also shown the highest micro hardness and wear-resistance properties due to its maximum crystallinity among all the HA coating.

Gartner ***et al*** (2022) [11] reported that Turning Seashell Waste into Electrically Conductive Particles. Biomaterials such as seashells are intriguing due to their remarkable properties, including their hierarchical structure from the nanometer to the micro- or even macroscopic scale. Transferring this nanostructure to generate nanostructured polymers can improve their electrical conductivity. Here, we present the synthesis of polypyrrole using waste seashell powder as a template to prepare a polypyrrole/$CaCO_3$ composite material. Various synthesis parameters were optimized to produce a composite material with an electrical conductivity of $2.1 \times 10{-}4 \pm 3.2 \times 10{-}5$ S/cm. This work presents the transformation of waste seashells into sustainable, electronically conductive materials and their application as an antistatic agent in polymers. The requirements of an antistatic material were met for a safety shoe sole.

Hussain *et al* (2021) [12] presented that the Effect of heat treatment on the synthesis of hydroxyapatite from Indian clam seashell by hydrothermal method. Hydroxyapatite (HA) powder has been successfully synthesized from low-cost Indian clam seashells by using hydrothermal method. The mixture of tri-calcium phosphate [$Ca_3(PO_4)_2$], heat-treated ball-milled clam sea shell ,and demineralized water are heat-treated at several temperatures (700℃, 800℃, 900℃, 1000℃ and 1100℃)for various time periods (1 h, 2 h, and 3 h) to perform the hydrothermal reactions .The maximum amount of crystalline HA with nearly stoichiometric phase can be obtained at 900℃ of heating temperature applied for 2 h of reaction time.

Hernandez *et al* (2021) [13] pointed out the Sea snail shells for synthesis of ceramic compounds reinforced with metallic oxide: Microstructural, mechanical and electrical behavior. The effect Cu_2O of formation in the $CaO \cdot Al_2O_3$ ceramic compounds synthesized by a powder processing method. For the synthesis, chemical compositions were prepared between $CaCO_3$ powder from sea snail shells, Al_2O_3 powder, and separate additions of Cu powder at 0.0%, 0.5%, 1.0%, 1.5%, and 3.0% by weight. The chemical compositions were subjected to a mix-milling process, then compacted in cylindrical samples and sintered at 1500ºC for their consolidation in a nitrogen-air atmosphere. The materials obtained possibly can be used in dental applications, materials with antimicrobial activity, or applied in telecommunication as radiofrequency oscillators, due to their electrical properties.

Alhari *et al* (2020) [14] pointed out the Green synthesis of silver nanoparticles from Neurada procumbens and its antibacterial activity against multi-drug resistant microbial pathogens. The fabrication of silver nanoparticles (Ag-NPs) using the extract of a xerophytic plant (Neurada procumbens) as a reducing agent. The fabricated Ag-NPs can effectively control multi-drug resistant gram-negative rods (MDR-GNRs), which were isolated from the Buraidah Central Hospital (BCH), Saudi Arabia. The predominant MDR-GNR bacteria included Klebsiella pneumoniae, Acinetobacter baumannii, and Escherichia coli. The Ag-NPs were examined by diverse spectral and analytical techniques, and then their antibacterial effects against MDR bacteria were determined. The present work illustrates that synthesized Ag-NPs from the aqueous leaf extract of Neurada procumbens show considerable antibacterial potential against MDR clinical isolates from different patient samples at BCH.

Tamilarasi *et al* (2020) [15] presented that Green synthesis of silver nanoparticles (Ag NPs) using Gomphrena globosa (Globe amaranth) leaf extract and their characterization. The silver nanoparticles were synthesized using silver nitrate as the precursor and an aqueous extract of fresh leaves of Gomphrena globosa (Globe amaranth) as the reducing and stabilizing agent. The active phytochemicals present in the leaves cause quick reduction of silver ions (Ag+) to metallic silver nanoparticles (Ag0). The formation of Ag nanoparticles was initially confirmed by visual observation through the color change of the mixture. The synthesized silver nanoparticles show excellent antibacterial activity against three grampositive bacteria (Staphylococcus aureus, Bacillus subtilis, Micrococcus luteus) and three gramnegative bacteria (Escherichia coli, Pseudomonas aeruginosa, and Klebsiella pneumoniae).

Mosaviniya ***et al*** (2019) [16] presented that Facile green synthesis of silver nanoparticles using Crocus Haussknechtii Bois bulb extract: Catalytic activity and antibacterial properties. The Green synthesis of silver nanoparticles (AgNPs) is of particular interest due to their catalytic and antibacterial properties. In this study, the extract of Crocus Haussknechtii Bois was used to synthesize small-sized AgNPs and the effective parameters were investigated. The experimental optimization of temperature and pH reveals that spherical nanoparticles with a size of about 10–25 nm could be obtained using 0.5 mL of $AgNO_3$ (20 mM) and 0.5 mL of the plant extract with total volume of 20 mL at pH = 7 and temperature of 75°C within 120 min. The catalytic activity of synthesized nanoparticles was evaluated in the degradation of a Congo Red dye in the presence of sodium borohydride. The results indicate that 16.67 µM Congo Red dye could be degraded in only 220 s . The rate of degradation is one of the highest values reported for catalytic reduction of Congo Red dye.

Moralesa ***et al*** (2019) [17] reported that Green synthesis of silver nanoparticles using Eucalyptus leucoxylon leaves extract and evaluating the antioxidant activities of extract .The green synthesis of silver nanoparticles (AgNPs), using two varieties of a natural extract of dark (D) or white (Wh) Salvia hispanica L. seeds, commonly named chia (Ch), as a reducing-stabilizing agent. Similarly, it was carried out a study on the effect of the variation of different physicochemical parameters, like aging time and storage temperature of the natural extract of dark Ch seeds, in the morphology, size and polydispersity of the prepared AgNPs. We found that the ideal conditions to do the green synthesis of AgNPs, are to use the Ch extract one day after it have been prepared and stored at 5 °C (1D C).Also determined that the synthesized AgNPs/D Ch have more antimicrobial activity against both bacteria, in comparation with AgNPs/W Ch (ZOI against E. coli, 18.5 mm; S. aureus, 14.9 mm).

Dhanaraj ***et al*** (2018) [18] presented that Conversion of waste sea shell (Anadara granosa) into valuable nanohydroxyapatite (nHAp) for biomedical applications. To reduce the pollution and give good value to waste shells, nanohydroxyapatite (nHAp) has been extracted from Anadara granosa waste with and without polymers by eco-friendly, product free and cost effective microwave irradiation method. The antibacterial effect of capped and uncapped HAp powder against pathogen bacterial strains Escherichia coli and Bacillaus cereus show the excellent antibacterial activity. The best nHAp composite is applied in the Dentin application.

Josh ***et al*** (2018) [19] pointed out the Green Synthesis of Silver Nanoparticles Using Pomegranate Peel Extracts and Its Application in Photocatalytic Degradation of Methylene Blue .The green synthesis of silver NPs (AgNPs) using pomegranate (Punica granatum) peel extract (PE) and its application in photocatalytic degradation of methylene blue (MB) dye were examined. AgNPs were rapidly synthesized within five minutes using pomegranate PE, which could degrade almost 89% of MB dye within 48 - 72 hours under sunlight irradiation; this finding indicates the potential of this natural product, although further exploration is needed.

Samro *et al* (2018) [20] focused that Antibacterial and Antioxidant Activity of Different Staged Ripened Fruit of Capsicum annuum and Its Green Synthesized Silver Nanoparticles. The aqueous extract of yellow-colored Capsicum annuum showed the highest antibacterial activity against Pseudomonas aeruginosa and also showed the highest antioxidant activity. Furthermore, silver nanoparticles were synthesized using the aqueous extract and characterized by UV-Vis, FTIR, SEM, and AFM analysis. The silver nanoparticles were investigated for its bactericidal activity. The silver nanoparticles produced using the extract of green-colored Capsicum annuum showed the highest bactericidal activity which was evidenced by protein leakage assay.

Vartooni *et al* (2016) [21] focused the Green synthesis of seashell supported silver nanoparticles using Bunium persicum seeds extract: Application of the particles for catalytic reduction of organic dyes In the present work, silver nanoparticles were immobilized on the surface of seashell using Bunium persicum seeds extract as a reducing and stabilizing agent. The seashell supported silver nanoparticles was characterized by FT-IR, XRD pattern, FE-SEM, EDS, TEM and TG-DTA. The diameter of Ag NPs on the seashell was predominantly found within the range 20–50 nm .This procedure has the advantages of very mild reaction conditions, clean reaction, elimination of organic solvents, toxic and dangerous reagents, and operational simplicity, which make it useful and attractive for the preparation of Ag NPs/seashell.

Vatandost ***et al (***2016) [22] presented that Green Synthesis of Silver Nanoparticles by Pepper Extracts Reduction and Its Electocatalytic and Antibacterial Activity. The aqueous pepper extract was used for reducing silver nitrate. The synthesized silver nanoparticles were analyzed with TEM, XRD and EDS. TEM image shows the formation of silver nanoparticles with average particle size of 20 nm which agrees well with the XRD data. The main advantage of using pepper extract as a stabilizing agent is that it provides long-term stability for nanoparticles by preventing particles agglomeration. To investigate the electrocatalytic efficiency of silver nanoparticles, silver nanoparticles modified carbon-paste electrode (AgNPs–CPE) displayed excellent electrochemical catalytic activities towards hydrogen peroxide (H_2O_2) and hydrogen evolution reaction (HER).

Chunfa Dong ***et al*** (2016) [23] focused that Wolfberry fruit (Lycium barbarum) extract mediated novel route for the green synthesis of silver nanoparticles. The green, simple and low cost process for production of well dispersed, small size silver nanoparticles with narrow distribution from 3 nm to 15 nm was described. In this method, silver nanoparticles were prepared in aqueous medium by employing wolfberry fruit extract as both reducing and stabilizing agent without utilizing any other capping and reducing agent. The generation of metallic nanoparticles was observed by change of color and the UV-vis absorption spectroscopy. The results show that the as-synthesized silver nanoparticles are highly crystalline in nature, spherical in shape. The reaction times, silver nitrate concentrations and wolfberry fruit extract amounts play crucial roles in the synthesis of small silver nanoparticles.

Ahmed *et al* ([2015) [24] focused that Green synthesis of silver nanoparticles using Azadirachta indica aqueous leaf extract. The simple approach was applied for synthesis of silver nanoparticles using Azadirachta indica aqueous leaf extract. The plant extract acts both as reducing agent as well as capping agent. To identify the compounds responsible for reduction of silver ions, the functional groups present in plant extract were investigated by FTIR. Results confirmed this protocol as simple, rapid, one step, eco-friendly, nontoxic and an alternative conventional physical/chemical methods. Only 15 min were required for the conversion of silver ions into silver nanoparticles at room temperature, without the involvement of any hazardous chemical.

Bindhu *et al* (2015) [25] focused that the green synthesis of silver nanoparticles using a natural extract of dark or white Salvia hispanica L. seeds and their antibacterial application the aqueous beetroot extract was used as reducing agent for silver nanoparticles synthesis. The synthesized nanoparticles were characterized using UV–visible spectroscopy, XRD and TEM. The surface plasmon resonance peak of synthesized nanoparticles was observed at 438 nm. As the concentration of beetroot extract increases, absorption spectra shows blue shift with decreasing particle size. The prepared silver nanoparticles were well dispersed, spherical in shape with the average particle size of 15 nm. The prepared silver nanoparticles reveal faster catalytic activity. This natural method for synthesis of silver nanoparticles offers a valuable contribution in the area of green synthesis and nanotechnology avoiding the presence of hazardous and toxic solvents and waste.

Ajitha ***et al*** (2015) [26] reported that Green synthesis and characterization of silver nanoparticles using Lantana camara leaf extract (LE). The AgNPs were prepared by simple, capable, eco-friendly and biosynthesis method using L. camara LE. This method allowed the synthesis of crystalline nanoparticles, which was confirmed by XRD and SAED patterns. The XPS analysis confirmed the formation of metallic silver and elucidates the surface state composition of AgNPs. . Decrement of particle size with an increment of leaf extract volume was evident in AFM, TEM images and also through a blue shift in the UV–vis spectra. The rate of formation and size of AgNPs were dependent on LE quantity. Meanwhile, these AgNPs exhibited effective antibacterial activity with the decrement of particle size against all tested bacterial cultures.

Vijay Kumar ***et al*** (2014) [27] focused that Green synthesis and characterization of silver nanoparticles using Boerhaavia diffusa plant extract and their anti bacterial activity. The Green synthesis of silver nanoparticles was carried out using Boerhaavia diffusa plant extract as a reducing agent. The biosynthesized AgNPs were characterized by SEM-EDAX, XRD, TEM, UV–Vis, and FT-IR spectroscopy techniques. UV–Vis spectroscopy of prepared silver colloidal solution showed absorption maxima at 418 nm. XRD and TEM analysis revealed that AgNPs are face-centered, cubic structure being spherical in shape with an average particle size of 25 nm. The AgNPs were tested for antibacterial activity against three fish bacterial pathogens viz., Aeromonas hydrophila, Pseudomonas fluorescens and Flavobacterium branchiophilum and they demonstrated highest sensitivity toward F. branchiophilum when compared to other two bacterial pathogens.

Nasrabad ***et al*** (2014) [28] presented that Green synthesis of silver nanoparticles using Eucalyptus leucoxylon leaves extract and evaluating the antioxidant activities of extract . In vitro antioxidant activity of essential oil and methanol extracts of Eucalyptus leucoxylon. Furthermore, the polar fraction of the extract was used as a reducing agent for the green synthesis of silver nanoparticles (Ag NPs). Antioxidant activities of the samples were determined by using three different test systems, namely DPPH and b-carotene/linoleic acid and reducing power. Synthesised Ag NPs were almost spherical in shape with an average diameter of about , 50 nm and synthesised within 120 min reaction time at room temperature.

Subba Rao ***et al*** (2013) [29] reported that Green synthesis and spectral characterization of silver nanoparticles from Lakshmi tulasi (Ocimum sanctum) leaf extract. The green synthesis of silver nanoparticles (AgNPs) using aqueous extract of Lakshmi tulasi (Ocimum sanctum) leaf as a reducing and stabilizing agent. AgNPs were rapidly synthesized using aqueous extract of tulasi leaf with $AgNO_3$ solution within 15 min. Characterization data reveals that the particles were crystalline in nature and triangle shaped with an average size of 42 nm. The zeta potential of AgNPs were found to be 55.0 mV. This large negative zeta potential value indicates repulsion among AgNPs and their dispersion stability.

Augustine ***et al*** (2013) [30] focused that a facile and rapid method for the black pepper leaf mediated green synthesis of silver nanoparticles and the antimicrobial study. The Green synthesis of nanoparticles is widely accepted due to the less toxicity in comparison with chemical methods. But there are certain drawbacks like slow formation of nanoparticles, difficulty to control particle size and shape make them less convenient. Here we report a novel cost-effective and eco-friendly method for the rapid green synthesis of silver nanoparticles using leaf extracts of Piper nigrum. The results suggest that this method can be used for obtaining silver nanoparticles with controllable size within a few minutes. The fabricated nanoparticles possessed excellent antibacterial property against both Gram-positive and Gram-negative bacteria.

Murugan ***et al*** (2012) [31] pointed out the green synthesis, characterization and evaluation of the biological activities of silver nanoparticles synthesized from Iresine herbstii leaf aqueous extracts .The synthesis and characterization of silver nanoparticles using Iresine herbstii and evaluation of their antibacterial, antioxidant and cytotoxic activity. The reaction mixture turned to brownish gray color after 7 days of incubation and exhibits an absorbance peak around 460 nm characteristic of Ag nanoparticle. Scanning electron microscopy (SEM) and EDX analysis showed silver nanoparticles were pure and polydispersed and the size were ranging from 44 to 64 nm. XRD studies revealed that most of the nanoparticles were cubic and face centered cubic in shape. The powerful bioactivity demonstrated by the synthesized silver nanoparticles leads towards the clinical use as antibacterial, antioxidant as well as cytotoxic agent.

Kouvaris ***et al*** (2012) [32] presented that Green synthesis and characterization of silver nanoparticles produced using Arbutus Unedo leaf extract.The silver nanoparticles were synthesized from aqueous silver nitrate through a simple and eco-friendly route using leaf broth of Arbutus unedo, which acted as a reductant and stabilizer simultaneously. The aqueous silver ions when exposed to the leaf broth were reduced and stabilized over long periods of time resulting in the green synthesis of surface functionalized silver nanoparticles. . The results revealed the formation of single crystalline Ag nanoparticles with a narrow size distribution for each sample. The particles, although discrete, were predominately coated with the organic leaf extract forming small aggregates, which makes them stable over long time periods and highly appropriate for coatings or biotechnology applications.

Mallikarjuna ***et al*** (2012) [33] focused that Phytochemical fabrication and characterization of silver nanoparticles by using Pepper leaf broth. The Pepper leaves extract acts as a reducing and capping agent in the formation of silver nanoparticles. A UV–Vis spectrum of the aqueous medium containing silver nanoparticles demonstrated a peak at 458 nm corresponding to the plasmon absorbance of rapidly synthesized silver nanoparticles that was characterized by UV–Vis spectrophotometer. The sizes of the synthesized silver nanoparticles were found to be in the range of 5–60 nm. The FTIR analysis of the nanoparticles indicated the presence of proteins, which may be acting as capping agents around the nanoparticles. This study reports that synthesis is useful to avoid toxic chemicals with adverse effects in medical applications rather than physical and chemical methods.

Harekrishna Bar ***et al*** (2009) [34] presented that Green synthesis of silver nanoparticles using seed extract of Jatropha curcas. The synthesis of silver nanoparticles has been reported using aqueous seed extract of Jatropha curcas. Formation of stable silver nanoparticles at different concentration of $AgNO_3$ gives mostly spherical particles with diameter ranging from 15 to 50 nm. The resulting silver particles are characterized using HRTEM, XRD and UV–vis spectroscopic techniques. XRD study shows that the particles are crystalline in nature with face centered cubic geometry.

Out of this review of literature, I came to conclude that no one had synthesis silver nanoparticles from piper nigrum with cardium seashell for bio-medical applications.

CHAPTER III

CHAPTER 3

MATERIALS AND METHODS

3.1 SEASHELL

A seashell or sea shell, also known simply as a shell, is a hard, protective outer layer usually created by an animal or organism that lives in the sea. The shell is part of the body of the animal. Empty seashells are often found washed up on beaches by beachcombers. The shells are empty because the animal has died and the soft parts have decomposed or been eaten by another animal. A seashell is usually the exoskeleton of an invertebrate (an animal without a backbone), and is typically composed of calcium carbonate or chitin. Most shells that are found on beaches are the shells of marine mollusks, partly because these shells are usually made of calcium carbonate, and endure better than shells made of chitin.

3.2 USES OF SEASHELL

Seashells can be a valuable resource and a range of industries are now looking at how they can be used, not just to improve profitability but also sustainability. Mined calcium carbonate is used in a range of industries such as construction materials, food supplement, pharmaceutics, animal feed, plastic production, and others but seashells offer a natural alternative. The top potential uses for seashells include use in:

- Poultry nutrition;
- Water purification;
- Retreating toxic waste;

- Organic fertilizer;
- Construction material.

3.3 HEALTHY BENEFITS OF PEPPER

- Prevents Any Sort of Cancer
- Good for Digestion
- Prevents Constipation
- Treats Skin Problems
- Good for Your Hair
- Aids in Weight Loss
- Treats Depression
- Helps in Treating Respiratory Diseases
- Reduces joint pain
- Detoxifies your body
- Anti – inflammatory properties
- Good for your brain
- Improves blood sugar
- Might be effective against cholesterol.

3.4 Silver nitrate

Silver nitrate is a chemical compound with the formula $AgNO_3$. It consists of an ionic bond between the silver cation (Ag^+) and the nitrate anion (NO_3^-). Due to the ionic nature of this compound, it readily dissolves in water and dissociates into its constituent ions.Silver nitrate is a precursor to many compounds of silver, including the silver compounds used in photography. When compared to silver halides, which are used in photography due to their sensitivity to light, $AgNO_3$ is quite stable when exposed to light.

3.4.1 Structure of $AgNO_3$

An illustration describing the structure of the silver nitrate molecule is provided below. It can be observed that silver has an oxidation number of +1 in this compound.

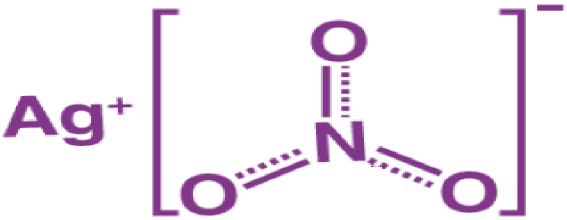

Figure : 3.1(Structure of $AgNO_3$)

The nitrate ion described above consists of one nitrogen atom which is surrounded by three oxygen atoms. The nitrogen-oxygen bonds in this ion are similar to each other. The formal charge assigned to the nitrogen atom is -1, whereas each oxygen atom holds a charge of -⅔. The net charge associated with the nitrate ion is -1, which is quenched by the +1 charge held by the

Ag^+ ion via an ionic bond in $AgNO_3$. It can be noted that the structure of the nitrate ion is stabilized by resonance.

3.4.2 Uses of Silver Nitrate

Silver nitrate has a wide range of applications in many fields such as biology, chemical synthesis, and medicine. Some of these uses of $AgNO_3$ are listed below.

- Silver nitrate is a very versatile compound because the nitrate ion can be replaced by other ligands that can bind to the silver ion.
- Due to the ability of this compound to form a precipitate of silver halides when treated with halide ions, it is used while making photographic films.
- Many silver-based explosives can be prepared with a precipitation reaction of silver nitrate.
- In the field of inorganic chemistry, halides are extracted with the help of this compound.
- The branch of chemistry known as analytical chemistry uses this reaction to check for the presence of halide anions such as the iodide, bromide, or chloride ions.
- Mixtures of alkenes can be separated with the help of this compound since the silver cation binds with alkenes in a reversible fashion.
- When diluted with water to a concentration of 0.5%, silver nitrate can serve as an antiseptic in many medical setups.

- A diluted solution of $AgNO_3$ can be administered to the eyes of a baby which is born to a mother suffering from gonorrhea, which combats the gonorrhoea bacteria and protects the baby from the onset of blindness.
- This compound is also known to be used for the treatment and the removal of unwanted warts in human beings.

3.4.3 Properties of Silver Nitrate

Some important physical and chemical properties of silver nitrate are listed in this subsection.

3.4.4 Physical Properties

- The molar mass of silver nitrate is 169.872 grams per mole.
- $AgNO_3$ has a colourless appearance in its solid-state and is odourless.
- In its solid state, it has a density of 4.35 grams per cubic centimetre. Its density in the liquid state at a temperature of 210^oC corresponds to 3.97 g/cm^3.
- The melting and boiling points of silver nitrate are 482.8 K and 713 K respectively. However, this compound tends to decompose at temperatures approaching its boiling point.
- Silver nitrate, like most ionic compounds, dissolves readily in water. Its solubility in water corresponds to 122 g /100mL at 0^oC and 256g / 100mL at a temperature of 25^oC
- The crystal structure of $AgNO_3$ is orthorhombic.

3.4.5 Chemical Properties

- The hazards of $AgNO_3$ include its toxic and corrosive nature.
- The reaction between silver nitrate and ethanol is explosive.
- The silver present in the silver nitrate compound is displaced by copper, which forms copper nitrate. The chemical equation for this reaction is given by $\mathbf{2AgNO_3 + Cu \rightarrow Cu(NO_3)_2 + 2Ag}$
- When heated to 440^oC, this compound completely decomposes to give oxygen, nitrogen dioxide, and silver.
- Silver nitrate on decomposition gives silver, oxygen gas and nitrite.

It can be noted that even though metal nitrates generally decompose to yield metal oxides, the decomposition reaction of silver nitrate gives rise to elemental silver because silver oxide decomposes at an even lower temperature than $AgNO_3$.

3.4.6 Applications of Silver Nitrate

Silver nitrate is broadly used in two fields – Medical and industrial applications. Silver nitrate is a precursor of many other silver compounds that are used. Hence, one of the uses of Silver Nitrate is in the preparation of other Silver compounds. Silver nitrate is a very caustic chemical. This is used in the preparation of other silver salts. Colloidal compounds of silver that are used in medicine are also prepared using silver nitrate. In photographic emulsions, Silver halides are used, and these, in turn, are prepared with Silver nitrate. This is also used in labs for volumetric analysis to determine, halides, thiocyanates etc.

3.4.7 Some of the Medical Applications of Silver Nitrate

- Eye drops for children: In the year 1881, it was first used in the manufacture of eye drops. This was used to treat or prevent any hereditary infections of the eye transmitted to the child from the mother. However, these days it is not used as a preventive remedy. It has been proven that bacteria, Gonococcal Bacteria which is a principal cause of eye infections are eliminated by this chemical.

- Some people have moles on their hands or bodies. Silver nitrate is used to cauterize and remove such moles.

- In the field of dentistry, it is used to heal ulcers in the mouth.

However, though it is known to be used in treatment to cure some problems as mentioned above, Silver Nitrate should not be consumed or used without doctor’s advice or consultation.

3.4.8 Some of the Industrial Applications of Silver Nitrate

- Electroplating: Such plating work is done on jewelry and watches to give a sophisticated finish and look. Silver Nitrate is used when Silver must be coated on Nickel.

- We all use mirrors in our day to day life. Mirrors reflect whatever is in front of it. In order to create such a surface that reflects, Silver Nitrate is used. A coating of Silver Nitrate is used on glass, which then makes the conversion of plain glass to mirror possible.

- It is also used in the manufacturing of many coloring agents like dyes and inks. Some people use hair dyes in which silver nitrate is added. In the textile industry, they use markers to mark on the fabric. Such markers also use Silver Nitrate. There are links that can never be removed, they are called indelible inks, which also use this chemical.

- Explosives are used to break rocks to lay roads etc: The manufacture of such explosives also uses silver nitrate and also includes other salts of silver like silver acetylide, silver azide, etc.
- Today's world is using digital photography. Earlier, photographs were taken with films that were washed and processed (called as Developing of photos). In the process of making photographic films, a small number of Silver halides (eg: silver bromide, silver chloride) was used. When stuck with light while taking photographs, there would be decomposition to elemental silver, which would leave an image. This could then be developed into a photo by using other chemicals.
- We all see different ceramic pottery in different colors. Silver Nitrate is used to add such colors in the ceramic works.
- Pesticide products that have Silver Nitrate as an active ingredient are used in the cut flower industry. These are used to prevent early or premature withering of plants and dropping of buds and flowers. Cut stems make ethylene, which helps to hasten the process of fruit ripening and aging of plants. When these stems are placed in a very dilute solution of Silver Nitrate then this process is delayed.

Thus, Silver Nitrate has its uses in various areas. However, it is important to be very careful in using this chemical as it can cause damage if improperly handled.

3.4.9 Impact of Light on Silver Nitrate

When Silver Nitrate is stored in labs, it is always advised to store them in dark bottles. There is a specific reason for this. Silver Nitrate is very sensitive to light. This means that the chemical will react when exposed to light. So, when this is left exposed to sunlight or any bright light, it will start to hydrolyze. This will result in the formation of black or brown colored silver oxide and nitric acid. If this is stored in dark bottles, and kept away from contact with direct light, this reaction can be minimized and hence can be stored for a longer duration.

3.4.10 Bulk Storage and Handling of Silver Nitrate

Silver Nitrate is an oxidizing agent, which means it will readily give out oxygen. Oxygen supports combustion or fire. Hence, while storing these chemicals, care should be taken to ensure that they are stored away from any chemical that is combustible or flammable. The reason is, that in case of a fire, the Silver Nitrate decomposes, can add to the fire by providing oxygen. Hence care should be taken to store them separately.

3.4.11 Adverse Health Effects of Silver Nitrate

Based on data available as of now following effects are caused by Silver Nitrate;

These are categorized as acute effects.

- Silver Nitrate is a caustic chemical. Hence this will cause irritation. When it is absorbed in the skin over a long period of time it causes a grayish discoloration of tissues. This phenomenon is called argyria.If inhaled, this will cause irritation and damage to mucous membranes.

- If Silver Nitrate is taken in by mouth, it can have dangerous effects and sometimes cause death also. It can cause vomiting, bloody diarrhea, dizziness and convulsions also. Some of the Chronic effects due to long term exposure to Silver Nitrate are:

- It can cause general depression, headache, and loss of mental capability. In some cases of people who have been exposed to Silver Nitrate, Cancer also has been observed.

- When somebody comes into contact with Silver Nitrate, the contact portion must be washed with large quantities of freshwater. They should be immediately provided with medical attention.

- Silver Nitrate is also highly toxic to fish and other aquatic life forms. Hence the disposal of this chemical also should be done in complete conformance with local laws and regulations.

- Silver Nitrate is also used in Criminal Investigations. Generally, fingerprints are found in crime scenes. One type of fingerprint, called the Latent print is not visible to the human eye. Such prints are left when sweat or natural body oils make contact with other surfaces. Investigators use a method called Latent Print development to solve or identify such prints. In such processes of developing the latent print, Silver Nitrate is used. In our skin secretions, there is some element of chlorides. Silver nitrate reacts with these secretions and forms silver chloride. These turn to gray color when exposed to UV light. Thus, this chemical helps in the field of criminal investigations also.

Table : 3.1 Properties of silver Nitrate

Molecular weight	169.87g/mol
Appearance	Colorless,solid,rhombic,crystals, having bitter, caustic metallic taste.
Odor	Odorless
Density	4.35g/cm^3[24℃]
Melting point	209.7℃ (409.5°F :482.8K)
Boiling point	440℃ (824°F :713K)
Solubility	1gm/0.4ml in water,30ml in alcohol at 25℃. slightly soluble in ether.

3.5 APPLICATIONS OF Ag-NPs IN NANOFIELD:

- Nanomaterials can exist naturally, be formed as by-products of combustion reactions, or be engineered specifically to fulfil a certain function.
- Nanomaterials are used in a wide range of industries, from healthcare and cosmetics to environmental preservation and air purification, due to their capacity to create materials in a specific way to perform a specified function.
- Carbon nanotubes can be utilised to morph aeroplane wings in aerospace. The nanotubes are combined in a composite form that bends when an electric voltage is applied**.**

- Baseball bats produced with carbon nanotubes are lighter and perform better, according to the sports industry. Antimicrobial nanotechnology, which is employed in things such as towels and mats used by athletes, is another example of nanoparticles in this business.
- Silver nanoparticles possess many valuable optical properties that have opened the door to new approaches in sensing and imaging applications, providing a wide range of detection modes such as colorimetric, dispersion techniques radiation, SERS and MEF, at extremely low detection limits. In addition, nanoparticles have made it possible to use diffusion imaging techniques and have brought valuable improvements to standard imaging techniques.
- Military applications for nanomaterials have also been developed. One example is the injection of movable pigment nanoparticles into the material of soldiers' uniforms to provide a better kind of camouflage. The military has also created sensor devices that can identify biological agents using nanomaterials such as titanium dioxide.
- Nano-titanium dioxide is also used in coatings to create self-cleaning surfaces like those found on plastic garden chairs. The coating is coated with a sealed film of water, and any dirt dissolves in the film, which is then removed by the following shower, thus cleaning the seats.
- Engineers may design photovoltaics (PV) and solar thermal devices with customised solar absorption rates by controlling the size, shape, and substance of the nanoparticle. Solar radiation absorption is substantially higher in nanoparticle based materials than in thin films of continuous sheets of material.

- The Sol-Gel technique is a way to make solid material out of nanoparticles. While it is considered a relatively recent industrial technology, it is widely employed in a variety of industries, including abrasive powder manufacturing, coatings manufacturing, and optical fiber manufacturing.

3.6 BIOLOGICAL APPLICATIONS OF Ag-NPs:

- **3.6.1 Antibacterial Activity of Ag NPs :**
- Ag NPs appear to be an alternative to antibiotics in terms of antibacterial activity and the capacity to overcome antibiotic resistance in bacteria. As a result, Ag NPs must be developed as antibacterial agents.
- Due to their huge surface-to-volume ratios and crystallographic surface structure, Ag NPs appear to be viable antibacterial agents among the many promising nanomaterials.
- The seminal paper reported by Sondi and Salopek-Sondi demonstrated the antimicrobial activity of Ag NPs against Escherichia coli, in which E. coli cells treated with Ag NPs showed the accumulation of Ag NPs in the cell wall and the formation of "pits" in the bacterial cell wall, eventually leading to cell death.

3.7 METHODS

3.7.1 CO-PRECIPITATION METHOD:

The simultaneous precipitation of a normally soluble component with a macro-component from the same solution by the formation of mixed crystals, by adsorption, occlusion or mechanical entrapment.

Co precipitation is a kind of precipitation where soluble compounds in a solution are eliminated during the course of precipitation. Precipitation is a process in which a solid is precipitated from a solution containing other ions. These ions are incorporated into the solid by adsorption on the surface of the growing particles, physical trapping in the porous space, or substitution in the crystal lattice. Adsorption is one of the main co precipitation mechanisms. It is a process in which a solid, or adsorbent, is added to a solution containing other ions, known as an adsorbent. In this case, the adsorbents are bound to the surface of the solid by physical or chemical interactions between the adsorbent and the adsorbent.Co-precipitation helps to hold the required cations close together in the reaction medium and lowers the temperature of decomposition, just as in the case of the sol– gel process.

3.7.2 ADVANTAGES :

Through different chemical reactions in the solution, the co-precipitation technique has the advantage of directly generating homogenous nanomaterials with tiny size and size dispersion.

- Easy and quick to prepare.
- Particle size and composition may be easily controlled
- A variety of ways to alter particle surface state and overall homogeneity
- It's cold outside.
- It saves energy.
- Doesn't need the use of an organic solvent.

3.7.3 DISADVANTAGES:

- Uncharged species are not included.

- Trace contaminants in the product may also precipitate.
- It takes time.
- Issues with batch-to-batch repeatability.

3.8 EXPERIMENTAL

3.8.1 PREPARATION OF SEA SHELL POWDER

The seashell was collected near the seashore of Muthu Nagar beach and the collected shells are cleaned under ultrasonicator for 3 hours .The cleaned shells are crushed, grinded, and makes into powdered by muffle furnace under 600°C for 2 hours.

Figure : 3.2 Cardium Seashell

Figure: 3.3 Ultrasonicator

3.8.2 PREPARATION OF PIPER NIGRUM

20g of pepper was powdered using mixer .Then the 20g of pepper and 200ml of distilled water was boiled at 100°C, the extract was filtered to obtained pure pepper solution.

Figure : 3.4 Piper Nigrum

3.8.3 PREPARATION OF SILVER NANOPARTICLES

First the beaker is washed thoroughly with ethanol.25g of seashell powder is dissolved in 125ml of pepper solution. Then the mixture is poured into a beaker and kept on a magnetic stirrer and stirred thoroughly for one and half hour at 70℃ heat is maintained and cooled. Then 21.233g of silver nitrate($AgNO_3$) was measured in digital balanced and mix it with the beaker containing seashell and pepper extract. The mixture is stirred at 700rpm until the precipitate is obtained. Now the color of the solution changes from light brown to dark brown color. The sample is filtered and heated in hot air oven at 120℃ . The dried sample is placed in muffle furnace at 600℃ . The precipitate thus obtained is finely powered. Thus the Silver nanoparticles are obtained

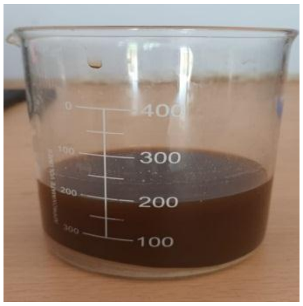

Figure: 3.5 (Brown sample)

Figure: 3.6(Black Sample)

The following equipments in the lab were used

- Muffle furnace
- Digital Balance
- Hot air oven.

CHAPTER IV

CHAPTER IV

RESULTS AND DISCUSSION

4.1 Introduction:

This present study is to investigate the chemical and bio-synthesis of the Ag_2O nanoparticles. The properties of nanostructures lead to the drastic potential applications. So in the present thesis the prepared Ag nanostructure have been subjected to XRD, EDAX and SEM analytic techniques and structural and surface morphology have been obtained respectively.

4.2 Structural analysis XRD:

The X-ray diffraction technique analyzed the crystalline phase, crystal structure, purity, and average crystalline size of the Ag_2O NPs. The XRD pattern of Ag_2O nanoparticles are shown in the figure 4.1 the 2θ ranges of 20° to 80° have been recorded. The XRD pattern of Ag_2O NPs shows good agreement with the JCPDS card number: 04-0783.The average crystalline size of Ag_2O NPs was calculated from the XRD pattern using the Debye Scherer formula

$$\mathbf{D = k\lambda/\beta \cos \theta}$$

Where,

- D is the gain size or particle size (nm)
- β is the full width at half maximum (FWHM) of a broad diffraction peak
- λ is the X-ray wavelength (1.5406 Å)

- θ is the Bragg's angle (degree)

- K is the Scherrer constant (0.94)

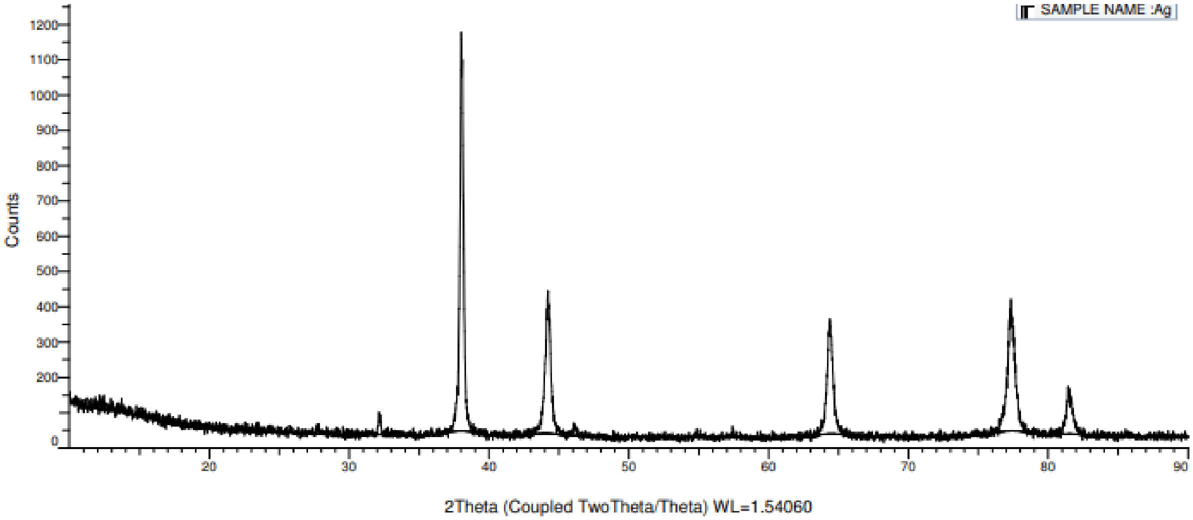

Fig 4.1 X - ray diffraction pattern of Silver oxide nanoparticles

Table 4.1 Calculation of size of silver oxide nanoparticle from XRD pattern.

Position 2Θ(degree)	**Mean Θ(degree)**	**FWHM β**	**Particle size D (nm)**
38.050	19.025	0.272	32
44.235	22.1175	0.395	23
64.395	32.1975	0.475	21
77.332	38.666	0.547	19

The average size of silver oxide nano particle is 24 nm.

The crystalline structure of the Ag_2O NPs was studied using XRD analysis, as shown in Figure. As shown in Figure 4.1, the crystalline existence and purity of as-prepared Ag_2O NPs were confirmed by studying the XRD pattern. The observed diffraction peaks observed at 2θ of 38.050, 44. 235, 64.395, and 77.332 were indexed to Bragg reflections (111), (200), (220), and (311), respectively. The XRD pattern was obtained as per the standard diffraction (JCPDS) file no: 04-0783 corresponding to the silver metallic nanoparticles of the crystalline face-centered cubic (fcc) planar geometry. The intensity of the peak corresponding to the (111) plane was greater than that of other planes, promoting the idea that Ag_2O NPs predominantly established along the (111) direction. Analysis of the X-ray diffraction (XRD) showed that most of the Ag_2O NPs were spherical. The average estimated crystallite size of the Ag_2O NPs estimated from the FWHM of the diffraction peak using the Scherrer equation, $D = K\lambda/\beta\cos\theta$, was found to be 24 nm.

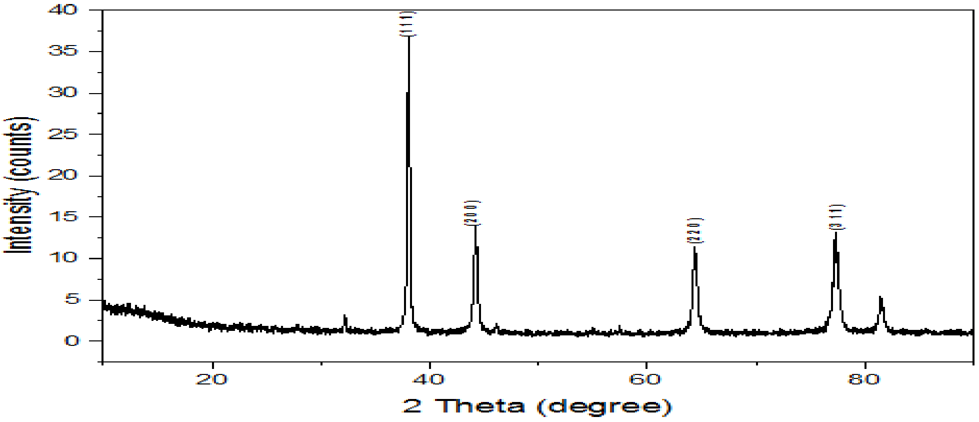

Figure : 4.2 XRD Pattern with hkl plane values.

Table 4.2 Comparison of experimental 2Ɵ with standard JCPDS file number : 04-0783.

S.No	**hkl**	**Piper Nigrum mediated Ag_2O NPs**	**Standard JCPDS Silver:04-0783**
		Experimental 2Ɵ	**Standard 2Ɵ**
1.	111	38.050	38.117
2.	200	44.235	44.279
3.	220	64.395	64.428
4.	311	77.332	77.475

4.3 CHARACTERISATION USING SEM:

Figure 4.3,4.4 and 4.5 shows the SEM images of prepared Ag_2O NPs. The SEM image of piper nigrum mediated Ag_2O nanoparticles is a flower like structure and the chemical synthesis Ag_2O nanoparticles flower shape surface morphology. In general, the decrease in particle size is inversely proportional to the surface volume of the material. Therefore the lower particle size material quickly penetrates the toxic elements as well as the bacterial surface that led the process of decomposition. The shape of nanoparticles depends on their interaction with stabilizers and the inductors around them and also their preparation method.

SEM Image of Ag_2O Nanoparticles

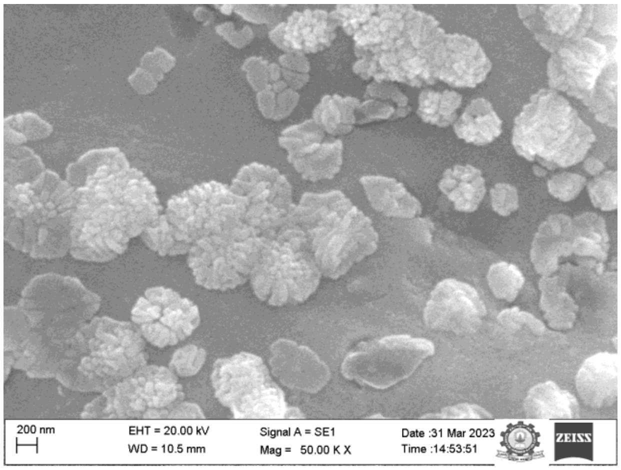

Figure : 4.3

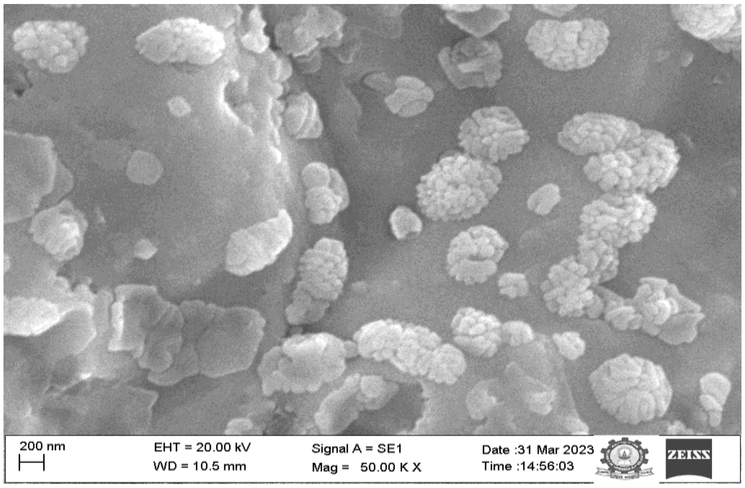

Figure :4.4

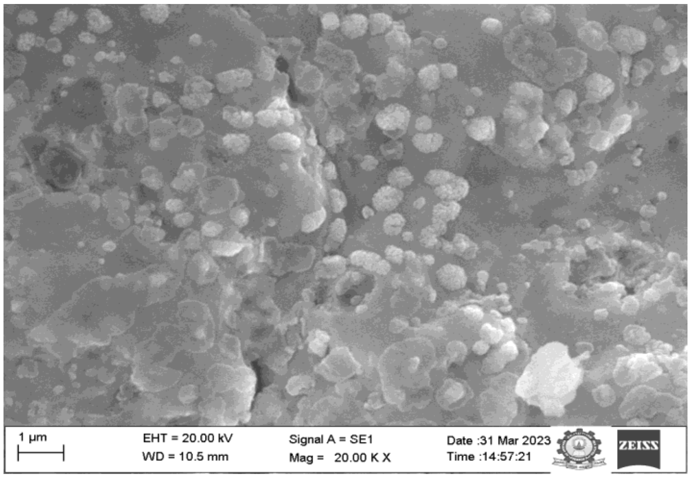

Figure : 4.5

4.4 CHARACTERIZATION USING EDAX:

Energy dispersive X-ray (EDX) composition analysis: Energy dispersive X-ray analysis (EDX), referred to as EDS or EDAX, is an x-ray technique used to identify the elemental composition of materials. The data generated by EDX analysis consist of spectra showing 32 peaks corresponding to the elements making up the true composition of the sample being analysed.

The purity of Ag_2O nanoparticles was analyzed by EDX pattern as revealed in Figure 4.6 shows Sharp and distinct peak of silver is observed at 3 keV. Thus, presence of sharp and intense peaks of Ag shows the high purity of synthesized nanoparticles. Elemental composition analysis by EDX presented strongest signal from silver (Ag) region and weaker signals from O and N atoms. It also showed that pure crystalline nature was only composed of silver

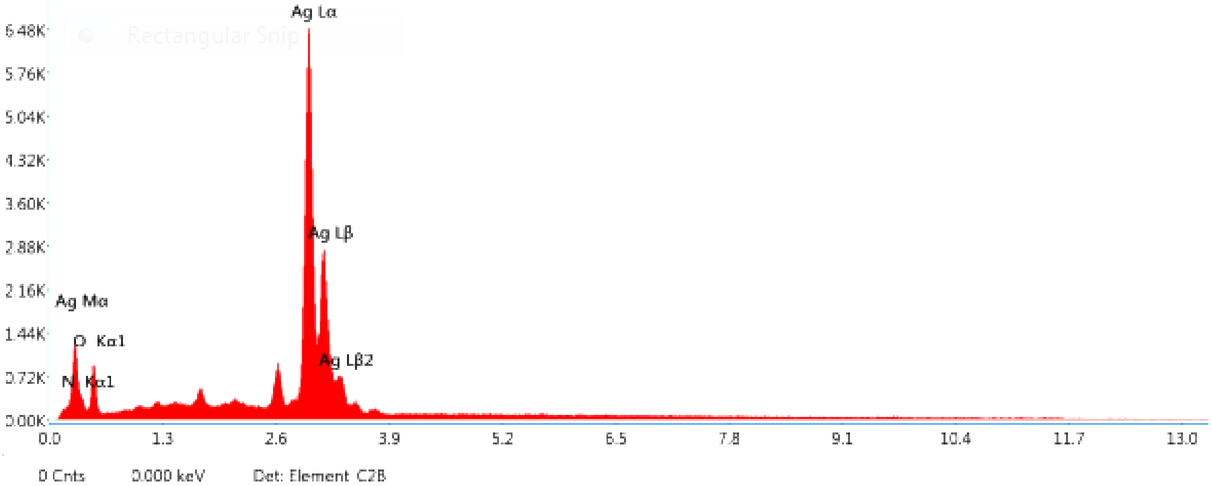

Figure:4.6 Energy Dispersive X-ray analysis (EDAX) of silver oxide nanoparticles

Table 4.3 : Elements with weight percentage in EDAX

Elements	Weight%
Ag	80.8
N	0.9
O	18.3

4.5 ANTI MICROBIAL TEST

4.5.1 WELL DIFFUSION TEST

The disk diffusion test which is also known as Kirby–Bauer test or diffusion test is a culture based microbial assay to check the susceptibility of any given sample or drug compound in drug discovery process and diagnostic setup. Agar well diffusion method is an extensively utilized procedure to assess the antimicrobial activity of any synthetic chemical molecule or plants/microbial extracts. The agar plate surface is inoculated by spreading a volume of the microbial inoculums over the entire agar surface. Then, a hole with a diameter of 6 to 8 mm is punched aseptically with a sterile cork borer or a tip, and a volume (20–100 µL) of the antimicrobial agent or extract solution at desired concentration is introduced into the well. Then, agar plates are incubated under suitable conditions depending upon the test microorganism. The antimicrobial agent diffuses in the agar medium and inhibits the growth of the microbial strain tested.

The Nutrient broth media and agar were autoclaved. The sterile media was used to culture the bacterial cells overnight at 37 °C. The autoclaved NB agar were plated on a standard petri dish and let to cool down. Once the agar is solidified, both the *E. coli* (ATCC 10536) and *S. aureus* (ATCC 25923) and were spread plated using a L-rod on to the NB agar plates. Sterile well cutter was used to punch in holes on the agar plate. 100 µl of the dissolved samples at different concentration were spread plated onto the punched in wells. To check the antimicrobial activity of the given samples and the zone of inhibitions was tabulated below with the plate images. After the incubation period, the zone of inhibition was measured and reported in millimeters (mm). All assays were performed in triplicate. The extracts were dissolved in distilled water and Chloramphenicol was used as control.

Table : 4.4 Antibacterial activity of the synthesized Ag_2O NPs

S. No	**Strain**	**Concentration level (µl)** **Zone of inhibition (mm)**				
		Control	**25**	**50**	**75**	**100**
1.	*E. coli*	20	-	11	13	15
2.	*S. aureus*	22	10	10	12	14

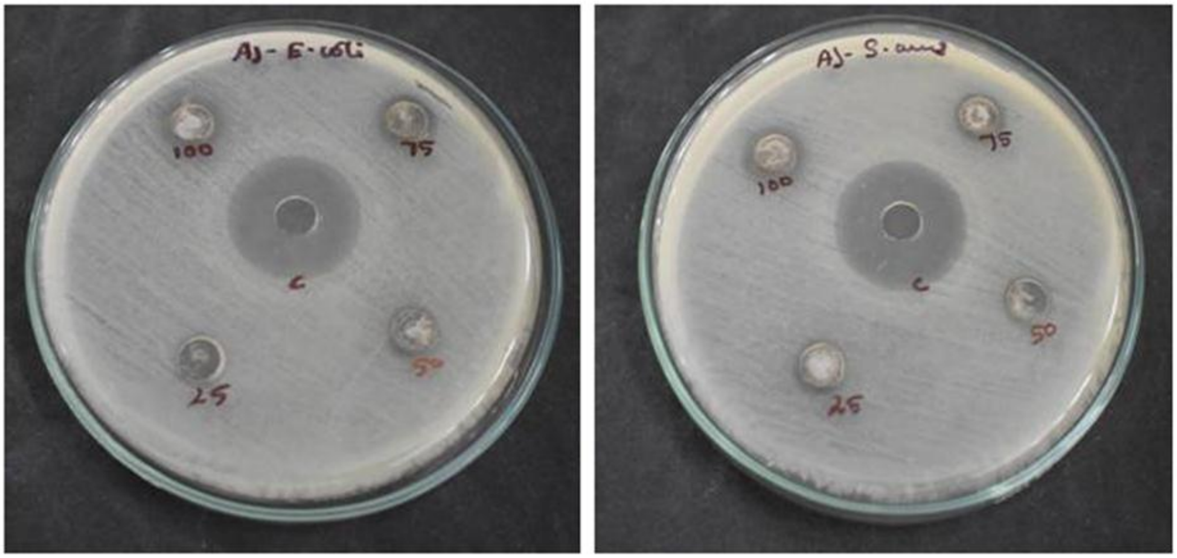

Figure : 4.7 Microbicidal potential of synthesized Ag_2O NPs

CHAPTER V

CHAPTER V

SUMMARY AND CONCLUSION

Ag_2O is one of the most useful metal oxide, which has many applications in different fields. A very remarkable and effective Silver Oxide nanostructured material is prepared using the simple co- precipitation method without any surfactants.

XRD:

- Strong peaks in XRD pattern specify the preferential crystal plane of the nanostructures.
- The grain size of the Ag_2O nanoparticles is 24nm.

EDAX:

The elemental analysis of the chemical compounds was investigated through EDS spectra NPs, the composition of the silver element is high compared to oxygen content.

SEM:

Ag_2O nanoparticles are basically composed of flower like structure and assembled together to yield morphology.

ANTI MICROBIAL TEST:

The well diffusion method was used to assess the antibacterial behaviours of the fabricated Ag_2O NPs that were assessed against a group of bacteria. It is a mixed group of various bacterial species and genera such as E.coli and S.Aureus having resistance to variety of antibiotics. Four holes were made in agar plate at four different concentration of Ag_2O NPs of 25 µl, 50 µl, 75 µl, 100 µl .The zone of inhibition was estimated by means of evaluating the diameter of the inhibition zone around Ag_2O NPs.

From all the results we observed that seashell, which is the source of calcium carbonate was not found in EDAX as well as in SEM images. However we are thinking that the presence of the calcium carbonate is not sufficient. So the work has to be improved further.The concentration can be varied to see the impact of the calcium in silver nanoparticles preparation.

The size, shape, and morphology of nanoparticles are all controlled by particular criteria such as reaction kinetics, temperature, pH, and so on, so that the synthesis method is selective in producing the nanoparticle that is desired.

Characterization of Ag_2O NP is a crucial step in determining their properties and learning about their composition, structure, and morphology. It also allows us to determine when the synthesis process is complete and assess its quality.

Physical and chemical methods can be adopted to prepare silver nanoparticles. Every year, hundreds of research articles detailing various Ag_2O NP synthesis strategies are published. We have just studied a few of the most important publications through this project, which largely deal with physical and chemical methods.

All known applications for metallic silver might employ nanosilver instead of silver to take advantage of nanosilver's unique features, according to the literature. Despite all of nanosilver's advantages, its environmental impact is problematic. These synthesis methods may necessitate the use of various raw materials, as well as the usage of hazardous products or wastes to produce reactions. However, there is various researches in the literature regarding nanosilver synthesis methods, but the most widely utilized methods in the industry are yet to be known.

As a result, we propose that researchers be directed to work on industry standard methods for manufacturing nanosilver. In the future, we'd like to carry on further research on nanoparticles, giving importance to bio synthesis of nanoparticles.

VI REFERENCES:

1. Charles P Poole And Frank K Owens; Introduction of nanotechnology, 30 May 2003.

2. J.J Kinsley, K.C Patil Wuhan University, Centre of Nano science and Nanotechnology;

3. S.K Prasad, Modern Concepts in Nanotechnology (2011).

4. Chand, Modern Physics,(2011)

5. H.S Dhanaraj, H.L.Bhat and K.C.Patil, Encyclopedia of Nanoscience and Nanotechnology;

6. Ying Wang; Nanostructures And Nanomaterial, Volume 2.

7. B.S. Murthy, P. Shankar And Baldev Raj; (2012), Textbook Of Nano science and Nanotechnology;

8. X.Feng,M.Z.Hu,H.S Nalwa, Encyclopedia Of Nanoscience and Nanotechnology.

9. Dutton Gribbin,John ,Richard Feynman; A Life In Science (1997).

10. Shahid Hussain., Zuber Ali Shah, Kazi Sabiruddin, Anup Kumar Keshri.,(2023) Characterization and tribological behaviour of Indian clam seashell-derived hydroxyapatite coating applied on titanium alloy by plasma spray technique, Journal of the Mechanical Behavior of Biomedical Materials.Vol 137.pp.105-550.

11. Stefanie Gärtner , Angelina Graf , Carla Triunfo , Davide Laurenzi , Stefan M. Schupp 4 , Gabriele Maoloni 3 , Giuseppe Falini and Helmut Colfen(2022), Turning Seashell Waste into Electrically Conductive Particles,International journal molecular science.vol.23.issue 13.pp.72-56.

12. Shahid Hussain and Kazi Sabiruddin(2021), Effect of heat treatment on the synthesis of hydroxyapatite from Indian clam seashell by hydrothermal method, Ceramics International.vol 47.issue 21.pp.29660-29669.

13. Jos´e G. Miranda-Hernandez , Carlos O. Gonzalez-Mor , H´ector Herrera-Hern´ andez , Enrique Hernandez ´ Sanchez ´ , Jos´e de Jesús A. Flores-Cuautle , Mayahuel Ortega-Avil´es(2021), Sea snail shells for synthesis of ceramic compounds reinforced with metallic oxide: Microstructural, mechanical and electrical behavior,Materials Today Communications.vol 28.pp.102-656.

14. Fahad A. Alharbi and Abdullah A. Alarfaj(2020), Green synthesis of silver nanoparticles from Neurada procumbens and its antibacterial activity against multi-drug resistant microbial pathogens, Journal of King Saud University – Science.vol 32.pp.1346-1352.

15. P. Tamilarasi and P. Meena(2020), Green synthesis of silver nanoparticles (Ag NPs) using Gomphrena globosa (Globe amaranth) leaf extract and their characterization, Materials Today: Proceedings.vol .33.pp.2209-2216.

16. Mohsen Mosaviniyaa , Towan Kikhavania, Marjan Tanzifia , Mohammad Tavakkoli Yarakib, Parnian Tajbakhshd , Aseman Lajevardie(2019), Facile green synthesis of silver nanoparticles using Crocus Haussknechtii Bois bulb extract: Catalytic activity and antibacterial properties. Colloid and Interface Science Communications. vol.33.pp.100-211.

17. Liliana Hernández-Moralesa , Heriberto Espinoza-Gomezb , Lucia Z. Flores-Lópeza, Erika Lis Sotelo-Barrerac , Alfredo Núñez-Riverac , Rubén Darío Cadena-Navac , Gabriel Alonso-Núñezc , Karla Alejandra Espinozaa(2019), Study of the green synthesis of silver nanoparticles using a natural extract of dark or white Salvia hispanica L. seeds and their antibacterial application, Applied Surface Science.vol.489.pp.952-961.

18. K.Dhanaraj, G.Suresh, (2018) Conversion of waste sea shell (Anadara granosa) into valuable nano hydroxyapitate for biological applications,vacuum.Vol .152.pp.222-230.

19. Sanket J. Joshi 1, Geetha S. J., Saif Al-Mamari and Ahlam Al-Azkawi .,(2018), Green Synthesis of Silver Nanoparticles Using Pomegranate Peel Extracts and Its Application in Photocatalytic Degradation of Methylene Blue.Jundishapur journal of natural pharmaceutical products vol.13.issue 3.pp.867-846.

20.AntonyV.Samrot.,N.ShobanaandRashmiJenna.,(2018), Antibacterial and Antioxidant Activity of Different Staged Ripened Fruit of Capsicum annuum and ItsGreenSynthesizedSilverNanoparticles.Bionanoscience vol.8.pp.632-646.

21. Akbar Rostami-Vartooni , Mahmoud Nasrollahzadeh , Mohammad Alizadeh (2016) Green synthesis of seashell supported silver nanoparticles using Bunium persicum seeds extract: Application of the particles for catalytic reduction of organic dyes, Journal of Colloid and Interface Science.vol 470.pp,268-275.

22. Elham Vatandosta , Fereshteh Chekinb, and Seyed Ahmad Shahidi Yasaghia(2016), Green Synthesis of Silver Nanoparticles by Pepper Extracts Reduction and Its Electocatalytic and Antibacterial Activity, Russian Journal of Electrochemistry, 2016, Vol. 52, No. 10, pp. 960–965.

23. Chunfa Donga. , Chuanliang Cao, Xianglin Zhangc , Yanlong Zhand , Xiangjie Wanga , Xiuzhi Yanga , Kui Zhouc , Xinhua Xiaoa , Bin Yuana(2014), Wolfberry fruit (Lycium barbarum) extract mediated novel route for the green synthesis of silver nanoparticles.International journal for light and electron optics.vol.130.pp.162-170.

24. Shakeel Ahmed, Saif Ullah, Mudasir Ahmad, Babu Lal Swami, Saiqa Ikram(2015), Green synthesis of silver nanoparticles using Azadirachta indica aqueous leaf extract. Journal of Radiation Research and Applied Sciences.vol.9.pp1-7.

25. M.R. Bindhu, M. Umadevi,(2015), Antibacterial and catalytic activities of green synthesized silver nanoparticles. Spectrochimica Acta Part A: Molecular and Biomolecular Spectroscopy.vol.135.pp.373-378.

26. B. Ajitha a, Y. Ashok Kumar Reddy, P. Sreedhara Reddy(2015), Green synthesis and characterization of silver nanoparticles using Lantana camara leaf extract. Materials Science and Engineering C.vol 49.pp.373-381.

27. P.P.N. Vijay Kumar ., S.V.N. Pammi , Pratap Kollu, K.V.V. Satyanarayana , U. Shameem(2014), Green synthesis and characterization of silver nanoparticles using Boerhaavia diffusa plant extract and their anti bacterial activity. Industrial Crops and Products.vol.52.pp.562-566.

28. Mehdi Rahimi-Nasrabadia ., Seied Mahdi Pourmortazavib , Seyed Ataollah Sadat Shandizc , Farhad Ahmadid,e and Hossein Batoolif(2014), Green synthesis of silver nanoparticles using Eucalyptus leucoxylon leaves extract and evaluating the antioxidant activities of extract, Vol. 28, No. 22, 1964–1969.

29. Y. Subba Rao , Venkata S. Kotakadi , T.N.V.K.V. Prasad , A.V. Reddy , D.V.R. Sai Gopal,(2013), Green synthesis and spectral characterization of silver nanoparticles from Lakshmi tulasi (Ocimum sanctum) leaf extract, Spectrochimica Acta Part A: Molecular and Biomolecular Spectroscopy.vol.103c.pp.156-159.

30. Robin Augustine .,Nandakumar Kalarikkal .,Sabu Thomas(2013), A facile and rapid method for the black pepper leaf mediated green synthesis of silver nanoparticles and the antimicrobial study.Applied Nanosciencs vol.4.pp.809-818.

31. C. Dipankar, S. Murugan.,(2012), The green synthesis, characterization and evaluation of the biological activities of silver nanoparticles synthesized from Iresine herbstii leaf aqueous extracts. Colloids and Surfaces B: Biointerfaces.vol.98.pp.112-129.

32. Pantelis Kouvaris, Andreas Delimitis, Vassilis Zaspalis, Dimitrios Papadopoulos, Sofia A. Tsipas , Nikolaos Michailidis.,(2012), Green synthesis and characterization of silver nanoparticles produced using Arbutus Unedo leaf extract, Materials Letters.vol.76.pp.18-20.

33. K. Mallikarjuna , N. John Sushma , G. Narasimha , L. Manoj , B. Deva Prasad Raju.(2012), Phytochemical fabrication and characterization of silver nanoparticles by using Pepper leaf broth, Arabian Journal of Chemistry.vol.7 issue6.pp.1099-1103.

34. Harekrishna Bar, Dipak Kr. Bhui, Gobinda P. Sahoo, Priyanka Sarkar, Santanu Pyne, Ajay Misra.(2009), Green synthesis of silver nanoparticles using seed extract of Jatropha curcas, Colloids and Surfaces A: Physicochemical and Engineering Aspects.vol.348 issue no.1-3pp,212-216.

ENHANCED ELECTRICAL PROPERTIES OF GREEN SYNTHESIS OF TiO_2 AND ZnO COMPACT LAYER ON PERVOSKITE SOLARCELLS

A project work report and submitted to

DEPARTEMENT OF PHYSICS

ST. MARY'S COLLEGE (AUTONOMOUS), THOOTHUKUDI

Affiliated to

MANONMANIAM SUNDARANAR UNIVERSITY,
THIRUNELVELI

In partial fulfilment of the requirements for the award of

MASTER OF SCIENCE IN PHYSICS

Submitted by

K. AROCKIA PUNITHA
Reg. No: 21SPPH02

Under the guidance of

Ms. P. PADMAVATHI M.Sc., M.Phil., SET.,

DEPARTMENT OF PHYSICS
ST. MARY'S COLLEGE (AUTONOMOUS),
THOOTHUKUDI.
Re-accredited with 'A+' Grade by NAAC
(2022-2023)

CERTIFICATE

This is to certify that this project work report entitled **"ENHANCED ELECTRICAL PROPERTIES OF GREEN SYNTHESIS OF TiO_2 AND ZnO COMPACT LAYER ON PEROVSKITE SOLAR CELLS"** is submitted to **ST. MARY'S COLLEGE (AUTONOMOUS), THOOTHUKUDI** in partial fulfilment of requirements for the award of **MASTER OF SCIENCE IN PHYSICS** and is a record of work done during the academic year **2022 – 2023** by **K. AROCKIA PUNITHA** (Register No: 21SPPH02)

Padmavathi P

Signature of the Guide

Padmavathi P

Signature of the Co-ordinator

Signature of the Director

Director
Self Supporting Courses
St. Mary's College (Autonomous)
Thoothukudi - 628 001.

Lucia Rose

Signature of the Principal

Principal
St. Mary's College (Autonomous)
Thoothukudi - 628 001.

12/4/23

Signature of the Examiner

DECLARATION

I hereby declare that the project work report entitled **"ENHANCED ELECTRICAL PROPERTIES OF GREEN SYNTHESIS OF TiO_2 AND ZnO COMPACT LAYER ON PEROVSKITE SOLAR CELLS"** is submitted to **ST. MARY'S COLLEGE, (AUTONOMOUS), THOOTHUKUDI** affiliated to **MANONMANIAM SUNDARANAR UNIVERSITY, THIRUNELVELI** for the award of the degree of Master of Science in Physics is my original work and that no part of this project work report has been submitted for any Degree, Diploma or other similar titles.

K. Arockia Punitha.

Station: Thoothukudi

Date: 10.4.2023

Signature of the Student

(K.AROCKIA PUNITHA)

ACKNOWLEGEMENT

On the very outset of this report, I feel obliged to our Almighty for his aid in the completion of this project work successfully.

I wish to record our profound gratitude to our Principal Rev. **Dr. Sr. A.S.J. Lucia Rose, M.Sc., B.Ed., M.Phil., PGDCA., Ph.D.** for her motivation.

I sincerely thank our Director of SSC**, Rev. Sr. Josephine Jeyarani, M.A., M.Phil.,** for her encouragement and support.

I wish to thank **Rev. Dr. Sr. JESSIE FERNANDO M.Sc., M.Phil., Ph.D.,** HOD & Associate professor for her inspirational words to complete this project work.

I am very thankful to Mrs. **P. PADMAVATHI M.Sc., M.Phil., SET.,** SSC Co-ordinator and my guide, for her efficient and effective guidance. She played a key role in preparation of this project.

I express my sincere thanks to **Dr. S VALANARASU M.Sc., M.Phil., Ph. D,** Assistant professor, Arulanandhar college, Karumathur, **Dr. A. MURUGESWARI M.Sc., Ph.D,** Assistant Professor, Anna University and **Dr. KARUNAKARAN M.Sc., M. Phil., Ph. D** Assistant professor, Alagappa Government college, Karaikudi, for their valuable support and guidance provided throughout this project.

I am deeply grateful to all the staff members of Department of Physics (SSC) for supporting me in all aspects.

I would like to thank **Tamil Nadu State council for Science and Technology [Grant number -PS 488]** for their financial support.

I wish to thank my superior, my community sisters and my friends for being a constant source of motivation.

ABSTRACT

TiO_2 and ZnO nano power were synthesized from banana stem and orange extract respectively. Single layer of TiO_2 and ZnO thin films were deposited on a cleaned glass substrates by spray pyrolysis method and also bilayer thin film of ZnO/TiO_2 are deposited on glass substrate by spray pyrolysis method. These films are annealed at 450 K. The resulting product was characterized by X-Ray Diffraction (XRD). X-ray diffraction confirmed the prepared nano structures and thin films as ZnO/TiO_2. Opto electronic properties, electrical properties are studied from UV, I-V and PL studies. Their morphology is studied from SEM.

CONTENT

LIST OF FIGURES

LIST OF TABLES

CHAPTER I

INTRODUCTION

1.1 INTRODUCTION:

Technological progress of modern society depends on the material science and engineering community's ability to conceive the novel materials with extraordinary combination of physical and mechanical properties [1,2]. Modern technology requires thin films for different applications. Thin films and its devices play an important role in the development of modern technology. Thin films are three-dimensional form of solid material, whose one dimension, called the thickness, is much smaller than the other two dimensions. Thin films are formed by atom to atom or molecule to molecule condensation process [3]. Their thicknesses are typically less than several microns. The limit of thickness may vary from a nanometer to a few micrometers depending upon the field of application. Thin film is very important material for technology because this type materials show different properties from its own bulk materials and this property provides lots of benefit. There are lots of thin film production methods [4]. Physical Vapour Deposition (PVD) and Chemical Vapour Deposition (CVD) are two most common types of thin-film coating. The physical techniques are vacuum evaporation, sputtering, spraying and painting while vapor deposition, oxidation, immersion plating, chemical bath deposition and electroplating are called chemical techniques. There are various methods to deposit semiconducting thin films such as chemical bath deposition (CBD) [5], vacuum evaporation [6], electro deposition [7], chemical vapor deposition [8], molecular beam epistaxis [9], pulsed laser deposition [10], thermal evaporation [11], etc. Among them CBD appears to be very suitable method for a large-scale fabrication of the semiconducting thin films.

The main advantages of this method are that it is a low-cost method and do not require any sophisticated instruments, and films can be prepared at low processing temperature [12]. A stack of thin films is called Multilayer. In this work bilayer of zinc and titanium thin film is coated by sparry method and its various structural characterization were studied.

1.2 DEPOSITIONS:

Thin film can be prepared by many physical and chemical techniques.

- Physical deposition
- Chemical deposition

1.2.1 PHYSICAL DEPOSITION:

Physical vapor deposition (PVD) is a family of coating processes in which thin films are deposited by the condensation of a vaporized form of the desired film material onto the substrate. This process is carried out in a vacuum at temperatures between 150 and 500°C. The average thickness of various PVD coatings is 2-5 microns.

Types PVD processes include:

- Cathodic arc deposition
- Electron beam physical vapor deposition
- Evaporative deposition
- Sputtering
- Ion plating

- Enhanced sputtering

These coatings are generally used to improve hardness, wear resistance and oxidation resistance. Thus, such coatings are used in a wide range of applications such as:

- Aerospace
- Automotive
- Surgical/Medical Dies and molds for all manner of material processing
- Cutting tools
- Firearms
- Optics

Thin films (window tint, food packaging, etc.)

1.2.2 CHEMICAL DEPOSITION:

Sol- gel technique

Chemical bath deposition

Spray pyrolysis technique

1.Plating

  - Electroplating technique
  - Electro less deposition

2.Chemical vapor deposition (CVD)

- Low pressure (LPCVD)
- Plasma enhanced (PECVD)
- Atomic layer deposition (ALD)

1.3 Thin films structure:

Different and complex chemical reaction occur during the deposition process depending on the technique employed and deposition parameters, such as substrate temperature, deposition rate, pressure, and alignment of vapor stream with substrate, which give rise to a variety of microstructures. The resulting microstructure in turn defines the physical and chemical properties of the film, which means that an appropriate management of these variables is essential to obtain tailored film properties.

- Amorphous thin films,
- Polycrystalline thin films,
- Epitaxial thin films.

1.4 Applications of thin films:

Thin film used in semiconductor devices, wireless communications, telecommunications, integrated circuits, rectifiers, transistors, solar cells, light-emitting diodes, photoconductors, light crystal displays, magneto-optic memories, audio and video systems, compact discs, electro-optic coatings, memories, multilayer capacitors, flat-panel displays, smart windows, computer chips, magneto optic discs, lithography, micro- electromechanical systems and multifunctional emerging coatings, as well as other emerging cutting technologies.

1.4.1Thin-film photovoltaic cells:

Thin-film technologies are also being developed as a means of substantially reducing the cost of solar cells. The rationale for this is thin-film solar cells are cheaper to manufacture owing to their reduced material costs, energy costs, handling costs and capital costs. This is especially represented in the use of printed electronics (roll-to-roll) processes. Other thin-film technologies, that are still in an early stage of ongoing research or with limited commercial availability, are often classified as emerging or third generation photovoltaic cells and include, organic, dye-sensitized, and polymer solar cells, as well as quantum dot, copper zinc tin sulfide, nanocrystal and perovskite solar cells.

1.4.2 Thin-film batteries:

Thin-film printing technology is being used to apply solid-state lithium polymers to a variety of substrates to create unique batteries for specialized applications. Thin-film batteries can be deposited directly onto chips or chip packages in any shape or size. Flexible batteries can be made by printing onto plastic, thin metal foil, or paper.

1.4.3 Biosensors and plasmonic devices:

Noble_metal thin films are used in plasmonic structures such as surface plasmon_resonance (SPR) sensors. Surface_plasmon_polaritons are surface waves in the optical regime that propagate in between metal-dielectric interfaces; in Kretschmann-Raether configuration for the SPR sensors, a prism is coated with a metallic film through evaporation. Due to the poor adhesive characteristics of metallic films, germanium, titanium or chromium films are used as intermediate layers to promote stronger adhesion. Metallic thin films are also used in plasmonic waveguide designs.

1.4.4 Thin-film bulk acoustic wave resonators (TFBARs/FBARs):

For miniaturizing and more precise control of resonance frequency of piezoelectric crystals thin-film bulk acoustic resonators TFBARs/FBARs are developed for oscillators, telecommunication filters and duplexers, and sensor applications.

1.5 Objective of the present work:

The objective of the present work is

- To synthesis of nano particles and thin films,
- To determine the structure using XRD and SEM.
- To find the opto electronic properties by UV spectroscopy.
- To find the electrical properties using I-V characteristics and PL studies.

CHAPTER II

LITERATURE REVIEW

Dundar *et al* (2019) [13] studied that the TiO2 thin films deposited onto window glassare practicable for air purification and self-cleaning applications. TiO2 films were deposited onto window glass by ultrasonic spray pyrolysis method. The effect of the deposition temperature on the morphological, structural, optical and surface chemical composition was examined to comprehend the factors affecting wettability and photocatalytic activity of the deposited TiO2 films. The TiO2 thin film deposited at 3508C exhibited the highest amount of oxygen defects and OH2 groups on the film surface, and high amount of Naþ (10 at%). This study showed, that transparent and super hydrophilic TiO2 thin films with the specific quantity of 0.2 mg cm22 and surface area of 600 cm2 is effective to degrade approximately 80% of MTBE and its intermediate product TBF; and is thereby prospective coating for self-cleaning and air purification applications.

Nadarajah *et al* (2013) [14] studied that Zinc Oxide (ZnO) thin films were deposited on glass substrates the spray pyrolysis technique. The films were subsequently annealed in ambient air from 300◦ C to 500◦ C. The morphology and structural properties of the thin films. The structural, electrical, and optical properties of the ZnO thin films were characterized using XRD, AFM, data acquisition unit, and UV-vis spectrophotometer. The grain size of the films increases with the increase of annealing temperatures. The XRD diffractogram revealed that the thermal annealed film at 500◦ C possesses good crystalline hexagonal wurtzite structure, with a preferred plane orientation along (002). The grain size estimated from FESEM analysis is in good agreement with XRD data.

The PL emission of the samples shows a narrow emission centered at 385 nm and a broad peak emission located at 594 nm and 672 nm. The ZnO films show an increase of transmission with the increase of annealing temperature. In particular, ZnO film annealed at 500∘ C achieves high light transmission of 96% in the visible range with low electrical resistivity of 0.82 Ω cm. These properties render that the ZnO film is attractive to optoelectronic device applications.

Bidier *et al* (2017) [15] studied that Ti-doped ZnO nanorods (NRs) have been deposited onto Si substrates at 93 °C by using chemical bath deposition method. FESEM images reveal a high-quality nanorods FTIR analysis confirmed a successful doping process, where the peak at 500 cm^{-1} represents the Ti–O bond. XRD analysis indicated the formation of hexagonal wurtzite structure with a very strong preferred orientation along c-axis and enhanced crystalline quality as a result of Ti doping. The results also, showed the important of doping process to improve the structural and optical qualities which offers novel potential applications in nano-optoelectronics field.

Liu *et al* (2021) [16] studied that low-temperature solution-processed ZnO has decided advantages in flexible and tandem solar cells, while its application encountered difficulties in perovskite optoelectronic devices due to chemical instability at the ZnO perovskite interface. It has been proven to be a result of protonation reaction between ZnO and organic cations in perovskite materials, thus accelerating the perovskite decomposition. The possibility for the application of ZnO in perovskite optoelectronic devices and makes it have more advantages in tandem devices based on perovskite materials, as well as device with Al-doped ZnO transparent electrode.

James *et al* (2021) [17] studied that Electron transport materials (ETMs) are considered a keystone component of third-generation solar cells. A metal oxide bilayer that combines ZnO and TiO_2 compact films (ZnO/TiO_2) is implemented as ETM for solution-processed Sb_2S_3 planar solar cells. This result can be attributed to three main factors: 1) reduced shunt and resistive paths; 2) improved extraction of photogenerated electron from Sb_2S_3 film to ETM; and 3) reduced trap states resulting in a suppressed charge recombination at the ETM/ Sb_2S_3. This metal oxide bilayer provides a promising strategy for overcoming the long-standing obstacles to the development of efficient Sb_2S_3 planar solar cells.

Shalan *et al* (2015) [18] studied that to fabricate nanostructured spheres composed of mixed metal oxides. ZnO/TiO_2 nanocomposites supported on FTO substrate which are used as the photo-anode electrode for Quasi solid state dye-sensitized solar cells (QS-DSSCs). Phase purity of the ZnO and TiO_2 phases of the composites shell has been studied by X-ray diffraction peaks analysis. The high efficiency and excellent long-term stability of the quasi-solid-state DSCs assembled with organic dye and the PA/PEG hybrid gel electrolyte indicate that they are promising for industrialization.

Shaikh *et al* (2018) [19] studied that a low-temperature (90°C) and directly grown anatase titanium dioxide (TiO_2) nanocrystalline film using successive ionic layer adsorption and reaction (SILAR) for perovskite solar cell and gas sensor applications. TiO_2 nanocrystalline electron transfer layer (ETL) improves the power conversion efficiency (PCE) of perovskite solar cells due to faster charge transport kinetics as well as slower charge recombination process. As-prepared anatase TiO_2 nanocrystalline film-based ammonia sensor demonstrated good repeatability, high selectivity, stability, and fast transition times, signifying its potentiality as room-temperature V_{OC}'s based gas sensor. Furthermore, the use of this novel process may in future find great potential in large-scale fabrication of perovskite solar cell and gas sensor models in practical applications.

Iqbal *et al* (2018) [20] studied that solar cells based on inorganic semiconductors were fabricated at various thermal-annealing temperatures using vapor deposition techniques. The active layer primarily consists of a bilayer comprising a hole transporting copper oxide-CuO and an electron transporting zinc oxide-ZnO nano particles. increasing temperature from 400 to 500 °C, respectively. The improved device performance at higher temperature is attributed to better crystal and interface quality. Both the CuO and ZnO can be used in the polymer-active layer to increase the absorption as well as collection of electrons. In this way, high-efficient quaternary blend hybrid organic solar cells can be achieved with good stability.

Zhou *et al* (2007) [21] studied that Aluminum doped zinc oxide (AZO) polycrystalline thin films were prepared by sol–gel dip-coating process on optical glass substrates. Zinc acetate solutions of 0.5 M in isopropanol stabilized by diethanolamine and doped with a concentrated solution of aluminum nitrate in ethanol were used. The content of aluminum in the sol was varied from 1 to 3 at %. Crystalline ZnO thin films were obtained following an annealing process at temperatures between 300°C and 500°C for 1 h. The electrical resistivity of the 780 nm thick 1 at % Al-doped ZnO film annealed at 500 °C reached 3.2×10^{-2} Ω cm, while a transmittance over 90% in the visible range was achieved.

Amjad *et al* (2022) [22] studied ZnO films co-doped with Mn and La were synthesized by the sol–gel technique. XRD analysis revealed that ZnO had a hexagonal structure. Mixed hexagonal and cubic phases appeared in ZnO containing Mn (1%) and La (1.5%). The grain size, d-spacing, unit cell, lattice parameters, atomic packing fraction, volume, strain, crystallinity, and bond length of co-doped ZnO films were determined as a function of doped ion contents. The maximum ‘n’ was obtained for ZnO film co-doped with 1% Mn and 1% La. Therefore, this film has maximum light scattering and is suitable for application in solar cells. The DSSC fabricated with ZnO film co-doped with 1% Mn and 1% La had 1.89% efficiency. This efficiency is 174% higher than that of the pristine ZnO-based DSSC.

Li *et al* (2016) [23] studied that resistance random access memory consisting of ZnO/TiO_2/Cu structure is demonstrated on a flexible and transparent PET/ITO substrate. To improve cell to cell uniformity, amorphous TiO_2 fabricated by atomic layer deposition is used for resistive switching material with ZnO film as a blocking layer. XPS survey scan showed chemical composition of the films and XPS depth profile of Ti 2p and O 1s analyses showed a homogeneous distribution of oxygen vacancies inside the TiO_2 film. BRS characteristic with good uniformity and long retention time was confirmed without using any electrical forming process. The device can be repeated for 30 cycles. The conduction mechanism of the PET/ITO/ZnO/TiO_2/Cu flexible device was thoroughly investigated and analyzed based on the filamentary theory.

R**ani *et al*** (2015) [24] studied that Titanium dioxide (TiO_2), Zinc oxide (ZnO) and bilayer TiO_2/ZnO (TZO) based cells have been developed and sensitized with five organic dyes and one cocktail dye composed of five dyes. Photovoltaic performance of TiO_2 and ZnO solar cell sensitized with six dyes is compared to that of bilayer TZO cells. TZO films have a higher efficiency with the five organic dyes than ZnO and TiO_2 solar cells, which is due to improved values of Voc and

Jsc. This may be due to the formation of energy barriers at the ZnO electrode/ electrolyte interface because of the presence of the TiO2 layer. This reduces the back electron transfer from CB of ZnO to I_3 in the electrolyte, thus reducing the recombination rate and improving the cell performance. Also, TZO film has high crystallinity, broad UV absorption and higher photosensitivity as compared to ZnO film. ZnO forms a compact layer between FTO/TiO_2 which benefits the fast electron transfer from TiO_2 to ZnO to FTO glass and reduces the charge recombination occurring at the ZnO/FTO interface. The lowest efficiency of TiO_2 based cells was with Xanthene dye which gives the best results with ZnO and photocatalytic degradation of dye by TiO_2.

Gareso *et al* (2018) [25] suited that Structural and optical properties of ZnO/TiO_2 bilayers thin films. ZnO thin films were prepared by dissolving zinc acetate dehydrated into a solvent of ethanol and then added tri ethanolamin. In the case of TiO_2 layers, tetra isoproxide was dissolved into ethanol and then added an acetate acid. The layer of ZnO was deposited first followed by TiO_2 layer on a glass substrate using a spin coating technique. The ZnO/TiO_2 bilayers were annealed at various temperatures from 300°C until 600°C for 60 minutes. The ZnO/TiO_2 thin films were coated on the glass substrate using sol-gel method. Based on the X-ray diffraction measurements, the grain size of the ZnO/TiO_2 decreases as annealing temperature increased, but it decreases after high annealing temperatures. The transmittance value of ZnO/TiO_2 increases with increasing the temperature that indicates that the improvement of the crystalline of the films.

Alam *et al* (2022) [26] Al- and Cu-doped ZnO nanostructured films in this study were deposited using a sputtering technique. Undoped ZnO, aluminum- and copper-doped ZnO thin films on FTO substrate via a facile room-temperature RF sputtering technique. The films revealed an average transmittance of ~80% in the visible region with low resistivity (2.9×10^{-4} Ω cm for Al–ZnO and 1.7×10^{-4} Ω cm for Cu–ZnO) and high carrier mobility (16.1 $cm^2\ V^{-1}\ s^{-1}$ for Al–ZnO and 13.2 $cm^2\ V^{-1}\ s^{-1}$ for Cu–ZnO). The low resistivity and high transmittance render these films suitable for application in transparent conductive electrodes of solar cells. Finally, the applicability of the prepared films was tested in solar cells. The Al-doped ZnO-based solar cells offered an efficiency of 0.492%, whereas the Cu-doped-ZnO-based solar cells exhibited the best performance with photocurrent of 4.985 mA cm−2 along with a power conversion efficiency of 0.56%, which were comparable vis-à-vis the values reported for solar cells. From these results, it can be clearly seen that the Cu–ZnO film shows the highest efficiency followed by the Al–ZnO thin film

Dehghanab *et al* (2019) [27] studied that $CH_3NH_3PbI_3$ planar-structure perovskite solar cells were fabricated with the configuration FTO/ZnO/ $CH_3NH_3PbI_3$/Au. ZnO nanoparticles were synthesized by the precipitation method. Three different deposition methods including spin-coating, spraying and successive ionic layer adsorption and reaction (SILAR) were applied to fabricate the ZnO films as electron transport layers. The best cell performance was achieved for the perovskite solar cell with a ZnO film coated by the spin method. The average efficiency was 7% without using any hole transport materials and 10.25% using spiro-OMeTAD as a hole transport material. The average efficiencies of the cells coated by the spraying and SILAR methods using spiro-OMeTAD, were found to be 8.64% and 7.7% respectively. This study demonstrates the versatility of the spray and SILAR coating methods and their potential for fabricating low-cost, large scale, flexible and mass-produced perovskite solar cells.

Liu *et al* (2019) [28] studied that to fabricate highly transparent conductive AZO thin films by using an aqueous solution process followed by an ultraviolet (UV) exposure technique at an annealing temperature as low as 200 °C, where the aluminum citrate complex was used as the Al doping source. Various of deposition parameters in the AZO thin films fabrication process were studied and optimized. the AZO thin films prepared from the Al citrate complex doping exhibited higher Al doping concentration and as a result, showing a better electrical property. The best AZO thin films demonstrated an optical transmittance higher than 85% in the visible spectra region and a lowest electrical resistivity of 4.8×10^{-3} Ω cm. The composition depth analysis showed that the simultaneous treatment of the AZO film by ultraviolet exposure and heat treatment could remove carbon species at a deeper thickness and as a result, improving the conductive stability of the AZO thin films. AZO thin films can be widely used in thin film solar cells and other low-temperature photoelectric device owing to their superior performance, low material costs and low-temperature processing.

Mbule *et al* (2018) [29] studied that transparent conductive aluminum-doped zinc oxide (AZO) thin films were deposited on a flat and nanostructured borosilicate glass substrates by using DC-magnetron sputtering. The aluminum doping concentration was kept at 3.3 wt% and the film thickness (100–400 nm) was varied. The thin films were then annealed at 250 °C for 1 h in nitrogen and/or argon atmosphere, respectively. AZO thin films were deposited on the flat and nanostructured borosilicate glass substrates and their photovoltaic properties were compared. The AZO thin films demonstrated different morphologies with surface roughness. The films were highly transparent in the visible range to the near-infra red region, with the optimum transparency showing from the film annealed at N_2 atmosphere. Power conversion efficiency recorded from AZO films deposited on flat substrate annealed at N_2 atmosphere was almost 8 times higher than that recorded from nanostructured substrate and was comparable to the power conversion efficiency recorded from ITO-based device.

Farhada *et al* (2019) [30] studied that cuprous oxide (Cu_2O) thin films have been grown on both soda lime glass (SLG) microscopy slides and Fluorine doped Tin Oxide (FTO) substrates by a modified SILAR method. The pH level of the cationic precursor, adjusted by adding acetic acid and sulfuric acid separately, as well as the concentration of anionic precursor (NaOH) were varied to elucidate their effect on the physical properties of the deposited films. The optical band gap of polycrystalline Cu_2O films estimated by the UV–VIS–NIR spectroscopy were found to be in the range of 2.05–2.15 eV for samples grown both on SLG and FTO substrate and consistent with the reported results in the literature. The electrical resistivities of the m-SILAR grown copper oxide thin films were found to be in the range of 180–380 **Ω**. cm which is much lower than those of the reported Cu_2O thin film grown by similar chemical methods.

Ma *et al* (2019) [31] studied that the low temperature processability and high charge carrier mobility, ZnO has been successfully employed in perovskite solar cells (PSCs) to act as the electron transport layer. Even so, because of the poor ZnO/perovskite interface chemical stability, achieving highly efficient and stable PSCs is still challenging the researchers. Therefore, the optimization of ZnO/perovskite interface by proper surface passivation has been developed for highly efficient PSCs. The optimized ZnO/TiOx annealing temperature was 250 C which exhibited the best device performance. The severe charge recombination of poor interface contact was efficiently suppressed and charge transfer was greatly enhanced by TiOx passivation, which was confirmed by TPV/TPC and TR-PL results. Finally, a highest PCE of 19.34% was achieved by using TiOx/ZnO ETL. Besides, the optimized devices showed good air stability.

Liu *et al* (2018) [32] studied that the properties of the perovskite solar cells (PSCs) are highly correlated with Fermi level, trap-state density and conductivity of inorganic electron transport layer. Metal elemental doping is an effective solution to largely improve the property of oxide semiconductor thin film. In this study, zinc dopant is successfully inserted into TiO_2 crystal lattice using low-temperature solution-processed route. We find that Zn-doped TiO_2 films possess less trap-state density and better conductivity, compared to undoped thin films, which contributes to the promotion of short circuit current. Zn-doped TiO_2 ETL originates from high electrical conductivity, low trap state density, and enhanced electron extraction. Consequently, Zn-doped TiO_2 -PSCs exhibit substantially enhanced performance compared with the undoped TiO_2 -based PSC in terms of the 27.5% improvement on PCE. More importantly, the Zn-doped TiO_2 fabricated by low-temperature solution-processable method bodes well as an useful ETL for economic flexible PSCs.

Lanjewar *et al* (2016) [33] studied about Pure and Ag doped ZnO photo electrode was successfully synthesized by sol gel spin coating and applied in Dye-sensitized solar cells (DSSCs). Ag dopant concentration is varied from 0 wt% - 17.13 wt% over weight of ZnO. Doping by Ag, the band gap is sharply reduced and resulting Ag:ZnO photoelectrode could absorb visible light range at the great extent. The largest reduction in band gap was achieved from 3.28 eV for pure ZnO film to 2.65 eV for Ag:ZnO with 10.3 wt% doping. Highest photo conversion efficiency (ɳ) and current density (mA/cm^2) obtained at optimum 10.3 Ag wt%. Moreover, fabricated DSSCs is very economical due to use of economical mercurochrome dye. Moreover, sol gel spin coating method is also economic synthesis method. Hence, Ag:ZnO DSSCs prepared in present work is economic and yet it gave 3.67 times enhanced I-V performance than pure ZnO DSSCs. This economical DSSC is hence, a potential candidate for solar cell applications.

Yinhua *et al* (2011) [34] studied that synthesis of ZnO architecture on a fluorine-doped SnO_2 (FTO) conducting glass pre-coated with nano porous TiO_2 film has been achieved by a one-step hydrothermal method at a temperature of 70 ıC. The effect of the reaction time on the morphology of the ZnO architecture has been investigated, and a possible growth mechanism for the formation of the ZnO architecture is discussed in detail. The growth time greatly affects the morphology of the obtained ZnO architecture. And a ZnO two-layer architecture only can be formed at a growth time of more than 1.5 h under the present experimental conditions. The dye-sensitized solar cells (DSSCs) are assembled with as-prepared composite film electrodes sensitized by N3 dye, LiI/I_2 electrolyte and a platinum flake counter electrode. ZnO nanorods grown on the bottom layer can provide efficient electron transportation channels to the nano porous TiO_2 film on the conducting substrate.

Rahman *et al* (2016) [35] studied about titanium dioxide (TiO_2) and zinc oxide (ZnO) bilayer film for pH sensing application will be presented. TiO_2/ZnO bilayer film with different speed of spin-coating process was deposited on Indium Tin Oxide (ITO), prepared by sol-gel method. This fabricated bilayer film was used as sensing membrane for Extended Gate Field- Effect Transistor (EGFET) for pH sensing application. TiO_2/ZnO bilayer film deposited at highest spin-speed exhibit highest sensitivity value which is 52.10 mV/pH. This result was supported with the thickness and AFM characterization. Increased of spin-speed has influence the sensitivity, thickness and AFM topology of the TiO_2/ZnO bilayer film. Highest spin-speed, which is 4000 rpm produce highest sensitivity with the lowest thickness, 24.63 nm and most uniform AFM topology.

Firdaus *et al* (2012) [36] studied that the preparation of ZnO and ZnO: TiO_2 thin films were conducted on glass prepared by sol-gel spray-spin coating technique. The performance and properties of nanostructured ZnO and ZnO: TiO_2 thin films at different thickness were investigated. the surface morphology ZnO thin films are porous and also formed aggregates of ZnO nanoparticles compare to composite ZnO: TiO_2 thin films are homogenous, well disperse particles and have high surface area. As increased the thickness, the size particle does not increase. The transmittance spectra revealed that all films had low average transmittance and transparency of film decreases with the increase of thickness and roughness. The optical band gap found to be increased with the increasing of the thin films thickness for ZnO thin films. The conductivity of ZnO found to be decreased as the thickness increase and conductivity for composite ZnO: TiO_2 thin films found to be higher than ZnO thin films.

Gareso *et al* (2022) [37] studied that the material properties of TiO_2, ZnO, and TiO_2/ZnO bilayer thin films fabricated by sol-gel spin coating technique after annealing. ZnO thin films were prepared by dissolving zinc acetate dehydrated into a solvent of ethanol and diethanolamine (DEA) was later added. Meanwhile, for TiO2 films, titanium tetra isopropoxide (TTIP) was dissolved into ethanol and an acetate acid was added. All film samples were annealed at different temperatures in the range of 400 – 600^{o}C for 60 minutes. The effective optical band gap energy of mixed TiO_2 and ZnO which was derived from Touch plot gave two regions at low and high energy. The optical band gap energy of the TiO_2 layer was higher than that of the mixed TiO_2 and ZnO layers. The refractive index (n), the extinction coefficient (k) and the dielectric constant showed similar behaviour in the single layer and mixed layer. Based on the optical characterization of TiO_2, ZnO and TiO_2/ZnO bilayer, these materials were suitable for application in optoelectronic devices.

CHAPTER-III

EXPERIMENTAL METHODS AND CHARACTERIZATION TECHNIQUE

3.1 INTRODUCTION:

Varies methods were used for the preparation of thin film. They can be classified into many types. The deposition process of a film can be divided into three basic phases:

- Preparation of the film forming particles (atoms, molecules, cluster)
- Transport of the particles from the source to the substrate
- Adsorption of the particles on the substrate and film growth

3.2 ZINC CHLORIDE:

Zinc chloride is the name of chemical compounds with the formula $ZnCl_2$ and its hydrates. Zinc chlorides, of which nine crystalline forms are known, are colorless or white, and are highly soluble in water [24]. This white salt is hygroscopic and even deliquescent. Samples should therefore be protected from sources of moisture, including the water vapor present in ambient air. Zinc chloride finds wide application in textile processing, metallurgical fluxes, and chemical synthesis.

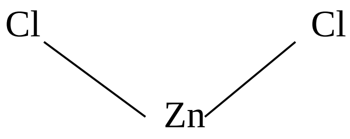

3.1 PROPERTIES OF ZINC CHLORIDE:

Chemical formula	$ZnCl_2$
Molar mass	136.315 g/mol
Appearance	white crystalline solid hygroscopic and very deliquescent.
Odor	Odorless
Density	2.907 g/cm3
Melting point	290 °C (554 °F; 563 K)
Boiling point	732 °C (1,350 °F; 1,005 K)
Solubility in water	432.0 g/ 100 g (25 °C)
Solubility	soluble in ethanol, glycerol and acetone.
Solubility in ethanol	430.0 g/100ml

3.2.1.1 PHYSICAL PROPERTIES:

Physical Properties of Zinc chloride Zinc chloride is solid at room temperature and has a white crystalline appearance. It is odorless. The solubility of this compound in water corresponds to 432g/100g. It is also soluble in acetone, ethanol, and glycerol. The four polymorphs of $ZnCl_2$ feature a tetrahedral 8 coordinate geometry between the Zn2+ ions and the Cl–Molten zinc chloride is highly viscous and has a relatively low electrical conductivity value.

3.2.1.2 CHEMICAL PROPERTIES:

Chemical Properties of Zinc chloride When $ZnCl_2$ is dissolved in water, the resulting solution is acidic in nature. The pH of an aqueous solution of zinc chloride with a concentration of 6M is 1. This compound reacts with ammonia to form complexes. Examples include $Zn(NH_3)_4Cl_2$ and $ZnCl_2(NH_3)_2$. When heated, the hydrated form of zinc chloride loses water and small quantities of ZnCl(OH) are obtained.

3.2.2 APPLICATION OF ZINC CHLORIDE:

Zinc chloride reacts with metal oxides (MO) to give derivatives of the idealized formula $MZnOC_2$. Addition citation(s) needed. This reaction is relevant to the utility of $ZnCl_2$ solution as a flux for soldering it dissolves passivating oxides, exposing the clean metal surface. Fluxes with $ZnCl_2$ as an active ingredient are sometimes called "tinner's fluid".

3.2.2.1 TEXTILE AND PAPER PROCESSING:

Concentrated aqueous solutions of zinc chloride (more than 64% weight/weight zinc chloride in water) have dissolving starch, silk, and cellulose. Relevant to its affinity for these materials, $ZnCl_2$ is used as a fireproofing agent and in fabric "refresheners" such as Febreze. Vulcanized fiber is made by soaking paper in concentrated zinc chloride

3.2.2.2 SMOKE GRENADES:

The zinc chloride smoke mixture ("HC") used in smoke grenades contains zinc Oxide, hexachloroethane and granular aluminum powder, which. When ignited, react to form chloride, carbon and aluminum oxide smoke, an effective smoke screen

3.2.2.3 DISINFECTANT AND WOOD PRESERVATIVE:

Dilute aqueous zinc chloride was used as a disinfectant under the name "Burnett's Disinfecting Fluid". From 1839 Sir William Burnett promoted its use as a disinfectant as well as a wood preservative. The Royal Navy conducted trials into its use as a disinfectant in the late 1840s, including during the cholera epidemic of 1849; and at the same time experiments were conducted into its preservative properties as applicable to the shipbuilding and railway industries. Burnett had some commercial success with his eponymous fluid. Following his death however, its use was largely superseded by that of carbolic acid and other proprietary products.

3.2.2.4 SKIN CANCER TREATMENT:

Zinc chloride has been used in alternative medicine to cause eschars, scabs of dead tissue, in an attempt to cure skin cancers. Various products, such as Cansema or "black salve", containing zinc chloride and sold as cancer cures have been listed by the (FDA) as fake with warning letters being sent to suppliers. Scarring and skin damage are also coated with escharotics substances.

3.3 TITANIUM ISOPROPOXIDE:

It is an alkoxide of titanium (IV) and appears as a liquid that is colorless to light yellow in form. Its odor is similar to Isopropyl Alcohol.

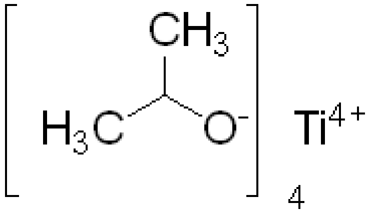

3.2 PROPERTIES OF TITANIUM ISOPROPOXIDE:

Melting Point	18 to 20 °C
Boiling Point	232 °C
Density	0.962 (g cm-3).
Molecular Weight	284.21532 [g/mol]
Exact Mass	284.146706
Flash Point	66°F
Topological Polar Surface Area	92.2
Covalently-Bonded Unit Count	5

3.3.2 APPLICATIONS OF TITANIUM ISOPROPOXIDE:

3.3.2.1 FIRE SAFETY PRECAUTIONS:

Spray water in large quantities. For spraying, alcohol foam, dry chemical, and carbon dioxide can also be used. All affected containers must be cooled with large quantity of water. Water should be sprayed from as large a distance as possible. It is also important not to allow sprayed water to settle in sewages and other water sources. Soak bulk liquid with cement powder, ash, or other commercial sorbents. Settled materials should be eliminated using suction hoses.

3.3.2.2 STORAGE DEVICE:

Dig a holding area (pond, lagoon etc.) to store this substance in liquid or solid form. Soil, sand bags, or foamed concrete may be used to control surface flow. For controlling water spill, natural barricades or spill control booms should be put in place. Other sources of ignition should be kept away from this substance. It should be stored away from water sources.

3.4 SPRAY PYROLYSIS:

Spray pyrolysis (SP) is a process in which a thin film is deposited by spraying a solution on a heated surface, where the constituents react to form a chemical compound. The chemical reactants are selected such that the products other than the desired compound are volatile at the temperature of deposition. This equipment for spray pyrolysis is composed of three zones:

(i) ultrasonic spray zone, which consists of the mist-generating system of a liquid source with an ultrasonic atomizer and the misted droplet-carrying system with air carrier gas;

(ii) (ii) heating zone in which the misted droplet is pyrolyzed in a preheated chamber; and

(iii) pumping zone, which consists of pumping evaporated/decomposed gases and trapping the produced powders. A simple schematic diagram of the ultrasonic spray pyrolysis method. This method is useful for obtaining ultrafine powders with small particle size (<1 μm), narrow size distribution (1–2 μm), high purity, high porosity, and large surface area.

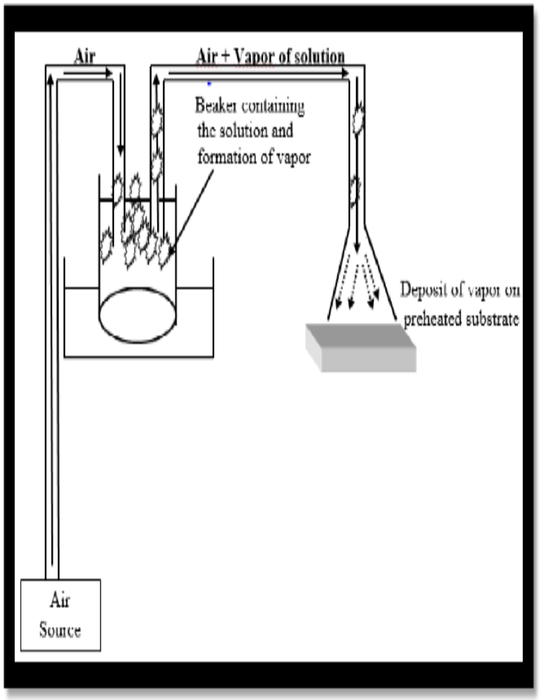

Fig 3.1 Spray pyrolysis method

Fig 3.2 Spray pyrolysis experimental setup

3.5 METHODS:

3.5.1 PREPARATION OF ZINC OXIDE NANOPARTICLE BY USING CO-PRECIPITATION METHOD:

10ml of banana stem extract is taken in a beaker with 100ml of distilled water. Then it is kept for constant stirring for 20 minutes using magnetic stirrer. Now 13.628 gram of zinc chloride is added into the beaker which is stirring. Then 50ml of ethanol is added to the beaker. The solution is kept at constant temperature of 60^{o}C along with constant stirring for minimum 5 hours. The next day the precipitate alone is kept as it is in the beaker and the remaining solution is washed. Now 100ml of distilled water and 50ml of ethanol is poured in to the beaker and kept at constant temperature of 60^{o}C along with constant stirring for 5 hours. The same procedure is repeated for 6 days. Then the synthesized material was kept at

120°C for 6 hours in a hot air oven, then the dried ZnO were crushed and it was kept at 650°C for 6 hours in the muffle furnace. Now the final product (ZnO) is obtained.

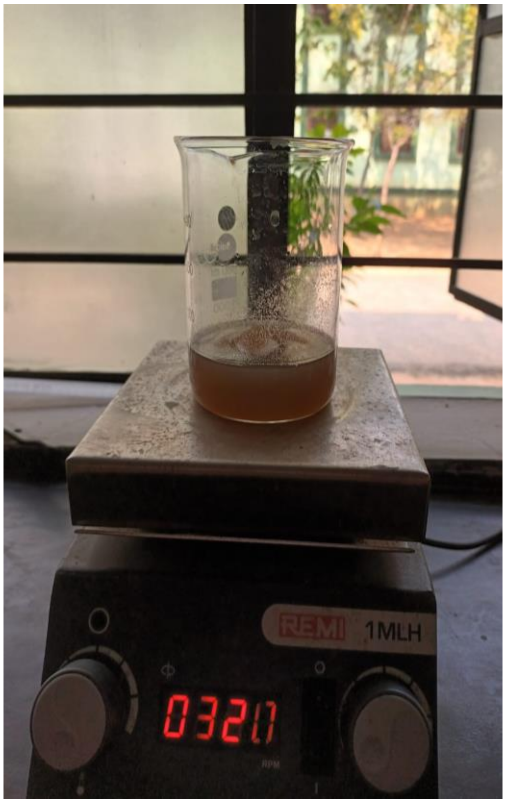

Fig.3.3 ZnO solution with banana extract

Fig.3.4 ZnO nanoparticle

3.5.2 PREPARATION OF TITANIUM DIOXIDE NANOPARTICLE BY USING CO-PRECIPITATION METHOD:

10ml of orange extract is taken in a beaker with 100ml of distilled water. Then it is kept for constant stirring for 20 minutes using magnetic stirrer. Now 15ml of titanium tetra isopropyl is added drop by drop into the beaker which is stirring. Then 50ml of ethanol is added to the beaker. The solution is kept at constant temperature of 60°C along with constant stirring for minimum 5 hours. The next day the precipitate alone is kept as it is in the beaker and the remaining solution is washed. Now 100ml of distilled water and 50ml of ethanol is poured in to the beaker and kept at constant temperature of 60^o C along with constant stirring for 5 hours. The same procedure is repeated for 6 days. Then the synthesized material was kept at 120^o C for 6 hours in a hot air oven, then the dried TiO_2 were crushed and it was kept at 700^{o}C for 6 hours in the muffle furnace. Now the final product (TiO2) is obtained.

Fig.3.5 Tio_2 solution of orange extract **Fig.3.6 Tio_2 particle in hot air oven**

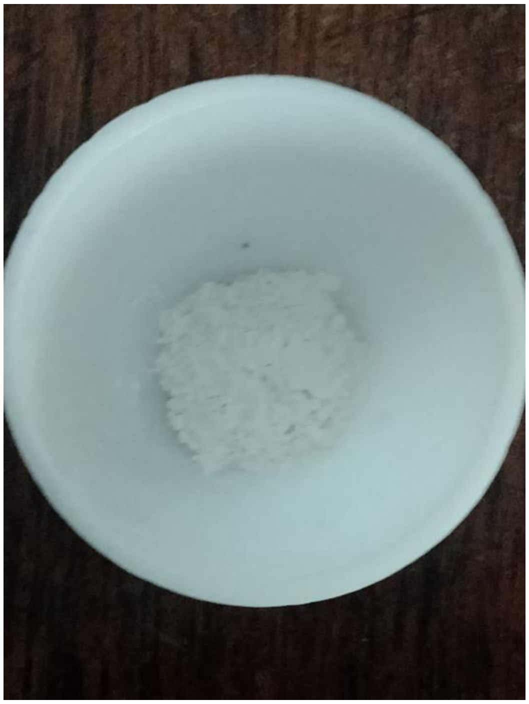

Fig.3.7 Tio_2 after the muffle furnace

3.6 SPRAY PYROLYSIS METHOD:

3.6.1 PREPARATION OF ZnO THINFILM:

By using spray pyrolysis method ZnO thin films have been deposited on the glass substrates. To prepare ZnO solution, the ZnO nano powder was added with 10 ml water and two drops of Hcl. The mixture was stirred for five minutes. ZnO solution was obtained. These solutions were used to prepare ZnO thin film. 2cm × 2cm glass substrates were used. Before using the substrates were washed with chromic acid and acetone. By using spray pyrolysis method ZnO thin film were deposited. Substrate was kept on the furnace, then the solutions was sprayed on the substrate

3.6.2 PREPARATION OF TiO_2THINFILM:

By using spray pyrolysis method TiO_2 thin films have been deposited on the glass substrates. To prepare TiO_2 solution, the TiO_2 nano powder was added with 2ml of acetile austinite, 2ml of water and 8 ml of Isopropyl alcohol are added. The mixture was stirred for five minutes. TiO_2 solution was obtained. These solutions were used to prepare TiO_2 thin film. 2cm × 2cm glass substrates were used. Before using the substrates were washed with chromic acid and acetone. By using spray pyrolysis method TiO_2 thin film were deposited. Substrate was kept on the furnace, then the solutions was sprayed on the substrate and annealed at 450°c in the furnace. The pressure given to the set up is1.5 $kgm^{-1}s^{-2}$.

3.6.3 PREPARATION OF ZnO/TiO_2 THINFILM:

By using spray pyrolysis method ZnO/TiO_2 thin films have been deposited on the glass substrates. To prepare ZnO solution, the ZnO nano powder was added with 10 ml water and two drops of HCl. The mixture was stirred for five minutes. ZnO solution was obtained. And to prepare a TiO_2, the TiO_2 nano powder was added to 2ml of acetyl austenite, 2ml of water and 8ml of isopropyl alcohol were added. Then the mixture was stirred for five minutes. TiO_2 solution was obtained. These solutions were used to prepare ZnO/TiO_2 thin film. 2cm × 2cm glass substrates were used. Before using the substrates were washed with chromic acid and acetone. By using spray pyrolysis method ZnO/TiO_2 thin film were deposited. Substrate was kept on the furnace, first the ZnO solution was coated on the substrate, then after two hours TiO_2 solution is coated on the ZnO, the substrate is annealed at 450°C in the furnace. The pressure given to the setup is $kgm^{-1}s^{-2}$.

CHAPTER IV

RESULTS AND DISCUSSION

4.1 INTRODUCTION:

This present study analyses the structural and electrical properties of green synthesized Tio_2 and ZnO compact layer for the application of perovskite solar cells. The properties of nano structures and thin films lead to the drastic potential applications. In this present work, ZnO and TiO_2 nanoparticles are prepared using banana stem extract and orange extract respectively. The as prepared ZnO and TiO_2 nanoparticles are coated in a glass substrate to get a thin film of ZnO/Tio_2 compact layer for the application of Perovskite solar cells.

4.2 X-RAY DIFFRACTION (XRD)

X-ray diffraction (XRD) is a powerful technique for determination of crystal structure and lattice parameters. The basic principles of X-ray diffraction are found in textbooks e.g., by Buerger, Klug and Alexander, Cullity, Tayler, Guinier, Barrett and Massalski. Figure 4.1 shows the schematics of X-ray diffractometer. Diffraction in general occurs only when the wavelength of the wave motion is of the same order of magnitude as the repeat distance between scattering centers. This condition of diffraction is nothing but Bragg's law and is given as,

$$\mathbf{2d \sin \Theta = n\lambda}$$

Where,

d = interplaner spacing

Θ = diffraction angle

λ= wavelength of x-ray

n = order of diffraction

For thin films, the powder technique in conjunction with diffractometer is most commonly used. In this technique the diffracted radiation is detected by the counter 86 tube, which moves along the angular range of reflections.

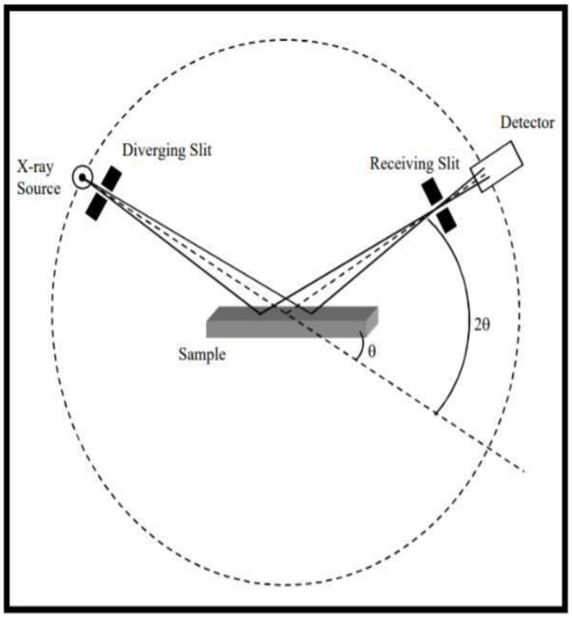

Fig 4.1 Schematic of X-ray diffractometer

The intensities are recorded on a computer system. The X- ray diffraction data thus obtained is printed in tabular form on paper and is compared with Joint Committee Power Diffraction Standards (JCPDS) data to identify the unknown material. The sample used may be powder, single crystal or thin film. The crystallite size of the deposits is estimated from the full width at half maximum (FWHM) of the most intense diffraction line by Scherrer's formula as follows

$$D = k\lambda / \beta \cos \Theta$$

Where, D is crystallite size, k is constant, λ is wavelength of X-ray used, ß is full width at half maxima of the peak (FWHM) in radians, Θ is Bragg's angle.

4.2.1 CHARACTERIZATION OF ZnO NANO PARTICLE USING XRD:

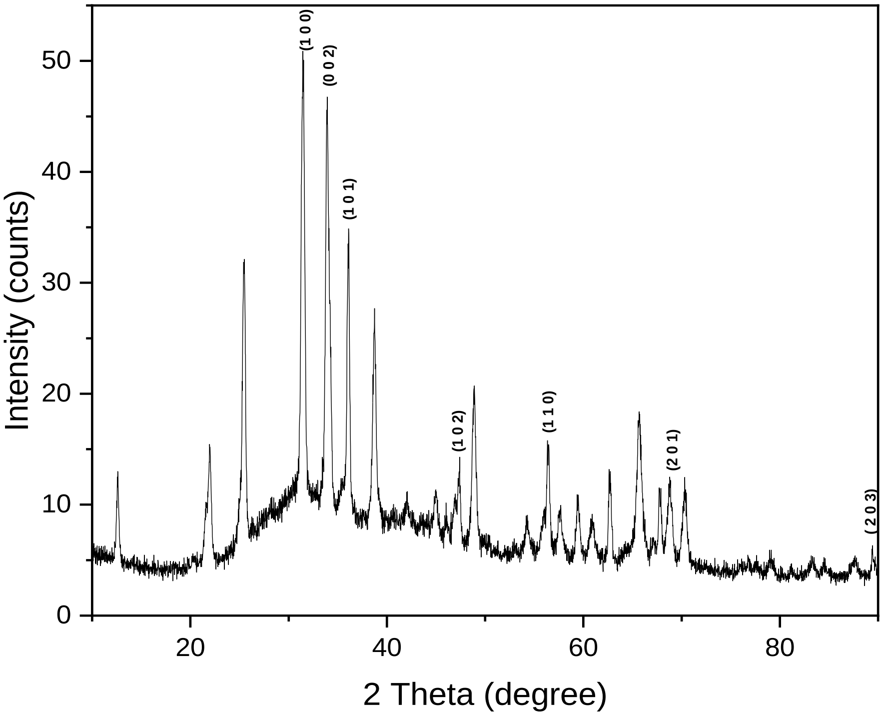

Fig. 4.2 XRD pattern of the synthesized ZnO

From Fig.4.2, it is observed that, the strong peaks were detected at 2θ values are 31.7°,36.07°,47.35°,56.4°,62.6°and 67.7° corresponding to the following lattice (hkl) planes:(100), (101), (102), (110), (103) and (112) respectively. It is also confirmed with the JCPDS 36-1451 which exhibits wurtzite. The peaks of the synthesized ZnO are in well agreement with that of the reference JCPDS file. There are no impurity peaks detected in the XRD which reveals that the as prepared ZnO nanoparticles exhibit high crystalline nature. The size of the particle is calculated using Debye Scherrer formula which is 22nm.

Table 4.1 Comparison of observed d spacing with standard JCPDS d spacing for ZnO nanoparticles.

S.No	2θ (Degree)	Observed d Spacing	Standard JCPDS d Spacing	hkl
1	31.46°	2.8414	2.817	100
2	36.07°	2.4878	2.4768	101
3	47.35°	1.9182	1.91183	102
4	56.42°	1.6295	1.62662	110
5	62.69°	1.4807	1.4779	103
6	67.78°	1.38134	1.3790	112

4.2.2 CHARACTERIZATION OF TiO_2 NANO PARTICLE USING XRD:

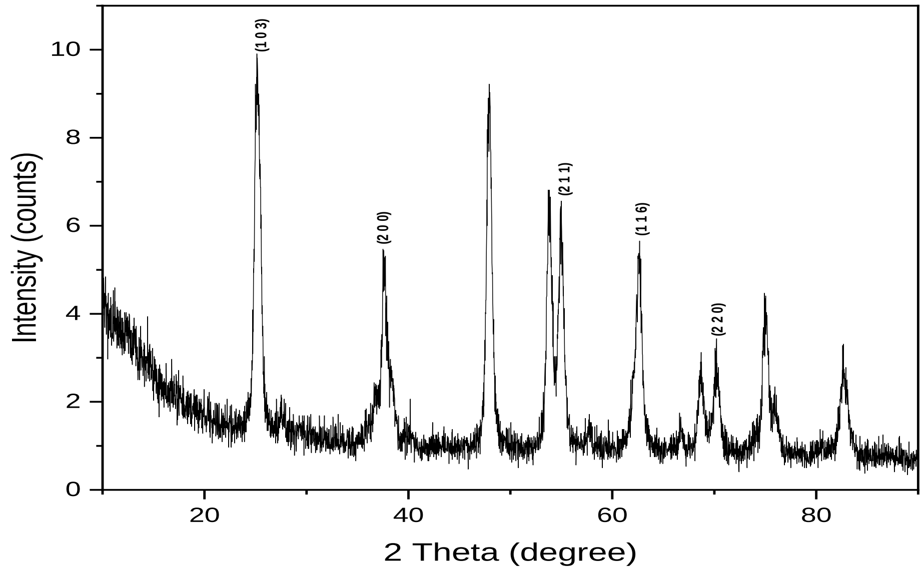

Fig. 4.3 XRD pattern of the synthesized TiO2

Table 4.2 Comparison of observed d spacing with standard JCPDS d spacing for TiO_2 Nano particle

S.No	2θ (degree)	Observed d Spacing	Standard JCPDS d spacing	hkl
1	25.28°	3.51921	3.52	103
2	37.62°	2.3886	2.38	200
3	53.82°	1.7018	1.892	211
4	62.61°	1.4823	1.364	116

From Fig.4.3, it is observed that, the strong peaks were detected at 2θ values are 25.28°,37.62°,53.82° and 62.61°and corresponding to the following lattice (h k l) planes:(103), (200), (211) and (116) respectively. It is also confirmed with the JCPDS 84-1285 which exhibits wurtzite. The peaks of the synthesized TiO_2 are in well agreement with that of the reference JCPDS file. There are no impurity peaks detected in the XRD which reveals that the as prepared TiO_2 nanoparticles exhibit high crystalline nature. The size of the particle is calculated using Debye Scherrer formula which is 14nm.

4.2.3 CHARACTERIZATION OF ZnO THIN FILM USING XRD:

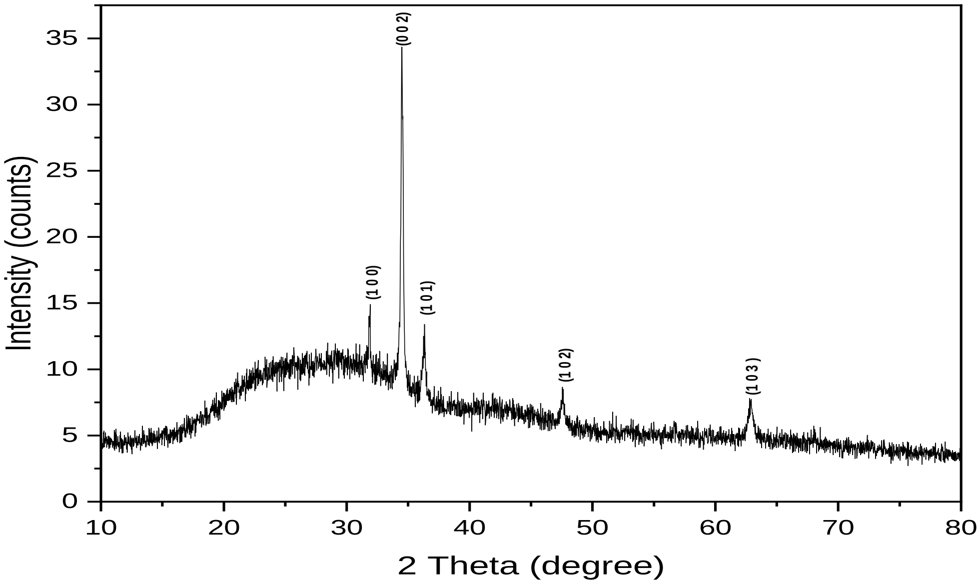

Fig. 4.4 XRD pattern of the Thin film ZnO

Table 4.3 Comparison of observed d spacing with standard JCPDS d spacing for ZnO Thin film

S. No	2θ (degree)	Observed d Spacing	Standard JCPDS d Spacing	hkl
1	31.84°	2.808	2.817	100
2	34.42°	2.597	2.64	002
3	36.3°	2.472	2.476	101
4	47.55°	1.910	1.911	102
5	62.8°	1.476	1.477	103

From Fig.4.4, it is observed that, the strong peaks were detected at 2θ values are 31.84°,34.42°,36.3°, 47.55° and 62.8°and corresponding to the following lattice (hkl) planes:(100), (002), (101) (102) and (103) respectively. It is also confirmed with the JCPDS 36-1451 which exhibits wurtzite. The peaks of the synthesized ZnO are in well agreement with that of the reference JCPDS file. There are no impurity peaks detected in the XRD which reveals that the as prepared ZnO thin film exhibit high crystalline nature. The size of the thin film is calculated using Debye Scherrer formula which is 52nm.

4.2.4 CHARACTERIZATION OF TiO_2 THIN FILM USING XRD:

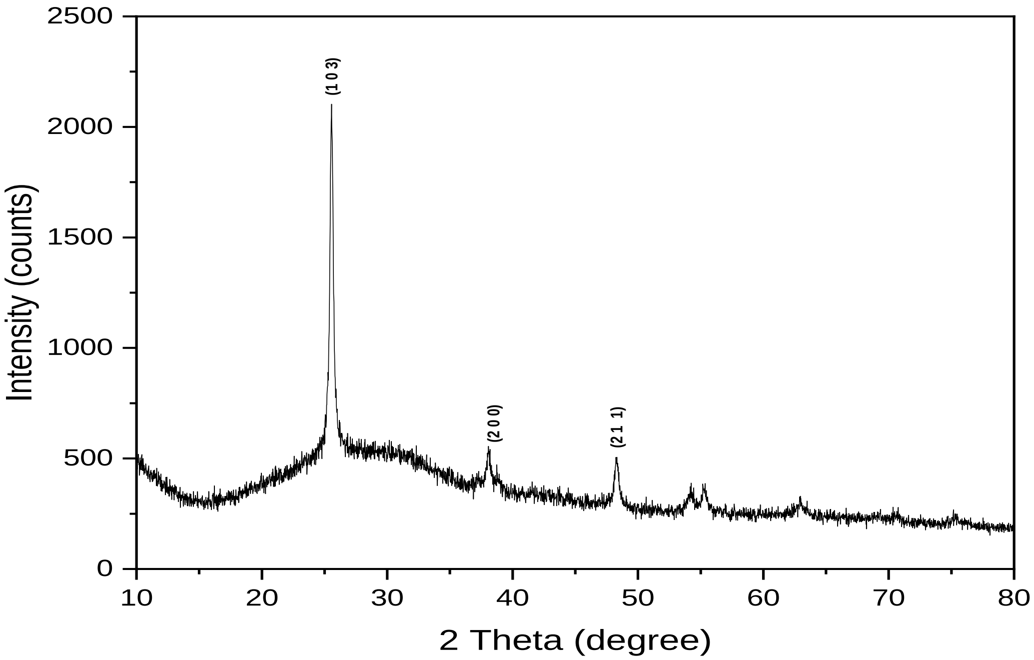

Fig. 4.5 XRD pattern of the thin film TiO2

Table 4.4 Comparison of observed d spacing with standard JCPDS d spacing for TiO_2 Thin film

S.No	2θ (degree)	Observed d value	Standard d value	hkl
1	25.56°	3.482	3.52	103
2	48.32°	1.882	1.892	200
3	55.24°	1.6651	1.665	211

From Fig.4.5, it is observed that, the strong peaks were detected at 2θ values are 25.56°,48.32°and 55.24°and corresponding to the following lattice (hkl) planes:(103), (200) and (211) respectively. It is also confirmed with the JCPDS 21-1272 which exhibits wurtzite. The peaks of the synthesized TiO_2 are in well agreement with that of the reference JCPDS file. There are no impurity peaks detected in the XRD which reveals that the as prepared TiO_2 thin film exhibit high crystalline nature. The size of the thin film is calculated using Debye Scherrer formula which is 33nm.

4.2.5 CHARACTERIZATION OF ZnO/TiO_2 THIN FILMS USING XRD:

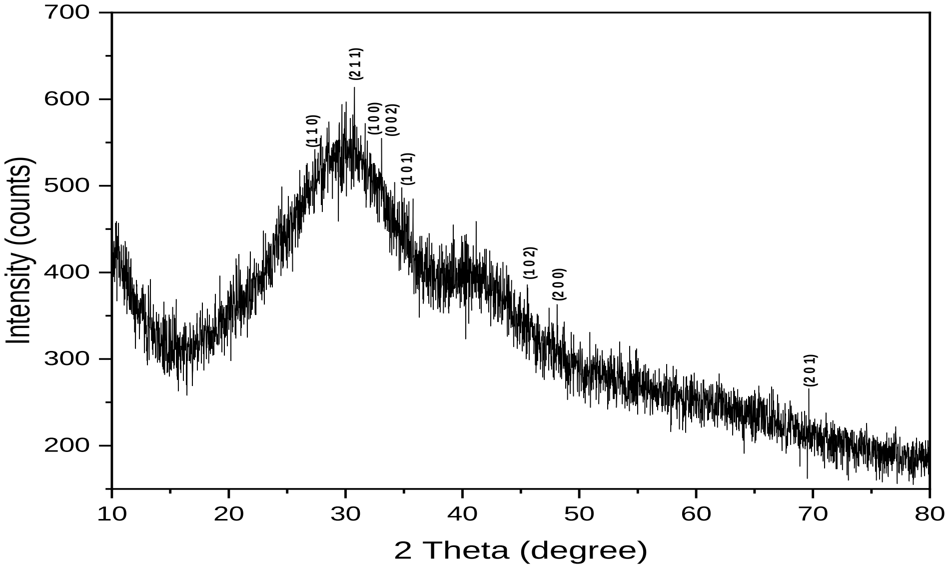

Fig. 4.6 XRD pattern of the thin film ZnO/TiO_2

Table 4.5 Comparison of observed d spacing with standard JCPDS d spacing of Tio_2 / ZnO Thin film

S. No	Observed d Spacing	Standed JCPDS d Spacing	ZnO/TiO_2	hkl
1.	2.897	2.904	TiO_2	211
2.	2.8233	2.817	ZnO	100
3.	2.5743	2.6047	ZnO	002
4.	2.487	2.544	TiO_2	101
5.	1.9881	1.911	ZnO	102
6.	1.3489	1.37	Zno	201

XRD pattern of ZnO/TiO_2 composite thin films are prepared using spray pyrolysis method. XRD graph of ZnO/TiO_2 annealed at temperature 450^0C show peaks which are corresponding to ZnO and TiO_2 in accordance with the JCPDS card.No.36-1451 and 21-1276. The high intense peaks are obtained at $2\theta = 31.66^o$, 34.8^o, 45.59^o, 69.6^o which are corresponding to the hexogonal structure of ZnO. The other three peaks are obtained at $2\theta=27.3^o$, 35.24^o, 30.75^o which are corresponding to anatase phase of TiO_2. There are no other phases of TiO_2 are present in the XRD pattern.

CHAPTER V

SUMMARY AND CONCLUSION

In this present investigation, ZnO nanoparticles are prepared using banana stem extract. TiO_2 nanoparticles are synthesized using orange fruit extract. The as prepared ZnO and TiO_2 nanoparticles are in nano range which is confirmed with the standard values. The size of the ZnO and TiO_2 are found using Debye Scherrer formula. The crystallite size of the ZnO and TiO_2 are 22nm and 14nm respectively. The thin film of ZnO/TiO_2 composite layer is coated by spray pyrolysis method. From the XRD pattern of ZnO/TiO_2 thin films, it is well noted that the peaks are in good agreement with the standard values.

REFERENCES

[1] Glocker & Shah I, 2002, "Handbook of Thin Film Process Technology", Institute of Physics vol.1,2.

[2] West R, 2003, John Willy & Sons, Singapore.

[3] Sadekar HK, Ghule AV & Sharma R, 2013, “Nanocrystalline ZnO thin films prepared by solution growth technique for photo sensor application”, Composite Part B, vol. 44, pp. 553–557.

[4] Meng Y, Huang K, Tang Z, Xu X, Tan Z, Liu Q, Wang C, Wu B, Wang C & Cao C, 2018, “The effect of Argon pressure dependent V thin film on the phase transition process of (020) VO_2 thin film”, Applied Surface Science, vol. 427, pp. 304-311.

[5] Akhtar MS, Malik MA, Riaz S, Naseem S & O'Brien P, 2015, “Optimising conditions for the growth of nanocrystalline ZnS thin films from acidic chemical baths”, Material Science in Semiconductor Processing, vol. 30, pp. 292–297.

[6] Chander S & Dhaka MS, 2015, “Physical properties of vacuum evaporated CdTe thin films with post-deposition thermal annealing”, Journal of Physica E, vol. 73, pp. 35-39.

[7] Xu J, Wang W, Zhang X, Chang X, Shi Z & Haarberg GM, 2015, “Electro deposition of ZnSe thin film and its photo catalytic properties”, Journal of Alloys Compounds, vol. 632, pp.778– 782.

[8] Mlowe S, Nyamen LD & Ndifon PT, 2015, “Aerosol assisted chemical vapor deposition (AACVD) of CdS thin films from heterocyclic cadmium (II) complexes”, Inorganica Chimica Acta, vol. 434, pp.181–187.

[9] Wu XJ, Zhang ZZ & Zhang JY, 2008 “Growth of FeSe on general substrates by metal-organic chemical vapor deposition and the application in magnet tunnel junction devices”, Thin Solid Film, vol. 516, pp. 6116–6119.

[10] Tseng YH, Yang CS, Wu CH, 2013, “Growth mechanism of CuZnInSe2 thin films grown by molecular beam epitaxy”, Journal of Crystal Growth, vol. 378, pp. 158–161.

[11] Khan TM, Zakria M, Ahmad M & Shakoor RI, 2014, “Optoelectronic study and annealing stability of room temperature pulsed laser ablated ZnO polycrystalline thin films”, Journal of Luminescence, vol. 147, pp. 97–106.

[12] Wei A, Zhao X, Liu J & Zhao Y, 2013, “Investigation on the structure and optical properties of chemically deposited ZnSe nanocrystalline thin films“, Physica B, vol. 410, pp. 120–125.

[13] Liu C, Wu W, Zhang D, Li Z, Ren G, Hana W & Guo W, 2021, “Effffective stability enhancement in ZnO-based perovskite solar cells by MACl modifification”, Journal of Materials Chemistry A, vol. 9, pp. 12161-12168.

[14] Jaimes A, Quintero O, Gamboa R, Flores A & Rincon M, 2021, “Functional ZnO/TiO2 Bilayer as Electron Transport Material for Solution-Processed Sb2S3 Solar Cells”, RRL Solar, vol. 5, no. 3, pp. 200764.

[15] Shalan A, Mourtada A, Rasly M, Moharam M, Cantu M & Rashad M, 2015, “Concordantly Fabricated Heterojunction ZnO-TiO2 Nanocomposites Electrodes via Co-precipitation Method for Efficient Stable Quasi-Solid-State Dye-Sensitized Solar Cells”, RSC advances, vol. 5, pp. 103095-103104.

[16] Shaikh S, Ghule B, Nakate U, Shinde, Satish P, Ekar U, Dwyer C, Kim K & Mane R, 2018, “Low-Temperature Ionic Layer Adsorption and Reaction Grown Anatase TiO2 Nanocrystalline Films for Efficient Perovskite Solar Cell and Gas Sensor Applications”, Scientific reports, vol. 8, pp. 11016.

[17] Iqbal K, Ikram M,· Afzal M &· Ali S, 2018, “Efficient, low-dimensional nanocomposite bilayer CuO/ZnO solar cell at various annealing temperatures”, Materials for renewable and sustainable energy, vol. 7, pp. 4 .

[18] Dundar I, Krichevskaya M, Katerski A & Acik I, 2018, “TiO2 thin films by ultrasonic spray pyrolysis as photocatalytic material for air purification”, Royal society open science, vol. 6, pp. 181578.

[19] Zhou H, Yi D, Yu Z, Xiao L, Li J, 2007, “Preparation of aluminum doped zinc oxide films and the study of their micro structure, electrical and optical properties”, Thin solid films, vol. 515. pp. 6909-6914.

[20] Zhang Q, Hou S & Li C, 2020, “Titanium Dioxide-Coated Zinc Oxide Nanorods as an Efficient Photoelectrode in Dye-Sensitized Solar Cells”, Nanomaterials, vol. 10, pp. 1598.

[21] Li H, Dong W, Wu W, Xi J & Ji Z, 2016, “Resistive switching characteristics of ZnO/a-TiO2 bilayer film fabricated on PET/ITO transparent and flexible Substrates”, Materials Research Bulletin, vol. 84, pp. 449–454.

[22] Rani M & Tripathi SK, 2015, “A Comparative Study of Nanostructured TiO_2, ZnO and Bilayer TiO2/ZnO Dye-Sensitized Solar Cells”, Journal of electronic materials, vol. 44, pp. 1151-1159.

[23] Gareso PL, Musfitasari & Juarlin E, 2018, “Optical and Structural Characterization of ZnO/TiO2 Bilayer Thin Films Grown by Sol-Gel Spin Coating”, Journal of Physics Conference series, vol. 979, pp. 012060.

[24] Alam M, Ansari M, Aamir M, Rehman M, Parveen N & Ansari S, 2022, “Preparation and Characterization of Cu and Al Doped ZnO Thin Films for Solar Cell Applications” Crystals, vol. 12, no.2, pp. 128.

[25] Dehghanab M & Behjat A, 2019, “Deposition of zinc oxide as an electron transport layer in planar perovskite solar cells by spray and SILAR methods comparable with spin coating”, RSC advances, vol. 9, pp. 20917-20924.

[26] Liu R, Chenc Y, Ding S, Li Y & Tian Y, 2019, “Preparation of highly transparent conductive aluminum-doped zinc oxide thin films using a low-temperature aqueous solution process for thin-film solar cells applications”, Solar energy materials and solar cells, vol. 203, pp. 110161.

[27] Mbule P, Wang D, Grieseler R, Schaaf P, Muhsin B, Hoppe H, Mothudi B & Dhlamini M, (2018) “Aluminum-doped ZnO thin films deposited on flat and nanostructured glass substrates: Quality and performance for applications in organic solar cells”, Solar energy, vol. 172, no. 2 pp. 219-224.

[28] Farhad S, Hossain M, Tanvir M, Akter R, Patwary M, Shahjahan M & Rahman M, 2019, “Structural, optical, electrical, and photoelectrochemical properties of cuprous oxide thin films grown by modified SILAR method”, Material Science in Semiconductor Processing, vol. 95, pp. 68-75.

[30] Ma J, Lin Z, Guo X, He J, Hu Z, Su J, Zhang J, Chan J & Hao Y, 2019, “Low temperature ZnO/TiOx electron-transport layer processed from aqueous solution

for highly efficient and stable planar perovskite solar Cells”, Materials Today Energy, vol. 14, pp. 100351.

[31] Lanjewar M & Gohel V, 2016, “Enhanced performance of Ag doped ZnO and pure ZnO thin films DSSCs prepared by sol gel spin coating”, Inorganic and Nano-metal Chemistry, vol. 47, no. 7, pp 1090-1096.

[32] Yinhua J, Xiaoli W, Wenl Z, Liang N & Yueming C, (2011) “Evolution of ZnO architecture on a nanoporous TiO2 film by a hydrothermal method and the photoelectrochemical performance”, Journal of Semiconductors, vol. 32, No. 3, pp 033005.

[33] Nadarajah K, Chee C & Tan C, 2013, “Influence of Annealing on Properties of Spray Deposited ZnO Thin Films”, Journal of Nanomaterials, vol. 2013, pp 146382.

[34] Khaleel R, Hashim M & Majeed S, 2022 “Synthesis of ZnO thin film by chemical spray pyrolysis using its nano powder”, Kuwait Journal of Science, vol.49, no.1, pp 1-11.

[35] Rahman R, Zulkefle M, Abdullah W, Rusop M & Herman S, 2015, “Characteristics of TiO2/ZnO Bilayer Film Towards pH Sensitivity Prepared by Different Spin Coating Deposition Process”, AIP Conference Proceedings, vol. 1733, pp 020059.

[36] Firdaus CM, Rizam MSB, Rusop M & Hidayah S,2012, “Characterization of ZnO and ZnO: TiO2 Thin Films Prepared by Sol-Gel Spray-Spin Coating Technique”, Procedia Engineering, vol.41, pp 1367-1373.

SYNTHESIS AND CHARACTERIZATION OF GO NANOPARTICLES BY MODIFIED HUMMER'S METHOD

A project work report and submitted to
DEPARTEMENT OF PHYSICS
ST. MARY'S COLLEGE (AUTONOMOUS), THOOTHUKUDI
Affiliated to
MANONMANIAM SUNDARANAR UNIVERSITY,
THIRUNELVELI
In partial fulfilment of the requirements for the award of
MASTER OF SCIENCE IN PHYSICS
Submitted by
J. MAHALAKSHMI
Reg. No: 21SPPH03
Under the guidance of
Ms. S. IRUDAYA SAHAYA LANCY M.Sc., M.Phil.,

DEPARTMENT OF PHYSICS
ST. MARY'S COLLEGE (AUTONOMOUS),
THOOTHUKUDI.
Re-accredited with 'A+' Grade by NAAC
(2022-2023)

CERTIFICATE

This is to certify that this project work report entitled **"SYNTHESIS AND CHARACTERIZATION OF GO NANOPARTICLES BY MODIFIED HUMMER'S METHOD"** is submitted to **ST. MARY'S COLLEGE (AUTONOMOUS), THOOTHUKUDI** in partial fulfilment of requirements for the award of **MASTER OF SCIENCE IN PHYSICS** and is a record of work done during the academic year **2022 – 2023** by **J. MAHALAKSHMI** (Register No: 21SPPH03)

5/4/23

Signature of the Guide

Padmavathi

Signature of the Co-Ordinator

Signature of the Director

Director
Self Supporting Courses
St. Mary's College (Autonomous)
Thoothukudi - 628 001.

Lucia Rose

Signature of the principal

Principal
St. Mary's College (Autonomous)
Thoothukudi - 628 001.

12/4/23

Signature of the Examiner

DECLARATION

I hereby declare that the project work report entitled **"SYNTHESIS AND CHARACTERIZATION OF GO NANOPARTICLES BY MODIFIED HUMMER'S METHOD"** is submitted to **ST. MARY'S COLLEGE, (AUTONOMOUS), THOOTHUKUDI** affiliated to **MANONMANIAM SUNDARANAR UNIVERSITY, THIRUNELVELI** for the award of the degree of Master of Science in Physics is my original work and that no part of this project work report has been submitted for any Degree, Diploma or other similar titles.

J. Mahalakshmi

Station: Thoothukudi **Signature of the Student**

Date: 05.04.2023 **(J. MAHALAKSHMI)**

ACKNOWLEGEMENT

On the very outset of this report, I feel obliged to our Almighty for his aid in the completion of this project work successfully.

I wish to record our profound gratitude to our Principal Rev. **Dr. Sr. A.S.J. Lucia Rose, M.Sc., B.Ed., M.Phil., PGDCA., Ph.D.** for her motivation.

I sincerely thank our Director of **SSC, Rev. Sr. Josephine Jeyarani, M.A., M.Phil.,** for her encouragement and support.

I wish to thank **Rev. Dr. Sr. JESSIE FERNANDO M.Sc., M.Phil., Ph.D.,** HOD & Associate professor for her inspirational words to complete this project work.

I owe a great deal to Mrs. **P. PADMAVATHI M.Sc., M.Phil., SET.,** SSC Co-Ordinator for supporting me throughout this project work.

I express my sincere thanks to **Ms. S. IRUDAYA SAHAYA LANCY M.Sc., M.Phil.,** for her valuable time and guidance provided throughout the successful completion of my project.

I am deeply grateful to all the staff members of Department of Physics (SSC) for supporting me in all aspects.

I acknowledge my deep sense of gratitude to my loving parents and friends for being a constant source of motivation.

ABSTRACT

Pure Graphene oxide nanoparticles was prepared by modified hummer's method. The resulting product was characterized by X-Ray Diffraction (XRD), Ultra Violet Visible Spectroscopy (UV-VIS), Scanning Electron Microscopy (SEM) with EDAX. X-ray diffraction confirmed the prepared nanostructures as Graphene oxide. The size of the particle is found to be 7nm. The structure of the as prepared nanoparticle is hexagonal which is confirmed with JCPDS file no.25 -284.Optical properties of Graphene oxide was studied by using UV spectroscopy. SEM image show that the surface morphology of the Graphene oxide nanoparticles. EDAX spectrum shows that the presence Carbon and Oxygen.

CONTENT

LIST OF FIGURES

LIST OF TABLES

CHAPTER-I

CHAPTER I

INTRODUCTION

1.1 INTRODUCTION:

In recent years, nanoscale materials have become essential in our daily lives, as they are included in electronic and opto electronic devices, biological applications, cosmetics. These nanoscale materials have large surface-to-volume ratio when compared with bulk materials. Semiconductor nanocrystals can exhibit unique properties, such as high extinction coefficients, rapid charge separation, good chemical, thermal, environmental stability and ease of synthesis. When the size is reduced to nanoscale, their physical, chemical, optical, electrical and photo response properties change drastically, resulting in unique properties. One of the most promising material is graphene oxide. Graphene is a novel material with outstanding electrical, thermal, optical properties, large surface area, high catalytic ability, distinguished biocompatibility, increased heterogeneous charge transfer rate, good stability etc., Hence it is used in a wide range of applications mainly in sensors, supercapacitor, gas sensing, photodegradation, Li-ion batteries, catalysis, drug delivery, and reduction of toxic metals. Compositing graphene with metal oxide prevents the restacking which in turn leads to increases in surface area and conductivity due to the synergetic effect. Graphene based materials are considered to be an important class of materials with a lot of applications. The rapid development of graphene-based materials for various applications particularly electrochemical sensors has been motivated by their unique structural features, high stability, novel physicochemical properties and low cost. In this present work, Hummer’s method is used to produce the pure graphene oxide nanoparticles and their structural and optical properties are studied.

1.2. NANO SCIENCE:

The prefix ‘nano’ is referred to a Greek prefix meaning ‘dwarf’ or something very small and depicts one thousand millionth of a meter (10^{-9} m). Nanoscience is the study of structures and molecules on the scales of nanometers ranging between 1 and 100 nm, and the technology that utilizes it in practical applications such as devices etc.., is called nanotechnology [1]. Nanoscience is a convergence of physics, materials science and biology, which deal with manipulation of materials at atomic and molecular scales. One of the most exciting elements of operating in the nanoworld is that things behave differently when you go ultra-small. Essentially, the physical and chemical properties of matter change. Consider a lump of gold, yellow in colour. If you were to break that lump into nanosized chunks, the gold would change colour depending on the size of the chunks. In the 10 to 100 nanometer range it can appear reddish (as well as orange, purple or green depending on the size or shape of the particle). Gold is also a catalyst when in this size regime but chemically inert at the micro/macro scale. Nanoscience is all about the ultra-small, but it has the potential to have an enormous impact on our lives.

1.3 NANO TECHNOLOGY:

Nanotechnology is viewed as a recent field of research and technology related to the synthesis and design of materials with diverse compositions, arrangement and having nanoscale dimension at least in one dimension [2]. Nanotechnology is one of the most promising technologies of the 21^{st} century. It is the ability to convert the nanoscience theory to useful applications by observing, measuring, manipulating, assembling, controlling and manufacturing matter at the nanometer scale. Richard Feynmann (American physicist, 1918-1988) was the first scientist who raised the first discussions about nanoscience in 1959, with a speech entitled "**There is a plenty of room at the bottom**". The term "Nanotechnology" was defined by Norio Taniguchi of the Tokyo Science University in a 1974 paper as follows: "Nanotechnology" mainly consists of the processing of separation, consolidation and deformation of materials by one atom or one molecule. Since that time the definition of nanotechnology has generally been extended to include features as large as 100nm.[3]. The National Nanotechnology Initiative (NNI) in the United States define Nanotechnology as "a science, engineering, and technology conducted at the nanoscale (1 to 100 nm), where unique phenomena enable novel applications in a wide range of fields, from chemistry, physics and biology, to medicine, engineering and electronics". This definition suggests the presence of two conditions for nanotechnology. The first is an issue of scale: nanotechnology is concerned to use structures by controlling their shape and size at nanometer scale. The second issue has to do with novelty: nanotechnology must deal with small things in a way that takes advantage of some properties because of the nanoscale.

1.4 NANOPARTICLES:

Nanoparticles and other nanostructures have captured the attention of both scientific and technological world. Nanoparticles have attracted a great deal of scientific interest as they are considered as a bridge between bulk materials and atomic or molecular structures. The nanoparticles or nanostructures often exhibit novel and considerably different physical and chemical properties in comparison to their bulk counter parts [4-5]. These nanostructures have size dependent properties. Thus, the properties of nanoparticles change as their size decreases and as the percentage of atoms at the surface of a material increases and becomes significant in relation to those which are in interior of the particle [6]. The material properties change as their size approaches the atomic scale. This is due to the surface area to volume ratio increasing, resulting in the material’s surface atoms dominating the material performance. Owing to their very small size, nanoparticles have a very large surface area to volume ratio when compared to bulk material, such as powders, plate and sheet. This feature enables nanoparticles to possess unexpected optical, physical and chemical properties, as they are small enough to confine their electrons and produce quantum effects. For example, copper is considered a soft material, with bulk copper bending when its atoms cluster at the 50nm scale. Consequently, copper nanoparticles smaller then 50nm are considered a very hard material, with drastically different malleability and ductility performance when compared to bulk copper. The change in size can also affect the melting characteristics; gold nanoparticles melt at much lower temperatures (300 °C for 2.5 nm size) than bulk gold (1064 °C). Moreover, absorption of solar radiation is much higher in materials composed of nanoparticles than in thin films of continuous sheets of material.

1.4.1 PROPERTIES OF NANOMATERIALS:

As the size is reduced to the nanometric scale, the exposed surface area increases and this favors the greater interaction between nearby atoms and molecules, giving rise to various interactions, attractions and repulsions that cause surface, electronic and quantum effects that affect to the optical, electric and magnetic behaviors of the materials. This means that with a very small amount of nanomaterial the properties of other materials can be modified and significantly improved, providing great potential and added value. An example of this will be polymers doped with carbon nanotubes, which make the doped material have a lightness, mechanical strength and functionality superior to metals.

1.4.2 TYPES OF NANOMATERIALS:

Nanomaterials can be grouped into different classifications, but one of the most important is according to their dimensions:

- Zero dimensional nanomaterials

A zero-dimensional structure is one in which all three dimensions are within the nanoscale range. Zero-dimension nanomaterials are considered as nanoparticles. Such as nanowires, nanodiamonds or quantum-dots. Fullerenes have potential application in medicine as they can be used as transport for drug release since they have good biocompatibility, are selective, retain biological activity and their size is small enough to be diffused. Carbon quantum-dots are carbon semiconductor nanostructures studied to replace conventional quantum-dots since they have the same fluorescence properties to be applied as biosensors but are biocompatible and their toxicity is much lower.

- One-dimensional nanomaterials

A one-dimensional structure is one in which two dimensions are within the nanoscale range. This classification includes nanotubes and carbon nanofibers. They also improve the electrical conductivity in adhesives and paints without modifying their chemical properties and prevent corrosion of the materials that are coated. Its electrical conductivity properties allow them to be used in the construction of anodes and cathodes and in the formulation of conductive inks that can be used in the construction of flexible electronic circuits.

- Two-dimensional nanomaterials

A two-dimensional structure is one in which is one dimensions is within the nanoscale. They are sheet-shaped materials. Among them are graphene, nanofilms, and nanocoating. Graphene is the most representative material and with the greatest potential for application in different fields such as medicine, where its application is investigated as a drug transport and release system or as a biosensor. In the energy sector since graphene can increase the life of a traditional lithium battery, charging it faster and keeping it running longer. In a filtration system, graphene oxide can form a membrane that acts as a barrier against liquids and gases allowing water purification.

- Three-dimensional nanomaterials

A three-dimensional material that has no dimension in the nanoscale. Within this classification are nanostructured materials, nanoparticle dispersions and multi-nanolayers. In this sense, tungsten oxide has been investigated as a material for the photoelectrochemical generation of hydrogen. The surface of the nanostructured semiconductor material absorbs solar energy and acts as an electrode for water electrolysis.[7]

1.5 APPLICATIONS:

- Food industry

In the food industry, nanotechnology has been utilized in order to enhance the delivery of food ingredients to target sites, increase flavor, inhibit bacterial growth, extend product shelf life and improve food safety. Use nano-capsule technology to change food based on user preferences. For example, one tasteless, colorless beverage contains nano-capsule of differently colored or flavored ingredients. Different microwave frequencies select which color or flavor is released.

- Medicine

Some of the most exciting breakthroughs in nanotechnology are occurring in the medical field, allowing medicine to become more personalised, cheaper, safer and easier to deliver. The potential for nanotechnology to improve drug-delivery systems for a range of diseases including cancer, heart disease, diabetes and other age-related illnesses is an area of intense research for scientists. This drug delivery method would reduce the dosage amount needed, target cancer cells rather than healthy cells, and reduce side effects. The technology is still being tested and undergoing approvals, but may see some real-world applications as early as 2016. Other exciting developments include the possibility of using nanotechnology to increase the growth of nerve cells (for example in a damaged brain or spinal cord), and using nanofibers to help regenerate damaged spinal nerves (currently being tested on mice).

- Energy

Nanotechnology is being used in a range of energy areas—to improve the efficiency and cost-effectiveness of solar panels, create new kinds of batteries, improve the efficiency of fuel production using better catalysis, and create better lighting systems.

- Auto motive

Nanoengineered materials are in a range of products including high-power rechargeable batteries, fuel additives, fuel cells and improved catalytic converters, which produce cleaner exhaust for longer periods.

- Environment

  Researchers are developing nanostructured filters that can remove virus cells and other impurities from water, which may ultimately help create clean, affordable and abundant drinking water. A nano fabric paper towel, which can absorb 20 times its weight in oil, can be used for oil-spill clean-up operations.

- Electronics

  Many new screen-based appliances (TVs, phones, iPads and so on) incorporate nanostructured polymer films known as organic light-emitting diodes (OLEDs). These screens are brighter, lighter and have a better picture quality, among other things. Transistors, the basic switches that enable all modern computing, have gotten smaller and smaller through nanotechnology. At the turn of the century, a typical transistor was 130 to 250 nanometers in size. Using magnetic random-access memory (MRAM), computers will be able to “boot” almost instantly. MRAM is enabled by nanometer-scale magnetic tunnel junctions and can quickly and effectively save data during a system shutdown or enable resume-play features.

- Textiles

Nanoscale additives in fabrics help resist staining, wrinkling and bacteria growth. Stain repellent and wrinkle-resistant threads woven in textiles. Body warmers use Phase Change Materials (PCMs) responding to changing body temperatures. Nano socks treated with silver nano particles. The silver acts against infection and odor. Nano-Tex has launched a new nanotechnology-based wrinkle free treatment that is said to offer an improved performance while preserving fabric strength and integrity providing an alternative to harsh traditional processes. Chemicals and processing methods reduce fabrics tear and tensile strength.

- Cosmetics

In cosmetics, nanoparticles are used for various purposes, including to enhance the delivery of active ingredients, improve the appearance and feel of products, and provide sun protection**.** Nanoparticles are often used as ultraviolet (UV) filters in cosmetics because of their UV protection properties. The main compounds used as UV filters in cosmetics that utilize nanotechnology are zinc oxide (ZnO) and titanium dioxide (TiO_2). These materials are commonly used because they are highly effective at blocking UV rays, non-toxic, and safe for use on the skin.

1.6. OBJECTIVE OF THE PRESENT WORK:

The objective of the present work is:

- To synthesize of graphene oxide nanoparticles by Hummer's method.
- To study the structural properties of the GO nanoparticles using XRD.
- To study the optical properties of the GO nanoparticles using UV spectroscopy.
- To analyse the surface morphological properties of the GO nanoparticles using SEM.

CHAPTER-II

CHAPTER II

LITERATURE REVIEW:

Sujiono et al., (2020) [8] studied graphene oxide (GO) based on coconut shell waste was successfully synthesized using a modified Hummers method, and the obtained GO was confirmed using XRD, FTIR, Raman spectroscopy, UV-Vis spectroscopy, and SEM-EDX. The XRD results showed that 71.53% of graphite 2H observed with GO sample tended to form a rGO phase. Meanwhile, FTIR spectroscopy confirmed the appearance of various oxygen-containing functional groups such as hydroxyl, carboxyl, alcohol, and epoxy within the GO structure. The value of the ID/IG intensity ratio of the GO sample was 0.89 with a 2D single layer and had a surface morphology with an abundance of granular particles with different size distributions. The analysis using the Tauc plot method shows that the value of the GO band gap energy was 4.38 eV, indicating its semiconductor properties.

Mayoli et al., (2020) [9] studied the graphene oxides (GO) were prepared by a ball milling process with potassium perchlorate as oxidizing agent and deionized water as milling medium. GO samples were synthesized at different processing times and compared with a sample prepared by the Hummer's method. The prepared graphene oxides have been studied by Fourier transform infrared (FTIR), Raman spectroscopies, powder X-ray diffraction (XRD), scanning electron microscopy (SEM) and transmission electron microscopy (TEM). FTIR spectroscopy indicates presence of oxygen-bearing functional groups on the surface, Raman spectroscopy, XRD, SEM and TEM analysis confirm GO formation in ball milling. TEM analysis shows that the particle size distribution of 40 nm and the distance between layers corresponds with nanomaterials suitable to medical applications. SAED pattern analysis indicated the crystalline nature of the sample.

Juarez et al., (2019) [10] studied the synthesis of graphene oxide based on the modified Hummer's method. First, the concentration of the reactants and the reaction conditions were optimized to improve the efficiency of the oxidation process of graphite. The Raman spectrum of the GO shows the typical D and G typical of graphite oxide materials. The contribution of the area under the band D to the total area is 98 %, confirming that almost the whole graphene was oxidized (high oxidation yield). Second, the reaction time was minimized to 12 h, without compromising the quality (as confirmed by micrography). Third, the production of toxic gases has been reduced. Fourth, a thermal treatment was introduced instead of the vacuum drying procedure traditionally used, greatly diminishing the overall graphite oxide processing time that includes: the reactant preparation, graphite oxidation process, rinsing and dispersion procedures, and drying.

Hou et al., (2019) [11] studied the Hummers' method, in which concentrated sulfuric acid (H_2SO_4) acts as the intercalator and potassium permanganate serves as the oxidant, is a commonly used method to prepare graphene oxide (GO). The amounts of intercalator and oxidant along with the particle size of graphite are important factors that affect the structure and properties of GO. In this study, Fourier-transform infrared spectroscopy, X-ray diffraction, Raman spectroscopy, ultraviolet–visible spectroscopy, scanning electron microscopy, dynamic light scattering, X-ray photoelectron spectroscopy, thermogravimetric analysis, and atomic force microscopy were used to characterize the effects of these factors on the structure and properties of GO. The results show that the amount of intercalator and oxidant clearly affect the types of oxygen-containing functional groups in the GO structure along with the oxidation degree of GO.

Aliyev et al., (2019) [12] studied the surface functional groups of GO layers and the oxidative debris (OD) stacked on them were investigated after OD was extracted. Analysis was performed successfully using Fourier transform infrared spectroscopy (FTIR), ultraviolet-visible spectroscopy (UV-Vis), X-ray photoemission spectroscopy (XPS), energy-dispersive X-ray spectroscopy (EDX), Raman spectroscopy, solid-state nuclear magnetic resonance spectroscopy (SSNMR), standardized Boehm potentiometric titration analysis, elemental analysis, X-ray diffraction (XRD), thermogravimetric analysis (TGA), scanning electron microscopy (SEM), and transmission electron microscopy (TEM). The analysis showed that graphene oxide layers, as well as oxidative debris contain different functional groups such as phenolic –OH, ketone, lactone, carboxyl, quinone and epoxy.

Shafai et al., (2018) [13] studied the TiO_2 NPs and graphene oxide-titanium dioxide (GO@TiO2) nanocomposite were synthesized and characterized by TEM, XRD UV–vis and SEM. From the optical absorption measurements, the energy band gap values were found to be 4.00, 3.78 and 3.5 eV for GO, TiO_2 and GO@TiO_2, respectively. From the spectroscopic studies, the photocatalytic degradation of examined insecticides by using GO@TiO_2 nanocomposite was found to be more efficient compared to the widely used TiO_2. The highest degradation rate among the examined insecticides was recorded for imidacloprid. Absorption spectroscopy confirmed that the insecticides are efficiently absorbed over the surface of the graphene oxide. These findings suggest the usefulness the fabricated GO@TiO_2 nanocomposite for degradation the examined toxic insecticides in water.

Antonio et al., (2018) [14] studied the preparation and characterization of hexamethylene diisocyanate (HDI)-functionalized GO. Different reaction conditions were tested to optimize the functionalization degree (FD), and detailed characterizations were conducted via elemental analysis, Fourier-transformed infrared (FT-IR) and Raman spectroscopies to confirm the success of the functionalization reaction. The morphology of HDI-GO was investigated by transmission electron microscopy (TEM), which revealed an increase in the flake thickness with increasing FD. The surface morphology of the samples was analyzed by TEM, and the images showed a raise in layer thickness with increasing extent of functionalization. TGA study revealed that the covalent grafting of HDI enhances the thermal stability of GO, ascribed to the crosslinking between neighbouring sheets. This thermal stability improvement is highly attractive for applications such as long-term electronics and electrothermal devices.

Durmus et al., (2018) [15] studied the EG were chemically oxidized to obtain GO nanosheets and successfully decorated with ZnO nanoparticles having an average particle size of 25–30 nm and synthesized with two-step sol-gel deposition method. Carbon/inorganic ratio of resulting nanocomposites was about 0.54/0.46 (w/w) and ZnO nanoparticles showed a well-defined 2D arrangement onto GO nanosheets based on the structural and morphological characterization works. It was concluded that such nanocomposite structure reduced the band gap of ZnO nanoparticles and thus increased its photocatalytic efficiency for the degradation of BF dye as a model compound in an aqueous medium. This study can provide a comprehensive technical information for the catalyst synthesis, characterization, and testing of performance issues and could prompt preparation of structurally designed and highly efficient composite catalysts.

Jin et al., (2018) [16] studied the hydrogen peroxide and its effects on GO. Here we tried to find experimental evidence that H_2O_2, which has been used as a terminating agent for residual potassium permanganate, directly influences the various properties of GO, leading to substantial changes. Moreover, we proved that all residual unreacted ions can be eliminated by filtration without any H_2O_2 addition for less defective GO. It has been widely studied by itself due to its unique physical and chemical properties, but GO is also known as a precursor for the solution-based bulk production of graphene.

Zaaba et al., (2017) [17] studied the structure and electrical properties of graphene oxide. GO was obtained from graphite flakes by using modified hummers method in which different from conventional hummer's method. In this method, the experiment was synthesized without sodium nitrate ($NaNO_3$) and ice bath, but carried out at room temperature. Prepared GO powders were then dissolved into different solvents, namely acetone and ethanol. Ethanol has advantages more than acetone in form of conductivity of electrical and solubility of GO. GO characterized using FTIR shows that both samples contain several functional groups such as hydroxyl, epoxy, carboxyl and carbonyl. Besides that, due to the lower diffraction peak of A-GO, XRD result shows the interlayer spacing of A-GO sample is slightly higher than E-GO sample.

Alyobi et al., (2017) [18] studied the Graphene's novel electrical, optical, and mechanical properties are affected both by substrate interaction and processing steps required to fabricate contacts and devices. Annealing is used to clean graphene devices, but this can lead to doping and defect changes and strain effects. There is often disagreement about which of these effects are occurring and which result in observed changes in Raman spectra. The effects of vacuum annealing on mechanically exfoliated pristine, suspended, and attached thin and thick few-layer graphene on SiO_2/Si are investigated here using scanning electron microscopy (SEM), Raman spectroscopy, and atomic force microscopy (AFM). Annealing at low temperature is sufficient to eliminate most of the defects. However, compressive strain is induced in the sheet by annealing at high temperature, and for thin regions increased substrate conformation leads to the apparent disappearance of the sheets. The intensity ratio of the 2D and G bands also reduces with induced compressive strain, and thus should not be used to detect doping.

Sharma et al., (2017) [19] studied the GO was prepared by exfoliation of graphite using modified Hummer's method and then reduced using hydrazine hydrate (reducing agent) to produce rGO. XRD, FESEM, Raman, FTIR spectrophotometer and TGA were used for characterization of GO and rGO. XRD images reveal crystalline structure for both GO and rGO. The d-spacing is observed to be reduced for rGO as compared to that for GO because of removal of oxygen containing functional groups. Intensity of FTIR peaks of oxide, hydroxyl and alkoxy groups decreases significantly on reduction. FESEM image shows more corrugated surface of rGO as compared to GO.

Alam et al., (2016) [20] studied the exfoliation of graphene by mechanical, chemical and thermal reduction and chemical vapor deposition and mentions their advantages and disadvantages. This article also indicates recent advances in controllable synthesis of graphene, illuminates the problems, and prospects the future development in this field. Recently graphene the noble material has brought a revolutionary change in the field of nanoelectronics. Its outstanding contribution is not only limited in nanoelectronics but also expanding in medical science, nanorobotics, commercial manufacturing of graphene synthesized products and so on.

Yu et al., (2016) [21] studied an improved $NaNO_3$ free Hummer's method by partly replacing $KMnO_4$ with K_2FeO_4 and controlling the amount of concentrated sulfuric acid. As compared to the existing $NaNO_3$-free Hummer's methods, this improved routine greatly reduces the reactant consumption while keeps a high yield. The obtained GO was characterized by various techniques, and its derived graphene aerogel was demonstrated as high-performance supercapacitor electrodes.

Safarpour et al., (2015) [22] studied the Partially reduced graphene oxide (rGO)/TiO_2 nanocomposite was firstly synthesized, and then, PES-based membranes were prepared by blending with rGO/TiO_2. In the rGO/TiO_2 nanocomposite, TiO_2 could uniformly disperse on the GO surface resulting in high hydrophilicity due to the presence of various hydrophilic functional groups on the surface of nanocomposite. Compared with TiO_2/PES and GO/PES membranes, rGO/TiO_2/PES membrane showed the best overall properties including the water permeability, fouling resistance and dye protein rejection. Considering the results of hydrophilicity, pure water flux, antifouling performance and dye rejection, the optimum concentration of 0.1 wt.% can be introduced for rGO/TiO_2 nanocomposite in the casting solution.

Tavakoli et al., (2015) [23] studied the synthesis of graphene nanosheets in the presence of pomegranate juice. In this approach, pomegranate juice was used not only as reductant but also as capping agent to form graphene nanosheets. At first, the improved Hummer method to oxidize graphite for the synthesis of graphene oxide (GO) was applied, and then the as-produced graphene oxide was reduced by pomegranate juice to form graphene nanosheets. Fourier transformed infrared (FT-IR), X-ray powder diffraction (XRD), scanning electron microscopy (SEM), energy dispersive spectrometry (EDS), high resolution transmission electron microscopy (HRTEM), atomic force microscopy (AFM) and Raman were used to characterize the samples. The results obtained from the characterization techniques proved high purity of the final products.

Chen et al., (2015) [24] studied the PVA films were prepared through aqueous solution method, and boric acid (BA) as well as graphene oxide (GO) was added to improve the mechanical and thermal properties. It was found that 5 wt % BA could increase the tensile strength threefold (from 23.3 to 67.7 MPa), and the incorporation of 0.2 wt % GO would provide additional percentage growth of 30% (from 67.7 to 88.5 MPa). Moreover, an enhancement of thermal stability of PVA film was found when boric acid or GO filler was added. The reinforcement mechanisms of both boric acid and GO were investigated, and a competitive phenomenon that the addition of boric acid would influence the reinforcement effect of GO sheets was found.

Kumar et al., (2015) [25] studied the global degree of oxidation in GO and to separate GO into fractions with more uniform extents of oxidation. Using the formation of GO stabilized oil-in-water emulsions, GO is separated into an emulsion fraction and a water fraction. We find GO sheets that stabilize the emulsion droplets are less oxidized than sheets suspended in water as shown by XRD, Raman spectroscopy, FTIR, elemental analysis and electrical conductance. The use of successive fractionation allows not only for the preparation of GO fractions with more narrowly defined properties, but also provides a method for characterizing GO batches.

Guerrero et al., (2015) [26] studied the Graphene oxide (GO) powders with different oxidation degree estimated through the relative intensity of the infrared absorption bands related to oxygen containing groups were prepared through variations of the Hummers method. The GO powders were analyzed by Transmission Electron Microscopy, Energy dispersive spectroscopy, X-ray Photoelectron Spectroscopy, Fourier Transform Infrared Spectroscopy, Raman spectroscopy, X-ray Diffraction, (UV-VIS) spectroscopy and Electrical Resistance measurements. Several square micron GO sheets with low wrinkling were obtained. FTIR shows presence of hydroxyl (-OH), epoxy (C-O-C), carboxyl (-COOH) and carbonyl (C=O) moieties and evidence of intermolecular interactions between adjacent groups. These interactions influence the exfoliation degree, the absorbance of the GO suspensions, as well as the electrical resistance, while the crystalline domain sizes, estimated from XRD and Raman do not show a noticeable behavior related with the composition and molecular structure.

Li et al., (2015) [27] studied the series GO/Ag_2CO_3 photocatalyst were synthesized by liquid phase deposition method. The effect of presence of GO on the surface property and visible light absorption of A$g_2CO_3$was investigated. Result shows that the GO/Ag_2CO_3 composite shows relative high surface area and enhancing visible light adsorption. When the coupling GO content was 0.5%, GO/Ag_2CO_3 exhibited the highest photocatalytic activity and stability. GO has good electrical conductivity which benefits the transfer of photo-generated electrons (e) in A to the surface of GO. The enhancement in electrons (e) and holes (h) separation could prevent Ag+ reduction by photo-generated electrons.

Yadav et al., (2014) [28] studied the graphene oxide/ carboxymethylcellulose /alginate (GO/CMC/Alg) nanocomposite blends were prepared by a simple solution mixing-evaporation method. The resulting structure, thermal stability, and mechanical properties of the blends were investigated by wide-angle X-ray diffractometry, Fourier transform infrared spectroscopy, Raman spectroscopy, scanning electron microscopy, thermogravimetric analysis, and mechanical testing. The obtained findings revealed that CMC, Alg, and graphene oxide were able to form a homogeneous mixture. When compared to a CMC/Alg blend, the incorporation of 1 wt% graphene oxide improved the tensile strength and young’s modulus by 40% and 1128%, respectively. In addition, the GO/CMC/Alg nanocomposite blend film showed a higher storage modulus than the CMC/Alg nanocomposite.

Song et al., (2014) [29] studied the graphene oxide (GO) films with two-dimensional structure were successfully prepared via the modified Hummer method. It is proven that redox method is a promising way to synthesize GO films on a large scale. Comprehensive characterizations of the properties of GO films were conducted. TEM and DFM analyses showed that GO sheets prepared in this study had single and double lamellar layer structure and a thickness of 2∼3 nm. X-ray diffraction (XRD) was selected to measure the crystal structure of GO sheet. Fourier transform infrared spectra analyzer (FT-IR) was used to certify the presence of oxygen-containing functional groups in GO films. The tests of UV-VIS spectrometer and TGA analyzer indicated that GO sheet possessed excellent optical response and outstanding thermal stability.

Cao et al., (2014) [30] studied the graphite oxide was prepared from natural flake graphite by Hummer’s method through liquid oxidization, and the reduced graphene oxide was obtained by chemical reduction of graphene oxide using NH_3. H_2O aqueous solution and hydrazine hydrate. The raw material graphite, graphite oxide, and reduced graphene oxide were characterized by X-ray diffraction (XRD), attenuated total reflectance-infrared spectroscopy (ATR-IR), and field emission scanning electron microscope (SEM). The results indicated that the distance spacing of graphite oxide was longer than that of graphite and the crystal structure of graphite was changed. The flake graphite was oxidized to graphite oxide and lots of oxygen-containing groups were found in the graphite oxide. In the morphologies of samples, fold structure was found on both the surface and the edge of reduced graphene oxide. the prepared GO is dispersed easily in solution. In this case, the modification of the GO is easy and it is suitable for GO application in composites and energy storage devices.

Perrozzi et al., (2014) [31] studied the fundamental characterization of graphene oxide (GO) and its future application perspectives. Morphology is discussed through optical microscopy, fluorescence microscopy, scanning electron microscopy, and atomic force microscopy studies. Chemical, structural, and vibrational properties are discussed through x-ray photoemission spectroscopy and Raman spectroscopy studies. Two easy characterization strategies, based on the correlation between x-ray photoemission spectroscopy and contact angle/optical contrast measurements are reported. Sensing and nano-biotechnology applications are discussed with focus on practical gas sensing and optical sensing, on the one hand, and on the toxicity issue of GO, on the other hand. Synthesis and post-synthesis treatments are also discussed, these latter with emphasis on lithography.

Frankberg et al., (2014) [32] studied the synthesis of graphene oxide by the modified Hummer's method and measuring the synthesis yield were investigated. The graphene oxide synthesis yield measurement, which was calculated to give a sufficiently small error of $\pm 0.08 \times 10^{-3}$ g mL^{-1}. Current results indicate that using a precursor graphite powder with smaller average particle size and changing the ultrasonic treatment parameters can increase the yield of graphene oxide synthesis by up to 70% (in g mL^{-1}), which was confirmed by the new measurement method.

Karteri et al., (2014) [33] studied the electrical characteristics of graphene oxide based thin film transistor with the polymer insulators such as polymethyl methacrylate (PMMA) and poly-4-vinylphenol (PVP). Graphene oxide (GO) nanosheets were prepared by using modified Hummer's method. The structural properties of GO nanosheets were characterized with Ultraviolet Visible (UV–vis), FT-IR spectroscopy and X-rays diffraction (XRD). Graphene oxide based thin film transistor (GO-TFT) was prepared by a spin-coating and thermal evaporation technique. The electrical characterization of GO-TFT was analyzed by output and transfer characteristics by using Keithley-4200 semiconductor characterization system (SCS). The mobility, threshold voltage, sub-threshold swing value and Ion/Ioff ratio. The transfer characteristics of GO based TFT device show a more dominating hole conduction over the electron conduction. This p-type semiconducting behavior of GO arises from the presence of various functional groups in GO.

Chang et al., (2014) [34] studied the Graphene oxide (GO) can be readily modified for particular applications due to the existence of abundant oxygen-containing functional groups. Graphene oxide-based materials (GOBMs), which are biocompatible and hydrophilic, have wide potential applications in biomedical engineering and biotechnology. In this review, the preparation and characterization of GO and its derivatives are discussed at first. Subsequently, the biocompatibility and tribological behavior of GOBMs are reviewed. Finally, the applications of GOBMs as lubricants in bio-tribological systems are discussed in detail. GO and its derivatives exhibit promising tribological properties as solid lubricants, oil based lubricant additives, water-based lubricant additives and fillers for polymer-based composite materials.

Dehghanzad et al., (2013) [35] studied the graphene oxide was successfully synthesized via oxidation of graphite, functionalized with dodecyl amine and then chemically reduced using hydrazine hydrate. The graphene oxide was also thermally reduced and exfoliated to obtain graphene. Different characterization methods including elemental, FTIR, XPS, Raman, TGA and XRD analyses were employed to deeply analyze the structure of the resulted materials. The results of different analysis mostly supported each other and demonstrated that different oxygen containing functional groups, those which were capable to grafting of dodecyl amine chains, have been created on the surface of graphite during the oxidation process at the expense of the increased defects. Structural changes of the materials during different stages of modification were also reflected in their amphiphilic characteristics and morphological features, evaluated using the contact angle experiments and SEM analysis, respectively. Thermally reduced and exfoliated graphene oxide exhibited near pure graphene characteristics by means of TGA and Raman analyses.

Chen et al., (2013) [36] studied an improved Hummer's method without using $\mathrm{NaN}O_3$ can produce graphene oxide nearly the same to that prepared by conventional Hummer's method. This modification does not decrease the yield of product, eliminating the evolution of $\mathrm{N}O_2/N_2O_4$ toxic gasses and simplifying the disposal of waste water because of the inexistence of Na+ and $\mathrm{N}O_3$ ions. For the first time, we also developed a prototype method of post-treating the waste water collected from the systems of synthesizing and purifying graphene oxide. The content of $\mathrm{M}n^{2+}$ ions in the purified waste water was measured to be lower than the guideline value for drinking water.

Yang et al., (2011) [37] studied the hybrid architecture of GO and ZNs with ZN attached onto GO sheets in parallel is presented in this article. The fabrication process includes introducing amino groups onto ZNs surface, followed by amidating with carboxyl groups of GO. The hybrid architecture preserved the morphology and crystallinity of the preformed ZNs and exhibited strong stability and reliability of the heterojunction structure. The assembling of this GO-based hybrid provides a new way to design semiconductor–carbon nanocomposites. surface. Transmission electron microscopy (TEM) image of the as-prepared hybrid reveals the morphology of the architecture of GO/ZNs hybrid. Fourier transform infrared spectroscopy (FTIR), X-ray diffraction (XRD), thermogravimetric analysis (TGA) ultraviolet–visible (UV–vis) and fluorescence spectroscopy were also performed to characterize the structure and properties of the GO/ZNs hybrid. Effective electron transfer from excited ZnO to GO sheets was confirmed from the luminescence quenching of yellow-green emission of ZNs.

Marcano et al., (2010) [38] studied the Hummers' method ($KMnO_4$, $NaNO_3$, H_2SO_4) is the most common method used for preparing graphene oxide. We have found that excluding the $NaNO_3$, increasing the amount of $KMnO_4$, and performing the reaction in a 9:1 mixture of H_2SO_4/H_3PO_4 improves the efficiency of the oxidation process. This improved method provides a greater amount of hydrophilic oxidized graphene material as compared to Hummers' method or Hummers' method with additional $KMnO_4$. Moreover, even though the GO produced by our method is more oxidized than that prepared by Hummers' method, when both are reduced in the same chamber with hydrazine, chemically converted graphene (CCG) produced from this new method is equivalent in its electrical conductivity. The mechanism for producing IGO with a more regular structure could be based on the formation of five-membered cyclic phosphate groups between the phosphoric acid and two vicinal diols formed on the graphite basal plane.

Kim et al., (2010) [39] studied the Graphite oxide sheet, now called graphene oxide (GO), is the product of chemical exfoliation of graphite and has been known for more than a century. GO has been largely viewed as hydrophilic, presumably due to its excellent colloidal stability in water. Here we report that GO is an amphiphile with hydrophilic edges and a more hydrophobic basal plane. Its amphiphilicity can be tuned by changing pH as it shuttles between water and the oil-water interface. Size-dependent amphiphilicity was also observed, leading to spontaneous interfacial size separation. It creates highly stable Pickering emulsions of organic solvents like colloidal particles and disperses insoluble solids in water like molecular surfactants.

Rattana et al., (2010) [40] studied the GO nanosheets were prepared by a chemical exfoliation technique. The structural and optical properties of the as-prepared GO nanosheets were characterized by Raman, FTIR, UV-vis and photoluminescence spectroscopy. The FTIR results confirmed the existence of oxygen-containing groups on the GO nanosheets and the photoluminescence spectra of GO nanosheets showed the emission peak in the visible regions. The C=O groups of GO nanosheets enable immobilization of various biomolecules through the covalent bonding. These results indicate that the GO nanosheets could be used as a promising new material for biological applications such as biofunctionalization and fluorescence biosensors.

Chen et al., (2009) [41] studied the rapid and mild thermal reduction of graphene oxide (GO) to graphene was achieved with the assistance of microwaves in a mixed solution of N, N-dimethylacetamide and water

(DMAc/H_2O). The mixed solution works as both a solvent for the produced graphene and a medium to control the temperature of the reactive system up to 165^0 C. The conductivity of graphene paper prepared by the microwave reduced product is about 104 times than that of GO paper. The yield of graphene prepared by this method is very high and production of gram level is easily achieved. The as-prepare graphene can be well dispersed in DMAc to form a stable colloid suspension in the concentration range of 1.0 mg mL. The suspension is useful for further modification of graphene and preparation of novel materials. The electrical conductivity of the MWG paper is about 104 times than that of GO paper.

Shen et al., (2009) [42] studied the preparation of graphite oxide (GO) from graphite through reaction with Benzoyl peroxide (BPO), complete exfoliation of GO into graphene oxide sheets, followed by their in situ reduction to reduced graphene oxide nanoplatelets. The mechanism of graphene oxide producing is mainly the generation of oxygen containing groups on graphene sheets. In addition, inserted BPO and expansion of CO_2 evolved during reaction will expand the distance between graphite layers, which are also main factors for exfoliation. Thermogravimetric analysis, Raman spectroscopy, and Fourier transform infrared spectroscopy indicated the successful preparation of GO. X-ray diffraction proved the mechanism of intercalation and exfoliation of graphite. Transmission electron microscopy and atomic force microscopy were used to demonstrate the structure of produced graphene oxide and reduced graphene oxide nanoplatelets.

CHAPTER-III

CHAPTER III

EXPERIMENTAL METHODS AND CHARACTERIZATION TECHNIQUES:

3.1. INTRODUCTION:

Carbon the most interesting material in the periodic table form stable allotropes and carbon-based nanomaterials due to its catenation properties. The different forms of carbon include graphite, diamond, fullerenes, graphene, carbon nanotube, charcoal and carbon dots etc. Graphene is the mother of all other allotropes of carbon which has drawn unprecedented interest owing to its intrinsic difference from other forms of carbon [43]. It constitutes a single layer sheet of sp2-bonded carbon atoms with densely packed honeycomb two-dimensional crystal lattice. Graphene oxide (GO) the precursor for graphene, has become one of the most widely researched materials of the last decade. It contains several oxygen-containing functional groups such as hydroxyl and epoxy groups which are located on the basal plane, and carboxy, carbonyl, phenol, lactone, and quinone groups at the sheet edges [44]. The GO is an insulator in nature because of the disruption of the graphitic structure arising from the oxygenated functional groups. The ionisation of different functional groups such as carboxylic acid and phenolic hydroxyl groups provide a negative charge on GO which make it favourable to an electrochemical reaction. Hence GO has been considered a promising material in electrochemical sensing [45].

3.2 MATERIAL IMPORTANCE:

Graphite oxide (GO), formerly called graphitic oxide or graphitic acid, is a compound of carbon, oxygen, and hydrogen in variable ratios, obtained by treating graphite with strong oxidizers and acids for resolving of extra metals. The maximally oxidized bulk product is a yellow solid with C:O ratio between 2.1 and

2.9, that retains the layer structure of graphite but with a much larger and irregular spacing.[46,47] The discovery of allotropes of carbon has transformed the electronic and optoelectronic industry due to their encouraging properties leading to a large spectrum of applications. An interesting characteristic of carbon is its ability to form many allotropes due to its covalency. In recent decades, various allotropes and forms of carbon have been discovered, including fullerenes, carbon nanotubes (CNTs), and graphene. Since the inception of nanotechnology, carbon allotropes based nanocomposites have become a leading sector of research due to their unique bonding properties. Fullerenes and carbon nanotubes-based polymer nanocomposites have attracted significant research interest due to their vast applications in various spheres of science and technology. The reduction of electrically insulating graphene oxide, which is exfoliated from graphite flakes, and use of the colloidal suspensions of reduced graphene oxide is one of the most promising ways to produce electrically conducting graphene-based platelets on large scale [48]. The bulk material spontaneously disperses in basic solutions or can be dispersed by sonication in polar solvents to yield monomolecular sheets, known as graphene oxide by analogy to graphene, the single-layer form of graphite.[49] Graphene oxide sheets have been used to prepare strong paper-like materials, membranes, thin films, and composite materials. Initially, graphene oxide attracted substantial interest as a possible intermediate for the manufacture of graphene.

3.2.1. STRUCTURE OF GRAPHENE OXIDE:

Graphene has two-dimensional structure consisting of a sp2 carbon network with thickness of one atom. Graphene has wide range of potential applications due to its excellent mechanical, thermal, and electrical properties. The structure and properties of graphite oxide depend on the particular synthesis method and degree of oxidation. It typically preserves the layer structure of the parent graphite, but the layers are buckled and the interlayer spacing is about two times larger (~0.7 nm) than that of graphite. Strictly speaking "oxide" is an incorrect but historically established name. Besides epoxide groups (bridging oxygen atoms), other functional groups found experimentally are: carbonyl (C=O), hydroxyl (-OH), phenol and for graphite oxides prepared using sulphuric acid (e.g. Hummers method) some impurity of sulphur is often found, for example in a form of organo sulfate groups.[50-55] The detailed structure is still not understood due to the strong disorder and irregular packing of the layers. The aliphatic regions in the layers with sp3 hybridized carbon atoms along with sp2 carbon atoms make the graphene oxide non-conducting. It is well known that the electrical conductivity can be restored in the carbon layers by reducing graphene oxide to graphene by chemical or thermal means. Though chemical methods are more widely used to make graphene and its composites, thermal reduction is cleaner, faster and more effective. Thermal reduction of graphene oxide to graphene also allows for quantitative estimation and control of oxygen bearing groups on the carbon layers.

3.2.2. SYNTHESIS OF GRAPHENE OXIDE:

GO, the basic framework of graphene was prepared by Brodie, Staudenmaier, Modified Hummers and Tour methods from graphite. It was first synthesised by a British chemist B.C. Brodie in 1855. He has successfully extracted GO by adding potassium chlorate to graphite containing fuming nitric acid solution. Staudenmaier improved the protocol by replacing fuming nitric acid solution with a mixture of fuming nitric acid and concentrated sulphuric acid. During these processes, an extreme level of safety is required to handle highly reactive potassium chlorate. Both of these processes are hazardous, time consuming and release toxic gases during the reaction. In 1957, William S Hummers and Richard E Offeman developed a rapid and relatively safe method for the preparation of GO from graphite using potassium permanganate ($KMnO_4$), sodium nitrate ($NaNO_3$) and concentrated sulphuric acid (H_2SO_4) as precursor materials. Later Hummers method was modified to achieve a higher degree of oxidation. Till date modified Hummer's method has been effectively used for the mass and high-quality production of GO. In 2010, a new recipe was introduced by Tour's group for the synthesis of GO with a greater degree of oxidation, which avoided the use of sodium nitrate and increased the amount of $KMnO_4$ and also introduced a new acid; phosphoric acid namely the Tour method. In this thesis, we choose the modified Hummer's method and Tour method for the preparation of GO. In modified Hummer's method 1.0 g graphite powder was dispersed in a concentrated solution of 30 mL H_2SO_4 for 20 minutes. After the addition of 0.5 g sodium nitrate at room temperature, the mixture was continuously stirred using a magnetic bead for 16 hrs, after which 3g $KMnO_4$ was added to the mixture. This addition was carried out in an ice bath to keep the temperature below 10^0C and further stirring was done for 2 hrs. The slurry was subsequently heated to 35^0C for another 3 hrs followed by the addition of 200mL of water. Then the temperature of the solution was raised to 90^0C and was heated for some more time. 10 mL of 30% hydrogen peroxide was slowly added and stirred the mixture overnight. Finally, the mixture was filtered and washed with 5% HCl and water until a neutral pH was obtained. In Tour method, we added 3 g of graphite powder and 18 g of $KMnO_4$ into a mixture of 360mL conc. H_2SO_4 and 40 mL phosphoric acid. Then the mixture was maintained at 50 °C with constant stirring for 12 hrs. The mixture was cooled down to room temperature and poured into a beaker containing flake ice (400mL) with vigorous stirring. 5mL of 30% H_2O_2 was added to the reaction mixture. It was then filtered and washed with 5% HCl and water. One of the biggest advantages of this protocol is the absence of $NaNO_3$, which minimizes the generation of toxic gases such as NO_2, N_2O_4 or ClO_2 in the reaction.

3.2.3 PROPERTIES OF GRAPHENE OXIDE:

Graphite oxide has attracted much interest as a possible route for the large-scale production and manipulation of graphene, a material with extraordinary electronic properties. Graphite oxide itself is an **insulator, almost a semiconductor, with differential conductivity between 1 and 5×10^{-3} S/cm at a bias voltage of 10 V.** However, being hydrophilic, graphite oxide disperses readily in water, breaking up into macroscopic flakes, mostly one layer thick.

TABLE 3.1. PROPERTIES OF GO

Reduction method	Chemically reduced
Color	Black
Form	Powder
Odor	Odorless
Sheet Dimension	Variable
Solubility	Insoluble
Dispersibility	Dispersed at low concentrations
Electrical conductivity	High
Thermal conductivity	High
Transmittance	About 98% of light
Electronic and electro chemical properties	Exceptional

3.2.4 APPLICATION OF GRAPHENE OXIDE:

Graphene and layered materials have made an impact on many different fields, and new applications are emerging every day. So, as for all evolving technologies, it is crucial to consider their safety.

- Graphene is many times stronger than steel, yet incredibly light weight and flexible.
- It is electrically and thermally conductive but also transparent.
- It is the world’s first 2D material and is one million times thinner than the diameter of a single human hair.
- Graphene is unique properties aloe for ground- breaking biomedical applications. Target drug delivery, improved brain penetration, DIY health testing kits and smart implants.
- The application of graphene and 2D materials for developing innovative and revolutionary medical devices that could improve health care.
- By combining graphene with paint, a unique graphene coating is formed which could signal the end of the decay of ships and cars through rust.
- The graphene based composite technique could be applied to brick and stone, to weatherproof houses, or even to food packaging to stop the transfer of water and oxygen molecules which causes food go off.
- Sporting goods are often the first to take up on a new materials development which has already been the case with the successful graphene enhanced tennis racket from head.
- A graphene based composite aircraft wing could drastically decrease weight, reduce the detrimental effects of lightning strike damage and increase fuel

efficiency and range. This could result in the world’s lightest, strongest, safest, greenest plane.

- That graphene and layered materials do not cause skin irritation after an acute exposure when they are made with non-irritating exfoliation agents.
- Graphene was repeatedly exposed to human bronchial epithelial tissue, and the scientists found that continual exposure over long periods of time did not induce a significant immune response. These results suggest that graphene could be safe for long-term workplace exposure.
- Biodegradation is the naturally occurring decomposition of materials by microorganisms, enzymes or other biological activity.
- It is important for materials to biodegrade to be considered safe, as the build-up of foreign materials can lead to ecological damage and health problems.
- The graphene itself can be biodegraded by a human enzyme.
- The biodegradation of graphene oxide in zebrafish, as a model for the gastrointestinal tract.
- Toxic effects were observed in some species but not others, and there were some changes to bacterial communities.
- The graphene and layered materials may reduce pollen vitality in the lab, but these effects are less evident in living organisms.
- Graphene oxide is also being explored for its applications in hydrogen storage. Hydrogen molecules can be stored among the oxygen-based functional groups found throughout the sheet.
- Graphene can be used as a coating to improve current touch screens for phones and tablets.
- It can also be used to make the circuitry for our computers, making them incredibly fast. Graphene can also spark the next generation of electronics.

- Graphene could see a smart phone which you could wear on your wrist or a tablet you could roll up like a newspaper.
- Indium- tin oxide is currently used for touch screens as it conducts well but it is brittle.
- A world's smallest transistor have already created using graphene.
- Batteries could be so flexible and light that they could be stitched into clothing or into the body.

3.2.5 PREPARATION TECHNIQUE:

Graphite oxide was synthesized from graphite powder by modified Hummer's method [56]. 2 g of graphite powder is added into 100mL of concentrated H_2SO_4 at room temperature. Under stirring, the mixture was cooled to 5^0C using an ice bath, and the temperature of the mixture was kept to be below 5^0C for 30min. 8g of $KMnO_4$ is then added gradually under stirring and cooling, so that the temperature of the mixture was not allowed to reach 10^0 C. 100mL distilled water was added into the mixture. And further diluted to approximately 300mL with distilled water. After that, 20mL of 30% H_2O_2 was added to the mixture to reduce the residual $KMnO_4$. The solid was filtered, washed with 5%HCl aqueous solution (800 mL) to remove metal ions and with distilled water until the pH was 6. The resulting graphite oxide (GO) was air dried for 24h.

3.3. CHARACTERIZATION TECHNIQUES:

3.3.1. INTRODUCTION:

The nanostructures can be characterized using various techniques such as XRD, SEM, TEM, AFM, UV, PL, Raman spectroscopy etc. The pure graphene oxide nanoparticles are subjected to XRD, UV, SEM EDAX with mapping, FTIR to the present work.

3.3.2. X-RAY POWDER DIFFRACTION:

X-ray diffraction pattern are formed when X-rays are focused on a crystalline material. X-ray scattering techniques are a family of non-destructive analytical technique which reveal information about the crystal structure, chemical composition and physical properties of materials and thin films. These techniques are based on observing the scattering intensity of an X-ray beam hitting a sample as a function of incident and scattered angle, polarization and wavelength or energy.

XRD is a rapid analytical technique primarily used for phase identification of a crystalline material and can provide information on unit cell dimensions. The analysed material is finely grind homogenized and average bulk composition is determined. Max Von Laue, in 1912 discovered that crystalline substances act as three dimensional diffraction gratings for X-ray wavelength similar to the spacing of planes in a crystal structures and atomic spacing X-ray diffraction is based on constructive interference of monochromatic X-rays and a crystalline sample.

3.3.3. DATA COLLECTION:

The intensity of the diffracted X-ray is continuously recorded as the sample and detector rotate through their respective angles. A peak in intensity occurs when the mineral contains lattice planes with d-spacing appropriate to diffract x-rays at that value of θ. Although each peak consists of two separate reflections (K_{a1}, K_{a2}) at small values of 2θ the peak locations overlap with K_{a2}appearing as a hump on the side of K_{a1}. Greater separation occurs at higher values of θ. Typically these combined peaks are treated as one. The 2λ position of the diffraction peak is typically measured as the center of the peak at 80% peak height.

3.3.4. DATA REDUCTION:

Results are commonly presented as peak positions at 2θ and X-ray counts (intensity) in the form of a table or an X-Y plot intensity (I) is either reported as peak height intensity, that intensity above background, or as integrated intensity, the area under the peak. The relative intensity is recorded as the ratio of the peak intensity to that of the most intense peak (relative intensity = I/$I_1 \times 100$).

3.3.5. DETERMINATION OF AN UNKNOWN SAMPLE:

The d-spacing of each peak is then obtained by the solution of the Bragg equation for the appropriate value of λ. Once all d-spacing have been determined, automated search/match routines compare the d's of the unknown to those of known materials. Because each mineral has a unique set of d-spacing, matching these d-spacing provides an identification of the unknown sample. A symmetric procedure is used by ordering the d-spacing in terms of the intensity beginning with the most intense peak. Files of d-spacing for hundreds of thousands of inorganic compounds are available from the international centre for diffraction data as Powder Diffraction File (PDF). Many other sites contain d-spacing of minerals such as the American mineralogist crystal structure database.

XRD can be used to:

- Determine crystal structure using Riveted refinement.
- Determine modal amounts of minerals (quantitative analysis)
- Characterize thin films samples
- Determine lattice mismatch between film and substrate and to inferring stress and strain
- Determine dislocation density and quality of the thin film by rocking curve measurements.

- Measure super lattices in multi-layered epitaxial structures
- Determine the thickness, roughness, and density of the film using glancing incidence X-ray reflectively measurements
- Make textural measurements such as the orientation of grains, in a polycrystalline sample.

3.4. ULTRA VIOLET SPECTROSCOPY:

UV/Vis spectroscopy is routinely used in analytical chemistry for the quantitative determination of different analyses, such as transition metal ions, highly conjucated organic compounds, and biological macromolecules. Spectroscopic analysis is commonly carried out in solutions but solids and gases may also be studied.

Molecules containing electrons or non-bonding electrons (n-electrons) can absorb the energy in the form of ultraviolet or visible light to excite these electrons to higher anti-bonding molecular orbital. The more easily excited the electrons the longer wavelength of light it can absorb. The UV spectrum records the wavelength of maximum absorption and the intensity of absorption.

Solutions of transition metal ions can be colored (ie., absorb visible light) because the electrons within the metal atoms can be excited from one electronic state to another. The colour of metal ion solutions is strongly affected by the presence of other species, such as certain anions or ligands. For instance, the colour of a dilute solution of copper sulfate is a very light blue adding ammonia intensifies the colour and changes the wavelength of maximum absorption.

Organic compounds, especially those with a high degree of conjugation (e.g. DNA, RNA, protein), also absorb light in the UV or visible regions of the electromagnetic spectrum. The solvents for these determinations are often water for water-soluble compounds, or ethanol for organic-soluble compounds. (Organic solvents may have significant UV absorption; not all solvents are suitable for use in UV spectroscopy Ethanol absorbs very weakly at most wavelengths.)

Solvent polarity and pH can affect the absorption spectrum of an organic compound. Tyrosine, for example, increases in absorption maxima and molar extinction coefficient when pH increases from water-soluble compounds, or ethanol for organic-soluble compounds. (Organic solvents may have significant UV absorption: not all solvents are suitable for use in UV spectroscopy. Ethanol absorbs very weakly at most wavelengths.) Solvent polarity and pH can affect the absorption spectrum of an organic compound. Tyrosine, for example, increases in absorption maxima and molar extinction coefficient when pH increases from 6 to 13 or when solvent polarity decreases. While charge transfer complexes also give rise to colors, the colors are often too intense to be used for quantitative measurement.

The Beer-Lambert law states that the absorbance of a solution is directly proportional to the concentration of the absorbing species in the solution and the path length. Thus for a fixed path length, UV/Vis spectroscopy can be used to determine the concentration of the absorber in a solution. It is necessary to know how quickly the absorbance changes with concentration. This can be taken from references (tables of molar excitation coefficients), or more accurately, determined from a calibration curve.

An UV/Vis spectrophotometer may be used as a detector for HPLC. The presence of an analyte gives a response assumed to be proportional to the concentration. For accurate results, the instruments response to the analyte in the unknown should be compared with the response to a standard; this is very similar to the use of calibration curves. The response (e.g., peak height) for a particular concentration is known as the response factor.

The wavelengths of absorption peaks can be correlated with the types of bonds in a given molecule and are valuable in determining the functional groups within a molecule. The Woodward-Fieserrules, for instance, are a set of empirical observations used to predict λ_{max} , the wavelength of the most intense UV/Vis absorption, for conjugated organic compounds such as dienes and ketones. The spectrum alone is not. however, a specific test for any given sample. The nature of the solvent, the pH of the solution, temperature, high electrolyte concentrations, and the presence of interfering Concentration is known as the response factor.

The wavelengths of absorption peaks can be correlated with the types of bonds in a given molecule and are valuable in determining the functional groups within a molecule. The Woodward-Fieserrules, for instance, are a set of empirical observations used to predict λ_{max} the wavelength of the most intense UV/Vis absorption. for conjugated organic compounds such as dienes and ketones. The spectrum alone is not. however, a specific test for any given sample. The nature of the solvent, the pH of the solution, temperature, high electrolyte concentrations, and the presence of interfering substances can influence the absorption spectrum. Experimental variations such as the slit width (effective bandwidth) of the spectrophotometer will also alter the spectrum. To apply UV/Vis spectroscopy to analysis, these variables must be controlled or accounted for in order to identify the substances present.

3.5. FOURIER TRANSFORM INFRARED SPECTROSCOPY:

FTIR spectra were recorded using Perkin Elmer, Spectrum Two. In infrared spectroscopy, IR radiation is passed through a sample and some of it is passed through (transmitted). The resulting spectrum represents the molecular absorption and transmission, creating a molecular fingerprint of the sample. Like a fingerprint, no two unique molecular structures produce the same infrared spectrum. This makes infrared spectroscopy useful for several types of analysis. FT-IR provides

- It can unknown materials
- It can determine the quality or consistency of a sample
- It can determine the amount of components in a mixture.

Fourier transform infrared spectroscopy (FT-IR) is a very interesting tool for the detection of the different functional groups present in a molecule and the identification of organic and inorganic compounds. It also gives important information about the vibration of chemical bonds in a molecule for different frequencies depending on the material and type of bonds. The basic principle of FTIR is "molecular transition between lower and higher vibrational energy levels by the absorption of electromagnetic radiation from the IR region".

In IR, the light of different wavelengths is incident on a sample surface in which different functional groups absorb the incident rays at different wavelengths causing a transition from the ground state to different excited states. During absorption, the molecules start to vibrate or rotate about their axis and peaks are formed at varying wavelengths. Vibrations can involve either a change in bond length (stretching) or bond angle (bending). The fundamental vibrational bands are calculated by the equations, 3N-5 for linear & 3N-6 for non-linear molecules, where N is the number of atoms. These absorption frequencies are helping to identify the type of functional group present in a given sample.

The FT-IR Spectrometers consists of three basic components; radiation source, interferometer and detector. The radiation emerging from a source is passed through an interferometer to the sample before reaching a detector. Upon amplification of the signal, in which high frequency contributions have been eliminated by a filter, then the data are converted to a digital form by an analog to digital converter and transferred to the computer for Fourier transformation.

3.6. SCANNING ELECTRON MICROSCOPY WITH ENERGY DISPERSIVE X-RAY:

Scanning Electron Microscopy, or SEM analysis, provides high-resolution imaging useful for evaluating various materials for surface fractures, flaws, contaminants or corrosion. Through SEM and EDX analysis, our metallurgical experts provide a thorough examination of material properties and give valuable insights to manufacturers.

SEM analysis is a powerful investigative tool which uses a focused beam of electrons to produce complex, high magnification images of a sample's surface topography. Once an area of interest has been identified on the sample and evaluated using SEM, our experts can dive deeper into the detail of the material using energy-dispersive x-ray spectroscopy, or EDX analysis.

Performing a visual analysis of a surface using scanning electron microscopy contributes to the identification of contaminates or unknown particles, the cause of failure and interactions between materials. In addition to surface evaluation, SEM analysis is utilized for particle characterization, such as wear debris generated during mechanical wear testing. The high magnification, high-resolution imaging of our SEM analysis supports the determination of the number, size, and morphology of small particles, allowing clients to understand the wear properties of their material. Energy dispersive x-ray spectroscopy, also referred to as EDX, EDS or EDAX, provides additional understanding of the surface material during the SEM analysis process. EDX analysis is used to acquire the elemental composition of a sample and allows for a more quantitative result than that provided by only SEM analysis. The combination of SEM and EDX analysis offers chemical composition and elemental investigation – providing a comprehensive metallurgical evaluation.

An electron beam with energy of 10–20 keV strikes the conducting sample's surface, causing X-rays to emit from the material, and the energy of the emitted X-rays depend on the material under examination. EDX does not fit under a technique for surface science, as the X-rays are generated in a region of about 2 microns in depth. By moving the electron beam across the material, an image of each element in the sample can be obtained. It generally takes long hours to acquire the images, as the intensity of the X-ray is low. The composition or amount of nanoparticles near and at the surface can be estimated using the EDX, provided they contain some heavy metal ions.

3.6.1. APPLICATIONS:

The SEM is routinely used to generate high-resolution images of shapes of objects and to show spatial variations in chemical compositions.

- Acquiring elemental maps or spot chemical analyses.
- Discrimination of phases based on mean atomic number (commonly related to relative density)
- Compositional maps based on differences in trace element “activators” (typically transition metal and rare earth elements)

Precise measurement of very small features and objects down to 50nm in size is also accomplished using the SEM. Back scattered electron images can be used for rapid discrimination of phases in multiphase samples. SEMs equipped with diffracted backscattered electron detectors can be used to examine micro fabric and crystallographic orientation in many materials.

CHAPTER IV

CHAPTER IV

RESULT AND DISCUSSION

4.1. Introduction

The modified Hummers method is used to prepare Graphene oxide nanoparticles. In this present work, the GO nanoparticles are subjected to XRD, UV, FTIR and SEM analysis.

4.2. Characterization using XRD

In this present investigation, XRD is used to analyse the crystal structure and verify the interplanar spacing of Graphene oxide nanoparticles. The strong high intense peaks are observed at $2\theta=26.6821^0$ along the (0 0 2) hkl plane, $2\theta=42.3686^0$ along the (1 0 0) hkl plane and $2\theta=77.6609^0$ along the (1 1 0) hkl plane respectively which are shown in Fig.4.1

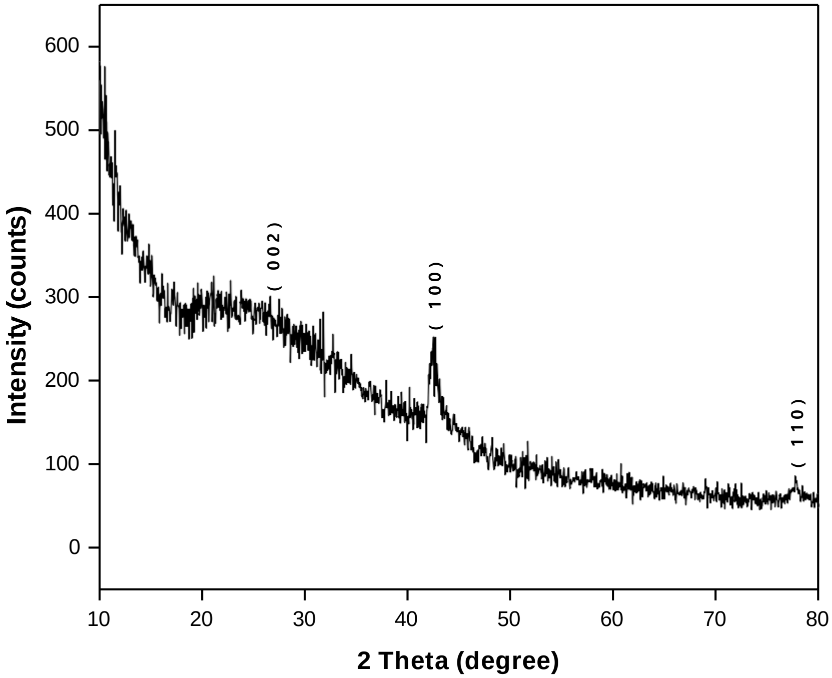

Fig.4.1. XRD pattern of Graphene oxide nanoparticles

The d-spacing values are in good agreement with the standard d –spacing values as confirmed with the JCPDS file no.25-284. From this data it is concluded that the as prepared Graphene oxide nanoparticles exhibit hexagonal structure. The standard and observed d-spacing values are presented in table.4.1

Table 4.1. Comparison of Observed d –Spacing values with JCPDS d – spacing values of as prepared Graphene oxide nanoparticles

S.No.	Observed d-spacing (Å)	JCPDS d-spacing (Å)	Observed 2θ (degree)	Hkl
1.	3.3411	3.3553	26.6821	0 0 2
2.	2.1333	2.1319	42.3686	1 0 0
3.	1.2295	1.2309	77.6609	1 1 0

From these experimental data, the average size of the GO nanoparticles are found out using the Debye Scherrer formula, $D=k\lambda/\beta \cos\theta$.The size of the particle is D=7nm. The average dislocation density is $\delta=5.7067\text{x}10^{15}$ lines/sq.m.

4.3. Characterization using UV

The analysis of UV-VIS absorbance spectra of the as prepared Graphene oxide nanoparticles are shown in Fig.4.2.It is indicated that graphene oxide possessed a good absorption. The maximum absorbance takes place in the region of 202nm range. The rest of the samples do not show any peaks, which is explained by reduction and substitution of oxygen functionalities.

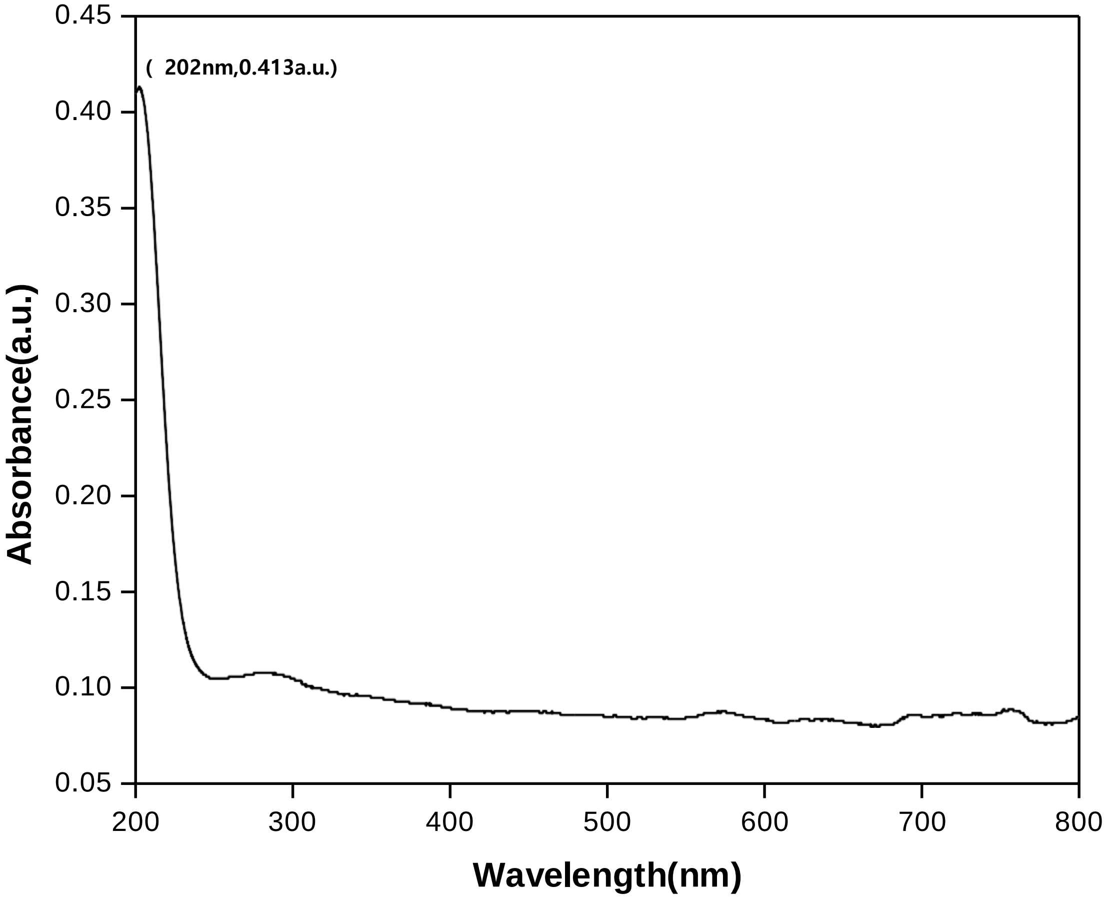

Fig.4.2. UV absorbance spectra of as prepared Graphene Oxide nanoparticles.

4.4. Characterization using SEM

The morphology of Graphene oxide nanoparticles have been investigated using SEM analysis. The images are as shown in Fig 4.3 and Fig.4.4

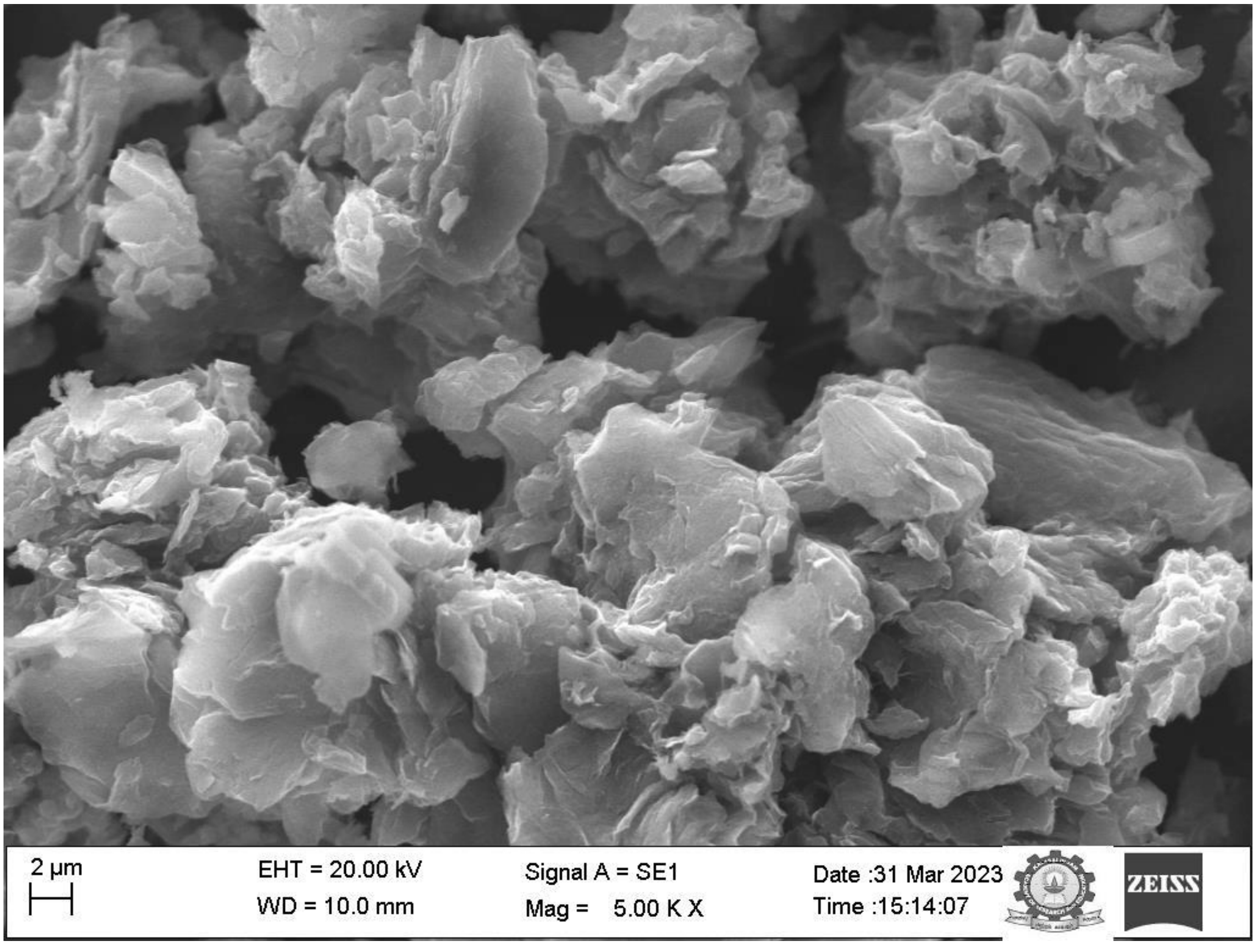

Fig.4.3 SEM image of as prepared Graphene oxide nanoparticles

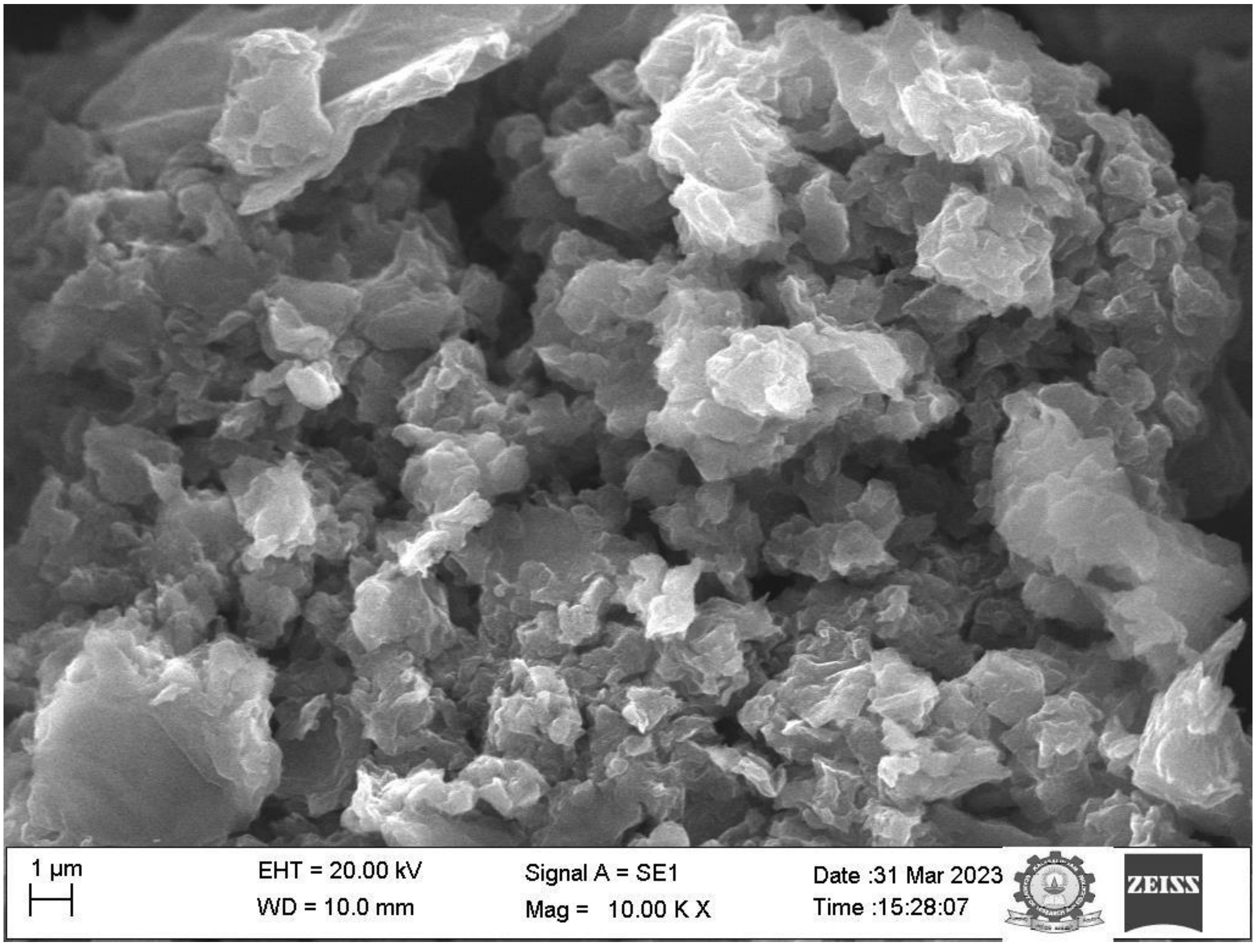

Fig.4.4 SEM image of as prepared Graphene oxide nanoparticles

The surface images of Graphene oxide nanoparticles show flower structure with pores. The particles are essentially formed as clusters which indicates the crystalline nature of the particles. The observation of some larger nanoparticles may be attributed to the fact that the particles have the tendency to agglomerate due to high surface energy of ultrafine particles.

4.5. Characterization using EDAX

The EDAX analysis shows that the final precipitate only contains C and O, indicating high purity of GO nanostructures and implying that the synthesised nanostructures are made entirely of carbon and oxygen nanoparticles. According to the EDAX report, the wt% of oxygen was 44.3 and Carbon was 55.7 percent which is close to the bulk GO weight percent. The EDAX spectrum is as shown in Fig. 4.5

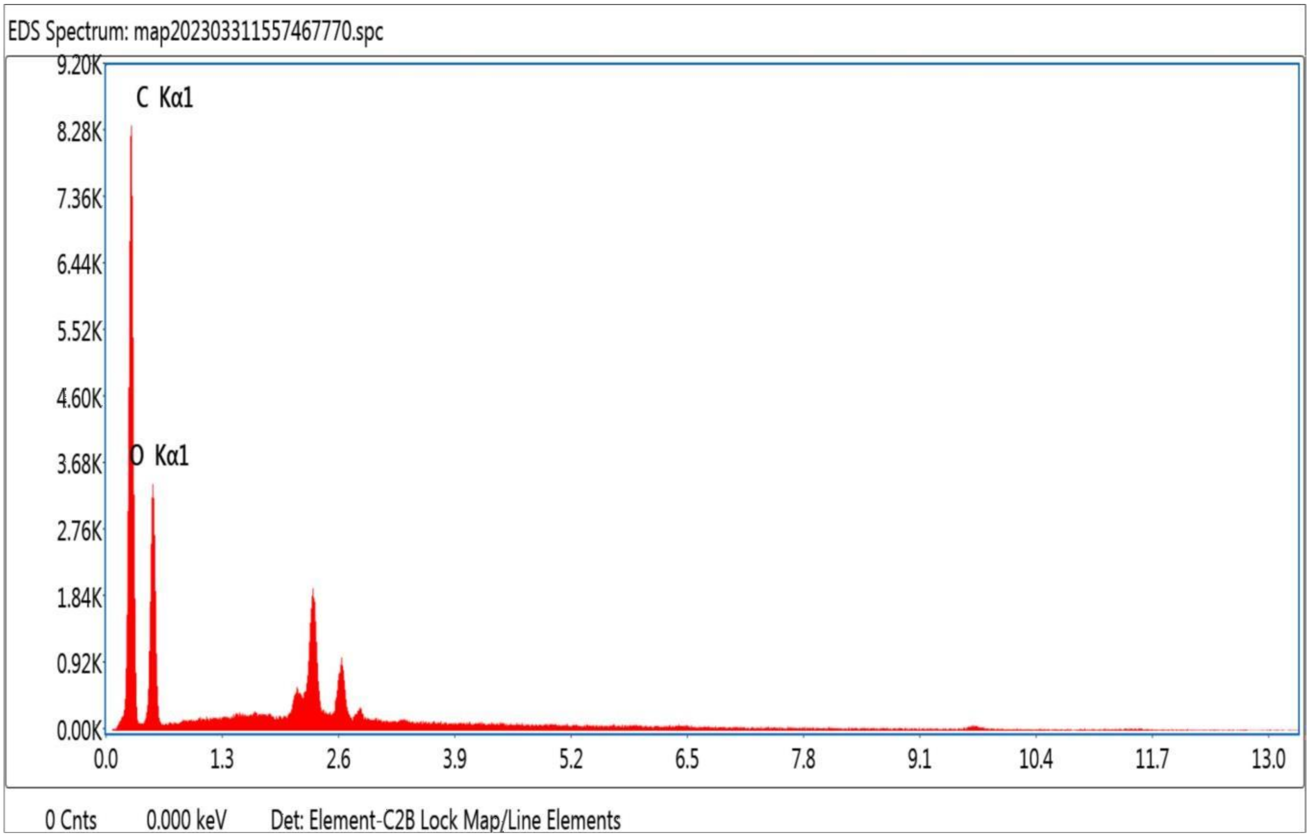

Fig.4.5 EDAX spectrum of as prepared Graphene oxide nanoparticles

CHAPTER-V

CHAPTER V

SUMMARY AND CONCLUSION

In this research work, pure GO nanoparticles are synthesised using modified Hummer’s method. The GO nanoparticles are subjected to XRD, UV, SEM and EDAX analysis to study the structural, optical and morphological properties of the GO nanoparticles. XRD studies clearly indicates that the particles are in nanorange. The average size of the particles are found using Debye Scherrer formula. The average size of the particle is found to be 7nm. It also exhibits hexagonal structure which is confirmed with JCPDS file no.25-284.From UV studies reveals that the as prepared GO possess good absorbance. The surface images of Graphene oxide nanoparticles show flower structure with pores which indicates the crystalline nature of the particles. EDAX spectrum shows the Carbon and Oxygen peaks which indicates the formation of GO nanoparticles.

VI. REFERENCE:

1. G. Schmid, (2004) Nanoparticles from Theory to Applications, Wiley-VCH, Weinheim.
2. R. Paull, J. Wolfe, P. Hébert, M. Sinkula, Nature Biotechnol., 21 (2003) 1144
3. B.S. Murthy, P. shankar and Baldev Raj; (2012), Text Book of Nanoscience and Nanotechnology.
4. J. H. Lee, Sensor and Actuat. B, 140 (2009) 319.
5. V. H. Grassian, J. Phys. Chem. C, 112 (2008) 1830
6. A. Roucoux, J. Schulz, H. Patin, Chem. Rev., 102 (2002) 3757.
7. Ying Wang; Nanostructures and Nanomaterials, Volume 2.
8. E.H. Sujiono, Zurnansyah, D. Zabrian Et al., (2020) “Graphene oxide-based coconut shell waste: synthesis by modified Hummer’s method and characterization”.
9. Francy Mayoli Casallas Caicedo, Enrique Vera Lopez, Et al., (2020) “Synthesis of graphene oxide from graphite by ball milling”.
10. Guillermo Santamaraa-Juarez, Estela Gomez-Barojas, Et al., (2019) “Safer modified Hummers’ method for the synthesis of graphene oxide with high quality and high yield.”
11. Yonggang Houa, Shenghua Lva, Leipeng Liua, Xiang Liua, (2019) “High-quality preparation of graphene oxide via the Hummers' method: Understanding the roles of the intercalator, oxidant, and graphite particle Size.”
12. Elvin Aliyev, Volkan Filiz, Muntazim. M., Khan, Young Joo Lee, Clarissa Abetz, and Volker Abetz, (2019) “Structural Characterization of Graphene Oxide: Surface Functional Groups and Fractionated Oxidative Debris.”

13. Nagi M. El-Shafaia, Mohamed E. El-Khouly, Maged El-Kemary, Mohamed S. Ramadana, Aly S. Derbalahe, Mamdouh S. Masouda, (2018) "Fabrication and characterization of graphene oxide–titanium dioxide nanocomposite for degradation of some toxic insecticides." Vol = 69, PP=315-323.
14. Jose Antonio Luceno-Sanchez, Georgiana Maties, Camino Gonzalez-Arellano, and Ana Maria Diez-Pascual, (2018) "Synthesis and Characterization of Graphene Oxide Derivatives via Functionalization Reaction with Hexamethylene Diisocyanate." Vol=8, PP=870.
15. Zehra Durmus, Belma Zengin Kurt, and Ali Durmus, (2018) "Synthesis and Characterization of Graphene Oxide/Zinc Oxide (GO/ZnO) Nanocomposite and Its Utilization for Photocatalytic Degradation of Basic Fuchsin Dye." Vol=4, PP=271-278.
16. Myung Jin Yoo, and Ho Bum Park, (2018) "Effect of Hydrogen Peroxide on Properties of Graphene Oxide in Hummers Method."
17. N.I. Zaabaa, K.L. Fooa, U. Hashima, S.J.Tanb, Wei-Wen Liua, C.H. Voona, (2017) "Synthesis of Graphene Oxide using Modified Hummers Method: Solvent Influence." Vol = 184, PP = 469-477.
18. Mona M. M. Alyobi, Chris J. Barnett and Richard J. Cobley, (2017) "Effects of Thermal Annealing on the Properties of Mechanically Exfoliated Suspended and On-Substrate Few-Layer Graphene." Vol=7, PP=349.
19. Neeru Sharma, Vikas Sharma, Yachana Jain, Mitlesh Kumari, Ragini Gupta, S. K. Sharma, and K. Sachdev, (2017) "Synthesis and Characterization of Graphene Oxide (GO) and Reduced Graphene Oxide (rGO) for Gas Sensing Application."

20. Md. Sajibul Alam Bhuyan, Md. Nizam Uddin, Md. Maksudul Islam, Ferdaushi Alam Bipasha, Sayed Shafayat Hossain, (2016) "Synthesis of graphene." Vol=6, PP=65-83.
21. Huitao Yu, Bangwen Zhan, Chaoke Bulin, Ruihong Li & Ruiguang Xing, (2016) "High-efficient Synthesis of Graphene Oxide Based on Improved Hummers Method." Vol=6, PP=36-143.
22. Jie Chen, Yadong Li, Yin Zhang, Yangguang Zhu, (2015) "Preparation and characterization of graphene oxide reinforced PVA film with boric acid as crosslinker."
23. Harish V. Kumar, Steven J. Woltornist, Douglas H. Adamson, (2015) "Fractionation and characterization of graphene oxide by oxidation extent through emulsion stabilization." Vol=98, PP=491-495.
24. Jesus Guerrero-Contreras, F. Caballero-Briones, (2015) "Graphene oxide powders with different oxidation degree, prepared by synthesis variations of the Hummers method." PP=1-12.
25. *Jiade Li1, Longfu Wei1, Changlin Yu1, Wen Fangl, Yu Xie, Wanqin Zhou, Lihua Zhu, (2015) "Preparation* and Characterization of Graphene Oxide/Ag2CO3 Photocatalyst and Its Visible Light Photocatalytic Activity."
26. Mahdie Safarpour, Vahid Vatanpour, Alireza Khataee, (2015) "Preparation and characterization of graphene oxide/TiO2 blended PES nanofiltration

    a. membrane with improved antifouling and separation performance."
27. Farnosh Tavakoli, Masoud Salavati-Niasari, Alireza badiei, Fatemeh Mohandes (2015) "Green synthesis and characterization of graphene nanosheets." Vol=63, PP=51-57.

28. Jianguo Song, Xinzhi Wang, and Chang-Tang Chang (2014) “Preparation and Characterization of Graphene Oxide.” Vol=2014, PP= 6 pages.
29. Ning Cao and Yuan Zhang (2014) “Study of Reduced Graphene Oxide Preparation by Hummers’ Method and Related Characterization.” Vol=2015, PP=5 pages.
30. Erkka J. Frankberga, Lijo Georgea, Alexander Efimova, Mari Honkanena, Jenni Pessib & Erkki Levänena (2014) “Measuring Synthesis Yield in Graphene Oxide Synthesis by Modified Hummers Method.” Vol=23, PP=755-759.
31. F Perrozzi, S Prezioso and L Ottaviano (2014) “Graphene oxide: from fundamentals to applications.” Vol=27, PP=21.
32. Ibrahim Karteria, ukru Karatas, Fahrettin Yakuphano glu. (2014) “Electrical characterization of graphene oxide and organic dielectriclayers based on thin film transistor.”
33. Jiade Li, Longfu Wei, Changlin Yu, Wen Fang, Yu Xie, Wanqin Zhou, Lihua Zhu. (2014) “Preparation and Characterization of Graphene Oxide/Ag2CO3 Photocatalyst and Its Visible Light Photocatalytic Activity.”
34. Mithilesh Yadav, Kyong Yop Rhee, S. J. Park, (2014) “Synthesis and characterization of graphene oxide/carboxymethylcellulose/alginate nanocomposites blends.”
35. Behzad Dehghanzad, Mir Karim Razavi Aghjeh, Omid Rafeie, Akram Tavakoli and Amin Jameie Oskooie (2013) “Synthesis and Characterization of Graphene and Functionalized Graphene via Chemical and Thermal Treatment Methods.”

36. Ji Chen, Bowen Yao, Chun Li, Gaoquan Shi (2013) “An improved Hummers method for eco-friendly synthesis of graphene oxide.” Vol=64, PP=225-229.
37. Yang Yang, Tianxi Liu (2011) “Fabrication and characterization of graphene oxide/zinc oxide nanorods hybrid.” Vol=257, PP=8950-8954.
38. T. Rattana, S.Chaiyakun, N.Witit-anun, N. Nuntawong, P. Chindaudom, S. Oaew,C. Kedkeaw, P. Limsuwan. (2010) “Preparation and characterization of graphene oxide nanosheets.” Vol=32, PP=759-764.
39. Jaemyung Kim, Laura J. Cote, Franklin Kim, Wa Yuan, Kenneth R. Shull, and Jiaxing Huang (2010) “Graphene Oxide Sheets at Interfaces.” Vol=132, PP=8180-8186.
40. Daniela C. Marcano, Dmitry V. Kosynkin, Jacob M. Berlin, Alexander Sinitskii, Zhengzong Sun, Alexander Slesarev, Lawrence B. Alemany, Wei Lu, and James M. Tour (2010) “Improved Synthesis of Graphene Oxide.” Vol=4, PP=4806-4814.
41. Wufeng Chen, Lifeng Yan, Prakriti R. Bangal (2009) “Preparation of graphene by the rapid and mild thermal reduction of graphene oxide induced by microwaves.”
42. Jianfeng Shen, Yizhe Hu, Min Shi, Xin Lu, Chen Qin, Chen Li, and Mingxin Ye (2009) “Fast and Facile Preparation of Graphene Oxide and Reduced Graphene Oxide Nanoplatelets.” Vol=21, PP=3514-3520.
43. W. Gao, (2015) Graphene Oxide: Reduction Recipes, Spectroscopy, and Applications, chapter 1.
44. Ayrat Dimiev, and Laboratory, (2017) Graphene Oxide Fundamentals and Applications, chapter 1.
45. K. N. Andre Geim, Nature Mater **6**, 1 (2007).

46. Hummers, W. S. Offeman, R. E. (1958). "Preparation of Graphitic Oxide". Journal of the American Chemical Society. **80** (6): 1339.
47. Sadri, Rad (2017). "Experimental study on thermo-physical and rheological properties of stable and green reduced graphene oxide nanofluids: Hydrothermal assisted technique". Journal of Dispersion Science and Technology. **38** (9):1302-1310.
48. W. Choi, I. Lahiri, R. Seelaboyina, Y. S. Kang, Solid State Mater. Sci., 35 (2010) 52.
49. Dreyer, D. R.; Park, S.; Bielawski, C. W.; Ruoff, R. S. (2010). "The chemistry of graphene oxide". Chemical Society Reviews. **39** (1): 228–240.
50. Schniepp H. C., Li J.L., McAllister M. J., Sai H., Herrera-Alonso M., Adamson D. H., Prud'Homme R.K., Car R., Saville D. A., Aksay I. A., (2006). "Functionalized Single Graphene Sheets Derived from Splitting Graphite Oxide". The Journal of Physical Chemistry B. **110** (17): 8535–8539.
51. Pandey D., Reifenberger R., Piner R., (2008). "Scanning probe microscopy study of exfoliated oxidized graphene sheets". Surface Science. **602** (9):1607.
52. Eigler S., Dotzer C., Hof F., Bauer W., Hirsch A., (2013). "Sulfur Species in Graphene Oxide". Chemistry: A European Journal. **19** (29): 9490–6.
53. Feicht Patrick, Kunz Daniel A., Lerf Anton, Breu Josef, (December 2014). "Facile and scalable one-step production of organically modified graphene oxide by a two-phase extraction". Carbon. **80**: 229–234.
54. Lerf Anton, He Heyong, Forster Michael, Klinowski Jacek, (June 1998). "Structure of Graphite Oxide Revisited‖". The Journal of Physical Chemistry B. **102** (23): 4477–4482.

55. Szabo Tamas, Berkesi Otto, Forgo, Peter, Josepovits Katalin, Sanakis, Yiannis, and Dimitris Petridis, Dekany Imre (2006-05-04). "Evolution of Surface Functional Groups in a Series of Progressively Oxidized Graphite Oxides". Chemistry of Materials. **18** (11): 2740–2749.
56. Vorrada Loryuenyong, Krit Totepvimarn, et al., (2013) “Preparation and Characterization of Reduced Graphene Oxide Sheets via Water-Based Exfoliation and Reduction Methods”. Volume-2013.

XRD, FTIR AND OPTICAL STUDIES OF FICUS BENGHALENSIS AERIAL ROOT DERIVED COBALT OXIDE NANOPARTICLE

A project work report and submitted to

DEPARTEMENT OF PHYSICS

ST. MARY'S COLLEGE (AUTONOMOUS), THOOTHUKUDI

Affiliated to

MANONMANIAM SUNDARANAR UNIVERSITY,

THIRUNELVELI

In partial fulfilment of the requirements for the award of

MASTER OF SCIENCE IN PHYSICS

Submitted by

P. MANGAIYARKARASI

Reg. No: 21SPPH004

Under the guidance of

Mrs. S. SARAVANA SELVI M.Sc., SET., B.Ed.,

DEPARTMENT OF PHYSICS

ST. MARY'S COLLEGE (AUTONOMOUS),

THOOTHUKUDI.

Re-accredited with 'A+' Grade by NAAC

(2022-2023)

CERTIFICATE

This is to certify that this project work report entitled **“XRD, FTIR AND OPTICAL STUDIES OF FICUS BENGHALENSIS AERIAL ROOT DERIVED COBALT OXIDE NANOPARTICLE”** is submitted to **ST. MARY’S COLLEGE (AUTONOMOUS), THOOTHUKUDI** in partial fulfilment of requirements for the award of **MASTER OF SCIENCE IN PHYSICS** and is a record of work done during the academic year **2022 – 2023** by **P. MANGAIYARKARASI** (Register No: 21SPPH04)

Signature of the Guide

Signature of the Co-Ordinator

Signature of the Director

Director
Self Supporting Courses
St. Mary's College (Autonomous)
Thoothukudi - 628 001.

Lucia Rose

Signature of the principal

Principal
St. Mary's College (Autonomous)
Thoothukudi - 628 001.

Signature of the Examiner

DECLARATION

I hereby declare that the project work report entitled **"XRD, FTIR AND OPTICAL STUDIES OF FICUS BENGHALENSIS AERIAL ROOT DERIVED COBALT OXIDE NANOPARTICLE.** is submitted to **ST. MARY'S COLLEGE, (AUTONOMOUS), THOOTHUKUDI** affiliated to **MANONMANIAM SUNDARANAR UNIVERSITY, THIRUNELVELI** for the award of the degree of Master of Science in Physics is my original work and that no part of this project work report has been submitted for any Degree, Diploma or other similar titles.

P. Mangaiyarkarasi

Station: Thoothukudi

Signature of the Student

Date: 05.04.2023

(P. MANGAIYARKARASI)

ACKNOWLEGEMENT

On the very outset of this report, I feel obliged to our Almighty for his aid in the completion of this project work successfully.

I wish to record our profound gratitude to our Principal **Dr. Sr. A. S. J. Lucia Rose, M.Sc., B.Ed., M.Phil., PGDCA., Ph.D.** for her motivation.

I sincerely thank our Director of SSC**, Rev. Sr. Josephine Jeyarani, M.A., M.Phil.,** for her encouragement and support.

I wish to thank **Rev. Dr. Sr. JESSIE FERNANDO M.Sc., M.Phil., Ph.D.,** HOD & Associate professor for her inspirational words to complete this project work.

I owe a great deal to Mrs. **P. PADMAVATHI M.Sc., M.Phil., SET.,** SSC Co-Ordinator for supporting me throughout this project work.

I express my sincere thanks to **Mrs. S. SARAVANA SELVI M.Sc., SET., B.Ed.,** for her valuable time and guidance provided throughout for the successful completion of my project.

I am deeply grateful to all the staff members of Department of Physics (SSC) for supporting me in all aspects.

I acknowledge my deep sense of gratitude to my loving parents and friends for being a constant source of motivation.

ABSTRACT

The main objective of nanotechnology is develop and improve every field with nanoparticle which are ultra small in size most importantly they exhibit super sensitivity extraordinary multi functionality and extremely low power consumption along with high surface to volume ratio so the demond of nanoparticle is hiked day by day. Especially, green synthesis of nanoparticle is welcomed due to environmental concern.

Thus the present work aims in producing cobalt oxide nanoparticle using green synthesis method with the help of arial root of ficus benhalensis and the studies XRD, FTIR, UV-vis, PL are planed to examine the synthesized material.

CONTENT

LIST OF TABLES

LIST OF FIGURES

CHAPTER I

1.1INDRODUCTION

Nanotechnologies are the design, characterization, production and application of structures, devices and systems by controlling shape and size at nanometre scale. [1] Nanotechnology is research and technological development at the atomic, molecular or macromolecular level in the length scale of approximately 1-100 nm range, to provide a fundamental understanding of phenomena and materials at the nanoscale and to create and use structures, devices and systems that have novel properties and functions because of their small or intermediate size [2]. The nanotechnology employs many physical and chemical processes to fabricate nano materials with unique properties. Through nanotechnology, we can develop new materials with sizes (at least in one dimension) less than 100 nm. These materials have vast range of applications such as nanomedicine, nanoelectronics, biomaterials, energy production and consumer products. Also, these materials have a variety of applications in agriculture, environment, information, communication and heavy industrys. For example, chemical properties take advantage of the large surface-to-volume ratio for catalysis, interfacial and surface chemistry.[3]

1.2 NANOPARTICLE

Nanoparticles can be defined as objects ranging in size from 1- 100 nm that due to their size may differ from the bulk material. The nanoparticles are of different shape, size and structure. It be spherical, cylindrical, tubular, conical, hollow core, spiral, flat, etc. or irregular and differ from 1 nm to 100 nm in size. The surface can be a uniform or irregular with surface variations. Some nanoparticles are crystalline or amorphous with single or multi crystal solids either loose or agglomerated.[5]

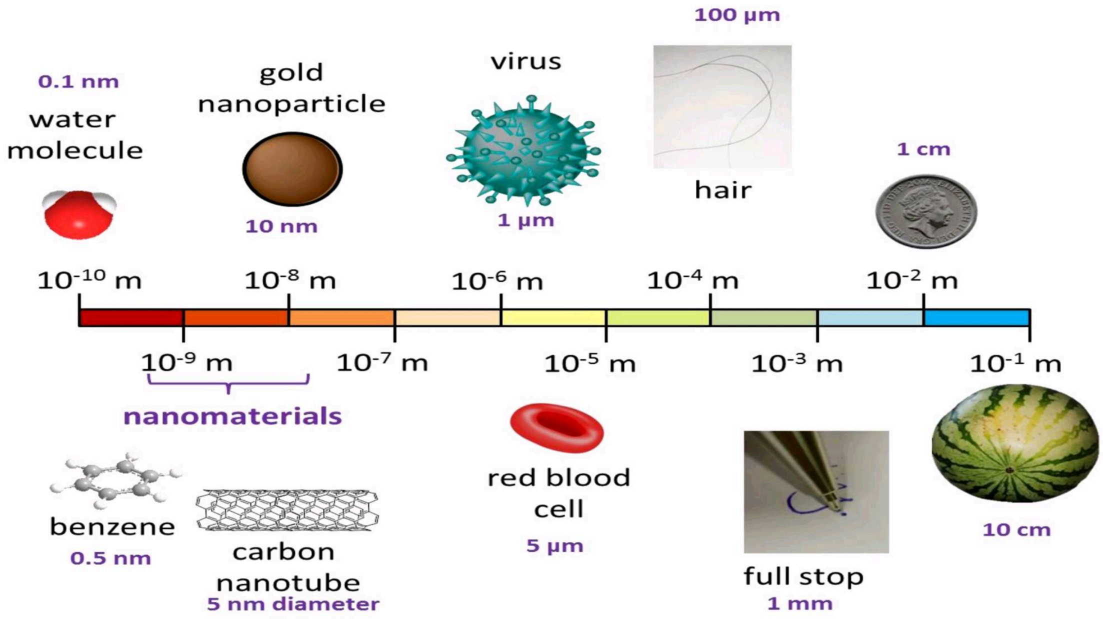

Figure 1.1 Sizes of various objects with nanoparticle

1.3 PROPERTIES OF NANOPARTICLE

Nanoparticles effectively form a bridge between bulk materials and atomic or molecular structures,

➢ Due to small size of nanoparticles, there are more atoms on the surface compared to the interior of the particles, which leads to large surface to volume ratio,

➢ The optical properties of nanomaterials are different from bulk materials of optical absorption peak of a semiconductor nanoparticle shifts to the short wavelength due to an increased band gap,

➢ Nanoparticles often possess unexpected visible properties because they are small enough to confine their electrons and produce quantum effects. For example, gold nanoparticles appear deep red to black in solution,

➢ Nano-size powder particles are potentially important in ceramics, powder metallurgy, in the achievement of uniform nano porosity and similar applications,

➢ When materials are made into nanoparticles their reactivity increase, These more reactive particles can enter the body through the skin, lungs etc,

➢ In optical properties the absorption occurs because electrons are induced by the photons of the incident light which make transitions between the lower lying occupied levels and higher unoccupied levels.[8].

1.4 CLASSIFICATION OF NANOPARTICLE

Classification is based on size is given bellow

- Zero- dimension (0D)
- One- dimension (1D)
- Two- dimension (2D)
- Three- dimension (3D)

1.4.1 ZERO DIMENSION (0D)

- 0D nanomaterials have all the dimension within nanoscale, i.e., no dimension is larger than 100 nm,
- The most commen representation of zero-dimensional nanomaterial is quantum dots.[10].

1.4.2 ONE DIMENSION (1D)

- In one dimensional, one dimension is outside the nanoscale, 1D assembly of functional nanoparticles (NPs) is more difficult to prepare due to its higher surface energy,
- Despite the fabrication difficulty, ID assembly of NPs exhibits many unique properties, and can directionally transport excitons, photons, phonons, so that it generates great interest in considerable applications in biomedicine, data storage, wave guiding, highly sensitive sensor, color display, microcircuits and others,

- 1-D material include nanotubes, nanorodes, and nanowires,

1.4.3 TWO DIMENSIONS (2D)

- In Two dimension, Two dimension is outside the nanoscale , 2D nanomaterial have shape-dependent characteristic and subsequent utilization as bulting blocks for the key components of nano device,
- 2D nanostructure have been investigated and developed their potential application in the filed of sensor, photocatalysts, nanocountainers, nanoreactors and templates for 2D structure of other material,
- This kind of material exhibit plate-like shape and includes graphene and other monolayer material such as black, and diatomic hexagonal boron nitrate.[11].

1.4.4. THREE-DIMENSIONAL NANOPARTICLE

- These are the nanomaterials that are not confined to the nanoscale in any dimension. These materials have three arbitrary dimensions above 100 nm. The bulk (3D) nanomaterials are composed of a multiple arrangement of nano size crystals in different orientations. It includes dispersions of nanoparticles, bundles of nanowires and nanotubes as well as multinanolayers (polycrystals) in which the 0D, 1D and 2D structural elements are in close contact with each other and form interfaces.[9].

1.5 APPLICATIONS OF NANOPARTICLE

Nanotechnology and nanomaterials can be used in all kinds of industrial sectors. They are usually found in the following;

❖ ELECTONICS

Carbon nanotubes are close to replacing silicon as a material for making smaller, faster and more efficient microchips and devices, as well as lighter, more conductive and stronger quantum nanowires. Graphene's properties make it an ideal candidate for the development of flexible touchscreens.

- **Energy**

A new semiconductor developed by Kyoto University makes it possible to manufacture solar panels that double the amount of sunlight converted into electricity. Nanotechnology also lowers costs, produces stronger and lighter wind turbines, improves fuel efficiency and, etc.

- **Biomedicine**

The properties of some nanomaterials make them ideal for improving early diagnosis and treatment of neurodegenerative diseases or cancer. They are able to attack cancer cells selectively without harming other healthy cells. Some nanoparticles have also been used to enhance pharmaceutical products such as sunscreen.

- **Environment**

Air purification with ions, wastewater purification with nanobubbles or nanofiltration systems for heavy metals are some of its environmentally-friendly applications. Nanocatalysts are also available to make chemical reactions more efficient and less polluting.

- **Food**

In this field, nanobiosensors could be used to detect the presence of pathogens in food or nanocomposites to improve food production by increasing mechanical and thermal resistance and decreasing oxygen transfer in packaged products.

- **Textile**

Nanotechnology makes it possible to develop smart fabrics that don't stain nor wrinkle, as well as stronger, lighter and more durable materials to make motorcycle helmets or sports equipment.[11]

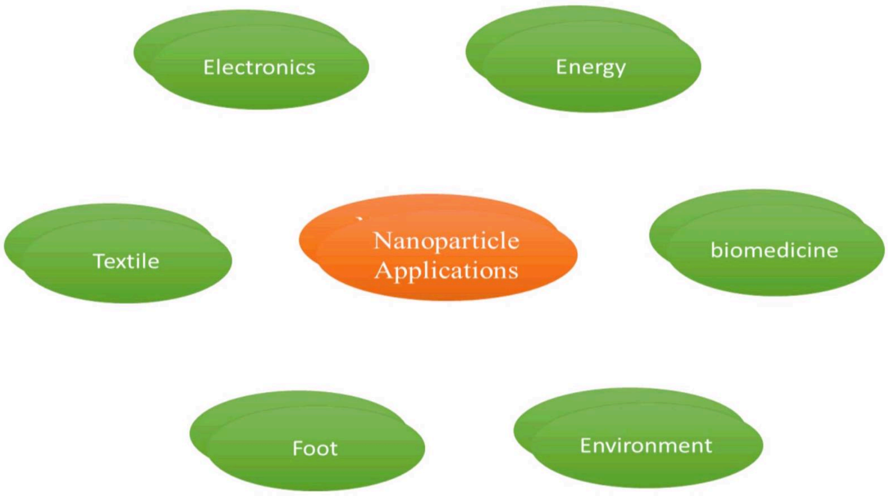

Figure 1.2 application of nanoparticle

1.6 FICUS BENGHALENSIS

The Banyan Tree is considered as the national tree of India. Its botanical name is Ficus Benghalensis. It belongs to the *Moraceae or mulberry* family of the plants. It is a type of plant which grows on another plant by germinating seeds in a crack of a host tree. This process is called *epiphyte*. There are about 800 different varieties of Ficus around the world. It is also called the Indian Fig Tree. This tree grows across a large area. Banyan trees are found in the Indian subcontinent. Some of its are also found in tropical subtropical parts of the world such as Florida. It can be 10–25 meters high. Its branches can span up to 100 meters. It can be seen all around India. Since ancient times it has been an integral part of villages in India. People still gather under these trees and have discussions and chats there. These banyan tree has great importance and it is considered sacred in the Hindu culture. There are many myths and legends associated with this tree. It is considered as the eternal tree.

They can grow very large in size. It has heavy and broad stems. This tree can spread indefinitely. They develop aerial roots from branches. These roots then come down to the ground and take roots in the ground and become trunks. As a result of tangles of roots and trunks a single tree can sometimes become a dense thicket. A banyan tree in **Andhra Pradesh** has the broadest canopy of any tree in the world.

It has large sized- elliptically shaped green leaves. These leaves are glossy and leathery. Young tree leaves are slightly reddish in the beginning. Two large scales cover the leaf buds. The scales abscise as the leaf ages. This tree bears their fruit in the form of *syconium* structure. The syconium of Ficus species provides food and shelter to fig wasps. Fig wasps are responsible for the pollination in the trees.

Figure 1.3 Ficus benghalensis with its aerial root

1.6.1 PROPERTIES OF FICUS BENHALENSIS

- It may show anti-diarrhoeal property,
- It may help with dysentery,
- It may show antidiabetic property,
- It may show anti-inflammatory property,
- It may help boost the immune system,

It may act as a blood purifier.

1.6.2 USE OF FICUS BENHALENSIS

There are multiple uses of the banyan tree. Each part of it can be used.

- It helps soil conservation,
- Its wood is very useful in furniture making. It can be used to make boxes, door panels and well curbs,
- It is also used in paper making,
- Its roots are very strong and are frequently used for tent poles,
- In some parts of India its leaves are used as plates during feasts,[14].

Nutrients	Value
Calories	27 kcal
Carbs	4.5 gm
Fat	0.6 gm
Protein	0.9 gm

Table 1.1 Nutrient values of Ficus benghalensis

1.7 COBALT NITRATE HEXAHYDRATE

Cobalt nitrate is the inorganic compound with the formula Co $(NO_3)_2xH_2O$. It is cobalt(II)'s salt. The most common form is the hexahydrate $Co(NO_3)_2 \cdot 6H_2O$, which is a red-brown deliquescent salt that is soluble in water and other polar solvents. [15].

Chemical formula	$Co\ (NO_3)_2 6H_2O$
Molar mass	291.03 g/mol
Melting point	57^0C
Density	1.88 g/cm^3
Solubility	2170 g/l

Table:2, properties of cobalt nitrate hexahydrate

1.7.1 PREPARATION

The hexahydrate is prepared treating metallic cobalt or one of its oxides, hydroxides, or carbonate with nitric acid;

$Co + 4\ HNO_3 + 4\ H_2O \rightarrow Co(H_2O)_6(NO_3)_2 + 2\ NO_2$

$CoO + 2\ HNO_3 + 5\ H_2O \rightarrow Co(H_2O)_6(NO_3)_2$

$CoCO_3 + 2\ HNO_3 + 5\ H_2O \rightarrow Co(H_2O)_6(NO_3)_2 + CO_2$

1.7.2 USES OF CABALT NITRATE

cobalt nitrate is used in surface treatment (as a corrosion inhibitor), in formulations, water treatment, battery production, petrochemicals, in the manufacture of dyes, glassware, textiles and as a catalyst.[16]

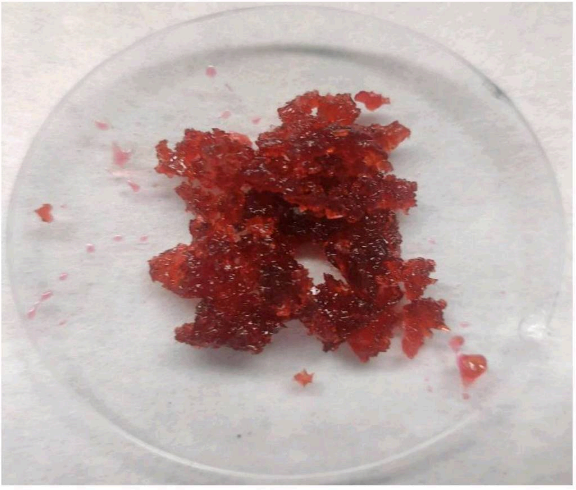

Figure 1.4 cobalt nitrate hexahydrate

1.8 SODIUM HYDROXIDE

Sodium hydroxide is also known as *lye* or *soda*, or *caustic soda*. At room temperature, sodium hydroxide is a white crystalline odorless solid that absorbs moisture from the air. It is a synthetically manufactured substance. When dissolved in water or neutralized with acid it releases substantial amounts of heat. Sodium hydroxide is highly corrosive. Sodium hydroxide is generally used as a solid or a diluted in a 50% solution. This chemical is used to manufacture soaps, rayon, paper, explosives, dyestuffs, and petroleum products. It is also used in processing cotton fabric, laundering and bleaching, metal cleaning and processing, oxide coating, electroplating, and electrolytic extracting. It is commonly found in commercial drain/ oven cleaners. Interestingly, sodium hydroxide has been studied for its use in the treatment of prion disease. [17].

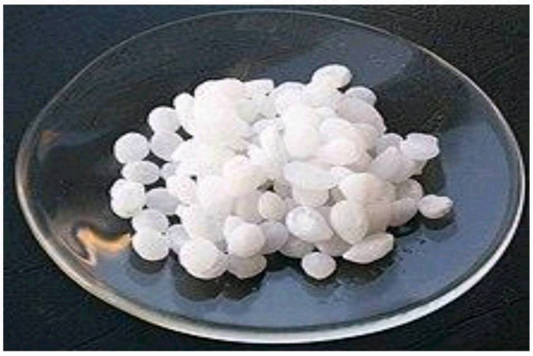
Figure 1.5 sodium hydroxide

1.8.1 PREPARATION OF SODIUM HYDROXIDE

A brine solution is electrolyzed using mercury cathode and carbon anode. Sodium metal, discharged at the cathode, combine with mercury to form sodium amalgam. Cl gas is evolved at the cathode. The amalgam is treated with water to give sodium hydroxide .

Reactions:

$2Na/Hg+2H_2O \rightarrow 2NaOH+H_2+Hg$ [18]

1.8.2 PROPERTIES OF SODIUM HYDROXIDE

- It is a white solid which has a melting point of 591K
- It is a stable compound.
- NaOH is bitter and has a soapy feel to it.
- It is highly soluble in water and moderately soluble in alcohol.
- Sodium hydroxide is strongly alkaline in nature

1.8.3 USES OF SODIUM HYDROXIDE

- In the refining of petroleum and vegetable oils.
- In the purification of bauxite for the extraction of aluminium.
- As a cleansing agent and in washing powder for machines, metal sheets etc.[17]

1.9 OBJECTIVES

- To synthesis cobalt oxide nanoparticle from the aerial root extract of Ficus Benghalensis,
- To analyze the structure of the sample through XRD and to identify the function groups present in sample through FTIR analysis,
- To analyze the optical properties of the sample through UV -Vis, Photoluminescence study.

CHAPTER II

Sirajual Haq et al (2021) [19] Synthesized Co_3O_4 NPs using P. nigrum leaves extract. For the production of nanoparticles, this process is easy, ecologically benign, the most efficient and less expensive. The structure of Co_3O_4 NPs was verified by XRD, and the sample calcined at 100 °C was amorphous. The amorphous phase evolves into a crystalline phase as the calcination rises. The XRD also confirms the cubic geometry of synthesized Co_3O_4 NPs. Because of the increase in particle size, the band gap energy decreases with temperature. The antibacterial activity of produced Co_3O_4 NPs was tested against Gram negative and Gram-positive bacteria, and the activity against Gram negative bacteria was shown to be quite strong. The antioxidant activity was performed then reduced the toxic effect of ABTS free radicals and the antioxidant activity of Co_3O_4 NPs calcined at 100 °C was significantly high than those calcined at high temperature, which might be due to the increase in particle size.

Mohammadi et.al (2021) [20] Made use of walnut green skin extract containing a high amount of phenolic compound, as a reducing agent to synthesize cobalt oxide. The nanoparticle were prepared by green synthesis identified and analyzed by SEM, XRD, FTIR, and VSM. The results of the scanning electron microscopy show that the nanoparticles were 80 nanometers in size. XRD studies showed that synthesized nanoparticles have a cubic crystal structure and an Fd3m group. Measuring the magnetic properties of the cobalt oxide nanoparticles synthesized by the VSM indicated that the synthesized nanoparticles had super-magnetic properties. The systematic study of the process was performed using Design Expert 10 software to determine the relationship between the four process variables, namely cobalt concentration, extract volume, time, and temperature effect. The square model was significant for the response variables. The optimum green synthesis parameters for producing Co_3O_4 nanoparticles are the cobalt nitrate (50 mmol), extract volume (10 ml), time (92 min), and temperature (53ºC). The SEM image showed that the sizes of the synthesized Co_3O_4 NPs ranged from 60 to 80 nm**.**

Kainat et.al (2021) [21] A facile and nonhazardous synthesis of Co_3O_4-NPs and MgONPs was reported using aqueous leaf extract of Hibiscus rosa sinensis as a potential reducing and stabilizing source. The FTIR analysis confirmed the successful capping of naturally occurring phyto constituents of the plant extract. The morphological examination via SEM and TEM showed the mean size of 27.72 for MgO-NPs and 18.98 for Co3O4-NPs. The NPs were investigated for multifaceted biological applications including bactericidal activity against urinary tract infection (UTI) isolates, leishmaniasis, larvicidal, antidiabetic antioxidant and biocompatibility studies. Our studies revealed that both the NPs were highly active against multidrug resistant UTI isolates as compared to traditional antibiotics. Both the NPs, in particular Co_3O_4-NPs also showed significant larvicidal and leishmanicidal activities against the Aedes Aegypti, the mosquitoes involve in the transmission of Dengue fever and lesihmaniatropica, respectively. Furthermore, the NPs significantly inhibited a-amylase and a-glucosidase, the key enzymes involved in the onset of Diabetes Mellitus (DM). Last but not least, the nonhazardous and biocompatible nature, make the Hibiscus rosa sinensis synthesized Co_3O_4-NPs and MgO-NPs as green, inexpensive and potential alternatives to be exploited as for biomedical applications.

Melvin S. Samuel et.al (2020) [22] Studied the GCoO-NPs were synthesized productively using the Jumbo Muscadine grape pulp extract (*Vitisro tundifolia*) and their structure were elucidated using XRD, FT-IR, UV–Vis spectrometry and SEM. The GCoO-NPs showed degradation 60 mg/100 mL concentration of AB-74 within 150 min (degradation with a rate constant of 0.043 min^{-1}). The dye degradation rates were extremely delicate to pH and worked best in the alkaline conditions. Further analysis is necessary to evaluate the degradation products to well comprehend the different decolorization mechanisms (adsorption vs degradation) for various azo dyes. Therefore, the synthesized GCoO-NPs had an excellent photocatalytic activity and the vital biological components in the NPs can treat microbesin future applications.

Muhamod hafeez et.al (2020) [23] Studied the synthesised Cobalt oxide nanoparticles (Co_3O_4-Nps) In this study, Co3O4-Nps were synthesized by using leaves extract of Populus ciliata (safaida) and cobalt nitrate hexahydrate as a source of cobalt. The prepared nanoparticles, were analyzed by various techniques such as FTIR, XRD, TEM and SEM. These techniques revealed the successful synthesis of cobalt oxide nanoparticles. Antibacterial activities of synthesized cobalt oxide nanoparticles were analyzed agaist gram positive and gram nagetive bacteria and it was found that by increasing concentation of cobalt oxide nanoparticles, antibacterial activity was increased**.**

Neda Akhlaghi et.al (2020) [24] Studied the synthesised Co_3O_4-Nps. In the current contribution, fenugreek leaves extract was successfully used for the synthesis of Co_2O_4 NPs. According to obtained results, high alkaline pH acts a critical role in the formation of cobalt NPs using biogenic compounds extracted from plant leaves. This factor significantly affects the crystallographic structure, and purity of the prepared NPs. Based on various advanced techniques were herein used, the obtained cobalt NPs possess high thermal stability, uniform hydrodynamic size distribution, high purity, and crystallite structure. The proposed biosynthetic process can be used to produce large quantities of Co_3O_4 NPs as a novel promising alternative to common chemical synthesis methods.

Suba A. Memon et.al (2020) [25] Synthesised and studied the Co_3O_4-Nps In this study, we have demonstrated a bio and eco-friendly protocol for the synthesis of Co_3O_4 NPs. The biogenic NPs were then characterized through versatile range of characterization techniques including XRD, SEM, EDS, UV–vis and DRS. Furthermore, the NPs were used to modify the GCE using Nafion as a binding agent making NPs sandwiched between itself and GCE surface. These NPs worked as catalytic current producers and enhanced the detection peak current response, resulting in the development of a sensitive electrode for tramadol drug detection. The electrochemical method is advantageous over other reported analytical methods due to their sensitivity, reproducibility, rapidity and accuracy. Using the modified GCE, under optimized parameters, the determination of tramadol was obtained with linear range of 0.5–45 μM and detection limit of 0.001 μM. The beautification of Nafion/Co3O4/GCE can provide excellent electrochemical stages due to combination of distended active surface area, strong adsorptive capability of the NPs and their specific interactions.

Murugan Perachiselvi et.al (2020) [26] Synthesised Co_3O_4 nanoparticles. formation of Co_3O_4 NPs is confirmed from XRD, further FTIR technique determines the functional group. The strong band of Co_3O_4 NPs was appeared below 690 cm^{-1}. SEM analysis reveals various particle sizes with a spherical shape. The average particle size of 478 nm using DLS. EDAX result showed elements of Co_3O_4 NPs. The result reveals as prepared NPs enhance the Cell viability. It depends on the time and concentration of NPs. The Cytotoxicity study result showed Co_3O_4 Nps less toxicity as well as biocompatibility and can be used for clinical purpose application.

Rajan Lakra et.al (2020) [27] Studied, cobalt oxide (Co_3O_4) nanoparticles have been synthesized using cobalt nitrate as its source by precipitation approach. The structural properties of the synthesized Co_3O_4 nanoparticles were studied using X ray diffraction (XRD). The XRD results confirm the crystalline nature of the nanoparticles. Further, scanning electron microscopy (SEM) was also performed to study the morphology of the synthesized Co_3O_4 nanoparticles. SEM micrograph shows that the Co_3O_4 nanoparticles are somewhat sphere like morphology and they are interlinked with each other.

Qing-Yun Chen et.al (2020) [28] Through an environmentally friendly and inexpensive method, of Co_3O_4 nanoparticles synthesize using the bread fungus as green materials. These nanoparticles calcined at 500°C had the smallest grain size, the uniform distribution, and the best light absorption. Furthermore, Co_3O_4 nanoparticles were used as a photocatalyst for overall water splitting under visible light irradiation without any cocatalyst and sacrificial agent. The evolution rates of the hydrogen and the oxygen increased by increasing the photocatalytic temperature, and the ratio of the hydrogen to oxygen is close to 2:1. In addition, Co_3O_4 photocatalyst had a good stability. Especially, Co_3O_4 calcined at 500°C showed a good photocatalytic performance. With in 5 h, the amount of hydrogen and oxygen is 259.4 and 135.7 $\mu molg^{-1}$, respectively. Therefore, the green synthesis of cobalt oxide is a promising method for overall water splitting.

S. Nallusamy et.al (2020) [29] Synthesised of cobalt oxide nano particles by co precipitation technique for electrochemical sensing of cholesterol in blood and the as-synthesized samples were characterized by FTIR and TEM techniques. 1.From the results it was observed that, the TEM of Co3O4 nanoparticles bring out the spherical agglomerate elements. The electrochemical belonging of cobalt oxide nanoparticles was examined with cyclic voltammetry. From the final observed results it was concluded that, the cobalt oxide nanoparticles have elevated electro-activity. The high conductivity of the nano particle makes it suitable for sensing the level of cholesterol in the analyte.

Onwudiwe et.al (2020) [30] Synthesised hydroxide and oxide forms of cobalt nanoparticle using Litchi cinensis. Our studies presented a facile green and cost effective synthesis of cobalt hydroxide $(Co(OH))_2$ and cobalt oxide (Co_3O_4) nanoparticles using the extract derived from Litchi cinensis, which provided the phytochemical compounds required for an environmental friendly route, to nanoparticles synthesis. The adopted methods involved two routes: boiling the aqueous solution of the fruit peel extract and precursor compound, and by microwave irradiation of the solution. The synthesized cobalt hydroxide were stable, well dispersed, spherical in shape and with size in the range of 26–40 nm, while the cobalt oxide showed an elongated rod-like morphology. The materials' characterization demonstrated that the synthesis approach impacted on both microscopic dimensions and crystallinity. In view of ecofriendly and cost-effective route, the present studies revealed that Litchi chinensis could be well utilized for the synthesis of well dispersed cobalt hydroxide and cobalt-oxide NPs, and may also be extended to other hydroxide and oxide forms of transition metals.

Kgosiemang et.al (2020) [30] Studied, the utilization of E. tirucalli aerial plant extract in green synthesis of MgO NPs and CoO NPs was successful. The secondary metabolites present in the aerial parts of E. tirucalli contained phytochemical constituents necessary to reduce cobalt and magnesium precursors to cobalt and magnesium oxide nanoparticles. The Hex and DCM extracts of E. tirucalli showed moderate anti-proliferative activity against MCF-7 breast cancer cells. On comparison, increased anti-proliferative activity was observed with CoO NPs. It is recommended that the Hex and DCM extracts as well as the CoO NPs be screened against a noncancerous breast cancer cell line to evaluate toxic selectivity of these extracts and nanoparticles against normal cells. This study is the first to report on synthesis of MgO NPs and CoO NPs from the aerial parts E. tirucalli, and their anti-proliferative activity against MCF-7 breast cancer cell lines, and has broaden the knowledge of possible biomedical applications of green cobalt and magnesium oxide nanoparticles.

Nur Oktri Mulya Dewi et.al (2019) [31] Synthesised and studied Co_3O_4 NPs was successfully synthesized by *Euphorbia heterophylla* L. leaves extract (ELE) which contained alkaloid as a weak base source for Co3o4 NPs synthesis. FT-IR spectrometry showed the presence of Co (II)-O and Co (III)-O bond at the wavenumber of 574 and 699 cm^{-1}, respectively. UV/Vis Spectroscopy indicated the typical peak of Co_3O_4 NPs was found at the maximum wavelength range of 200-350 and 380-600 nm. The particle size distribution of Co_3O_4 NPs was 69.75 nm. XRD result of Co_3O_4 NPs had the 2θ diffraction peaks at of 31.1953°; 38.5401°; 44.8076°; 50.2027°; 59.2743° and 65.1419°. The Co_3O_4 NPs band gap energy was 1.53 eV. TEM image showed that morphology of Co_3O_4 NPs was spherical shaped with the size of particle about ~17 nm. The photocatalytic activity of Co_3O_4 NPs was carried out for the methylene blue degradation in 63.105% under irradiation of visible light for 3 hours.

B.A Omaran et.al (2019) [32] Investigated the capability of Aspergillus brasiliensis ATCC 16404 to mycosynthesize Co_3O_4-NPs. Methods and Results: Mycelial cell-free filtrate of A. brasiliensis ATCC 16404 was applied for mycosynthesis of Co_{3O}4-NPs. The preliminary indication for the formation of Co_3O4-NPs was the change in colour from yellow to reddish-brown. One-factor-at a time-optimization technique was applied to determine the optimum physicochemical conditions required for the mycosynthesis of Co_3O_4-NPs and they were found to be: 72 h for reaction time, pH 11, 30°C, 100 rev min _1 for shaking speed in the darkness using 4 mmol l _1 of $CoSO_4$.7H2O and 5_5% of A. brasiliensis dry weight mycelium (w/v). The mycosynthesized Co_3O_4-NPs were characterized using various techniques: spectroscopy including UV/Vis spectrophotometry, dynamic light scattering (DLS), zeta potential measurement, energy-dispersive X-ray analysis, Fourier transform infrared spectroscopy and Xray diffraction; and vibrating sample magnetometry and microscopy including field emission scanning electron microscopy and high-resolution transmission electron microscopy. Spectroscopic techniques confirmed the formation of Co_3O_4- NPs and the microscopic ones confirmed the shape and size of the mycosynthesized Co3O4-NPs as quasi-spherical shaped, monodispersed nanoparticles with a nano size range of 20–27 nm. The mycosynthesized Co_3O_4 NPs have excellent magnetic properties and exhibited a good antimicrobial activity against some pathogenic micro-organisms.

Siddique et.al (2019) [33] Studied the green and eco-friendly synthesis and characterization of cobalt oxide nanoparticles using leaf extract of Citrus medica plant. The crystalline nature and functional groups analysis of cobalt oxide Nps was confirmed by X-ray diffraction and diffused reflectance infra-red spectroscopy respectively. The band gap of the Nps was calculated using Tauc plot. Scanning microscope analysis was carried out to get an insight to the structural morphology of the catalyst. The catalyst was found to be very active for the degradation of methyl orange dye using a very small amount of catalyst (0.006 g) using ultra violet radiation source. Approximately, 90% of the dye (Initial Conc. 10 mg L^{-1}) was degraded in 60 min at natural pH (6.5). The dye degradation increased with increase in pH of the solution, due to the enhanced production of OH radicals, at higher pH values. Different experimental parameters like catalyst amount, agitation speed, initial pH of the solution, initial concentration of dye and recycling of the catalyst were varied to test the performance of the catalyst

P. Saravanakumar et.al (2018) [34] Studied an eco-friendly green synthesis of cobalt oxide nanoparticles using seed extract of piper nigrum was investigated. Synthesized nano Cobalt oxide were characterized using UV-Vis, FT-IR spectroscopic techniques and AFM. UV spectra showed the maximum absorbance of 268 and 305 nm due to the excitation of surface Plasmon vibrations in the cobalt oxide nanoparticles formation. FTIR spectrum exhibited the characteristic band at 704 cm^{-1} which indicated the O-Co-O bridging vibration of Co_3O_4 nanoparticles. Photocatalytic degradation of Crystal violet under UV-irradiation was also investigated. Undoped and Ce ion doped cobalt oxide nanoparticles possess photocatalytic activity while the latter shows enhanced degradation efficiency percentage and can be used as an effective photocatalyst.

N. Matinise et.al (2018) [35] Synthesised, spinel Co_3O_4 nanoparticles through a simple green method using Moringa *oleifera* extract. The electrochemical performances were evaluated by cyclic voltammetry, electrochemical impedance spectroscopy and galvanostatic charge discharge. The loaded spinel Co_3O_4 nanoparticles on nickel foam electrode exhibited an excellent electrochemical performance, and thus could be a promising electrode material candidate for supercapacitors. Owing to its simplicity of synthesis, low cost and excellent electrochemical performance, this green method may hold abundant potential for assembly of other nanostructured electrode materials for high-performance hybrid supercapacitors.

Shikha Dubey et.al (2018) [36] Studied the cobalt oxide nanoparticle. A novel green synthesis of cobalt oxide (Co_3O_4) nanoparticles using latex of Calotropis procera via simple Precipitation method at room temperature was investigated. An extensive characterization of the product was carried out using X-ray diffractometry (XRD), Differential scanning calorimetry (DSC), Transmission electron microscopy (TEM), Energy dispersive X-ray spectroscopy (EDX), Fourier transform infrared spectroscopy (FTIR) and UV–Visible spectroscopy. The results of the characterization confirmed that the synthesized nanomaterial is highly dispersed. TEM analysis revealed that the nano particles are having an average size around 10 nm. The eco-toxic investigation suggested that the particles are non-toxic and safes towards the environment. This green strategy proves to be an effective, fast, simple and cost-effective approach for the synthesis of Co_3O_4 nanoparticles for various applications.

Ismat Bibi et.al (2017) [37] Synthesised Cobalt oxide NPs using P. granatum peel extract cobalt nitrate hexahydrate at low temperature and characterized by advanced techniques. The synthesized cobalt oxide size was in the range of 40–80 nm. The

PCA was evaluated by degrading RBO 3R dye under solar light irradiation. In response photoactivity of cobalt oxide NPs under solar light irradiation, 78.45% degradation of RBO 3R was achieved within 50 min of irradiation. It can be concluded that the P. granatum peel extract has considerable number of bioactive compounds and able to reduce and stabilize the cobalt oxide NPs. The method is simple and cost effective, which could be used for the synthesis of cobalt oxide NPs in nano-size range. This technique could also be extended for the synthesis of other metal NPs since this method is eco-benign and cost effective**.**

Rama Koyyati et.al (2016) [38] Studied the synthesised cobalt nanoparticles form *Raphanus sativus var. longipinnatus* leaf extract and characterized using various techniques such as UV-visible spectrophotometry, Fourier transform infrared spectrometry and Scanning electron microscopy coupled with Energy dispersive micro analysis. The spectroscopic methods confirmed the formation of cobalt nanoparticles and the microscopic technique confirmed the shape and size of the cobalt nanoparticles as spherical with an average particle size of 80nm. Antibacterial activity of the synthesized nanoparticles was measured by disc diffusion method. The cobalt nanoparticles showed effective antibacterial activity against Gram negative bacteria.

Thi Toan Nguyen et.al (2016) [39] Reduced graphene oxide sheets decorated with cobalt oxide nanoparticles (Co_3O_4/rGO) were produced using a hydrothermal method without surfactants. Both the reduction of GO and the formation of Co_3O_4 nanoparticles occurred simultaneously under this condition. At the same current density of 0.5 A g^{-1}, the Co_3O_4 /rGO nanocomposites exhibited much a higher specific capacitance (545 F g^{-1}) than that of bare Co_3O_4 (100 F g^{-1}). On the other hand, for the detection of H_2O_2, the peak current of Co_3O_4/rGO was 4 times higher than that of Co_3O_4. Moreover, the resulting composite displayed a low detection limit of 0.62 mM and a high sensitivity of 28,500 mA mM^{-1} cm^{-2} for the H2O2 sensor. These results suggest that the Co_3O_4/rGO nanocomposite is a promising material for both supercapacitor and non-enzymatic H_2O_2 sensor applications.

A. Diallo et.all (2015) [40] Reported on the bio-synthesis and the main physical properties of p-type Co_3O_4 nanoparticles for the first time by a completely green chemistry process using Aspalathus Linearis's natural extract as an effective chelating agent. Their surface/interface and optical properties are reported. In addition to the X-ray diffraction investigations, the Raman, and infrared as well as X-ray photoelectron spectroscopies confirmed the single phase of the Co_3O_4 nanoparticles. As their average size was low as ⟨fparticle⟩ ~3.6 nm, the reticular atomic planes were under a slight compressive state.

M.Yarestani et.al (2014) [41] Cobalt oxide (Co_3O_4) nanoparticles synthesised by hydrothermal method using mixture of cobalt(II)chloride, Triton X-100 and KOH in an autoclave at 180 °C for 6 h followed by heating at 400 ºC for 3 h in air. The product have been characterized by Fourier transform infrared (FT-IR), UV-Vis spectroscopy, powder X-ray diffraction (XRD), scanning electron microscopy (SEM) and transmission electron microscopy (TEM). Optical properties of the Co_3O_4 nanoparticles have revealed the presence of two band gaps, viz. 2.9 and 2.4eV. Data from vibrating sample magnetometer (VSM) confirm the purity of the product along with single phase paramagnetic behavior.

Katalin Sinko et.al (2011) [42] Studied various liquid-phase syntheses of CoO and Co_3O_4. The experiments focus on two synthesis routes: the coprecipitation and the sol–gel methods combined with thermal decomposition. The effect of synthesis route, the type of precursors (cobalt nitrate/chloride) and precipitation agent (carbonate, hydroxide, oxalic acid, and ammonia), the chemical compositions, pH, application of surfactants (PDMS, Triton X-100, NaDS, NaDBS, TTAB, ethyl acetate, citric acid), and the heat treatments on the properties of particles were investigated. The particle size and distribution have been determined by dynamic light scattering (DLS). The phases and the morphology of products have been analysed by XRD and SEM. The coprecipitation technique is less able to shape the particles than sol–gel technique. PDMS can be applied efficiently as surfactant in preparation methods. The finest particles (around 85 nm) with narrow polydispersity (70–100 nm) and spherical shape could be achieved by using sol–gel technique in medium of 1-propanol and ethyl acetate.

Mark Allen et.al (2003) [43] The protein cage of the 12-subunit ferritin-like protein from *Listeria innocu* for the synthesis of two cobalt oxide minerals, Co_3O_4 and Co(O)OH. Reaction of Co(II) with H_2O_2 at pH 8.5 under either elevated temperature (65 °C) or ambient temperature (23 °C) resulted in the formation of cobalt oxide nanoparticles encapsulated within the protein cage. At elevated temperatures, Co_3O_4 was formed while at lower temperature the oxyhydroxide Co(O)OH was found. Mineral particles, commensurate in size with the internal dimensions of the protein (5 nm), were imaged by transmission electron microscopy and shown to be surrounded by the intact protein cage. The minerals were investigated by electron diffraction and revealed a crystalline Co_3O_4 phase and an amorphous Co(O)OH phase. Further investigation of these composite materials using size exclusion chromatography, gel electrophoresis, dynamic light scattering, and *ú* potential measurements indicated that the mineral was encapsulated within the protein cage giving rise to properties of both the mineral and protein component.

CHAPTER III

3.1 METHODS AND METHODOLOGY

About 5g of aerial roost of ficus bengalensis was initially washed, crushed and added with deionized water. Then it was heated at 70^0C-75^0C for 1/2 an hour. Then the heated solution is filtered using Wattmen filter paper. Thus the extract was obtained. IM cobalt nitrate hexahydrate solution is added with extract and the entire solution is allowed to stirrer for ½ an hour. Color of the solution was observed as dark pink color. After an ½ hour, IM NaOH solution is added, to the resultant solution drop by drop. changing of color was observed. Till dark blue formation this was continued 30 minutes stirring was allowed in the solution. After that PH of the solution is checked and found out as 5 then continuous water washing was done. till the reach of neutral PH. For 12 hours the resultant material was kept at hot air oven at 105 °C. The dried material was collected and grained well followed by calcined at 500°C for 3 hours and the sample is collected. At last, 7.079g sample is collected, and named as MMC.

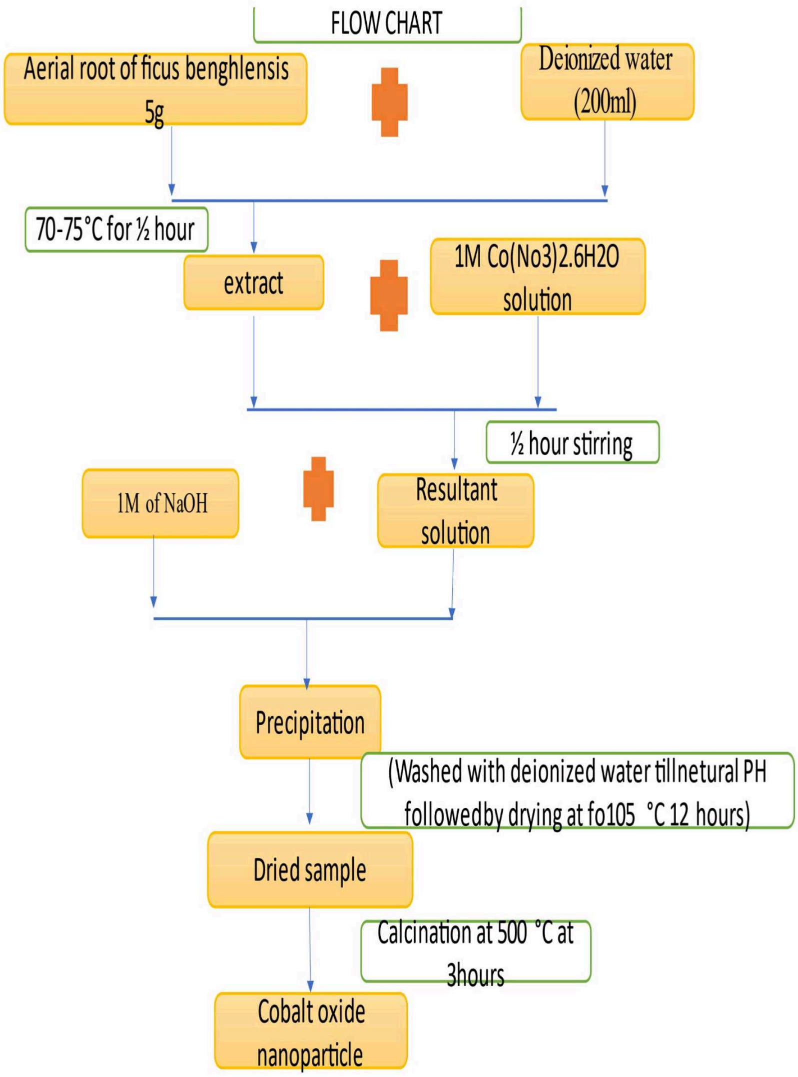
FLOW CHART
Aerial root of ficus benghlensis 5g
Deionized water (200ml)
70-75°C for ½ hour
extract
1M Co(No3)2.6H2O solution
½ hour stirring
1M of NaOH
Resultant solution
Precipitation
(Washed with deionized water tillnetural PH followedby drying at fo105 °C 12 hours)
Dried sample
Calcination at 500 °C at 3hours
Cobalt oxide nanoparticle

3.3 X-RAY DIFFRACTION

Max von Laue and Co., in 1912, discovered that crystalline substances act as three-dimensional diffraction gratings for X-ray wavelengths similar to the spacing of planes in a crystal lattice [43]. X-ray diffraction is now a common technique for the study of crystal structures and atomic spacing. X-ray diffraction is based on constructive interference of monochromatic X-rays and a crystalline sample. These X-rays are generated by a cathode ray tube, filtered to produce monochromatic radiation, collimated to concentrate, and directed toward the sample The interaction of the incident rays with the sample produces constructive interference (and a diffracted ray) when the following conditions satisfy yields the Bragg’s law:

$$n\lambda=2d\sin\theta$$

where n is an integer, λ is the wavelength of the X-rays, d is the interplanar spacing generating the diffraction, and θ is the diffraction angle. This law relates the wavelength of electromagnetic radiation to the diffraction angle and the lattice spacing in a crystalline sample. These diffracted X-rays are then detected, processed, and counted. By scanning the sample through a range of 2θ angles, all possible diffraction directions of the lattice should be attained due to the random orientation of the powdered material. Conversion of the diffraction peaks to d-spacings allows identification of the compound because each compound has a set of unique d-spacings. Typically, this is achieved by comparison of d-spacings with standard reference patterns. [45].

Figure 3.1 XRD Instrument

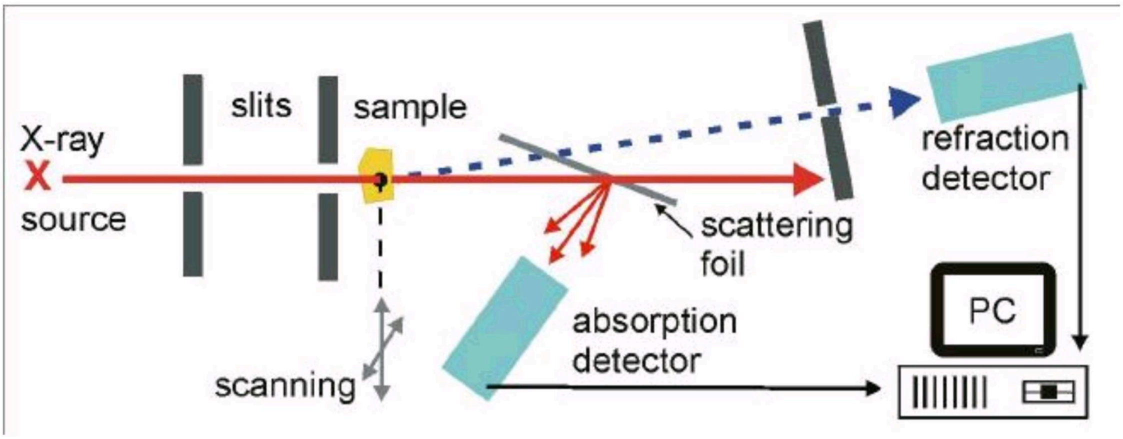

Figure 3.2 process behind the XRD spectrum

3.3.1 APPLICATIONS OF XRD

- Characterization of crystalline materials,

- Identification of fine-grained minerals such as clays and mixed clays that are difficult to determine optically,
- Determinations of unit sell dimensions,
- Measurement of sample purity,
- Determine crystal structures using Rietveld refinement,
- Determine of modal amounts of minerals (quantitative analysis),
- Determining lattice mismatch between film and substrate and to inferring stress and strain,
- Determining dislocation density and quality of the film by rocking curve measurements,
- Measuring super lattices in multi-layered epitaxial structures,
- Determining the thickness, roughness and density of the film using glancing incidence X-ray reflectivity measurements,
- Make textural measurements, such as the orientation of grains, in a polycrystalline sample. [45]

3.4 FOURIER TRANSFROM INFRA-RED SPECTROSCOPY

The instrument that determines the absorption spectrum for a compound is called a spectrophotometer. Fourier transform spectrophotometer provides the IR spectrum much more rapidly compared to the traditional spectrophotometer. Fig. 1.1 schematically illustrates the main component of a simple FTIR spectrophotometer. The instrument produces a beam of IR irradiation, which is emitted from a glowing black-body source. Subsequently, the beam passes through into interferometer where the spectral encoding takes place.[46] The recombination of beams with different in path lengths in the interferometer creates constructive and destructive interference called an interferogram. The beam now enters the samples compartment and the sample absorbs specific frequencies of energy, which are uniquely characteristic of the sample from the interferogram. Then, the detector measures the special interferogram signal in energy versus time for all frequencies simultaneously. In the meantime, a beam is superimposed to provide a reference (background) for the instrument operation. Finally, the desirable spectrum was obtained after the interferogram automatically subtracted the spectrum of the background from the sample spectrum by Fourier transformation computer software. [47]

Figure 3.3: FTIR Instrument.

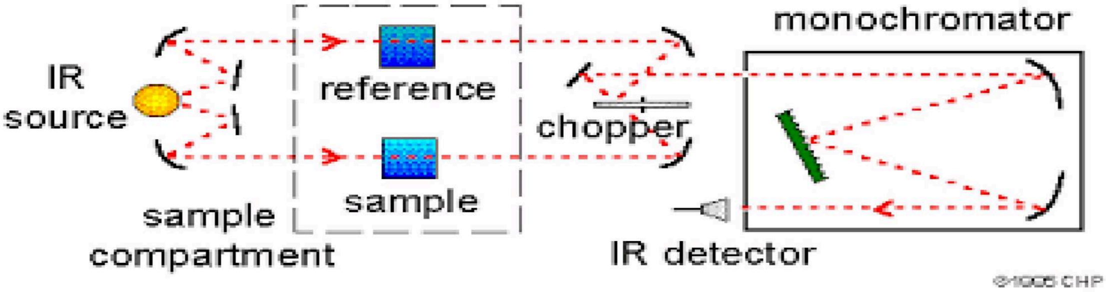

Figure:3.4, process behind the FTIR spectrum

3.4.1APPLICATIONS

- Pharmaceutical research
- Forensic investigation
- Polymer analysis
- Environmental and water quality analysis method
- High resolution experiments
- Kinetic reaction on the microsecond time scale.

3.4.2 ADVANDAGE OF FTIR:

➢ Speed: Because all of the frequencies are measured simultaneously, most measurements by FTIR are made in a matter of seconds rather than several minutes. This is sometimes referred to as the Felgett advantage.

➢ Sensitivity: Sensitivity is dramatically improved with FTIR many reasons. The detectors employed are much more sensitive, the optical throughout is much higher which results in much lower noise levels, and the fast scans a enable the addition of several scans in order to reduce the random measurement noise to any desired level.[47]

3.5 UV-VISIBLE SPECTROSCOPY:

UV-Visible Spectroscopy is based on chemical compounds absorption of ultraviolet or visible light, which results in the formation of different spectra. The interaction of light and matter is the basis of spectroscopy. Excitation and de-excitation occur as matter absorbs light, resulting in the formation of a spectrum.

When matter absorbs ultraviolet light, the electrons within it become excited. This leads them to transition from a ground state (an energy state with a low quantity of energy) to an excited state (an energy state with a relatively large amount of energy associated with it). It's worth noting that the difference between the energies of the electron's ground and excited states is always equal to the quantity of ultraviolet or visible energy it absorbs.

The most significant disadvantage of using a UV-VIS spectrometer is the amount of time it takes to prepare for usage. When employing UV-VIS spectrometers, proper setup is essential. Outside light, electrical noise, and other impurities that could interfere with the spectrometer's reading must be removed. [48]

Figure:3.5 UV-Vis Instrument

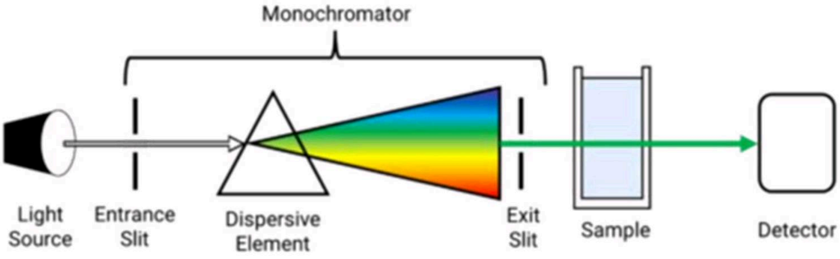

Figure 3.6: process behind the UV- vis spectrum

3.5.1APPLICATIONS

- Mainly it is used for qualitative and quantitative determinations such as enzyme assays, molecular weight determination,

- Ts routinely used in analytical chemistry for the quantitative determination of different analytes, such as metal ions, highly conjugated organic compounds, and biological macromolecules,
- Spectroscopic analysis is commonly carried out in solutions but solids and gases may also be studied.[48]

3.6 PHOTOLUMINESCENCE SPECROSCOPY

Photoluminescence refers to a form of luminescence that results from photoexcitation. Simply, photoluminescence occurs when a material emits light after absorbing a photon from an external light source. In photoluminescence spectroscopy, you can measure the intensity of emitted light as a function of wavelength by using an optical spectrometer. We recommend that you also use a high energy light source to stimulate all of the available electrons into their excited energy state.

There are several ways of categorising phenomena within photoluminescence. It is firstly important to consider that both radiative and non-radiative emissions will occur within your sample. As a form of radiative emission, photoluminescence can then be separated into two main classifications **fluorescence and phosphorescence**. These both have different energy transition pathways, and therefore very different lifetimes. One main way of quantifying photoluminescence efficiency is by measuring the photoluminescent quantum efficiency (PLQE) of a sample. You could also measure its photoluminescent quantum yield (PLQY). For measuring bulk material properties, you will need a high energy excitation source and a spectrometer. [49]

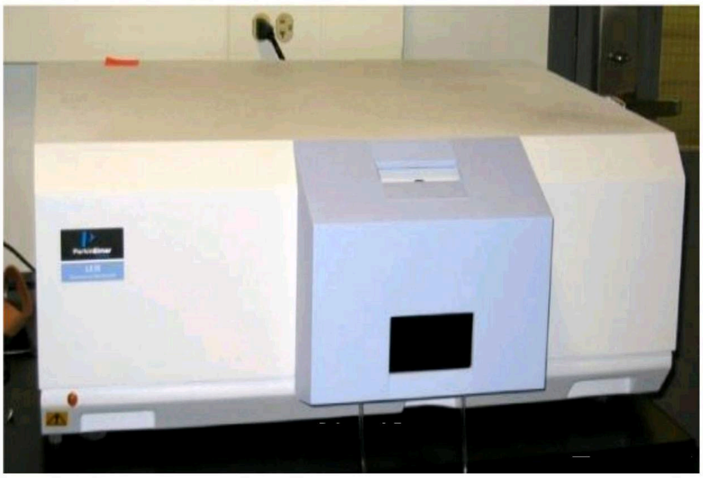

Figure 3.8: Photoluminasence spectrum.

CHAPTER IV

4.1 XRD RESULT

XRD patterns of the prepared Co_2O_4 nanoparticle show amorphous nature. Xrd pattern of the synthesized Co_2O_3 nanoparticle is given by in figure (4.1). The observed weak peaks are at the 2θ values of 31.35^0, 36.85^0, 59.47^0, 65.25^0. The particle size of the Co_2O_3 nanoparticle corresponding to the above 2θ values is found as 18.24nm, 27.76nm, 15.17nm, 20.85nm. This is done with the Debye Scherrers equation,

$$\mathbf{D = k\lambda/\beta \cos\theta}$$

$\beta \longrightarrow$ full width half maximum (radian)

$k \longrightarrow$ scattering angle (degree)

$\boldsymbol{\lambda} \longrightarrow$ x ray wave length (A^0) ($\boldsymbol{\lambda}$=1.5406 A^0)

$k \longrightarrow$ the correction factor(k=0.94)

$D \longrightarrow$ crystallite size of material(nm)

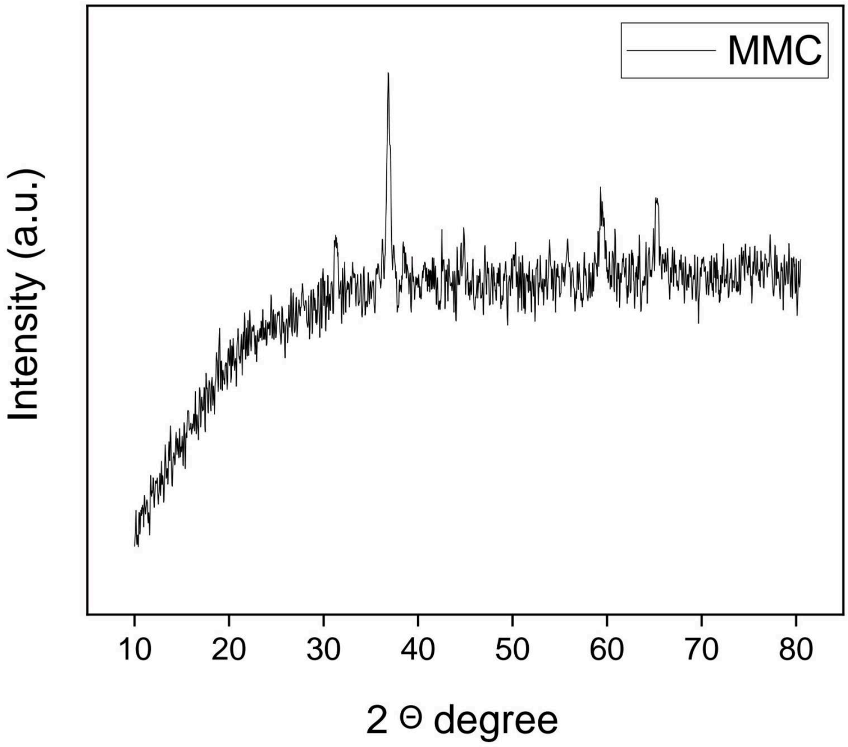

Figure 4.1 x-ray diffraction

S.No	**2θ (degree)**	**Full width Hafe maximum**	**Particle size (nm)**
1	**31.3528**	**0.4723**	**18.24**
2	**36.8583**	**0.3149**	**27.76**
3	**59.4733**	**0.6298**	**15.17**
4	**65.2505**	**0.4723**	**18.24**

Table 4.1 particle size from XRD analysis

4.2 FTIR RESULT

FTIR was used to perform an analysis of the potential functional group of Co_3O_4. Figure 4.3. The absorption band at 578.65 cm^{-1} was assigned to Co-O stretching which confirms the strong of Co_3O_4. Nanoparticle and 667.77 cm^{-1} was assigned to the bridging vibration of O- Co-O. The 667.75 cm^{-1} band is characteristic of Co^{2+}–O vibration in a tetrahedral site, and the band 578.65 cm^{-1} is attributable to the Co^{3+}–O vibration in an octahedral site of the Co3O4 lattice.[51]

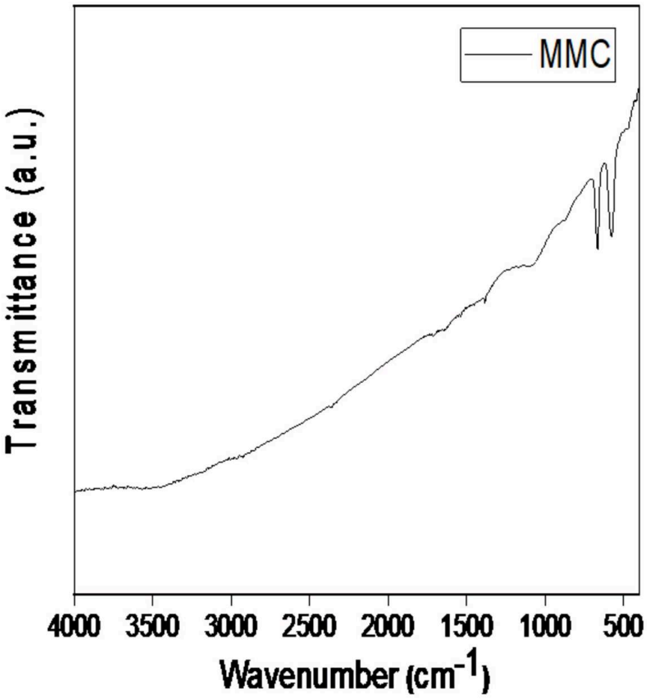

Figure 4.2: Fourier transformation spectrum

4.3 UV RESULT

The formation of the cobalt (III) oxide NPs was confirmed by the UV–Visible spectrometry (Fig. 4.2). The as-prepared cobalt (III) oxide NPs display an absorption maximum at 210 nm, which is characteristic absorption peak of Co (III) oxide NPs. This band owes its existence due to surface Plasmon resonance band and the broad peak representing the wide size distribution of these particles.[52]. The band gap energy 5.9eV of Co_3O_4 nanoparticles is higher than the bulk material. (3.19) [51]. This blue shift of the band gap energy may due to quantum confinement effect which inturns of confirms the nanoscale nature of Co_3O_4 particle prepared in the present work.

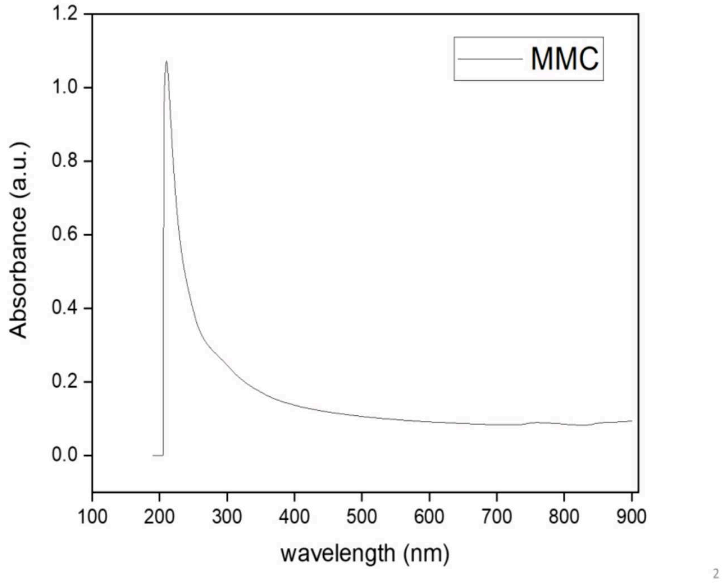

Figure 4.3 UV-vis sepctrum

4.4 PHOTOLUMINESCENCE (PL) SEPCTRUM

The photoluminescence (PL) excitation spectra of Co_3O_4 nanoparticle was recorded at room temperature, Figure 4.3.[53]. The two bands observed near 400 nm (400nm,468nm) may be due to the oxygen vacancy created within the nanocrystalline particle that stabilized the cubic spinel structure of the Co3O4 nanoparticles.[54]. Upon excitation at 400nm, materials shows two distinct emission peaks; Near Band Edge UV emissions at 400 nm, and visible emissions positioned at 468 nm. Origin of near band edge emission was attributed to the radiative annihilation of excitons, while the visible emission was attributed to the radiative annihilation of photo-generated holes.[53].

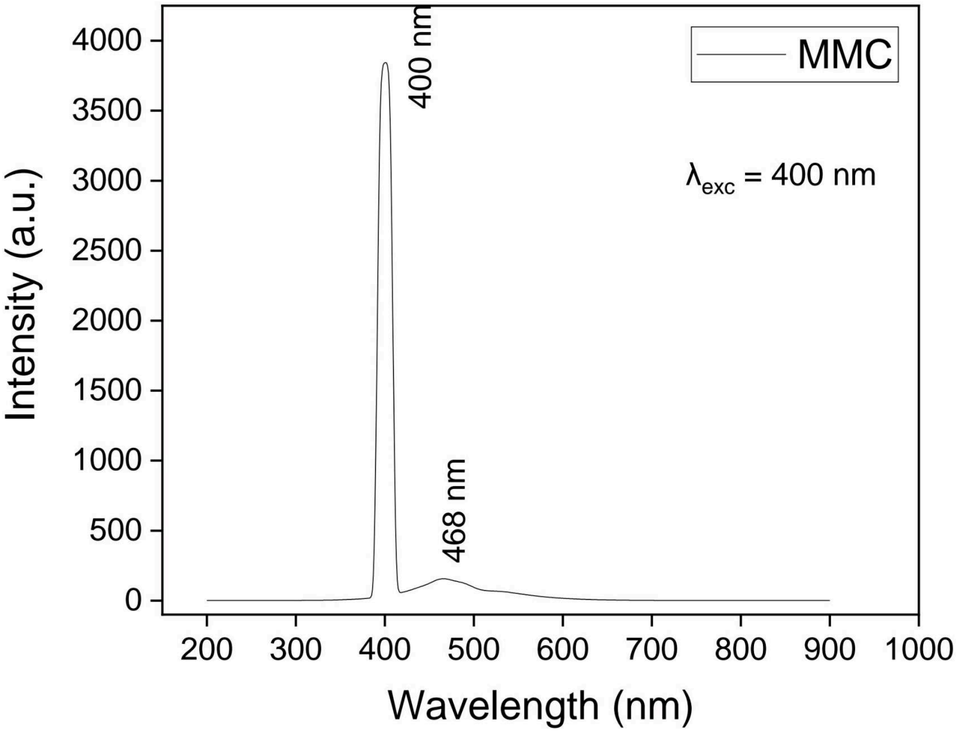

Figure 4.4: Photoluminescence result

CHAPTER V

5.1 CONCLUSION

In this work, aerial root of Ficus Benghalensis was used in the preparation of Co_3O_4 nanoparticle via green synthesized method. The produced Co_3O_4 nanoparticle was characterized through XRD, FTIR, UV and PL analysis. The results were analyzed and interpreted. With the help of XRD analysis, the nature of the sample was confirmed as amorphous and particle size of the sample lied between 15 – 30 nm. From FTIR analysis, functional groups of the sample were identified and their assignments were found. From UV analysis, UV band gap energy (5.9eV) was determined. From PL analysis, optical properties of the sample were analyed.

REFERENCE

1. Roger W. Whatmore Nanotechnology—what is it? Should we be worried? (2006)

2. Karthikeyan Subramani1, Abdelbary Elhissi2, Usha Subbiah3 and Waqar Ahmed Introduction to nanotechnology (2019)

3. K. Shimizu, INC 2, USA, 2006.

4. George M. Whitesides, Nanoscience, Nanotechnology, and Chemistry

5. Anu Mary Ealias and Saravanakumar M P, A review on the classification, characterisation, synthesis of nanoparticles and their application.

6. Machado S, Pacheco J G, Nouws H P A, Albergaria J T and Delerue-Matos C 2015 Characterization of green zero-valent iron nanoparticles produced with tree leaf extracts *Sci. Total Environ.* **533** 76–81.\

7. Dutton Gribbin,John ,Richard Feynman; A Life In Science (1997).

8.R.K mohapatra PHI Delhi, Engineering chemistry with laboratory experiment (2015)

9. Dr. R. K. Mohapatra, *M.Sc., M.Phil., M.B.A., Ph.D.* Faculty (Chemistry), GCE Keonjhar , NANOMATERIALS

10. Lipsen, minho and averio , international librian nanotechnology "backgrounds information on nanotechnology"

11. https:/www.iberdrola>nanotechnology- application

12. Murugesu s, Selamat J, perumal V,phytochemistry pharmacological and recent application of ficus benhalensis and ficus religiosa.

13. tutorialspoint-com/botanical-name-of-banyan -tree#:~:text

14.https://pmc/article/pmc87072

15.en.wikipedia.orgmwiki/cobalt-nitrate

16.pubchem.ncbi.nic.gov/compound/sodium-hydroxide

17. toppr.com/ask/content/concept/sodium-hydroxide-preparation

18. (byjus.com)/chemistry/caustic-soda-preparation

19. Sirajul Haq1 , Farwah Abbasi1, Manel Ben Ali et.al.., Green synthesis of cobalt oxide nanoparticles and the effect of annealing temperature on their physiochemical and biological properties , express(8) (2021)

20. Ali Talha Khalil, Muhammad Ovais,et.al., Physical properties, biological applications and biocompatibility studies on biosynthesized single phase cobalt oxide (Co3O4) nanoparticles via *Sageretia thea* (Osbeck.) (2021)

21.Sayed Zia Mohammadi, Batoul Lashkari,et.al, Green synthesis of Co3O4 nanoparticles by using walnut green skin extract as a reducing agent by using response surface methodology,(2021)

22. Melvin S. Samuela, E. Selvarajanb et.al, Green synthesis of cobalt-oxide nanoparticle using jumbo Muscadine (*Vitis rotundifolia*): Characterization and photo-catalytic activity of acid Blue-74,(2020)

23. Muhammad Hafeez1 , Ruzma Shaheen1,et.al., Green synthesis of cobalt oxide nanoparticles for potential biological applications.(2020)

24. Neda Akhlaghi a, Ghasem Najafpour-Darzi, et.al., Facile and green synthesis of cobalt oxide nanoparticles using ethanolic extract of Trigonella foenumgraceum (Fenugreek) leaves,(2020)

25. Murugan Perachiselvi, J. Jenson Samraj, et.al., Facile Synthesis of Cobalt OxideNanoparticle for Biological Studies, vol 8,No5, (2020).

26. Rajan Lakra a, Rahul Kumar et.al.., Synthesis and characterization of cobalt oxide (Co3O4) nanoparticles,(2020)

27. Qing-Yun Chen,a,* Sajjad U, et.al., Temperature effect on green-synthesized Co3O4 nanoparticle as photocatalyst for overall water splitting,(2020)

28. S. Nallusamy a,⇑, K. Sujatha b, Experimental analysis of nanoparticles with cobalt oxide synthesized by coprecipitation method on electrochemical biosensor using FTIR and TEM (2020)

29. Damian C. Onwudiwe a,b,∗, Murendeni, et.al., Eco-friendly synthesis, structural properties and morphology of cobalt hydroxide and cobalt oxide nanoparticles using extract of Litchi chinensis,(2020)

30. Ipeleng Kopano Kgosiemang, Relebohile Lefojane, Green synthesis of magnesium and cobalt oxide nanoparticles using *Euphorbia tirucalli*: Characterization and potential application forbreast cancer inhibition,(2020).

31. Nur Oktri Mulya Dewi1, Yoki Yulizar et.al., Green synthesis of Co3O4 nanoparticles using *Euphorbia heterophylla* L. leaves extract: characterization and photocatalytic activity,(2019)

32. B.A. Omran, H.N. Nassar et.al., Novel mycosynthesis, ,(2019) of cobalt oxide nanoparticles using Aspergillus brasiliensis ATCC 16404—optimization, characterization and antimicrobial activity.

33. Mohsin Siddique*, Noor Muhammad Khan. (2019), Green synthesis of cobalt oxide nanoparticles using Citrus medica leaves extract: characterization and photo-catalytic activity.

34. P. Saravanakumar et al., (2018) Piper Nigrum Mediated Green Synthesis, Charecterization of Undoped Cobalt Oxide and Cerium Ion Doped Cobalt Oxide Nanoparticles.

34. N. Matinise , a), N. Mayedwa et.al., (2018), Green Synthesis of Cobalt (II, III) Oxide Nanoparticles using Moringa Oleifera Natural Extract as High Electrochemical Electrode for Supercapacitors.

35. Shikha Dubey a, Jay Kumar et.al., (2018), Facile and green synthesis of highly dispersed cobalt oxide (Co3O4) nano powder: Characterization and screening of its eco-toxicity.

36. Ismat Bibi, Nosheen Nazar et.al.,(2017), Green and eco-friendly synthesis of cobalt-oxide nanoparticle: Characterization and photo-catalytic activity.

37**.** Rama Koyyati1,2, Karunakar Rao Kudle et.al., (2016), Evaluation of

Antibacterial and Cytotoxic activity of Green Synthesized Cobalt Nanoparticles using Raphanus sativus var. longipinnatus Leaf Extract.

38. Thi Toan Nguyen a, Van Hoa Nguyen, et.al., (2016), Facile synthesis of cobalt oxide/reduced graphene oxide composites for electrochemical capacitor and sensor applications.

39. A. Diallo, A.C. Beye, et.al., (2015), Green synthesis of Co_3O_4 nanoparticles via Aspalathus linearis: Physical properties.

40. M. Yarestani, A.D. Khalaji, et.al., (2014), Hydrothermal synthesis of cobalt oxide nanoparticles: Its optical and magnetic properties.

41. Katalin Sinkó1, Géza Szabó1, et.al.,(2011), Liquid-Phase Synthesis of Cobalt Oxide Nanoparticles.

42. Mark Allen, Debbie Willits, et.al., (2003), Constrained Synthesis of Cobalt Oxide Nanomaterials in the 12-Subunit Protein Cage from *Listeria innocua* .

43. Friedrich, W.; Knipping, P.; von Laue, M. Interferenz-Erscheinungen bei Rontgenstrahlen. Sitzungsber. Math.-Phys. Classe Koniglich-
Bayerischen Akad. Wiss.Munchen. (1912), 303–322.

44. Andrei A. Bunaciu, et.al., (2015), X-Ray Diffraction: Instrumentation and Applications.

45. Leon A, Reuquen P, Garin C, Segura R, Vargas P, Zapata P, Orihuela PA (2017) FTIR and Raman characterization of TiO_2 nanoparticles coated with polyethylene glycol as carrier for 2-methoxyestradiol. ApplSci 7(1):49.

46. M.A. Mohamed, J. Jaafar, et.al., chapter 1, FOURIER TRANSFROM INFRA RED spectroscopy.

47. Rostami-Vartooni, A., Nasrollahzadeh,M., Salavati-Niasari,M., Atarod,M., 2016. Photocatalytic degradation of azo dyes by titanium dioxide supported silver nanoparticles prepared by a green method using Carpobrotus acinaciformis extract. J. Alloys Compd.689, 15–20 .

48. www.techologynetworks.com ,uv applications.

49. ossila.com/en-tecnology in/page/photoluminescence.

50. K. Prema Latha, C. prema, S. Meenakshi sundar, (2018), Synthesis and characterization of cobalt oxide Nanoparticle.

51. S. Vijayakumar A. Kiruthika Ponnalagi S. Nagamuthu G. Muralidharan, (2013), Microwave Assisted Synthesis of Co3O4 Nanoparticles for Highperformance Supercapacitors.

52. S. Farhadi, M. Javanmard, G. Nadri, Characterization of cobalt oxide nanoparticles prepared by the thermal decomposition, Acta Chim. Slov. 63 (2016) 335-343.

53. Owolabi M. Bankole, et.al., (2020 Microwave-Assisted Synthesis of Cobalt Oxide/Reduced Graphene Oxide (Co_2O_4–rGo) Composite and its Sulfite Enhanced Photocatalytic Degradation of Organic Dyes),

54. A.B. Vennela, D. Mangalarani. et.al (2019), structural and Optical Properties of Co_3O_4 nanoparticle prepared by sol-gel Technique for photocatalytic applications.

55. Owolabi M. Bankole,et.al., Microwave-Assisted Synthesis of Cobalt Oxide/Reduced Graphene Oxide (Co3O4–rGo) Composite and its Sulfite Enhanced Photocatalytic Degradation of Organic dyes.

STRUCTURAL AND MORPHOLOGICAL STUDIES OF FICUS BENGHALENSIS AERIAL ROOT DERIVED COBALT OXIDE NANOPARTICLE

A project work report and submitted to
DEPARTEMENT OF PHYSICS
ST.MARY'SCOLLEGE(AUTONOMOUS), THOOTHUKUDI
Affiliated to
MANONMANIAM SUNDARANAR UNIVERSITY,
THIRUNELVELI
In partial fulfilment of the requirements for the award of
MASTER OF SCIENCE IN PHYSICS
Submitted by
A. MECKANCY
Reg. No: 21SPPHO5
Under the guidance of
S. SARAVANA SELVI Msc., SET.,B.Ed.,

DEPARTMENT OF PHYSICS
ST. MARY'S COLLEGE (AUTONOMOUS), THOOTHUKUDI.
Re-accredited with 'A+' Grade by NAAC
(2022-2023)

CERTIFICATE

This is to certify that this project work report entitled **"STRUCTURAL AND MORPHOLOGICAL STUDIES OF FICUS BENGHALENSIS AERIAL ROOT DERIVED COBALT OXIDE NANOPARTICLE"** is submitted to **ST. MARY'S COLLEGE (AUTONOMOUS), THOOTHUKUDI** in partial fulfilment of requirements for the award of **MASTER OF SCIENCE IN PHYSICS** and is a record of work done during the academic year **2022 – 2023** by **A.MECKANCY** (Register No: 21SPPH05)

S. Saravanan

Signature of the Guide

Padmavathi

Signature of the Co-Ordinator

Signature of the Director

Director
Self Supporting Courses
St. Mary's College (Autonomous)
Thoothukudi - 628 001.

Lucia Rose

Signature of the principal

Principal
St. Mary's College (Autonomous)
Thoothukudi - 628 001.

12/4/23

Signature of the Examiner

DECLARATION

I hereby declare that the project work report entitled **"STRUCTURAL AND MORPHOLOGICAL STUDIES OF FICUS BENGHALENSIS AERIAL ROOT DERIVED COBALT OXIDE NANOPARTICLE"** is submitted to **ST. MARY'S COLLEGE, (AUTONOMOUS) ,THOOTHUKUDI** affiliatedto **MANONMANIAM SUNDARANARUNIVERSITY, THIRUNELVELI** for the award of the degree of Master of Science in Physics is my original work and that no part of this project work report has been submitted for any Degree, Diploma or other similar titles.

A. Meckancy

Station: Thoothukudi

Signature of the Student

Date: 5.4.2023

(A. MECKANCY)

ACKNOWLEGEMENT

On the outset of this report, I feel obliged to our Almighty for his aid in the completion of this project work successfully.

I wish to record our profound gratitude to our Principal **Rev**. **Dr. Sr. A. S. J. LUCIA ROSE,M.S.,B.Ed.,M.Phil.,PGDCA.,Ph.D.,** for her motivation.

I sincerely thank our Director of SSC**, Rev .Sr. JOSEPHINE JEYARANI, M.A., M.Phil.,** for her encouragement and support.

I wish to thank **Rev. Dr. Sr. JESSIE FERNANDO M.Sc., M.Phil., Ph.D.,** HOD & Associate professor for her inspirational words to complete this project work.

I owe a great deal to **Mrs. P. PADMAVATHI M.Sc., M.Phil., SET.,** SSC Co-Ordinator for supporting me throughout this project work.

I express my sincere thanks to **Mrs. S.SARAVANA SELVI Msc.,SET.,B.Ed.,** for her valuable time and guidance provided throughout for the successful completion of my project.

I am deeply grateful to all the staff members of Department of Physics (SSC) for supporting me in all aspects.

I acknowledge my deep sense of gratitude to my loving parents and friends for being a constant source of motivation.

ABSTRACT

The main objective of nanotechnology is to develop and improve every field with nanoparticles which are ultra small in size. Most importantly, they exhibit super sensitivity, extraordinary multi-functionality and extremely low power consumption along its high surface to volume ratio. so the demand of the nanoparticle is hiked day by day especially, green synthesis of nanoparticle is welcomed due to environmental concern.Aeial root of ficus benghalensis is chosen to synthesize the nanoparticle and the material is planned to study morphologically. Morphology of the synthesized Co_3O_4 nanoparticle will be studied using SEM-EDX, BET surface analysis and Raman study is planned to analysis the structure of the sample.

Thus the present work aims in producing cobalt oxide nanoparticles using co-precipitation technique with the help of aerial root of Ficus Benghalensis and the studies are used to analysis the sample both morphologically and structurally.

CONTENT

LIST OF TABLES

LIST OF FIGURES

1.Introduction

Nano is a prefix used to describe one millionth or 10^{-9} of something.The concept of nanotechnology was introduced by physics nobel laureate Richard P Faynman. A nano particle or ultrafine particle is usually define as a particle of matter having size between 1 to 100 nanometer diameter. Nanoparticles are usually distinguished from microparticle (1-1000μm), fine particle (100 to 250 nm), coarse particle (2500 to 10000 nm),Because of their smaller size. This smaller size drives very different physical and chemical properties.

Nanoparticle occur widely in nature and are object of study in many science such as chemistry, physics, geology and biology. In general, the small size of nanoparticle lead to a lower concentration of point defect compared to their bulk counterparts, But they do support a varity of dislocation that can be visualized using high resolution electron microscope. Nanotechnology is now widely considered to have the potential to bring benefits in the following areas such as drug development , water decontamination , information and communication technologies , and material sciencs.

1.1 NANOTECHNOLOGY

Nanotechnology is viewed as an upcoming field of research and technology related to the synthesis and design of materials with diverse compositions, arrangement and having nanoscale dimension at least in one dimension [1]. Nanotechnology is one of the most promising technologies of the 21st century. It is the ability to convert the nanoscience theory to useful applications by observing, measuring, manipulating, assembling, controlling and manufacturing matter at the nanometer scale. The National Nanotechnology Initiative (NNI) in the United States define Nanotechnology as “a science, engineering, and technology conducted at the nanoscale (1 to 100 nm), where unique phenomena enable novel applications in a wide range of fields, from chemistry, physics and biology, to medicine, engineering and electronics”. This definition suggests the presence of two conditions for nanotechnology. The first is an issue of scale: nanotechnology is concerned to use structures by controlling their shape and size at nanometer scale. The second issue has to do with novelty: nanotechnology must deal with small things in a way that takes advantage of some properties because of the nanoscale.

1.2 NANOPARTICLE

Nano particles are particles between 1 to 100 nanometers in size . Particles are further classified according to diameter . Ultrafine particles are the same as nano particles and between 1 and 100 nanometers in size , fine particles have size between 100 and 2,500 nanometers , and coarse particle research is currently an area of intense scientific interest due to a wide variety of potential application in biomedical , optical and electronic fields [2-4] . In principle any collection of atoms bonded together with a structural radius of < 100 nm can be considered a nano particle . For e.g. , metal clusters (agglomerates of metal atoms) , large molecules , such as proteins , and even hydrogen - bonded assemblies of water molecules , which exist in water at ambient temperatures . Various synthesis of nanoparticle should consider the following conditions:

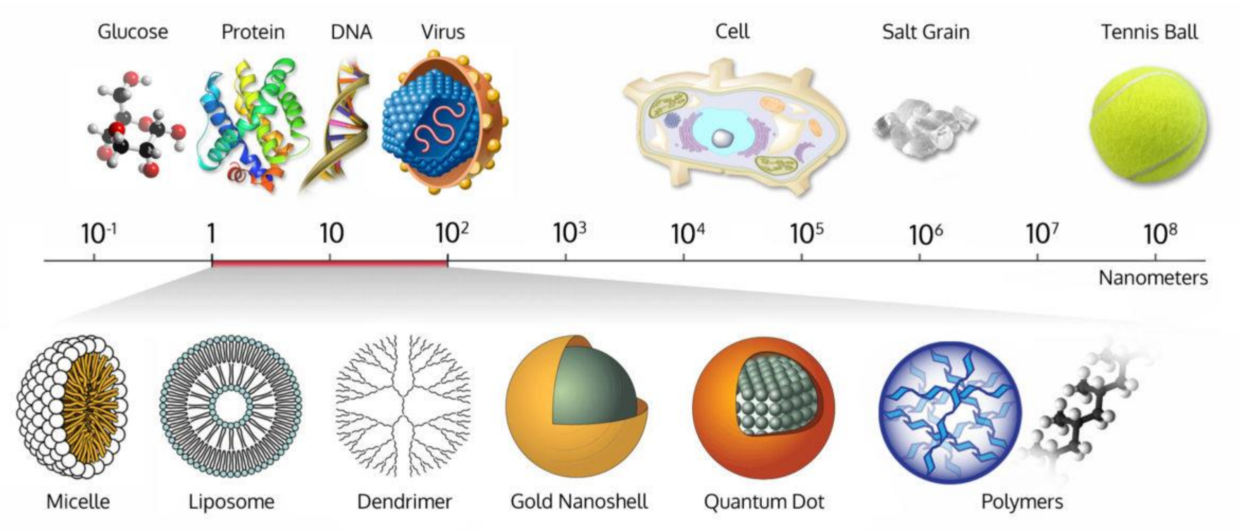

Fig 1.1 Size of various materials compared to nanoparticle

- Control of particle size, shape, crystal structure and composition distribution,
- Improvement of the purity of nanoparticles,
- Control of aggregation,
- Stabilization of physical properties, structures and reactants,
- Higher reproducibility.

1.3 TYPES OF NANOPARTICLE

Organic and inorganic nanoparticles are the two basic types of nanoparticles. Micelles, dendrimers, liposomes, hybrid and compact polymeric nanoparticles fall within the first category. Fullerenes, quantum dots, silica, and metal nanoparticles make up the second group. The appearance, size, and chemical properties of nanoparticles are also used to classify them. Some of the most important classes of nanoparticles are based on physical and chemical characteristics

1. **Carbon – based Nanoparticle:**

Examples of carbon – based Nanoparticle are cabon Nanotube and fullerence. These nanomaterial are used in structural reinforcement since they are 100 times stonger then steel. Good conductivity, high strength, structure, electron affinity are all attractive features of these material.

2. **Ceramic Nanoparticle:**

Ceramic nanoparticle have high heat resistance and chemical inertness. Researchers are paying close attention to these inorganic non-metallic solid because of their unique properties. It has been used effectively as a drug delivery system for several diseases like cancer and bacterial infection.

3. **Metal Nanoparticle:**

Metal nanoparticle are prepared fron metal precursors and can be synthesized by chemical, electrochemical or photochemical method. Metal nanoparticle are utilized across several research field, including detection and imaging of biomolecules and also in environmental and bioanalytical application.

4. **Semiconductor Nanoparticle:**

Semiconductor material have qualities that are intermediate between metals and non-metals, as well as large band gaps. Their properties are significantly attered by band gap tuning. As a result, they are crucial in photo catalysis, photo optics and electronic devices.

5. **Polymeric Nanoparticle:**

Polymeric Nanoparticle are organic based nanoparticle. Depending upon the preparation method, polymeric nanoparticle got structure like nanocapsules or nanospheres. They are used in drug delivery and diagnostics. Drug delivery system with polymeric nanoparticles are highly biodegradable and biocompatible.

6. Liquid Nanoparticle:

Liquid nanoparticle are generally spherical with a diameter ranging from 10 to 100 nm. Their structure consists of a solid core made of lipid and a matrix containing soluble lipophilic molecules and external core is stabilized by surfactants and emulsifiers. Liquid nanoparticles are used in gene therapy.

Based on their dimensionalities, nanomaterials are placed into four different classes [5].

❖ Zero-dimensional nanomaterials (0-D):

The nanomaterials in this class have all their three dimensions in the nanoscale range. Examples are quantum dots, fullerenes, and nanoparticles.

❖ Zero-dimensional nanomaterials (0-D):

The nanomaterials in this class have all their three dimensions in the nanoscale range. Examples are quantum dots, fullerenes, and nanoparticles.

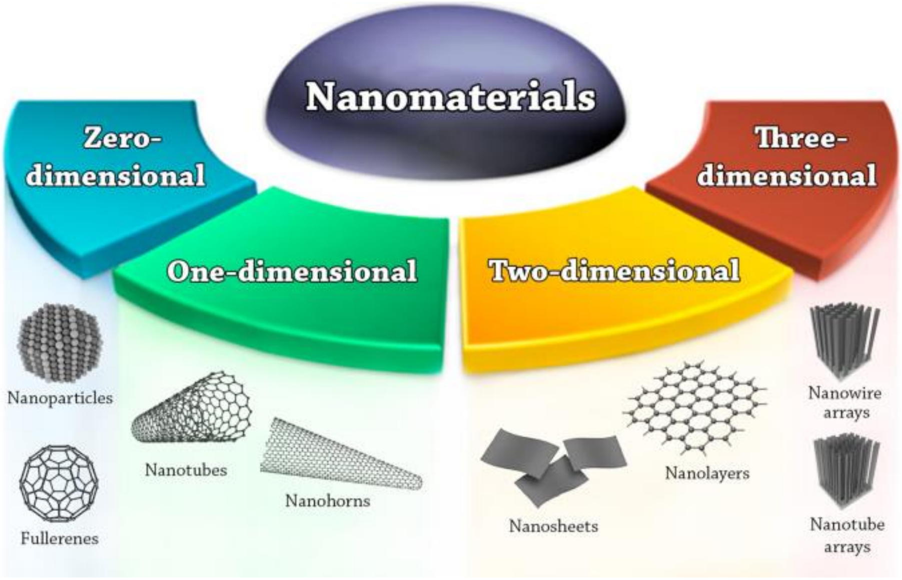

Fig 1.2 Dimensions of nanostructure

- **One-dimensional nanomaterials (1-D):**

  The nanomaterials in this class have one dimension outside the nanoscale. Examples are nanotubes, nanofibers, nanorods, nanowires, and nanohorns.

- **Two-dimensional nanomaterials (2-D):**

  The nanomaterials in this class have two dimensions outside the nanoscale. Examples are nanosheets, nanofilms, and nanolayers.

- **Three-dimensional nanomaterials (3-D) or bulk nanomaterials**:

  In this class the materials are not confined to the nanoscale in any dimension. This class contains bulk powders, dispersions of nanoparticles, arrays of nanowires and nanotubes.

1.4 PROPERTIES OF NANOPARTICLES

1. Due to small size of nanoparticles, there are more atoms on the surface compared to the interior of the particles, which leads to large surface to volume ratio.
2. Nano-size powder particles are potentially important in ceramics, powder metallurgy, in the achievement of uniform nano porosity and similar applications.
3. When materials are made into nanoparticles their reactivity increase. These more reactive particles can enter the body through the skin, lungs etc.
4. In optical properties the absorption occurs because electrons are induced by the photons of the incident light which make transitions between the lower lying occupied levels and higher unoccupied levels of the material.

1.5 APPLICATIONS OF NANOPARTICLE

❖ Cosmetics and sunscreen

The sunscreen including nanoparticles such as titanium dioxide provides numerous advantages . The UV protection property of titanium oxide and zinc oxide nanoparticles as they are transparent to visible light as well as absorb and reflect UV rays found their way to be used in some sunscreens . Some lipsticks use iron oxide nanoparticles as a pigment[6] .

❖ Electronics

The higher necessity for large size and high brightness displays in recent days that are used in the computer monitors and television is encouraging the use of nanoparticles in the display technology . For example nanocrystalline lead telluride , cadmium sulphide , zinc selenide and sulphide , are used in the light emitting diodes (LED) of modern displays [7]. The development in portable consumer electronics such as mobile phones and laptop computers led to the enormous demand for a compact , lightweight and high capacity batteries . Nanoparticles are the ideal choice for separator plates in batteri

- **Catalysis**

Catalysis Nanoparticles contain high surface area that offers higher catalytic activity . Due to their extremely large surface to volume ratio the nanoparticles function as efficient catalyst in the production of chemicals [8]. One of the important application is the use of platinum nanoparticles in the automotive catalytic converters as they reduce the amount of platinum required due to very high surface area of the nanoparticles thus reducing the cost significantly and improving performance . Some chemical reactions for example , reduction of nickel oxide to metal nickel (Ni) is performed using nanoparticles .

- **Medicine**

Nanotechnology has improved the medical field by use of nanoparticles in drug delivery . The drug can be delivered to specific cells using nanoparticles [9] . The total drug consumption and side effects are significantly lowered by placing the drug in the required area in required dosage . This method reduces the cost and side effects . The reproduction and repair of damaged tissue (Tissue engineering) can be carried out with the help nanotechnology . The traditional treatments such as artificial implants and organ transplants can be replaced by tissue engineering . One such example is the growth of bones carbon nanotube scaffolds . The use of gold in medicine is not new . In Ayurveda ,an Indian medical system , gold is used in several practices .

- **Food**

The improvement in production , processing , protection and packaging of food is achieved by incorporating nanotechnology . For example a nanocomposite coating in a food packaging process can directly introduce the anti - microbial substances on the coated film surface . One of the example is the canola oil production industry includes nanodrops , an additive designed to transfer the vitamins and minerals in the food .

- **Construction**

Nanotechnology has improved the construction processes by making them quicker , inexpensive and safer . For example when nanosilica (SiO_2) is mixed with the normal concrete , the nanoparticles can improve its mechanical properties , and also improves its durability [10] . The addition of haematite (Fe_2O_3) nanoparticles increases the strength of the concrete . Steel is the most widely available and used material in the construction industry . The properties of steel can be improved by using nanotechnology in steel for example in bridge construction the use of nano size steel offers stronger steel cables . The other important construction material is glass . Extensive research is being performed on the application of nanotechnology in construction glass.

1.6 COBALT NITRATE HEXAHYDRATE

Cobalt nitrate is the inorganic compound with the formula $Co(NO_3)_2 \cdot xH_2O$. It is cobalt (II)'s salt. The most common form is the hexahydrate $Co(NO_3)_2 \cdot 6H_2O$, which is a red-brown deliquescent salt that is soluble in water and other polar solvent [11]. As well as the anhydrous compound $Co(NO_3)_2$, several hydrates of cobalt(II) nitrate exist. These hydrates have the chemical formula $Co(NO_3)_2 \cdot nH_2O$, where $n = 0, 2, 4, 6$.

Fig 1.3 Cobalt nitrate hexahydrate

Use and reaction

It is commonly reduced to metallic high purity cobalt. It ca be absorbed on to various catalyst supports for use in Fischer–Tropsch catalysis.It is used in the preparation of dyes and inks. Cobalt(II) nitrate is a common starting material for the preparation of coordination such as complex cobaloximes, carbonatoteraamminecobalt (III) [12], and others.

Table 1.1 Properties of Cobalt nitrate hexahydrate

Formula	$Co(NO_3)_2 . 6H_2O$
Molar Mass	182.943 g/mol
Melting Point	100 ^{0}C
Density	2.49 g/cm
Appearance	Red Crystalline

Production

The cobalt nitrate hexahydrate is prepared treating metallic cobalt or one of its oxides, hydroxides, or carbonate with nitric acid:

$$Co + 4\ HNO_3 + 4\ H_2O \rightarrow Co(H_2O)_6(NO_3)_2 + 2\ NO_2$$

$$CoO + 2\ HNO_3 + 5\ H_2O \rightarrow Co(H_2O)_6(NO_3)_2$$

$$CoCO_3 + 2\ HNO_3 + 5\ H_2O \rightarrow Co(H_2O)_6(NO_3)_2 + CO_2$$

Application of cobalt nanoparticle

- In micro-electronics,
- As a magnetic nanoparticles with numerous uses in microbatteries, nanowires, specific alloy and catalyst applications,
- In catalysis, superconductors, electronic ceramics and other fields as an important inorganic material,
- As a catalyst and catalyst carriers,
- As an electrode active materials,
- For glass, porcelain colorants and pigments,
- Chemical industry oxidants,
- Senior goggles and other filter materials,
- As carbides,
- In temperature and gas sensors,
- In electrochromic devices,
- In enamels, grinding wheels, and solar energy absorbers.

1.7 SODIUM HYDROXIDE

It is also known as lye and it an inorganic compound with the formula NaOH. sodium hydroxide is a white crystalline odorless solid that absorbs moisture from the air. It is a manufactured substance. When dissolved in water or neutralized with acid it liberates substantial heat. Sodium hydroxide is very corrosive. It is generally used as a solid or a 50% solution. Other common names include caustic soda and lye. Sodium hydroxide is used to manufacture soaps, rayon, paper, explosives, dye stuffs and petroleum products. It is also used in processing cotton fabric, laundering and bleaching, metal cleaning and processing oxide coating, electroplating and electrolytic extracting. It is commonly present in commercial drain and oven cleaners.

Fig 1.4 Sodium Hydroxide

Table 1.2 Properties of sodium hydroxide

Formula	NaOH
Molar Weight	39,997 g/mol
Density	2.13g/cm^3
Boiling Point	1,388^o C
Melting Point	318 ^{o}C

Production

sodium hydroxide was produced by treating sodium with calcium hydroxide in a metathesis reaction which takes advantage of the fact that sodium hydroxide is soluble, while calcium carbonate is not. This process was called causticizing [13].

$$Ca(OH)_{2(aq)} + Na_2CO_{3(s)} \rightarrow CaCO_{3(s)} + 2\ NaOH_{(aq)}$$

Sodium hydroxide is also produced by combining pure sodium metal with water. The byproducts are hydrogen gas and heat, often resulting in a flame.

$$2\ Na_{(s)} + 2\ H_2O_{(l)} \rightarrow 2\ NaOH_{(aq)} + H_2$$

Uses of sodium hydroxide

- For making soaps and detergents it is used. Sodium hydroxide is used for hard bar soap, while potassium hydroxide is used for liquid soap preparation[15-16],
- Sodium hydroxide is used more often than potassium hydroxide because it is cheaper and a smaller quantity is needed,

- As drain cleaners that contain sodium hydroxide convert fats and grease that can clog pipes into soap, which dissolves in water,
- For making artificial textile fibres ,
- In the manufacture of paper. Around 56% of sodium hydroxide produced is used by industry, 25% of which is used in the paper industry ,
- In purifying bauxite ore from which aluminium metal is extracted. This is known as Bayer process,
- In de-greasing metals, oil refining, and making dyes and bleaches,
- In water treatment plants for pH regulation,
- To treat bagels and pretzel dough, giving the distinctive shiny finish.

1.8 FICUS BENGHALENSIS

Ficus Benghalensis Tree is a large plant and it is a national tree. It has been used for thousands of years and has become an essential plant in the medicinal field. Ficus Benghalensis varies in morphology, growth habit, flower color, leaves, stems, and chemical composition. It is available throughout the year in different regions of the world. It grows in evergreen except in some dry areas where it remains leafless for a very short time due to dryness and shortage of water.The most famous characteristic of banyan is its beautiful flavor . Flowering occurs from May to August. Ficus Benghalensis has leaves, which are very large, glossy green, leathery and elliptical in shape. Young leaves seem to be an attractive reddish tinge. Ficus Benghalensis tree fruit color at ripening time change from orange to red . It is also used as ornamental plant in different regions of the world .

Table 1.3 Scintific Classification of aeial Benghalensis

Kingdom	Plantae
Division	Magoliophyta
Class	Mahnoliopsida
Order	Utricales
Family	Moraceas
Genus	Ficus
Species	Benghalensis

AERIAL ROOT

The roots that grow outside the soil or above the ground are called aerial roots. Prop roots, stilt roots, breathing roots and climbing roots are four different types of aerial roots. Ficus Benghalensis has a special type of roots, that is, aerial prop roots. Aerial roots help to anchor the plant firmly, while also contributing to the uptake of water and nutrients. aerial roots play an important part in providing oxygen for respiration. Oxygen enters a mangrove through lenticels, thousands of cell-sized breathing pores in the bark and roots. These plants are very sturdy and often have trunk-like stems. The aerial roots help keep them grounded so they don’t fall over.

Fig 1.5 Aerial root of Ficus Benghalensis

Uses of aerial root

- Cures burning sensation,
- Cures ulcers,
- Cures painful skin diseases,
- Cures inflammation and toothache,
- Used in hair fall control and makes hair strong from roots.

1.9 OBJECTIVE OF PRESENT WORK

- ➢ To synthesis cobalt oxide nanoparticle from aerial root of ficus benghalensis .
- ➢ Sturctural analysis of the synthesized cobalt oxide will be studied using ramam study.
- ➢ Morphology of the synthesized cobalt oxide nanoparticle will be studied using SEM-EDX, BET surface analysis study.

2.REVIEW OF LITERATURE

Ramesh vinayagam et al.(2023)[14]studied about synthesis of cobalt oxide nanoparticles (CONPs) mediated by leaf extract of *Muntingia calabura* using a rapid and simple method and evaluation of its photocatalytic activity against methylene blue (MB) dye. UV–vis absorption spectrum showed multiple peaks with an optical band gap of 2.05 eV, which was concordant with the literature. FESEM image signified the irregular-shaped, clusters of CONPs, and EDX confirmed the existence of the Co and O elements. The sharp peaks of XRD spectrum corroborated the crystalline nature with a mean crystallite size of 27.59 nm. FTIR image revealed the presence of various phytochemicals present on the surface and the bands at 515 and 630 cm^{-1} designated the characteristic Co–O bonds. VSM studies confirmed the antiferromagnetic property with negligible hysteresis. The high BET specific surface area (10.31 m^2/g) and the mesoporous nature of the pores of CONPs signified the presence of a large number of active sites, thus, indicating their suitability as photocatalysts. Hence, the CONPs synthesized herein could be applied to degrade other xenobiotics and the treatment of industrial wastewater and environmentally polluted samples.

Parvathiraja Chelliah et al.(2023)[15] studied about, biosynthesis of cobalt oxide (Co_3O_4) nanoparticles using Curcuma longa plant extract.The cubic structure and spherical shape of Co_3O_4 nanoparticles were estimated by using XRD and TEM characterizations. Plant molecules aggregation and their agglomerations on the nanoparticles were established from FTIR and EDX spectroscopy. Multiple cobalt valences on the oxygen surfaces and their reaction, bonding, and binding energies were analyzed from XPS measurements. The biogenic Co_3O_4 nanoparticles were executed against gram-positive (Staphylococcus aureus—S.aureus) and gram-negative (Escherichia coli—E. coli) bacteria. A gram-positive bacterial strain exhibited great resistivity on Co_3O_4 nanoparticles. Degradation of organic dye pollutants on the Co_3O_4 nanoparticles was performed against methylene blue (MB) dye under the conditions of visible light irradiation. This research work achieved enhanced degradation potency against toxic organic dye and their radicals are excited from visible light irradiations. Absorption light and charged particle recombinations are reformed and provoked by the plant extract bio-molecules. Furthermore, the biosynthesized Co_3O_4 nanoparticles determined the potency of bacterial susceptibility and catalytic efficacy over the industrial dye pollutants.

R. Vandamar Poonguzhali et al.(2023)[16] study about,A fresh lemon juice-assisted auto-combustion method was implemented for the synthesis of Co_3O_4 nanoparticles (Co_3O_4 NPs). The structural, vibrational, optical, and morphological properties of prepared Co_3O_4 NPs were investigated at 350 °C. The effects of lemon juice and heat treatment on the physicochemical properties of Co_3O_4 nanoparticles were investigated. XRD was used to investigate the structure, lattice constant, and crystallite size of Co_3O_4 NPs. FT-IR spectroscopy was used to investigate the functional groups and vibrational modes of unheated and heated Co_3O_4 NPs. Unheated and heated Co_3O_4 NPs had energy band gaps of 3.14 eV and 3.4 eV, respectively. TEM micrographs of heat-treated Co_3O_4 NPs confirm the nanoscale range of the particles, which agrees well with the crystallite size determined by XRD. LPG based sensor behavior of Co_3O_4 nanoparticles has been tested with various aspects of sensing parameters. The result shows that the prepared nanoparticles can be a promising sensing material for toxic gases like LPG,Co_2 and NH.

Govindasamy et al.(2022)[17], studied about Psidium guajava leaf extracts are used to stabilize the synthesis of cobalt oxide nanoparticles. The biosynthesized cobalt oxide nanoparticles were investigated using UV-visible spectroscopic analysis. Additionally, Fourier-transform infrared spectroscopy revealed the presence of carboxylic acids, hydroxyl groups, aromatic amines, alcohols and phenolic groups.

The X-ray diffraction analysis showed various peaks ranging from 32.35º to 67.35º . The particle size ranged from 26 to 40 nm and SEM images of green synthesized P. guajava cobalt oxide nanoparticles showed agglomerated and non-uniform spherical particles. The anti-bacterial activity of green synthesized P. guajava cobalt oxide nanoparticles was evaluated against Gram-positive Staphylococcus aureus and Gram-negative Escherichia coli with a 7 to 18 mm inhibitory zone. These results confirmed that green synthesized P. guajava cobalt oxide nanoparticles have a potential photocatalytic and anti-bacterial activity and also reduced cell viability against MCF-7 breast cancer and HCT 116 colorectal cancer cells.

Srivastava et al.(2022)[18] studied about,orange peel extract mediated cobalt oxide nanoparticles from cobalt nitrate hexahydrate. The orange peel extract has Citrus reticulata, which is a key biological component that acts as a ligand and a reducing agent during the formation of nanoparticles. Additionally, the same nanoparticles were also obtained from various precursors for phase and electrochemical behavior comparisons. The prepared Cobalt oxide-nanoparticles were also sulfurized and phosphorized to enhance the electrochemical properties. The synthesized samples were characterized using scanning electron microscopic and X-ray diffraction techniques. The cobalt oxide nanoparticle showed a specific capacitance of 90 F/g .The phosphide-based nanoparticles offer more than 85% capacitance retention after 5000 cycles. This study offers a green strategy to prepare nanostructured materials for energy applications.

Ramasamy et al.(2022)[19] studied about,green synthesis of Cobalt oxide nanoparticles using Pisonia alba leaf extract . For instance, the use of biological materials such as plants is usually safe. Plants also contain reducing and capping agents. The characteristics of the CoNPs were determined by various analyses, including X-ray diffraction (XRD), Fouriertransform infrared (FTIR), Field emission scanning electron microscopy (FeSEM), Energy dispersive X-ray spectroscopy

(EDX) and Dynamic light scattering method (DLS). Characterization techniques confirmed that the formation of nanoparticles and also they stabilized the nanoparticles.

Bekele et al.(2022)[20] studied about, synthesized Co_3O_4 NPs within various volume ratios in the presence of Solanum tuberosum leaf extract as a green alternative template. the green-synthesized Co_3O_4 NPs were characterized using XRD, SEM, EDX, TEM, HRTEM, SAED, FTIR, and UV-DRS. Moreover, the synthesized NPs were used as green alternative and costeffective nanoelectrodes for the detection of CA and ascorbic acid. SEM-EDX and TEM including HRTEM and SAED indicates that the greensynthesized Co_3O_4 NPs were too crystalline having spherical structure without any secondary phase and foreign materials. In addition, the FTIR analysis confirms the role of leaf extract of Solanum tuberosum as both capping and reducing agents that prevent the overgrowth of Co_3O_4 NPs and also indicates the formation of Co-O stretching. UV-DRS result suggests the energy band gap for Co_3O_4 NPs synthesized with the volume ratio of 1 : 2, 1 :1, and 2 :1 was deduced to be 1.77, 1.83, and 2.19 eV, respectively.

RajanLakra , et al. (2021) [21] studied about , synthesized cobalt oxide nanoparticles from cobalt nitrate as its source by precipitation approach . The structural properties of the synthesized Co_3O_4 nanoparticles were studied using X ray diffraction (XRD) . The XRD results confirm the crystalline nature of the nanoparticles . Further , scanning electron microscopy (SEM) was also performed to study the morphology of the synthesized Co_3O_4 nanoparticles . SEM micrograph shows that the Co_3O_4 nanoparticles are somewhat sphere like morphology and they are interlinked with each other.

C.T.Anuradha et al (2021)[22] studied, a facile biological benign synthesis of cobalt oxide nanoparticles is obtained using Citrus limon (C. limon) fruit extract at diferent annealing temperature. XRD assessment afrms the unique facets (2 2 0, 3 1

1, 4 0 0, 5 1 1 and 4 4 0 planes) of Co_3O_4 nanoparticles. XRD and FTIR studies confrmed that C. limon fruit extract was the principle, reducing as well as stabilizing agent for this green synthesis process. The morphology of Co_3O_4 nanoparticles is obtained by FESEM techniques at distinct annealing temperature. The antibacterial and antifungi activities of synthesized nanoparticles have higher antibacterial and antifungi activity than the standard drug against gram (+) and gram (−) bacteria like Staphylococcus aureus, Streptococcus mutans, Klebsiella pneumoniae, Escherichia coli and antifungi activity hostile to Aspergillus favus and Aspergillus niger which are depicted in this work.

Mohammadi et al.(2021)[23] studied, cobalt oxide nanoparticles prepared by green synthesis method .The nanoparticle were prepared by green synthesis identified and analyzed by SEM, XRD, FTIR, and VSM. RSM was used to find out the best parameters in the production of conalt oxide nanoparticles. The optimum green synthesis parameters for producing cobalt oxide nanoparticles are concentration of cobalt nitrate salt (50 mmol), extract volume (10 ml), time (92 min), and temperature (53 ◦C). The SEM analysis showed that the sizes of the synthesized cobalt oxide nanoparticle ranged from 60 to 80 nm. The magnetic properties of cobalt oxide nanoparticle were assessed by VSM .

Sirajul Haq et al.(2021)[24] studied, the cobalt oxide nanoparticles synthesized via green method using Piper nigrum (P. nigrum) leaves extract and were calcined at different temperatures. The crystalline nature was studied through x-ray diffractometer(XRD). With increasing calcination, the amorphous phase transitioned to the crystalline phase. Diffuse reflectance spectroscopy (DRS)was used to observe UVVisible light absorbance phenomenon, and Tauc’s plot was used to calculate the band gap energy, which was found to decrease with calcination. Scanning electron microscopy (SEM)was used to analyze the surface morphology, and Fourier transform infrared (FTIR)spectroscopy was used to classify the surface functional groups. Antibacterial and antioxidant potentials of cobalt oxide NPs were found to decrease with increasing calcinations temperature.

Syed Yawar Saeed et al.(2020)[25] studied nanoparticles prepared by green synthesis method. In this study, cobalt oxide nanoparticles were synthesized from roots extract of Ziziphus Oxyphylla Edgewby using cobalt chloride hexahydrate. After the successful synthesis of nanoparticles, various methods were used to analyze these nanoparticles, including Fourier transform infrared spectroscopy, scanning electron microscopy, x-ray diffraction analysis, and energy dispersive analysis of x-ray. Scanning electron microscopy images reveal the spherical and irregular structure of Co_3O_4 - NPs shaving a particle size between 40 to 60 nm. It is suggested that Co_3O_4 - NPs could be of great importance in medical science for their antimicrobial activity antioxidant, antileishmanial, cytotoxic, hemolytic, larvicidal activities, anticholinergic, anti-diabetic, and anti-cancer activities.

Hafeez et al (2020)[26] studied about,Cobalt oxide nanoparticles. Now a days green methods of synthesis of these NPs are preferred over other methods because of associated benefits. In this study, Co_3O_4- Nps were synthesized by using leaves extract of Populus ciliata (safaida) and cobalt nitrate hexa hydrate as a source of cobalt. The synthesized NPs were analyzed by different techniques such as fourier transform spectroscopy (FTIR), x-ray diffraction (XRD), transmission electron microscopy (TEM) and scanning electron microscopy (SEM). Antibacterial activities of the synthesized Co_3O_4 - Nps were evaluated against gram negative and gram positive bacteria and found active against Escherichia coli (E. coli), Klebseilla pneumonia (K. pneumonia), Bacillus subtillus (B.subtillus) and Bacillus lichenifermia (B. lichenifermia).

Demain C.onwudiwe et al.(2020)[27] Prepared Cobalt hydroxide and cobalt oxide nanoparticles (NPs) using extract of Litchi cinensis, cobalt acetate tetrahydrate by a rapid microwave-assisted method. Structural and morphological characterization of the synthesized NPs were carried out using X-ray diffractometry (XRD), scanning electron microscopy (SEM), transmission electron microscopy (TEM), and fourier transform infrared spectroscopy (FTIR). The XRD patterns revealed that the cobalt hydroxide obtained via the two approaches were the β form, with space group of P-3ml, and the product from the microwave route yielded particles with higher crystallinity. TEM analysis showed that the $Co(OH)_2$ nanoparticles have similar spherical morphologies and monodispersity. Cobalt oxide nanoparticles, were obtained by the calcination of the hydroxide species and resultant loss of both the water molecule and the phytochemical component of the particles, and showed elongated rod like morphology. This green approach, without the use of any chemical reagent, proves to be an efficient, simple, fast and cost effective route for the synthesis of $Co(OH)_2$ and Co_3O_4 NPs which may be used in various applications.

Mohsin Siddique et al.(2020)[28] studied about, the green and eco-friendly synthesis and characterization of cobalt oxide nanoparticles using leaf extract of Citrus medica plant. The crystalline nature and functional groups analysis of cobalt oxide Nps was confirmed by X-ray diffraction and diffused reflectance infra-red spectroscopy respectively. The band gap of the Nps was calculated using Tauc plot. Scanning microscope analysis was carried out to get an insight to the structural morphology of the catalyst. The catalyst was found to be very active for the degradation of methyl orange dye using a very small amount of catalyst (0.006 g) using ultra violet radiation source. Approximately, 90% of the dye (Initial Conc. 10 mg L^{-1}) was degraded in 60 min at natural pH (6.5). The dye degradation increased with increase in pH of the solution, due to the enhanced production of OH radicals, at higher pH values. Different experimental parameters like catalyst amount, agitation speed, initial pH of the solution, initial concentration of dye and recycling of the catalyst were varied to test the performance of the catalyst.

S. Samuela et al.(2020)[29] studied about, the GCoO-NPs. Nanoparticles were synthesized productively using the Jumbo Muscadine grape pulp extract (Vitis rotundifolia) and their structure were elucidated using XRD, FT-IR, UV–Vis spectrometry and SEM. The GCoO-NPs showed degradation of 60 mg/100 mL concentration of AB74 within 150 min (degradation with a rate constant of 0.043 min^{-1}). The dye degradation rates were extremely delicate to pH and worked best in the alkaline conditions. Further analysis is necessary to evaluate the degradation products to well comprehend the different decolorization mechanisms (adsorption vs degradation) for various azo dyes. Therefore, the synthesized GCoO-NPs had an excellent photocatalytic activity and the vital biological components in the NPs can treat microbes in future applications.

Syed Sauban Ghani et al.(2020)[30] studied about cobalt Nanoparticle. Cobalt nanoparticles (CoNPs) were successfully synthesized by green synthetic route using metal salts and flower extracts of a wild plant Calotropis gigantea which act as reducing as well as the stabilizing agent. The synthesized Cobalt nanoparticles (CoNPs) were characterized using various techniques such as UV-visible spectrophotometry and Fourier transform infrared spectrometry. Size characterization of the samples was made by Dynamic light-scattering (DLS) and Transmission electron microscope (TEM).The antibacterial activities of cobalt nanoparticles (Co NPs) were studied under varying concentrations of CoNPs with respect to Staphylococcus aureus and Escherichia coli.

Yoki Yulizar et al. (2020)[31] studied Cobalt oxide Nanoparticle. Cobalt oxide nanoparticles (NP) have been successfully formed using Moringa oleifera leaves extract (MLE) through two phases's system of hexane–water. Co_3O_4 NP was further characterized using UV-Vis DRS, FT-IR, TEM, SEM-EDX, XRD and UV-Vis spectrophotometer. FTIR spectra of Co_3O_4 NP had strong absorption bands at wavenumbers of 538 and 670 cm^{-1} . The bandgap energy value of Co_3O_4 NP was 1.43 eV. In addition, the characterization of SEM and TEM showed that the morphology of Co_3O_4 NP was in the spheres form with particle sizes around 73 nm. The photocatalytic activity of Co_3O_4 NP was carried out for methylene blue (MB) photodegradation. Co_3O_4 NP had photodegradation activity against MB under visible light irradiation of 91% for 120 min.

S. Ajarem et al.(2020)[32] studied about synthesis of Cobalt oxide nanoparticles was assessed by the aqueous extract of red algae and their utilization as cytotoxicity, antioxidant, anticoagulant, antibacterial, and anti-cancer properties. UV–Vis, SEM, TEM, FTIR, EDAX, XRD, and TGA are tools used for characterization purposes. The size of the cobalt oxide nanoparticle crystal of 28.2 ± 7.8 nm was measured based on the X-ray diffraction analysis. Cobalt oxide nanoparticle biological properties such as determination of the antibacterial properties of cobalt oxide nanoparticle by the zone of inhibition method and the minimum inhibitory concentration (MIC) were determined using a dilution broth agar test. Cobalt oxide nanoparticle indicated higher antibacterial than oxytetracycline standard antibiotics. According to these context findings, cobalt oxide nanoparticle would be used as a medicinal aid along with its anti –cytoto xi and effect on bacteria and cancer.

Yameen Ahmed et al (2019)[33] studied the formation of cobalt oxide nanoparticle. cobalt oxide nanoparticles can be fabricated using a reduction technique that is cheaper, environmentally friendly, and best compared to other conventional techniques. In summary, authours have established a facile green method to synthesize low-cost copper oxide and cobalt oxide NPs by using Spinacia oleracea leaf extract . These nanoparticles have many properties and applications. They possess antimicrobial catalytic property and also they can be used in energy storage materials, gas sensors etc The synthesized NPs were examined by various techniques such as UV-Vis, XRD, EDX, and SEM. These techniques confirmed the successful synthesis of cobalt oxide NPs.

N. Matinise et al. (2019)[34],studied about the fabrication of Cobalt (II, III) oxide nanoparticles through a green synthetic method using Moringa Oleifera extract. The electrochemical activity, crystalline structure, morphology, isothermal behaviour and optical properties of cobalt oxide nanoparticles were studied using various characterization techniques. The X-ray diffraction (XRD) and Energy Dispersive X-ray Spectroscopy (EDS) analysis confirmed the formation of cobalt oxide nanoparticles.

Mulya Dewi et al.(2019)[35], studied Co_3O_4 NPs.They were prepared by green synthesis method using Euphorbia heterophylla L. leaves extract (ELE). Co_3O_4 NPs were characterized by FTIR Spectrometry, UV- Vis Spectroscopy, Particle Size Analyser (PSA), X- Ray Diffraction (XRD) and UV- Vis DRS. The FT-IR results showed the presence of Co (II)- O bond and Co (III)- O bond at the wavenumber of 574 and 699 cm^{-1} , respectively. XRD characterization showed that Co_3O_4 NPs had diffraction peaks at 31.1953°, 38.5401°, 44.8076°, 50.2027°, 59.2743° and 65.1419°.TEM image showed that morphology of Co_3O_4 NPs was spherical shaped with the particle size of ~17 nm.The photocatalytic activity of Co_3O_4 NPs was carried out for the methylene blue degradation in 63.105% under irradiation of visible light for 3 hours.

Urabe et al. (2019)[36] studied,cobalt oxide nanoparticles were synthesized using Camellia sinensi leaves and Apium graveolens extract which is a green method of nanoparticles synthesis that does not introduce harmful substances into the environment and ensures cost effectiveness. The particle size was calculated to be in the range of 21–55 nm. These cobalt oxide nanoparticles inhibited the growth of S. aureus, P. aerugino. Therefore, it is pertinent to conclude that the cobalt nanoparticles could be used in the treatment of diseases and infections caused by these organisms

S. Alwin David et al.(2019)[37] ,studied about synthesized cobalt oxide nanoparticles drived from biomaterials like plant extract , bacterium and fungus . Currently , researchers have focused their concentration on the biosynthesis of nanoparticles using biomaterials containing phenols , carbonyls , amines , carbohydrates , proteins and amino acids which act as bio - templates , reducing agents , stabilizing agents , capping agents and chelating agents for nanoparticles . This article also discussed the reports of characterization of cobalt oxide nanoparticles by UV - Vis spectroscopy , diffuse reflectance spectroscopy (DRS) , X - ray diffraction (XRD) , Fourier - transform infrared spectroscopy (FTIR) , selected area electron diffraction (SAED) , scanning electron microscopy (SEM) , high resolution scanning electron microscopy (HRSEM) , transmission electron microscopy (TEM) , high resolution transmission electron microscopy (HRTEM) which were carried out by various researchers.

Maryam Fallahi et al.(2019)[38] studied aboult, cobalt oxide nanoparticle synthesized using Cirsium vulgare leaves extract and characterized using various technique such as X-ray diffraction (XRD), scanning electron microscope (SEM),and transmission electron microscope (TEM).These method conformed the formation of cobalt oxide nanoparticle, and the microscopic technique confirmed the size of the cobalt oxide nanoparticle is about 20nm.The results showed this modified electrode can be applied as a suitable and an efficient catalyst for the oridation of L-cysteine.The oxidation current are directly proportional to the L-cysteine concentration. Simpicity, precision, and being inexpensive are the main advantage of this electrode.

Masoud Salavat et al.[39] studied about the preparation of Co_3O_4 nanoparticles from a solid precursor N - N - bis (salicylaldehyde) -1,2 phenylenediimino cobalt (II) ; Co (salophen) has been achieved via two simple steps : firstly , the Co (salophen) precursor was precipitated from the reaction of cobalt (II) acetate and N - N ' - bis (salicylaldehyde) -1,2 - phenylenediimino ; H_2salophen ; in propanol under nitrogen condition ; then , cubic phase Co_3O_4 nanoparticles with the size of mostly 30-50 nm could be produced by thermal treatment of the Co (salophen) in air at 773

K for 5 h . The as synthesized products were characterized by powder X - ray diffraction (XRD) , Fourier transform infrared spectroscopy (FT - IR) , transmission electron microscopy (TEM) , X - ray photoelectron spectroscopy (XPS) , and scanning electronic microscopy (SEM) . These results confirm that the resulting oxide was pure single - crystalline Co_3O_4 nanoparticles .

Shikha Dubey et al.(2018)[40] studied, green synthesis of cobalt oxide (nanoparticles using latex of Calotropis procera via simple precipitation method at room temperature was investigated. An extensive characterization of the product was carried out using X-ray diffractometry (XRD), Differential scanning calorimetry (DSC), Transmission electron Microscopy (TEM), Energy dispersive X-ray spectroscopy (EDX), Fourier transform infrared spectroscopy (FTIR) and UV–Visible spectroscopy. The results of the characterization confirmed that the synthesized nanomaterial is highly dispersed. TEM analysis revealed that the nano particles are having an average size around 10 nm. The eco-toxic investigation suggested that the particles are non-toxic and safe towards the environment. This green strategy proves to be an effective, fast, simple and cost effective approach for the synthesis of cobalt oxide nanoparticles for various applications.

Saravanakumar et al. (2018)[41], studied green synthesis of cobalt oxide nanoparticles using seed extract of piper nigrum. Synthesized nano Cobalt oxide were characterized using UV-Vis, FT-IR spectroscopic techniques and AFM. UV spectra showed the maximum absorbance of 268 and 305 nm due to the excitation of surface Plasmon vibrations in the cobalt oxide nanoparticles formation. FTIR spectrum exhibited the characteristic band at 704 cm^{-1} which indicated the O-Co-O bridging vibration of cobalt oxide nanoparticles. Hence it can be used as a catalyst for the removal of dyes from contaminated water resource. The Cerium doped cobalt oxide Nanoparticles exhibit enhanced photocatalytic activity and can be efficiently used as photocatalyst in the process of removal of organic dyes and used for environmental cleaning and water purification.

IsmatBibi et al.(2017)[42] studied, synthesis of Cobalt - oxide nanoparticles using Punica granatum peel extract and cobalt nitrate hexahydrate at low temperature . The synthesized cobalt - oxide NPs were characterized using X - ray powder diffraction , scanning electron microscopy , energy - dispersive X - ray , atomic force microscopy , fourier transform infrared spectroscopy and UV - visible techniques . The cobalt - oxide NPS were in highly uniform shape and size was in the rang of 40-80 nm . Photo catalytic activity (PCA) of the synthesized NPs was evaluated by degrading Remazol Brilliant Orange 3R (RBO 3R) dye and a degradation of 78.45 % was achieved (dye conc . 150 mg / L) using 0.5 g cobalt - oxide NPs for 50 min irradiation time . In view of eco - benign and cost - effective nature , the present investigation revealed that P. granatum could be used for the synthesis of cobalt - oxide NPs for photo - catalytic applications.

F.chekin et al.(2016)[43] studied about ,green synthesis of pure cobalt oxide nanoparticles (CoO-NPs) in aqueous medium using gelatin. The main advantage of using gelatin as stabilizing agent is that it provides long-term stability for nanoparticles by preventing particles agglomeration. The particles have been characterized using X-ray diffraction (XRD), transmission electron microscope (TEM), scanning electron microscopy (SEM), energy dispersive X-ray (EADX), and thermogravimetric analysis (TGA). TEM image shows the formation of CoO-NPs with average particle size of 28 nm which agrees well with the XRD data. The XRD results showed pure cobalt oxide crystalline nature with crystallite size of 25 nm which agrees well with the TEM results. A sensor towards the glucose detection is fabricated by spiking of CoO NPs into carbon paste.

J.K.Sharma et al.(2015)[44] studied about, green synthesis of cobalt oxide nanoparticles cobalt oxide nanoparticle using leaves extract of plant Calotropis gigantea and characterized by X - ray diffraction (XRD) , UV - vis spectroscopy , scanning electron microscopy (SEM) , transmission electron microscopy (TEM) and energy dispersive X - ray spectroscopy (EDX) . The green synthesized cobalt oxide nanoparticle showed excellent catalytic effect on the thermal decomposition of ammonium perchlorate (AP) and burning rate of composite solid propellants (CSPs) . Kinetics of slow and rapid thermal decomposition has been investigated by isoconversional and ignition delay methods , respectively . Moreover , the electrocatalytic performance of green synthesized cobalt oxide nanoparticle in dye - sensitized solar cells (DSSC) has also been evaluated . The cyclic voltametry

A diallo et al.(2015)[45]studied about, the green synthesis of high-purity amorphous Co_3O_4 quasi-spherical nanoparticles (⟨fparticle⟩ ~3.57 nm) by green process using the natural extract of A. Linearis as an effective bio-reduction/bio-oxidizing chemical agent. Thermal annealing at ~400°C during 2 h under normal air conditions allows the acquisition of crystallized single-phase.Co_3O_4 nanoparticles were substantiated by the EDS, XRD, Raman, ATR-FTIR, and XPS investigations.

3. PREPARATION OF COBALT OXIDE

About 5 g of aerial roost of ficus benghalensis was initially washed , crushed and added with deionized water. Then it was heated at 70^0C - 75 ^{0}C for 1/2 an hour . Then the heated solution is filtered using Wattmen filter paper . Thus the extract was obtained . IM cobalt nitrate hexahydrate solution is added with extract and the entire solution is allowed to stirrer for ½ an hour. Colour of the solution was observed as dark pink colour. After an ½ hour, IM NaOH solution is added, to the resultant solution drop by drop. changing of colour was observed. Till dark blue formation this was continued 30 minutes stirring was allowed in the solution. After that PH of the solution is checked and found out as 5 then continuous water washing was done . till the reach of neutral PH. For 12 hours the resultant material was kept at hot air oven at 105 °C. The dried material was collected and grained well followed by calcined at 500°C for 3 hours and the sample is collected . At last , 7.079g sample is collected, and named as MMC

3.1 flow chat

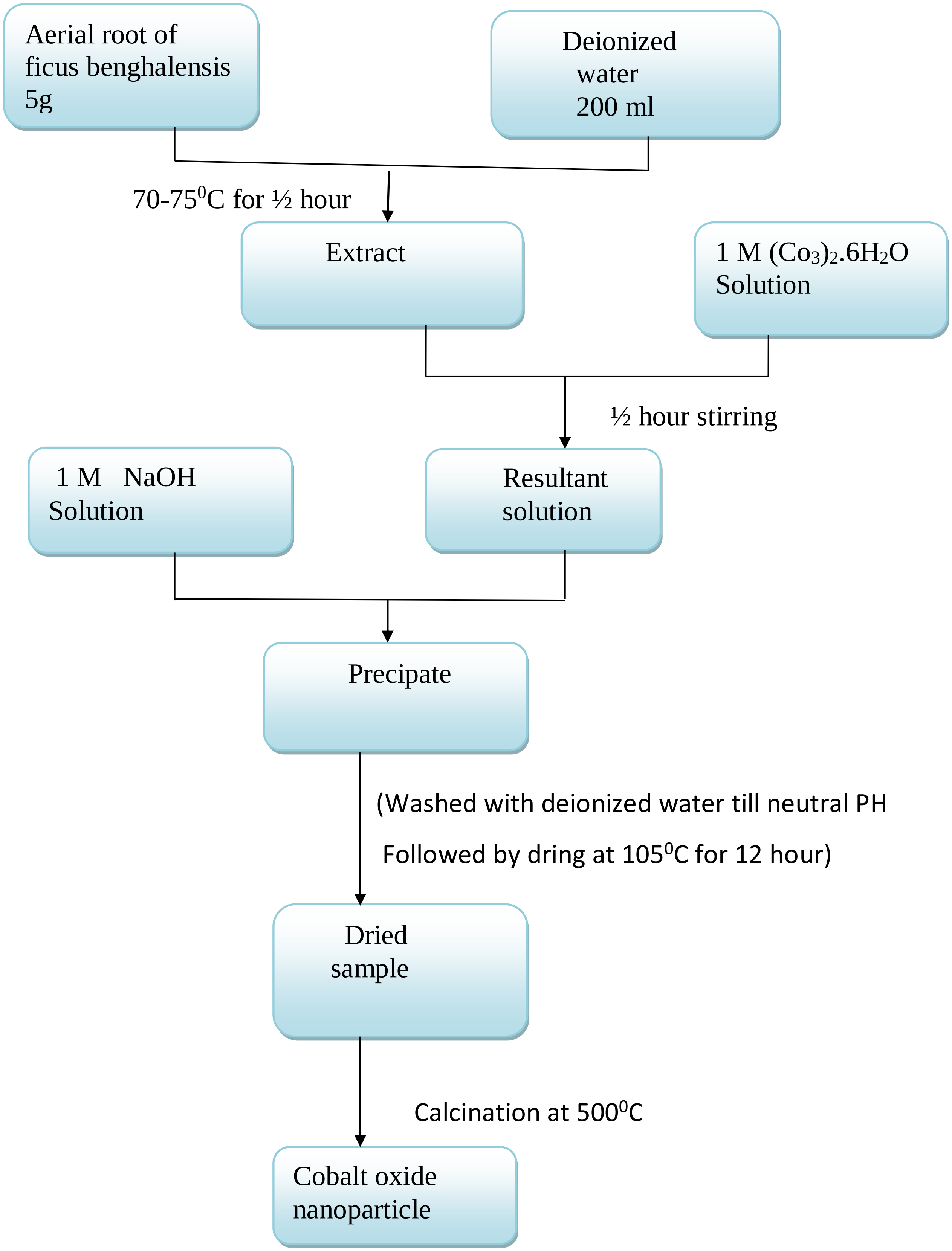
Aerial root of ficus benghalensis 5g
Deionized water 200 ml
70-75^{0}C for ½ hour
Extract
1 M $(Co_3)_2.6H_2O$ Solution
½ hour stirring
1 M NaOH Solution
Resultant solution
Precipate
(Washed with deionized water till neutral PH
Followed by dring at 105^{0}C for 12 hour)
Dried sample
Calcination at 500^{0}C
Cobalt oxide nanoparticle

3.2 CO-PRECIPITATION METHOD

The co-precipitation technique involves the precipitation of metal in the form of hydroxide from a salt precursor with the help of a base in a solvent. Co-precipitation is the most widely used procedure for preparing a precursor of mixed oxides. Co-precipitation is a very common reaction for the synthesis of NPs. In the typical co-precipitation reaction, the feature of different solubility of salts in water is taken advantage of. As reagents, two or more water-soluble salts are used that react with each other. One or more salts that are water-insoluble are formed in the liquid phase. When the concentration of this product crosses the solubility product value in the reaction media precipitation takes place.

There are three main mechanisms of co-precipitation method

- Inclusion,
- Occlusion,
- Adsorption.

Advantages

- Easy and quick to prepare,
- Particle size and composition may be easily controlled,
- A variety of ways to alter particle surface state and overall homogeneity,
- It's cold outside,
- It saves energy,
- Doesn't need the use of an organic solvent.

Disadvantages

- Uncharged species are not included,
- Trace contaminants in the product may also precipitate,
- It takes time,

- Issues with batch-to-batch repeatability,
- When the reactants have highly differing precipitation rates, this approach fails [46].

3.3 CHARACTERIZATION TECHNIQUE

Characterization and analytical techniques are methods used to identify, isolate or quantify chemicals or materials or to characterize their physical properties. They include microscopy, light scattering spectroscopy, chromatography, gravimetric and other measurements used in chemistry and material science. The nanostructure has to be characterized by using various techniques such as SEM, TEM, UV, FTIR, XRD, BET, RAMAN ,etc. The cobalt nanoparticle are subjected to SEM, EDAX, Elecrochemical analysis, BET surface area analysis ,in the present work.

3.3.1 Scanning Electron Microscope (SEM)

Scanning electron microscope uses a focused beam of high energy electrons to generate a variety of signals at the surface of solid specimens. The signal that derive from electron sample interactions reveal information about the sample including external morphology, chemical composition and crystalline structure and orientation of materials making up the sample. In most applications data are collected over a selected area of the surface of the sample and a two- dimensional image is generated that displays spatial 33 variations in these properties. Areas ranging from approximately 1 cm to 5 microns in width can be imaged in a scanning mode using conventional SEM techniques. The SEM is also capable of performing analyses of selected point locations on the sample[47].

Fig 3.3.1 Scanning electron microscope

Intrumantation

Essential components of all SEM include the following:

- Electron Source
- Electron Lense
- Sample Stage
- Detectors for all signals of interest
- Display / Data output devices
- **Infrastructure Requirements**:
    - Power Supply
    - Vacuum System
    - Cooling system
    - Vibration-free floor
    - Room free of ambient magnetic and electric Fields

Application

The SEM is routinely used to generate high-resolution images of and to show spatial variations in chemical compositions.

1) Acquiring elemental maps or spot chemical analyses,
2) Discrimination of phases based on mean atomic number,
3) Compositional maps based on differences in trace element “.

Precise measurement of very small features and objects down to 50nm in size is also accomplished using the SEM. Back scattered electron images can be used for rapid discrimination of phases in multiphase samples. SEM is equipped with diffracted backscattered electron detectors can be used to examine micro fabric and crystallographic orientation in many materials[48].

3.3.2 Energy dispersive X-ray (EDX)

Energy dispersive X-ray analysis (EDX), referred to as EDS or EDAX, is an x-ray technique used to identify the elemental composition of materials. The basic principle of EDX is a generation of X-rays from a specimen through the electron beam. The X-rays are generated according to the characteristics and nature of the elements present in the sample. Hence, this technique also can be used to measure the energy of emitted X-rays. The data generated by EDX analysis consist of spectra showing peaks corresponding to the elements making up the true composition of the sample being analysed.

Fig 3.3.2 Energy dispersive X-ray instrument

The components of the EDX

1. Excitation source (electron beam or x-ray beam),
2. X-ray detector,
3. Pulse processo,r
4. Analyzer.

Advantages

- Improved quality control and process optimization,
- Rapid identification of contaminant and source,
- Full control of environmental factors, emissions etc,
- Greater on-site confidence, higher production yield
- Identifying the source of the problem in process chain.

3.3.3 RAMAN spectroscopy

When light interacts with molecules in a gas, liquid, or solid, the vast majority of the photons are dispersed or scattered at the same energy as the incident photons. This is described as elastic scattering, or Rayleigh scattering. A small number of these photons, approximately 1 photon in 10 million will scatter at a different frequency than the incident photon. This process is called inelastic scattering, or the Raman effect. Raman scattering produces scattered photons with a different frequency depending on the source and the vibrational and rotational properties of the scattered molecules. Raman spectroscopy works on the principle of Raman scattering. It is used to study materials by chemists and physicists.It is used to study the vibrational, rotational and low-frequency modes of the molecules.

Fig 3.3.3 Raman spectrometer

Types of Raman Spectroscopy

1. Resonance Raman Spectroscopy (RRS),
2. Surface-enhanced Raman Spectroscopy (SERS),
3. Micro-Raman Spectroscopy,
4. Non-linear Raman Spectroscopic Techniques.

Applications

- Raman spectroscopy works on the basis of Raman effect and finds applications in various fields like nanotechnology to understand the structure of nanowires, biology and medicine where the low-frequency DNAs and proteins are studied and chemistry to understand the structure of molecules and their bonds,
- Raman scattering is used in remote sensing and planetary exploration,
- Raman scattering is used to sense the minerals in Mars,
- Raman spectroscopy is used to analyze a wide range of materials, including gases, liquids, and solids. Highly complex materials such as biological organisms and human tissue can also be analyzed by Raman spectroscopy,
- For solid materials, Raman scattering is used as a tool to detect high-frequency phonon and magnon excitations,
- Raman lidar is used in atmospheric physics to measure the atmospheric extinction coefficient and the water vapour vertical distribution,
- Stimulated Raman transitions are also widely used for manipulating a trapped ion's energy levels, and thus basis qubit states,
- Raman spectroscopy can be used to determine the force constant and bond length for molecules that do not have an infrared absorption spectrum,
- Raman amplification is used in optical amplifiers,
- Raman spectroscopy has been used to investigate nucleic acids, in biological systems by a vibrational tag[49].

3.3.4 Brunauer - Emmett – Teller (BET)

Brunauer-Emmett-Teller (BET) theory aims to explain the specific surface area of materials. It is Directly measures surface area & pore size distribution. BET theory applies to systems of multilayer adsorption, and usually utilizes probing gases that do not chemically react with material surfaces as adsorbates to quantify specific surface area. It gives important information on their physical structure as the area of a materials surface affects how that solid will interact with its environment. Many properties such as dissolution rates, catalytic activity, moisture retention, and self life are often correlated to a material's surface area. The specific surface area of the BET sample is determined by the physisorption of an inert gas, typically nitrogen, argon, or krypton, on the sample surface. The surface area determination should be carried out at a constant temperature. Specific surface area is a scale-dependent property, with no single true value of specific surface area definable, and thus quantities of specific surface area determined through BET theory may depend on the adsorbate molecule utilized and its adsorption cross section.

Fig 3.3.4 Brunauer-Emmett-Teller instrument

Application

❖ Cement and concrete

The Measurement of the specific surface area using the BET method is useful for comparing different cements. This may be performed using adsorption isotherms measured in different ways, including the adsorption of water vapour at temperatures near ambient, and adsorption of nitrogen at 77 K (the boiling point of liquid nitrogen). Different methods of measuring cement paste surface areas often give very different values, but for a single method the results are still useful for comparing different cements.

❖ Activated carbon

Activated carbons has strong affinity for many gases and has an adsorption cross section of 0.162 nm^2 for nitrogen adsorption at liquid-nitrogen temperature (77 K). BET theory can be applied to estimate the specific surface area of activated carbon from experimental data, demonstrating a large specific surface area, even around 3000 m^2/g [50].

❖ Catalysis

In the field of solid catalysis, the surface area of catalysts is an important factor in catalytic activity. Inorganic materials such as mesoporous silica and layered clay minerals have high surface areas of several hundred m^2/g calculated by the BET method, indicating the possibility of application for efficient catalytic materials.

Advantages

- Nitrogen, Argon, Krypton are available as adsorbate gases,
- Several instrument options to ensure best fit for material.

4. RESULT AND DISCUSSION

This present study is to investigate the chemical and bio-synthesis of the Co_3O_4 nanoparticles. The properties of nanostructures lead to the the drastic potential applications. So in the present thesis the prepared Cobalt oxide nanostructure have been subjected to RAMAN, EDAX, SEM and BET surface analysis, Electro chemical analysis analytic techniques and structural and surface have been obtained respectively.

4.1 Scanning Electron Microscope (SEM) Analysis

The morphology of Co_3O_4 nanoparticles was investigated by SEM. Figure 4.1 shows the SEM image of the as-prepared Co_3O_4 nanoparticles. From the SEM image, it is clearly evident that the product consists of extremely fine particles with sphere-like morphologies that appreciably aggregated as clusters due to the extremely small dimensions and high surface energy of the obtained nanoparticles. The SEM image shows irregular particle agglomerates of the product, indicating that the synthesized Co_3O_4 is actually composed of numerous nanoparticles with a uniform size, and these particles undergo further aggregation to form porous agglomerate structure.

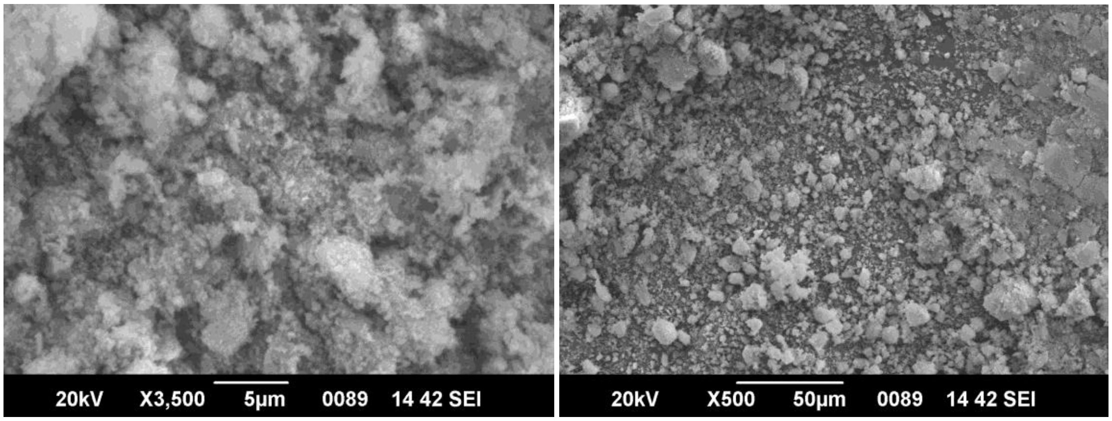

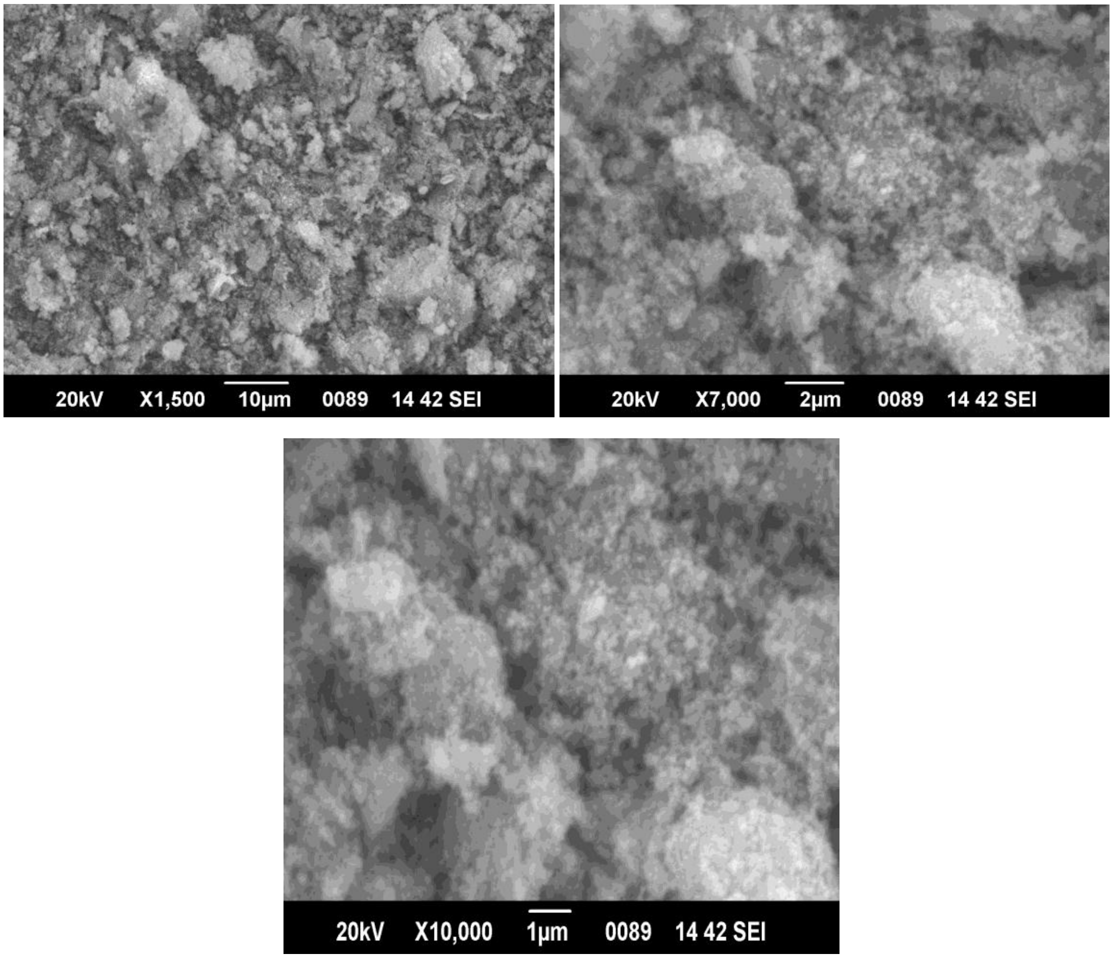

Fig 4.1 SEM image of cobalt oxide nanoparticle

4.2 Energy Dispersive X-ray (EDX) spectrum Analysis:

Fig 4.2 shows energy dispersive x-ray analysis of cobalt oxide nanoparticle. The elemental composition of the synthesized Co_3O_4-NPs was also evaluated from EDX analysis. From the graph, it is confirmed that the presence of Co and O peaks alone and no other impurities were identified and this shows the phase purity of the samples which supports the X-ray diffraction pattern of the samples.Table 4.1 shows the elemental composition of cobalt and oxygen present in the sample. The atomic percentage of Co and O were found to be 52.2% and 47.8% which is in good agreement with the literature .

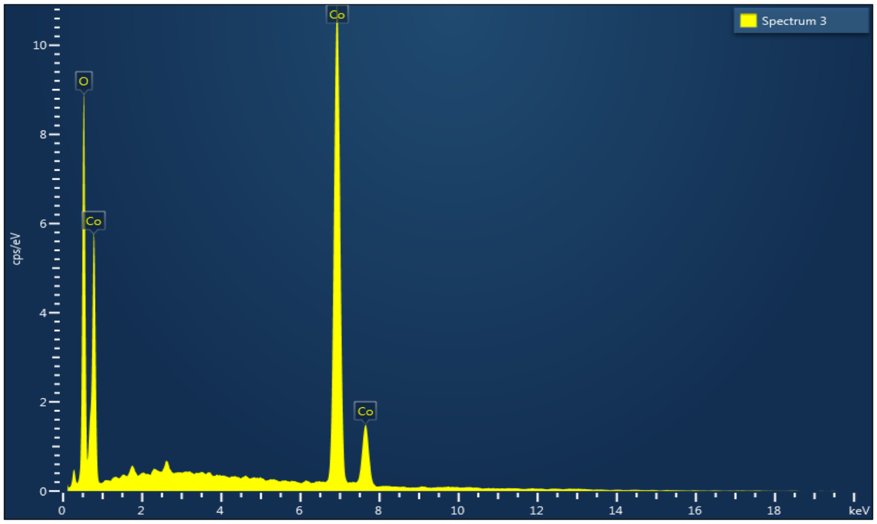

Fig 4.2 EDX image of cobalt oxide nanoparticle

Table 4.2 EDX of Cobalt oxide nanoparticle

S.No	Elements	Weight %	Atomic %
1.	O	19.91	47.8
2.	Co	80.09	52.2

4.3 RAMAN analysis

Raman scattering is very sensitive to the microstructure of nanocrystalline materials, it is also used here to clarify the structure of the Co_3O_4 nanoparticles. As shown in Fig. 4.3 shows four obvious peaks located at around 183.9, 467.3, 515.6, and 676.09 cm^{-1}, corresponding to the four Raman-active modes of Co_3O_4 nanoparticle. The Raman bands with medium intensity located at 183.9, 467.3 and 515.6 cm^{-1} have the $F_2g^{(1),}$ Eg and $F_2g^{(2)}$ symmetry, respectively. The strong band at about 676.09 cm^{-1} is attributed to the characteristics of the octahedral sites ($Co^{III}O_6$), which is assigned to the A_1g species in the O_h spectroscopic symmetry.

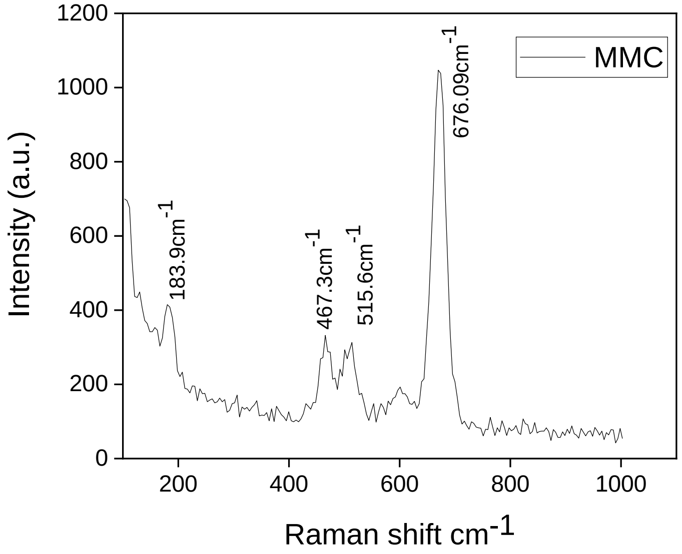

Fig 4.3 Raman image of cobalt oxide nanoparticle

4.4 BET surface analysis

The nitrogen absorption – desorption isotherm was drawn for the cobalt oxide nanoparticle. (Figure 4.4 a) presence of type – IV isotherm in the nitrogen absorption – desorption graph reveals the existence of mesopores in the sample. BET specific surface area and BJH desorption pore volumes are 139.439 m^2/g, 0.553 cm^3/g respectively. Figure 4.4 b represent the pore size distributation graph. Various peak values observed in the graph are listed as 1.55 nm, 2.14 nm, 2.49 nm, 4.51 nm, 5.42 nm, 6.77 nm,10.9 nm. This wide range of the values indicates the presence of mesopores in the sample. From the BJH pore size distribution absorption, it is revealed that more number of pures have the radius of 1.554nm.

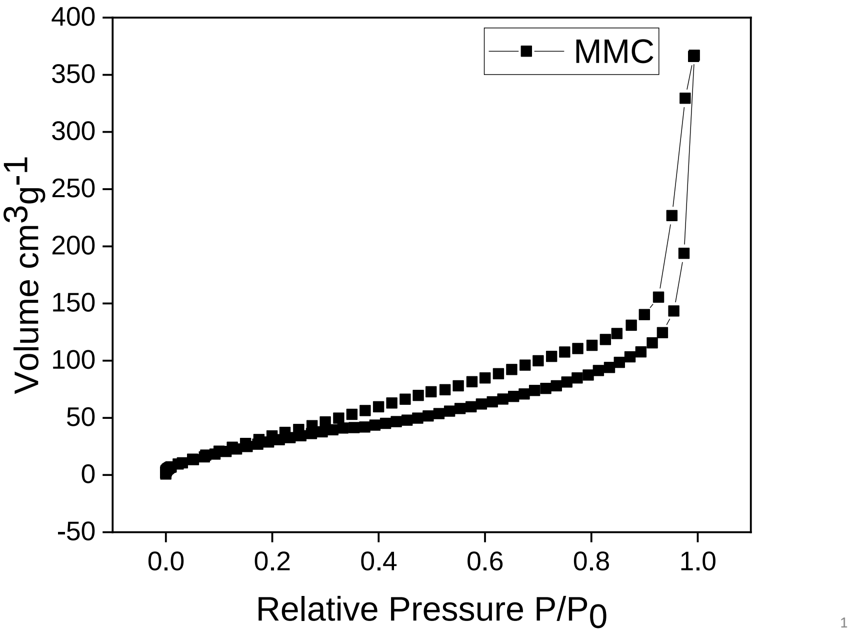

Fig 4.4- a N$_2$ absorption desorptionof cobalt oxide nanoparticle

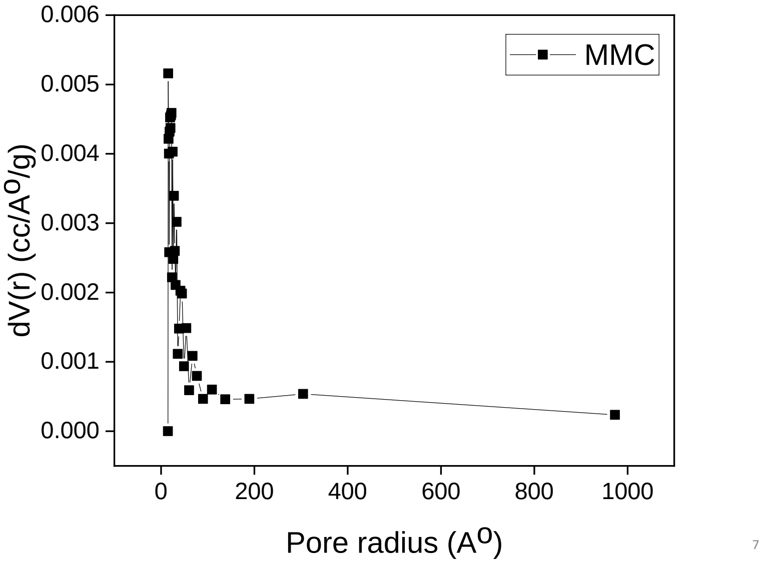

Fig 4.4- b Pore size distribution of cobalt oxide nanoparticle

5. CONCLUSION

In this work, aerial root of banyan treee was used in the preparation of Co_3O_4 nanoparticle via co-precipitation method. The synthesized Co_3O_4 nanoparticle was finely ground and collected. Morphology of the synthesized Co_3O_4 nanoparticle was studied using SEM-EDX, BET surface analysis and RAMAN study. With help of SEM analysis it is clearly evident that product consist of extremely fine particles with sphere like morphologies. From EDX analysis, presence of Co and O was confirmed and no impurities were identified. From RAMAN analysis, it is confirmed that the sample had four Raman-active modes.BET surface analysis revealed that more number of mesopores were present in the Co_3O_4 nanoparticle. Additionally BET specific surface area and pore volumes were found 139.439 $m^{2/}g$, 0.553 cm^3/g respectively.

REFERENCE

[1] R.Paull,J. Wolf,p.Heber,M.Sinkula,Nature Biotechnol.,21 (2003)1144

[2] S. Ayyapan , S. mahadevan , P.chandramohan , M. Srinivasan ,P. john Philip & Baldev Raj .,(2010) " Influence of Co_2 ion concentration on the size , Magnetic properties , and purity of Co FeO4 spinel ferrite nano particles " .

[3]. Fun chin , suk ; Iyer , K.Swaminathan ; Raston , Colin.L ; saundaers , Martin., (2008) " Size selective synthesis of superparamagnetic nano particle in thin fluids under continuous flow condition ".

[4] Nigel Smith , colin L. Raston , martin saunders , Robert Woodward , annayaMandal , MD ., “ properties of Nanoparticle” Reviewed by April Cashin - Garbutt , MA (Cantab) .

[5] Nadeem Joudeh and Dirk Link.,(2022) “ Nanoparticle classifcation, physicochemical properties, characterization, and applications: a comprehensive review for biologists “ .

[6] Wiechers .J .W ,and Musee.,N.,(2010) Engineered Inorganic Nanoparticles and Cosmetics : Facts , Issues , Knowledge Gaps and Challenges 6

[7] Teng W, Jeng S, Kuo, C .,(2008) “liquid crystal” displays 33 1663–5

[8] Crooks R M, Zhao M, Sun L I, Chechik V and Yeung L E E K 2001 Dendrimer-Encapsulated Metal Nanoparticles : Synthesis , Characterization , and Applications to Catalysis 34 181–90

[9] Ganesh K and Archana D 2013 Review Article on “Targeted Polymeric Nanoparticles ”

[10] Nazari A and Riahi S 2011 Composites : Part B “The effects of SiO 2 nanoparticles on physical and mechanical properties of high strength compacting concrete Compos”. Part B 42 570–8

[11] Dallas Donaldson, Detmar Beyersmann, "Cobalt and Cobalt Compounds" in Ullmann's Encyclopedia of Industrial Chemistry”. Wiley-VCH, Weinheim, 2005.

[12] Schlessinger, G. (1960). "Carbonatotetramminecobalt(III) Nitrate". *Inorganic Syntheses*. 6: 173–175

[13] Deming, Horace G. (1925). General Chemistry:' An Elementary Survey Emphasizing Industrial Applications of Fundamental Principles '(2nd ed.). New York: John Wiley & Sons, Inc. p. 452.

[14] Ramesh Vinayagam , Akshatha Hebbar , P. et al (2023).'Green synthesized cobalt oxide nanoparticles with photocatalytic activity towards dye removal volume' 216 part 4 114766

[15] Parvathiraja Chelliah , Saikh Mohammad Wabaidur et al.(2023)' Green Synthesis and Characterizations of Cobalt Oxide Nanoparticles and Their Coherent Photocatalytic and Antibacterial Investigations Parvathi'

[16] Vandamar Poonguzhali , R., Ranjith Kumar .E,. et al.' Natural lemon extract assisted green synthesis of spinel Co_3O_4 nanoparticles for LPG gas sensor application ' volume 377 , 15 February 2023, 133036

[17] Rajakumar Govindasamy , Vaishnavi Raja et al, (2023) 'Green Synthesis and Characterization of Cobalt Oxide Nanoparticles Using Psidium guajava Leaves Extracts and Their Photocatalytic and Biological Activities'.

[18] Rishabh Srivastava , Shiva Bhardwaj et al,(2022) 'Waste Citrus reticulata Assisted Preparation of Cobalt Oxide Nanoparticles for Supercapacitors'

[19] Thenmozhi Ramasamy, Sukithra Elango ,et al (2022) , "Green Synthesis and Characterization of Cobalt Nanoparticles from Pisonia Alba Leaf" volume 10 :pp 534-540

[20] Eneyew Tilahun Bekele , H. C. Ananda Murthy et al,'Solanum tuberosum Leaf Extract Templated Synthesis of Co_3O_4 Nanoparticles for Electrochemical Sensor and Antibacterial Applications' Volume 2022, Article ID 8440756, 15 pages.

[21] Rajan Lakra a , Rahul Kumar b , Dhirendra Nath Thatoi a , Prasanta Kumar

Sahoo a , Ankur Soam a ,(2020) “Synthesis and characterization of cobalt oxide (Co_3O_4) nanoparticles ”.

[22] C.T. anuradha, p raji,(2021) “Citrus limon fruit juice-assisted biomimetic synthesis, characterization and antimicrobial activity of cobalt oxide (Co_3O_4) nanoparticles”.

[23] Sayed Zia Mohammadi. a , Batoul Lashkari. a , Azita Khosravan, b. (2022) , “Green synthesis of Co_3O_4 nanoparticles by using walnut green skin extract as a reducing agent by using response surface methodologe” (https://www.sciencedirect.com/journal/surfaces-and-interfaces).

[24] Sirajul Haq1, Farwah Abbasi , Manel Ben Ali. (2021) “cobalt oxide nanoparticles and the effect of annealing temperature on their physiochemical and biological properties”, (https://doi.org/10.1088/2053-1591/ac1187)

[25] Syed Yawar Saeed1 , Kanwal Mazhar2, Laiba Raees , Asma Mukhtiar , Farooq Khan and Muhammad Khan ,(2021), ”Green synthesis of cobalt oxide nanoparticles using roots extract of Ziziphus Oxyphylla Edgewits characterization and antibacterial activity” . (https://doi.org/10.1088/2053-1591/ac9350)

[26] Muhammad Hafeez1 , Ruzma Shaheen , Bilal Akram , Zain-ul-Abdin , Sirajul Haq , Salahudin Mahsud , Shaukat Ali and Rizwan Taj Khan.,(2020) “Green synthesis of cobalt oxide nanoparticles for potential biological applications”.

[27] Damian C. Onwudiwe , Murendeni P. Ravele , Elias E. Elemike c,(2020) “Eco-friendly synthesis, structural properties and morphology of cobalt hydroxide and cobalt oxide nanoparticles using extract of Litchi chinensis”. . http://www.elsevier.com/locate/nanoso

[28] Mohsin Siddique, Noor Muhammad Khan, Muhammad Saeed, Sajid Ali and Zarbad Shah.,(2020) “ Green synthesis of cobalt oxide nanoparticles using Citrus medica leaves extract: characterization and photo-catalytic activity”.

[29] Melvin S. Samuela , E. Selvarajanb , Thangavel Mathimanic , Needhidasan

Santhanamd , Tran Nhat Phuonge , Kathirvel Brindhadevif,, Arivalagan Pugazhendhig,“Green synthesis of cobalt-oxide nanoparticle using jumbo Muscadine (Vitis rotundifolia): Characterization and photo-catalytic activity of acid Blue-74”.

[30] Syed Sauban Ghani1*, Farheen Ghan, (2020),. “Green Synthesis and Antibacterial Activity of Cobalt Nanoparticle from Calotropis gigantae”.

[31] Yoki Yulizara, Dewangga Oky Bagus Apriandanub and Yessi Pratiwi c,(2020) “Formation of Co_3O_4 Nanoparticles Using Moringa oleifera Leaves Extract through Two Phases System of Hexane-Water and their Photocatalytic Activity” Vol. 982, pp 9-13.

[32] Jamaan S. Ajarem, Saleh N. Maodaa, Ahmed A. Allam , Mohamed M. Taher and Mohamed Khalaf,.(2020)“Benign Synthesis of Cobalt Oxide Nanoparticles Containing Red Algae Extract: Antioxidant, Antimicrobial, Anticancer, and Anticoagulant Activity”. (https://doi.org/10.1007/s10876-021-02004-9)

[33] Yameen Ahmed, Jamshid Hussain , Farman Ullah and Sohaib Asif,(2020) “Green synthesis of copper oxide and cobalt oxide nanoparticles using Spinacia oleracea leaf extract “.

[34] N. Matinise, N. Mayedwa, X. G. Fuku, N. Mongwaketsi, and M. Maaza,.(2020),. “ Green synthesis of cobalt (II, III) oxide nanoparticles using Moringa Oleifera natural extract as high electrochemical electrode for $^{\text{supercapacitors”.}}$

[35] Nur Oktri Mulya Dewi , Yoki Yulizar1, Dewangga Oky Bagus Apriandanu,(2019),.“Green synthesis of Co_3O_4 nanoparticles using Euphorbia heterophylla L. leaves extract: characterization and photocatalytic activity”.

[36] Aliyaa A. Urabe and Wisam J. Aziz,(2019),. “biosynthesis of cobalt oxide (Co_3O_4) nanoparticles using plant extract of Camellia sinensis (L.) Kuntze and Apium graveolens L. as the antibacterial application”. WNOFNS 24 (2019) 356-364

[37]Ishmatbibi, Nosheennazar, et al, “ Green and eco friemdly synthesis of cobalt oxide nanaoparticle:characterization and photo catalytic activity”, volume 28, Issue

19.

[38] Maryam Fallahi1 & Banafsheh Norouzi1,(2020) “Synthesis of cobalt oxide nanoparticles using Cirsium vulgare leaves extract and evaluation of electrocatalytic effects on oxidation of L-cysteine.

[39]Masoudsalavathi-niasari, Afsanehkhansari, “synthesis and characterization of cobalt oxide nanoparticle by thermal treatment process.”

[40] Shikha Dubey a , Jay Kumar b , Ashok Kumar b , Yogesh Chandra Sharma a,(2018)“Facile and green synthesis of highly dispersed cobalt oxide (Co_3O_4) nano powder: Characterization and screening of its eco-toxicity”.

[41] Saravanakumar,P. muthukumar,M. “Piper Nigrum Mediated Green Synthesis, Charecterization of Undoped Cobalt Oxide and Cerium Ion Doped Cobalt Oxide Nanoparticles”. PP. 918-923

[43] Ismat Bibi ,A. Nosheen Nazar ,A.(2019) “Green synthesis of iron oxide nanoparticles using pomegranate seeds extract and photocatalytic activity evaluation for the degradation of textile dye”

[44] J.K.Sharma ' PratibhaSrivastava ' GurdipSingh M.ShaheerAkhtar S.Ameen Green synthesis of Co_3O_4 nanoparticles and their applications in thermal decomposition of ammonium perchlorate and dye - sensitized solar cells (https://doi.org/10.1016/j.mseb.2014.12.012) Volume 193

[45] Diallo,A. Beye,a.c. “ Green synthesis of Co_3O_4 nanoparticles via Aspalathus linearis: Physical properties”.

[46] https://www.sciencedirect.com/topics/materialsscience/coprecipitation

[47] Valencia, S.; Vargas, X.; Rios, L.; Restrepo, G.; Marın, J. M. Sol–Gel and Low Temperature Solvo Thermal Synthesis of Photoactive NanoTitanium Dioxide. J. Photochem. Photobiol. A 2013, 251, 175–181. DOI: 10.1016/j.jphotochem.2012.10.025

[48] Vasconcelos, D.C., Costa, V.C., Nunes, E.H., Sabioni, A.C., Gasparon, M.,

Vasconcelos, W.L., 2011. Infrared spectroscopy of titania sol-gel coatings on 316L stainless steel. Mater. Sci. Appl. 2, 1375–1382

[49] Nakayama, Atsuko; Suzuki, Kazuya; (1996) Elecronic and magnetic properties of Activated carbon fibers". Bull. Chem. Soc. Jpn. 69 (2): 333–339.

EFFECT OF DESPOSITION CYCLES OF AS-DEPOSITED ZnO THIN FILMS PREPARED BY SILAR METHOD

A project work report and submitted to

DEPARTEMENT OF PHYSICS

ST. MARY'S COLLEGE (AUTONOMOUS), THOOTHUKUDI

Affiliated to

MANONMANIAM SUNDARANAR UNIVERSITY,

THIRUNELVELI

In partial fulfilment of the requirements for the award of

MASTER OF SCIENCE IN PHYSICS

Submitted by

M.MOHAMED SHIFANA

Reg. No: 21SPPH06

Under the guidance of

Dr. A. Nirmala Shirley M.Sc., B.Ed., M.Phil., Ph.D.,

DEPARTMENT OF PHYSICS

ST. MARY'S COLLEGE (AUTONOMOUS),

THOOTHUKUDI.

Re-accredited with 'A^{+}' Grade by NAAC

(2022-2023)

CERTIFICATE

This is to certify that this project work report entitled **"EFFECT OF DEPOSITION CYCLES OF AS - DEPOSITIED ZnO THIN FILMS PREPARED BY SILAR METHOD"** is submitted to **ST. MARY'S COLLEGE (AUTONOMOUS), THOOTHUKUDI** in partial fulfilment of requirements for the award of **MASTER OF SCIENCE IN PHYSICS** and is a record of work done during the academic year **2022 – 2023** by **M.MOHAMED SHIFANA** (Register No: 21SPPH06)

A. Nirmala Shirley

Signature of the Guide

Padmavathi

Signature of the Co-Ordinator

Signature of the Director

Director
Self Supporting Courses
St. Mary's College (Autonomous)
Thoothukudi - 628 001.

Lucia Rose

Signature of the principal

Principal
St. Mary's College (Autonomous)
Thoothukudi - 628 001.

12/4/23

Signature of the Examiner

DECLARATION

I hereby declare that the project work report entitled **"EFFECT OF DEPOSITION CYCLES OF AS-DEPOSITIED ZnO THIN FILMS PREPARED BY SILAR METHOD"** is submitted to **ST. MARY'S COLLEGE, (AUTONOMOUS), THOOTHUKUDI** affiliated to **MANONMANIAM SUNDARANAR UNIVERSITY, THIRUNELVELI** for the award of the degree of Master of Science in Physics is my original work and that no part of this project work report has been submitted for any Degree, Diploma or other similar titles.

M. Mohamed Shifana

Signature of the Student

Station: Thoothukudi

Date: 5. 4. 23

(M.MOHAMED SHIFANA)

ACKNOWLEGEMENT

First of all, I thank GOD of all creations, for showering his divine mercy and grace in completing this project work successfully.

I wish to record my profound gratitude to our Principal Rev. **Sr. Dr. A. S. J. Lucia Rose, M.Sc., B.Ed., M.Phil., PGDCA., Ph.D.** for her motivation.

I sincerely thank our Director of **SSC, Rev. Sr. Josephine Jeyarani, M.A., M.Phil.,** for her encouragement and support.

I wish to thank **Rev. Sr. Dr. JESSIE FERNANDO M.Sc., M.Phil., Ph.D.,** HOD & Associate professor for her inspirational words to complete this project work.

I owe a great deal to Mrs. **P. PADMAVATHI M.Sc., M.Phil., SET.,** SSC Co-Ordinator for supporting me throughout this project work.

I express my sincere thanks to **Dr. A. Nirmala Shirley M.Sc., B.Ed., M.Phil., Ph.D.,** for her valuable time and guidance provided throughout for the successful completion of my project.

I am deeply grateful to all the staff members of Department of Physics (SSC) for supporting me in all aspects.

I acknowledge my deep sense of gratitude to my loving parents and friends for being a constant source of motivation.

ABSTRACT

Zinc Oxide (ZnO) is an important material for various applications in electronics, optoelectronics, biomedical and sensing. ZnO thin films were prepared by SILAR Method for various cycles. Zinc Chloride and Distilled Water were used as cationic and anionic precursors for the thin film. ZnO thin films were grown by optimizing the concentration of cationic and anionic precursors of immersion cycle and immersion time. The crystal structure of the films was studied by X-Ray Diffraction. Optical properties were studied by Photoluminescence, FTIR, UV Visible spectroscopy and thickness of film was calculated. Effect of deposition cycles on structural and optical properties were reported.

LIST OF TABLES

LIST OF FIGURES

CHAPTER 1

1.1 INTRODUCTION

Being a part of nanotechnology, a thin film is a layer of material ranging from fractions of a nanometer (monolayer) to several micrometer in thickness. Thin refers to the value less than about 1 micron (10,000 Å, 1000nm).

Historically Bunsen and Grove first obtained thin metal films in a vacuum system in 1852. The limit of thickness may vary from a nanometer to a few micrometers depending upon the field of application. Thin film studies have directly or indirectly advanced many new areas of research in solid state physics and chemistry, which are based on characteristic of the thickness, geometry, and structure of the film . At the initial stages, investigation on the thin films was made out of scientific curiosity, particularly for their significantly different properties from those of the same material in bulk form. However the acquired capability of controlling properties of the thin films in subsequent years, helped immensely the use of thin films in electronic optoelectronics and other devices and as a result the electronics industry has become the greatest beneficiary of thin film technology. On the other hand, the thin film technology contributes to the development of microelectronics, by reducing the sizes of semiconductor devices to two dimensions. Thin films are formed mostly by deposition using either physical or chemical methods. Thin films with both crystalline and amorphous structure, have immense importance in the era of high technology. Thin film materials are the key elements of continued technological advances made in the fields of semiconductor, microelectronic devices, magnetic thin films in recording devices, magnetic sensors, gas sensors, antireflective coatings, photoconductors, IR detectors, interference filters, solar cells, polarizers, superconducting films, anticorrosive, decorative coatings piezoelectric devices, transparent electrodes, solar cells, and photo catalyst .

Thin film deposition process involves three main steps:

a) production of the appropriate atomic, molecular, or ionic species,

b) their transport to the substrate through a medium,

c) condensation on the substrate, either directly or via a chemical and/or electrochemical reaction, to form a solid deposit.

There are various methods to deposit semiconducting thin films such as chemical bath deposition (CBD) [1], vacuum evaporation [2], electro deposition, chemical vapor deposition [3], molecular beam epitaxy [4], pulsed laser deposition [5], thermal evaporation [6], etc. Among them CBD appears to be very suitable method for a large scale fabrication of the semiconducting thin films. The main advantages of this method are that it is a low-cost method and do not require any sophisticated instruments, and films can be prepared at low processing temperature [7].

In this project, we deal with the preparation and characterization of ZnO. The ZnO is extremely an attractive replacement material for indium tin oxide due to its good optical and electrical properties coupled with the low cost, non-toxicity and abundance in nature of Zn. In this work, Zinc Oxide thin films were coated by SILAR method and its structural, optical properties and thickness were studied.

1.1 APPLICATION OF THIN FILM

Thin film finds its application in various fields which are listed below.

1.2.1 Engineering/Processing

a) Hard coatings for cutting tools

b) Protection afainst high temperature corrosion

c) Self-supporting coatings of refractory metals for rocket nozzles, crucibles, pipes

1.2.2 Optics

a) Highly reflecting coatings (laser mirrors)

b) Beam splitter and thin film polarizer

c) Integrated optics

1.2.3 Electronics

a) Passive thin film elements (Resistors, Condensers, Interconnects)

b) Active thin film elements (Transistors, Diodes)

c) Integrated Circuits (VLSI, Very Large Scale Integrated Circuit)

1.2.4 Biomedicine

a) Biocompatible implant coatings

b) Neurological sensors

1.2.5 Sensorics

a) Data acquisition in aggressive environments and media

b) Biological Sensorics

1.3 SILAR METHOD

One of the modern chemical deposition methods is successive ion layer adsorption and reaction (SILAR) method. Generally, this method consisted of two important processes, namely adsorption of ion onto the substrate and reaction of the adsorbed ion layer will be observed. During the deposition process, cleaned substrate will be dipped into different solutions (containing cationic and anionic precursors). Adsorption is an exothermic process. The adsorption is a surface phenomenon between ions and surface of substrate and is possible due to attraction of force between ions in the solution and surface of the substrate. These forces may be cohesive forces or van-der-waals forces or chemical attractive forces. Atoms or molecules of substrate surface are not surrounded by atoms or molecules of their kind on all sides. Therefore, they possess unbalanced or residual force and hold the substrate particles. Thus, atoms can be holding on the surface of the substrate. The factors like temperature of solution, pressure, nature of the substrate, concentration of the solution, area of the substrate etc., of the compound. Dividing the measured overall film thickness by number of reaction cycles, growth rate can be determined. This gives a numerical value for growth rate under the given conditions. If the measured growth rate exceeds the lattice constant of the material, a homogeneous precipitation in the solution could have taken place. In practice, however, the thickness increases typically less than or greater than a monolayer. Thus, the process involves an alternate immersion of the substrate in a solution containing a soluble salt of the cation of the compound to be grown. The substrate supporting the growing film is rinsed in highly purified deionized water after each immersion. The facts affecting the growth phenomena are the quality of the precursor solutions, their pH values, concentrations, counter ions, individual rinsing and dipping time. In addition, complexing agent and pretreatment of the substrate have been shown to affect the SILAR method. Basically, film thickness, morphology and composition could be controlled through immersion-reaction cycle [8].This method was first reported in 1985 by Ristov and co-workers [9].

1.3.1 ADVANTAGE OF SILAR METHOD

- Non-formation of precipitate in solution
- Save material costs
- Does not need vacuum chamber
- Low deposition temperature, energy saving
- Good growth rate of films
- Thickness, particle size and morphology of the films can be easily controlled by changing the deposition cycle
- Stoichiometry of deposited material can be controlled by changing the concentration of precursor solution
- Thin films can be deposited onto any type of substrate
- Deposition on large area
- Simple and inexpensive method

1.4 AIM OF THE PRESENT WORK

- To prepare the ZnO thin film by SILAR Method
- To analyse the structure of the ZnO thin film by X-Ray diffraction.
- To analyse the Optical properties of ZnO thin film by Photoluminescence (PL), UV-VIS and FTIR
- To analyse the Thickness of ZnO thin film

1.5 MATERIALS STUDIED

1.5.1 ZINC OXIDE

Zinc oxide is an inorganic compound with the formula ZnO. It is a white powder that is insoluble in water. Zinc oxide, with its unique physical and chemical properties, such as high chemical stability, high electrochemical coupling coefficient, broad range of radiation absorption and high photostability, is a multifunctional material. In materials science, ZnO is a polar II–VI compound semiconductor whose ionicity resides at the order line between the covalent and ionic semiconductors. It is an intrinsic n-type semiconductor because of deviation from stoichiometry and the presence of intrinsic defects such as O vacancies (VO) and Zn interstitials (Zin) [10].

Thin films of ZnO have been deposited using spray pyrolysis, electron beam evaporation, chemical deposition, electro deposition, vacuum evaporation, successive ionic layer adsorption and reaction (SILAR) technique [11]

1.5.2 STRUCTURE OF ZINC OXIDE

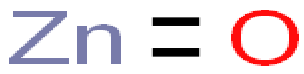

Fig.1.1 Structure of Zinc Oxide

1.5.3 PROPERTIES OF ZINC OXIDE

Chemical formula	ZnO
Molar mass	81.406g/mol
Appearance	White solid
Density	$5.606 g/cm^3$
Melting point	1974℃ (3585°F;2,247k)
Boiling point	2,360℃ (4,280°F;2,630k)
Band gap	3.3Ev
Magentic susceptibility	$-27.210^{-6}\ cm^3$/mol
Refractive index (n_D)	2.013,2.029

TABLE 1.1 PROPERTIES OF ZINC OXIDE

1.5.4 APPLICATION OF ZINC OXIDE

ZnO has got a wide array of applications. The reactivity of ZnO makes it ideal to be used as a precursor for obtaining other compounds of Zn. ZnO has proved to be a boon for materials science as it has got a combination of unique properties like UV absorption, anti-microbial properties, steady thermal and optical properties. Be it ceramics, lubricants, ointments, adhesives or the rubber industry ZnO has got a very significant contribution [12]

1.5.4.1 Rubber Manufacture

The rubber industry is responsible for consuming about 50% of the ZnO that produced globally. ZnO along with stearic acid are a must for activating the process of vulcanization in rubber manufacture**.**

1.5.4.2 Medical uses

Fine particles of ZnO have anti-microbial and deodorizing qualities and hence they are used for packaging purposes. These properties along with its ability of neutralizing acids make it ideal for use in antiseptic creams, healing creams etc. They are also an important component in toothpastes and dental prosthetics. Due to its ability to absorb ultraviolet light, ZnO is also used in sunscreens lotions and sun block creams to prevent sunburns. ZnO is also used in the making of cigarette filters as it helps in removing harmful substances like H_2S and HCN without affecting the flavour.

1.5.4.3 Food Additives

ZnO is usually added to food products as a source of Zn which is considered to be a necessary nutrient as it helps in the performance of various physiological activities like growth and proper functioning of the sexual organs. ZnO is also added to fodder as a Zn supplement for livestock. Zinc oxide is used to manufacture zinc gluconate which is nowadays found in cold prevention lozenges.

1.5.4.5 Electronic Applications

The wide band gap of ZnO enables it to be used for the purpose of making LEDs and laser diodes. Transparent Thin-Film Transistors (TTFT) can also be fabricated with ZnO. Nanorod sensors made of ZnO are devices that detect fluctuations in electric current passing through the wires as a result of the adsorption of gas molecules**.**

1.5.4.5 Anti Corrosive Coatings

Zinc oxide is an excellent inhibitor of fungi, mildew and mold Paints which have ZnO are usually used as anti-corrosive coatings for various metals like galvanized Zn which is especially hard to protect as it makes organic coatings brittle and unsuitable for adhesion. ZnO paints on the other hand maintain their flexibility and adhesive properties for years on end. The UV blocking abilities of ZnO also play an important role in improving the resilience of the paint. Unlike some lead pigments that are available commercially, ZnO is impervious to the effect of Sulphur compounds that are present in the atmosphere.

1.6 ZINC CHLORIDE

Zinc chloride is the name of chemical compound with the formula $\mathrm{ZnC}l_2$ and its hydrates. Zinc chloride, of which nine crystalline forms are known, are colourless or white, and are highly soluble in water[13]. $\mathrm{ZnC}l_2$ itself is hygroscopic and even deliquescent. Samples should therefore be protected from sources of moisture including the water vapour present in ambient air. Zinc chloride finds wide application in textile processing, metallurgical fluxes, and chemical synthesis. No mineral with this chemical composition is known aside from the very rare mineral simonkolleite.

1.6.1 STRUCTURE OF ZINC CHLORIDE

Fig. 1.2 Structure of Zinc Chloride

1.6.2 PROPERTIES OF ZINC CHLORIDE

Chemical formula	$ZnCl_2$
Molar mass	136.31 5g/mol
Appearance	White crystalline solid hygroscopic and very deliquescent
Odor	Odorless
Density	2.907g/cm^3
Melting point	290℃(554°F,563 K)
Boling point	732℃ (1350°F ,1005K)
Solubility in water	432.0g/100g (25°C)
Solubility in alcohol	430.0g/100ml

Table 1.2 properties of zinc chloride

1.6.3 PHYSICAL PROPERTIES

Zinc chloride is solid at room temperature and has a white crystalline appearance. It is odourless. The solubility of this compound in water corresponds to 432g/100g. lt is also soluble in acetone, ethanol, and glycerol. The four polymorphs of $ZnCl_2$ feature a tetrahedral coordinate geometry between the Zn^{2+}ions and the Cl^- molten zinc chloride is highly Viscous and has a relatively low electrical conductivity value.

1.6.4 CHEMICAL PROPERTIES

When $ZnCl_2$ is dissolved in water, the resulting solution is acidic in nature. The pH of an aqueous solution of zinc chloride with a concentration of 6M is 1. This compound reacts with ammonia to form complexes. Examples include $Zn(NH_3)_4Cl_2$ and $ZnCl_2(NH_3)_2$. When heated, the hydrated form of zinc chloride loses water and small quantities of ZnCl(OH) are obtained.

1.6.5 APPLICATION OF ZINC CHLORIDE

1.6.5.1 METALLURGICAL FLUX

Zinc chloride reacts with metal oxides (MO) to give derivatives of the idealized formula $MZnOCl_2$. Additional citation(s) needed. This reaction is relevant to the utility of $ZnCl_2$ solution as a flux for soldering. It dissolves passivating oxides, exposing the clean metal surface. Fluxes with $ZnCl_2$ as an active ingredient are sometimes called "tinner's fluid".

1.6.5.2 IN TEXTILE AND PAPER PROCESSING

Concentrated aqueous solutions of zinc chloride (more than 64% weight/weight zinc chloride in water) have dissolving starch, silk, and cellulose.

Relevant to its affinity for these materials, $ZnCl_2$ is used as a fire proofing agent and in fabric "refresheners" such as Febreze. Vulcanized fibre is made by soaking paper in concentrated zinc chloride**.**

1.6.5.3 SMOKE GRENADES

The zinc chloride smoke mixture("HC") used in smoke grenades contains zinc Oxide, hexachloroethane and granular aluminium powder, which then ignited, react to form chloride, carbon and aluminiumoxide smoke, an effective smoke screen

1.6.5.4 FINGERPRINT DETECTION

Ninhydrin reacts with amino acids and amines to form a colored compound "Ruhemann's purple" (RP). Spraying with a zinc chloride 10 Solution forms a l: l complex RP:$ZnCl(H_2O)_2$, which is more readily detected as it fluoresces more intensely than RP.

1.6.5.5 DISINFECTANT AND WOOD PRESERVATIVE

Dilute aqueous zinc chloride was used as a disinfectant under the name "Burnett's Disinfecting Fluid". From 1839 Sir William Burnett promoted its use as a disinfectant as well as a wood preservative. The Royal Navy conducted trials into 1849 and at the same time experiments were conducted into its preservative properties as applicable to the ship building and railway industries. Burnett had some commercial success with his eponymous fluid. Following his death however, its use was largely superseded by that of carbolic acid and other proprietary products**.**

1.6.5.6 SKIN CANCER TREATMENT

Zinc chloride has been used in alternative medicine to cause eschars, Scabs of dead tissue, in an attempt to cure skin cancers. Various products, such as Cansema or "black salve", containing zinc chloride and sold as cancer cures have been listed by the (FDA) as fake with warning letters being sent to suppliers. Scarring and skin damage are associated with escharotic substances.

1.7 SODIUM HYDROXIDE

Sodium hydroxide is also known as lye or soda, or caustic soda At room temperature, sodium hydroxide is a white crystalline odorless solid that absorbs moisture from the air. It is a synthetically manufactured substance. When dissolved in water or neutralized with acid it releases substantial amounts of heat, which may prove sufficient to ignite combustible materials. Sodium hydroxide is highly corrosive. [14]

1.7.1 STRUCTURE OF SODIUM HYDROXIDE

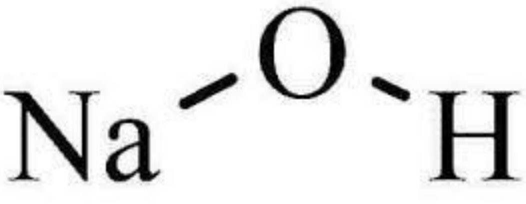

Fig.1.3 Structure of Sodium Hydroxide

1.7.2 PROPERTIES OF SODIUM HYDROXIDE

Chemical formula	NaOH
Molar mass	39.9971g/mol
Odor	Odorless
Density	2.13 g/cm^3
Melting point	323℃ (613°F ;596 k)
Boiling point	1,388℃ (2,530°F; 1,661 k)
Magnetic Susceptibility	-15.8. 10^{-6} cm^3/ mol(aq)
Refractive index (n_D)	1.3576

TABLE 1.3 PROPERTIES OF SODIUM HYDROXIDE

1.7.3 APPLICATION OF SODIUM HYDROXIDE

1.7.3.1 Manufacturing of Soap

Sodium hydroxide is used to make soap. It is one of the prime constituents of the soap manufacturing process. It is also called Lye. When its solution is mixed with fats and oils, it results in a chemical reaction called saponification. The fats and oils are made of organic acids. These acids react with sodium in the alkaline solution to form esters or organic salts. These organic salts are the prime constituents of soaps we use every day.

1.7.3.2 Home Applications

One of the prime uses of caustic soda in daily life is cleansing. It is a corrosive solution that can easily clean different utensils and tools without any hassle. In fact, many cleaning products contain sodium hydroxide. It is recommended not to use it directly with bare hands. The best examples of caustic soda used at home are drain cleaners, oven cleaners, tile cleaners, etc. It can easily remove fat, grease, grime, etc., from the trickiest corners of the floor, kitchen tops, and appliances. The cleaning process becomes very simple.

1.7.3.3 Industrial Uses

The sodium hydroxide used in industries is diverse. It is also used for different reactions done in laboratories as well. In the pharmaceutical industry, sodium hydroxide is used to formulate different kinds of medicines that are used for various purposes. These medicines deliver excellent therapeutic effects in the form of sodium salts too. In the paper industry, caustic soda is used to make pulp and manufacture paper. Sodium hydroxide is used to manufacture aluminium products in the aluminium industry. It is also used in making soaps, detergents, surfactants, etc.

1.8 DISTILLED WATER.

Distilled water is water that has been boiled into vapour and condensed back into liquid in a separate container. Impurities in the original water that do not boil below or near the boiling point of water remain in the original container. Thus, distilled water is one type of purified water [15].

CHAPTER 2

LITERATURE REVIEW

Gani yergaliuly,et.,al.,(2022) reported that ZnO thin films deposited at ambient temperature and barometric pressure by the sequential ionic layer adsorption and reaction method (SILAR) was carefully studied in this work. Ethanol and distilled water (DW) were alternatively used as a solvent for preparation of ZnO precursor solution. Superficial morphology, crystallite structure, optical and electrical characteristics of the thin films of various thickness are examined applying X-ray diffraction (XRD) system, scanning electron microscopy, the atomic force microscopy, X-ray photoelectron spectroscopy, ultraviolet–visible spectroscopy, photoluminescence spectroscopy, Hall effect measurement analysis and UV response study. XRD analysis confirmed that thin films fabricated using ethanol or DW precursor solvents are hexagonal wurtzite ZnO with a preferred growth orientation (002). Furthermore, it was found that thin films made using ethanol are as highly crystalline as thin films made using DW. Nano-flower morphology was observed for ZnO films grown using distilled water and ethanol while the surfaces of films grown with high SILAR cycle number are covered with nanostructures. Interestingly, for the samples grown in ethanol solvent the grain size decrease from~24 to~19 nm and was observed by an increase of the SILAR deposition cycles up to 50. ZnO thin films prepared using aqueous solutions possess high optical band gaps. However, films prepared with ethanol solvent have low resistivity (10^{-2} Ω cm) and high electron mobility (750 cm^2 /Vs). The ethanol solvent-based SILAR method opens opportunities to synthase high quality ZnO thin films for various potential applications. [16]

P. Sreedev, et., al., (2022) examined that ZnO is a hexagonal wurtzite semi conducting material, which finds numerous applications in the modern world. In thin film form ZnO shows unique properties such as high surface to volume ratio, piezo electric properties etc. Due to these mentioned properties ZnO thin films are considered as one of the most important material base for sensor application. The performance of the sensing materials will depend up on the method of synthesis, crystal structure and morphology of the samples. So structural and morphological identifications of the samples are essential before any sensor application. Hence the current work was done in two stages. In the first stage ZnO thin films were synthesized from 0.05M and 0.1M precursor medium using 50 dip cycles of SILAR method. Thus prepared samples were annealed for 350 °C for two hours. Obtained films were investigated with UV-Visible, XRD and SEM analysis. Transmittance and absorption spectrum of samples were compared. The transmittance for 0.05M sample was found to be more, whereas absorbance of 0.1M sample was more. Comparing with standard data XRD peaks were identified for each samples. From the comparative intensity study of XRD peaks, 0.1M sample was observed to be more crystalline. From the observed h,k,l values lattice parameters of each samples was determined and was reported. Values were found to be comparable with literature values which confirm the hexagonal structure of ZnO. Crystallite sizes were determined using Scherer formula and it was found to be comparable for each samples. The SEM images revealed the morphology of the samples. It infers that surface roughness was more for 0.1M sample. [17]

Aishwarya Santhamoorthy, et., al., (2021) determined that ZnO thin films were deposited onto the glass substrates using successive ionic layer adsorption and reaction (SILAR) technique by varying the deposition cycles from 25 to 100 in steps of 25 cycles. The effect of deposition cycles on the structural, morphological, optical and electrical properties was investigated and reported. Structural analysis revealed the formation of the hexagonal wurtzite crystal structure of ZnO with the preferential plane orientation of (1 0 0) for all deposition cycles. For the film deposited at 25 cycles alone, we observed the meagre diffraction peak at 2θ= 21.27 corresponds to (1 0 1) plane of the orthorhombic phased zinc sulphate, which indicated the incomplete formation of zinc ammonium complex from the precursor. Morphological analysis revealed the formation of nanorod-like morphology for the deposition cycles of 25 and 50, whereas it was found to be deformed at 75 and 100 cycles. The optical bandgap of the deposited thin films was decreased as a function of deposition cycles. However, at 75 deposition cycles, the bandgap was increased to 3.2468 ± 0.0026 eV, and it could be attributed to the variation in the density of states near the conduction band. A significant reduction in the grain resistance of the films at 50 and 100 deposition cycles explained the low resistivity of ZnO thin films. In addition, the negative values of the Hall coefficient indicated the n type semiconducting property of ZnO thin films. Linear relation from the I–V characteristics elucidated Ohmic behaviour. Thus, the investigated surface properties of ZnO thin films varied as a function of number of deposition cycles. [18]

Kiran, et., al., (2019) studied and reported that Zinc oxide thin films were grown on the amorphous glass substrate using Successive Ionic Layer Adsorption and Reaction (SILAR) technique at room temperature. The various preparative parameters were optimized to obtain good quality films. The as-grown films were annealed at 350° C for 2 h in air. The comparative study of the annealed and the as-grown thin films of ZnO were done for structural, optical and electrical studies. Polycrystalline nature was depicted from the x-ray diffraction (XRD) patterns. The peak intensity of as-grown ZnO thin films enhances after annealing. The average grain size calculated from XRD patterns was 17.66 nm for as-grown, while it increased to 24.66 nm after annealing. The band gap of as-grown ZnO thin films was relatively higher and was found to be 3.80 eV. After air annealing, the band gap decrease to 3.58 eV. The current-voltage characteristics showed nearly ohmic behavior with decrease in the film resistance, after annealing in air. N-type conductivity was confirmed from the TEP measurement. [19]

Sreedev p, et., al., (2019) reported that SILAR method was adopted for the synthesis of 0.025M ZnO thin films prepared for 15 dip cycles and annealed for 450℃ for 1 hour. The optical property of the prepared sample was investigated with UV visible and FTIR spectrometers. Thus obtained inferences of transmittance and absorbance was used to calculate parameters like absorption coefficient, extinction coefficient, band gap energy, refractive index and reflectance. It was observed that transmittance and absorbance show lower percentage over visible range. Band gap energy was found to be 3.75eV. Bandgap energy and refractive index was found to be comparable with the literature values. With these obtained values and due to the simplicity of the procedure, it was suggested that SILAR is a good method for ZnO thin film synthesis. [20]

Nilam B Patil,et.,al.,(2018) studied that the ZnO thin film sensor was developed by a low-cost sol–gel spin coating technique on a glass substrate. The structural, morphological, surface compositional, optical and electrical properties of the ZnO thin film were studied using XRD, FESEM, XPS, HRTEM, FTIR and UV–VIS techniques. The gas sensing performance of ZnO thin film is studied at different operating temperature for various gases like $\mathrm{N}O_2$, $\mathrm{N}H_3$, $\mathrm{C}H_3\mathrm{OH}$, $\mathrm{C}l_2$ and $H_2\mathrm{S}$. The ZnO thin film sensor was highly selective towards $\mathrm{N}O_2$ gas with a maximum response of 12.3 at 100 ppm concentration at 200 °C operating temperature. ZnO film sensor can also detect low concentration of $\mathrm{N}O_2$ gas up to 5 ppm with the response of 4.1. The ZnO thin film sensor showed excellent repeatability, high stability and moderate response and recovery time, for $\mathrm{N}O_2$ gas in the 5–100 ppm concentration range. All the gas sensing results indicated that the ZnO thin film can stand as good sensor for NO_2gas detection. [21]

M. Nirmala, et., al., (2017) examined that ZnO thin films were prepared by Successive Ionic Layer Adsorption and Reaction method. Thickness of the prepared films were calculated by Gravimetric method. The structure of the prepared films was analyzed by XRD. It revealed that the prepared films are polycrystalline in nature with hexagonal structure. The characteristics peaks were identified and the structural parameters were calculated and presented. SEM micrograph showed the morphology of the prepared film as flower like morphology in higher magnification which can be applicable for photovoltaic cell. The type of transition and bandgap was estimated from optical analysis. The bandgap was found to be 3.2eV. Then the optical parameters such as absorption coefficient, extinction co efficient, were calculated and presented.[22]

Sara Marouf, et., al., (2017) studied that ZnO films have been successfully synthesized via sol–gel dip coating method on glass substrates. This process eliminates the addition of basic or acid solutions containing foreign elements, high temperature and complex systems. In the present contribution, the effects of aging time on the morphological, structural and optical properties of ZnO films were investigated systematically. Morphological analysis revealed that thin films prepared from aged sol were relatively smoother with minimum surface roughness and the heavily aged samples exhibits nanorods morphology. Experimental results have shown that the prepared zinc oxide thin films by this method have higher crystallinity spectra as compared to other methods. Moreover, the optical transparency of films was significantly enhanced by aging the solution for longer times. An optimum sol aging time was determined for thin film formation providing a useful guideline for the process control purposes. These results meant that ZnO films prepared from the sol with longer aging time were still suitable for practical applications. [23]

A. Raidou, et., al., (2014) reported that Zinc oxide (ZnO) thin films have been deposited using a SILAR (Successive Ionic Layer Adsorption and Reaction) technique, which is based on the alternate dipping of substrate in the solution and distilled water. The precursors for ZnO films were dilute aqueous solution $ZnSO_4$ complexed with NH_3. XRD measurement showed that the films were crystallized in the wurtzite phase type with preferred orientation (002). X-ray photoelectron spectroscopy (XPS) was used to monitor changes in oxidation state of ZnO thin films. The SEM micrographs revealed different shapes of ZnO thin films, which depend of various deposit parameters. Optical properties study exhibits direct band gap nature with band gap energy 3.12 eV and 3.32 eV, depending on the PH. [24]

N. Nagarani, et., al., (2013) concluded that ZnO thin films have been prepared on to glass substrate by spin coating method. Zinc acetate dihydrate, isopropyl alcohol and diethanolamine were used as starting material, solvent and stabilizer respectively. The prepared films were annealed at different temperature from 350ºC to 550℃. The crystal structure and orientation of the films were investigated by using X-ray diffraction (XRD). The Scherrer formula was used to calculate the grain size of the films. From UV spectra the optical energy band gap was evaluated (3.27 eV-3.31eV). The surface morphology of the film was analysed by Scanning Electron Microscope (SEM). The surface morphology of the film is homogeneous and continuous. The films showed high transparency (>90%) in the visible region. When the annealing temperature was increased above 450°C, transmittance was decreased. This may be due to diffusion of impurity ions from the sodalime glass. [25]

Pay-Yu-Lee, et., al., (2013) reported that fabrication of a ZnO PD by SILAR involved the use of ethylene glycol. The average diameter of ZnO was around 100 nm. In addition, the obtained hexagonal ZnO thin films grew along the c-axis and with stronger intensity at the peak (002) plane; further, the films had a smooth surface morphology and showed high transparency in the visible spectral range. The fabricated ZnO PD was visible-blind with a cutoff wavelength around 350 nm. Under a 10 V applied bias, the measured dark current was 2.58µA and the photocurrent was 803 µA, and hence, the responsivities were 68.5 A/W for the ZnO PD. [26]

Raidou, et., al., (2013) recorded that zinc oxide (ZnO) thin films were deposited onto the glass substrates by a successive ionic layer adsorption and reaction method, which is based on the alternate dipping of substrate in a zinc sulphate solution complexed with NH_4OH and distilled water heated at 75℃. The time duration for which a substrate is dipped in the distilled water, plays an important role. The structural analyses from X-ray diffraction patterns displayed the formation of polycrystalline ZnO with high orientation along c-direction (002). The optical band gap was found to be declined from 3.3 to 3.27 eV. X-ray photoelectron spectroscopy indicates that the ZnO films were free of decomposed precursor residues in the bulk. [27]

N. Lehraki, et., al., (2012) studied that Zinc oxide (ZnO) thin films were deposited by spray pyrolysis technique using different precursors. Three starting solutions salts namely: zinc acetate, zinc chloride and zinc nitrate were used. The properties of these solutions and their influence upon ZnO films growth rate are investigated. The obtained results indicate that the dissociation energy of the starting solution plays an important role on films growth rate. A linear relationship between the solution dissociation energy and the growth rate activation energy was found. However, the surface tension of the used solution controls the droplet shape impact. Both solution surface tension and dissociation enthalpy alter the microstructure of the formed film. Films deposited with zinc acetate were characterized by a smooth surface, dense network and high transparency. SEM image reveals that film deposited with zinc chloride exhibits better crystallinity. While films deposited with acetate and nitride precursors are composed with micros crystallites embedded in an amorphous phase. Zinc acetate solution yielded to film with higher transmittance by comparison to films prepared with zinc chloride and zinc acetate precursors. [28]

Shih-Chang-Shei, et., al., (2012) investigated that ZnO thin films obtained by SILAR at different temperature treatments in ethylene glycol (75–180℃) With an increase in the temperature, preferential growth occurred along the c-axis, and high-intensity peaks due to the (0 0 2) plane were observed in the XRD spectrum; further, the obtained films had a smooth surface and showed good transparency in the visible spectral range. The films deposited at temperatures below 95℃ showed a rapid decrease in their transparency, eventually becoming white. At very high temperatures (>145 ◦C), only slight enhancement of the crystal quality was observed and the growth rate decreased. PL and XPS data revealed that the temperature treatment significantly affects the distribution of defects in the films. At low temperatures, a large number of these defects, mostly oxygen defects attributable to $Zn(OH)_2$in the films, were observed. However, the concentration of these defects reduced at high temperatures. Thus, we concluded that the quality and the structural and optical properties of the thin films depended strongly on the temperature treatment. Furthermore, temperature treatment was confirmed to play an important role in ZnO film deposition instead of post thermal annealing after the film growth. [29]

A Sakthivelu, et., al., (2011) reported that ZnO thin films were deposited by simple Successive Ionic Layer Adsorption and Reaction (SILAR) technique. The influence of reactant concentration on the structural, optical and morphology of the film was studied. X-ray diffraction study revealed that the film had preferential orientation along the plane (002). ZnO films deposited with higher concentration of precursor solution showed clear improvement in crystallinity. All micro structural parameters of the films were calculated. The surface morphology of the films revealed that grain size depended on the molarity of the precursor solution. Transmittance over the visible range exceeded 75% for all molarity of the films. For molarity increase, the transmittance of the film decreased. The band gap of the film was situated in the range 3.32 eV - 3.08 eV and decreased with the increase of the molarity. [30]

Zaiul Raza Khan, et., al., (2011) studied that all samples had hexagonal wurtzite structure. The crystallites sizes were measured using XRD data and were found to be in the range of 18 - 24 for ZnO thin films on quartz substrates prepared by sol-gel technique with 0.80 M zinc acetate solutions. Films had been characterized using optical and structural measurements. All the films exhibited high transmittance (91% - 95%) in the range of 400 nm to 800 nm, thus making the films suitable for optoelectronic devices, for instance as window layers in solar cells. The films showed a direct transition in the range 3.24 eV. The film had the strong emission band at 383 nm and also a broad emission peak centered at 550 nm visible region. The FTIR spectrum of the film had the characteristics ZnO absorption band at 482 cm^{-1}[31]

A. Kathalingam, et., al., (2010) found that ZnO thin film was deposited on a zinc plate using a chemical bath of zinc acetate (Zn$(O_2CCH_3)_2$) and ethylenediamine ($C_2N_2H_8$) at various temperatures. Different substrates were used and their effect on the chemical bath deposition of ZnO were investigated. The crystallite size and band gap energy were found to depend on the bath temperature. The band gap decreased as the crystallite size increased. The bath temperature was found to influence the growth of ZnO crystallites: at temperatures above 50°C, good crystalline film was produced. The pH range 9.5–10.5 was found to be the most suitable for CBD growth of ZnO. The use of zinc as the substrate is conducive to smooth adsorption of zinc ions on the surface and it results in a high-quality coating. A decrease in the band gap was observed upon increasing the bath temperature and size of the crystallites. [32]

A. Raidou, et., al., (2010) stated that ZnO films were obtained by successive immersion of a substrate in an aqueous solution containing: $\mathrm{ZnS}O_4$ with different molarities, 6ml/100ml 13.15 M aqueous ammonia solution and in deionised water heated at different temperatures. The X-ray diffraction analysis showed that the films were polycrystalline with zincite hexagonal structure with the preferential orientation of (002) plane. The study of surface morphology revealed that deposited ZnO films took many shapes: nanorods, Nano prisms, flowerlike, needles, spindles and hexagonal structures. Obtained ZnO films exhibited a high transmittance of 90% in visible band, and optical band gap of 3.27 eV. The optical direct band gap decreased with increasing bath temperature. [33]

M. Smirnov, et., al., (2010) studied that Zinc oxide (ZnO) thin films were deposited onto glass substrates by spin-coating method, from a precursor solution containing zinc acetate, ethanol and ammonium hydroxide. After deposition, the films were heated at a temperature of 100 °C in order to remove unwanted materials. Finally, the films were annealed at 500℃ for complete oxidation. X-ray diffraction showed that ZnO films were polycrystalline and had a hexagonal (wurtzite) structure. The crystallites were preferentially oriented with (0 0 2) planes parallel to the substrate surface. The films had a high transparency (more than 75%) in the spectral range from 450 nm to 1300 nm. The analysis of absorption spectra showed the direct nature of band-to-band transitions. The optical bandgap energy ranges between 3.15eV and 3.25eV. Some correlations between the processing parameters (spinning speed, temperature of post deposition heat treatment) and structure and optical characteristics of the respective thin films were established. [34]

A. Ghosh, et., al. (2008) reported that Zinc oxide thin films were grown by successive ionic layer adsorption and reaction technique at room temperature. The as-grown films were annealed at different temperatures, viz. 350, 400, 450, and 500℃ in air atmosphere for 2 hours. Effect of annealing on the physical properties of ZnO thin films has been studied. XRD analysis revealed the polycrystalline nature for ZnO thin films with hexagonal phase. The films were highly oriented along (1 0 0) and (1 0 1) planes, an enhancement in these peaks was the significance of the post-deposition annealing treatment on ZnO thin films. The grain size was also increased from 8.65 to 18.39 nm for as-grown sample (at room temperature) to 450 ℃. The optical studies of the samples show that the energy band gap was decreased in accordance with the annealing temperature. Optical absorption study revealed direct band gap nature with band gap energy in the range 3.24–3.14 eV depending on the annealing temperature. The results of optical studies were strengthened by photoluminescence (PL) studies. [35]

Siti Nuurul Fatimah Hasim, et., al., (2009) studied that ZnO thin films had been successfully synthesized by thermal evaporation of pure zinc at 900℃ under the flow of different percentages of argon and oxygen gases. The films were characterized by X-ray diffraction (XRD), variable pressure scanning electron microscopy (VPSEM), energy dispersive X-ray spectroscopy (EDS) and UV–vis spectroscopy. The aim of this paper was to study the influence of the oxygen percentage on the structural and morphological properties of the ZnO films. VPSEM results show that very thick needle structures were produced at high oxygen percentages. EDS results revealed that only Zn and O were present in the sample, indicating a composition of pure ZnO. XRD results showed that the ZnO synthesized under different quantities of oxygen were crystalline with the hexagonal wurtzite structure. UV–Vis spectroscopy results indicated that the optical band gap energies from the transmission spectrum are between 3.62 and 3.69 eV for ZnO thin films. [36]

M. Bouderbala, et., al., (2008) studied that Undoped ZnO thin films of different thicknesses were prepared by r.f. sputtering in order to study the thickness effect upon their structural, morphological, electrical and optical properties. The results suggest that the film thickness seems to have no clear effect upon the orientation of the grains growth. Indeed, the analysis with X-ray diffraction show that the grains were always oriented according to the c (0 0 2)-axis perpendicular to substrate surface whatever the thickness was. However, the grain size was influenced enough by this parameter. An increase in the grain size versus the thickness was noted. For the electrical properties, measurements revealed behaviour very dependent upon thickness. The resistivity decreased from 25 to 1.5×10^{-3} Ω cm and the mobility increased from 2 to 37 cm^2V^{-1} s^{-1} when the thickness increased from 70 to 1800 nm while the carrier concentration seemed to be less affected by the film thickness and varied slightly remaining around 1020 cm^{-3} . Nevertheless, a tendency to a decrease was noticed. The optical measurements showed that all the samples had a strong transmission higher than 80% in the visible range. A slight shift of the absorption edge towards the large wavelengths was observed as the thickness increased. This result showed that the band gap was slightly decreases from 3.37 to 3.32 eV with the variation film thickness vary from 0.32 to 0.88 mm. [37]

V. R. Shinde, et., al., (2007) reported that zinc oxide (ZnO) thin films were deposited onto the glass substrates by a novel chemical method, which is based on the alternate dipping of substrate in an alkaline zinc nitrate solution and double-distilled water containing H_2O_2(1%) at room temperature. The time duration for which the substrate is dipped in the precursor solution, played an important role and it had been shown in this work that the time period for which a substrate is dipped in dilute H_2O_2solution, which we referred as reaction period, affected significantly on the structural, surface morphological and optical properties. The structural analyses from X-ray diffraction (XRD) patterns displayed the formation of polycrystalline ZnO with no preferred orientations. The scanning electron micrographs (SEM) revealed the spongy and powdery clusters for low reaction period, which was converted to uniform spherical grains with increase in reaction period. The optical band gap was found to be declined from 3.28 to 3.12 eV with increase in reaction period. [38]

Hong Seong Kang, et., al., (2003) explained that ZnO thin films on (001) sapphire substrates had been deposited by pulsed laser deposition (PLD). After post-annealing treatment in the oxygen ambient, the optical properties of ZnO thin films were characterized by photoluminescence (PL). The structural properties of ZnO thin films were characterized by XRD. Crystallinity of ZnO film was enhanced at annealing temperature above 700℃. As the post-annealing temperature increases, intensity of UV (380 nm) peak decreased while the intensity of visible (about 490-530 nm) peak increased, carrier concentration decreased and resistivity increased. Structural, electrical and optical properties of ZnO films had been investigated for the application of light emission device. [39]

Jae-Min-Myoung, et., al., (2002) examined the series of ZnO films with various thicknesses were prepared on (0001) sapphire substrate by PLD. All the films showed strong (0001) preferred orientation because of its lowest surface energy. It is found that the crystalline quality, electrical and optical properties of the films strongly depended on the film thickness and showed large change around the film thickness of $4000A^0$ both FWHM values of DCXRC and carrier concentration determined by Hall measurements decreased with increase in the film thickness and, for the films thicker than $4000A^0$, they were saturated. The RT-PL measurements showed that, for the films thinner than the position of the near band-edge emission exhibits large shift towards the lower-energy side while, for the films thicker than 4000A°, it approached to the value of bulk ZnO. These results are attributed to the fact that the films thinner than 4000A°were under the severe tensile strain and it decreasesd with increase in the film thickness further. Therefore, it was believed that the films thicker than 4000A° were almost strain-free and exhibited the near-bulk ZnO properties. [40]

M. Purica, et., al., (2002) studied that transparent and conductive ZnO thin films had been prepared by a method derived from chemical vapor deposition using Zn ($C_5H_7O_{22}$) as Zn source. The deposited thin ZnO layers of ~0.1 μm thickness on Si and InP semiconductor substrates, have been investigated with respect to the crystalline phase by X-ray diffraction (XRD), and surface morphology by atomic force microscopy (AFM). Spectrophotometric measurements in the ultraviolet-visible-near infrared spectral range and optoelectrical measurements of ZnO semiconductor heterostructures had been performed. In XRD the preferential orientation of the crystallites for prepared ZnO films were (112) on (111)-Si substrate and (002)-wurtzite c-axis orientation perpendicular to the surface of

(100)-oriented InP substrate; the dimensions of grain sizes were in the range of 18– 40 nm .[41]

CHAPTER 3

3.METHODOLOGY

Various methods were used for the preparation of thin film and they can be classified into two major types

- Chemical deposition
- Physical deposition

3.1 CHEMICAL DEPOSITION

In this method a fluid precursor underwent a chemical change at a solid surface leaving a solid layer. A normal example was the formation of soot on a cool object when it was placed inside a flame. As the fluid was surrounding the solid object, deposition happens on the surface, in a particular direction; thin film from chemical deposition techniques tends to be conformal, rather than directional. Chemical deposition was further divided by the phase of the precursor.

3.1.1 ELECTROPLATING

In electroplating, an ionic metal was required with electrons to form a non-ionic coating on a substrate. A common system consisted of a chemical solution with the ionic form of the metal, an anode which may be made up of the metal being plated (a soluble anode) or an insoluble anode (usually carbon, platinum, titanium, lead, or steel), and finally, a cathode where electrons were supplied to produce a film of non-ionic metal.

3.1.2 SOL GEL

The sol-gel process is a wet-chemical technique and widely used for the fabrication of both glassy and ceramic materials. Such method was used for the fabrication of materials (typically metal oxides) starting from a colloidal solution (sol) that acts as the precursor for an integrated network polymer. In this chemical procedure, the ‘sol’ (or solution) gradually evolves towards the formation of a gel-like biphasic system containing both a liquid phase and solid phase whose morphologies range from discrete particles to continuous polymer network.

3.1.3 ATOMIC LAYER DEPOSITION (ALD)

This method used gaseous precursor to deposit conformal thin films one layer at a time. The process was divided into two separate reactions, run in sequence and repeated for each layer, in order to confirm total layer saturation before beginning the next layer. Hence one reactant was deposited first and then the second reactant was deposited. In that time a chemical reaction occurred on the substrate, forming the desired composition.

3.1.4 DIP COATING

During dip coating, the substrate is immersed in the coating solution. As it is withdrawn, a liquid layer was entrained on the substrate. The thickness of this entrained solution was determined by the withdrawal speed.

3.1.5 SPIN COATING

This was also known as spin casting, which used a liquid precursor deposited onto a smooth substrate which was subsequently spun at a high velocity to centrifugally spread the solution over the a upon the viscosity of the solution. Repeated depositions were carried out to increase the thickness of films as desired. Thermal treatment was often carried out in order to crystallize the amorphous spin coated film. Such crystalline films could exhibit certain preferred orientations after crystallization on single crystal substrates.

3.2 PHYSICAL VAPOR DEPOSITION

Physical vapor deposition (PVD) is a vaporization coating technique that involved the transfer of material at the atomic level. The process can be described according to the following sequence of steps

- The material to be deposited is converted into a vapor by physical means (high-temperature vacuum or gaseous plasma)
- The vapor was transported to a region of low pressure from its source to the substrate.
- The vapor underwent condensation on the substrate to form a thin film.

Typically, PVD processes were used to deposit films with thickness in the range of a few nanometers to thousands of nanometers. However, they could also be used to form multilayer coatings, graded composition deposits, very thick deposits, and free standing structures.

PVD thin film technology covered a rather broad range of deposition techniques, including electron-beam or hot-boat evaporation, reactive evaporation, and ion plating. PVD techniques also included processes based on sputtering, whether by plasma or by an ion beam. PVD is also used to describe the deposition from arc sources that may or may not be filtered. In general, this process could be divided into two groups.

- Evaporation
- Sputtering

Evaporation refers to thin film being deposited by thermal means, whereas in the sputtering mode the atoms or molecules are dislodged from the solid target through the impact of gaseous ions (plasma). Both methods have been further developed into several specific techniques.

3.2.1. THERMAL EVAPORATION

Thermal evaporation works by vaporizing the target material using thermal energy from a tungsten heating element or an electron beam. After vaporization, the material is transported through a high pressure vacuum and was deposited onto the substrate where it condensed and grows into a solid film. This method could be used to deposit pure metals, nonmetals, oxides and nitrides. It is most often used to deposit electrically conductive metallic layers on the solar cells, OLED displays, and thin film transistor

3.2.2 ELECTRON BEAM EVAPORATOR

In electron-beam evaporation the target material was deposited in a crucible which is designed to match the heating and power density of the electron-beam. To avoid contamination of the target material in the evaporation stage, the crucible should not be prone to evaporation or erosion at high temperatures. Typical deposition rate for electron beam evaporation range from 1 to 10 nanometers per second**.**

3.2.3 MOLECULAR BEAM EPITAXY (MBE)

This is one of the common methods of depositing single crystals. It was invented in the late 1960s at Bell Laboratories by J. R. Arthur and Alfred Y. Cho. This requires high or ultra-vacuum. The most important property of MBE is the slow deposition rate (typically less than 1000 nm per hour), which allows the films to grow epitaxially. In this process slow streams of an element could be directed at the substrate, so that material deposits one atomic layer at a time. Compound like gallium arsenide was usually deposited by repeatedly applying a layer of one element (i.e., gallium), then a layer of the other (i.e., As), so that the process is chemical, as well as physical. The beam of material can be generated by either physical means (that is, by a furnace) or by a chemical reaction (chemical beam epitaxy). During operation, reflection high energy electron diffraction (RHEED) was used for monitoring the growth of the crystal layers.

3.2.4 SPUTTERING

Sputtering deposition worked by transferring ions from a target material onto a substrate material using plasma, often argon, in a vacuum chamber. While sputtering deposition techniques vary in their specifics, the basic setup and operation follows. The target material was connected to a negatively charged cathode and the substrate was connected to a positively charged anode. Free electrons accelerated toward the anode and collided with the argon atoms, converting them into positively charged ions. The argon ions then accelerate toward cathode and collide with the target material, releasing atoms which were deposited onto the substrate surface. Sputtering deposition found its earliest application in production of computer hard disks and is now used extensively in integrated circuit processing, production of anti-reflective or high emissivity film coated glass, cutting tool coating, and coating of CDs and DVDs.

Three sputtering techniques are the most employed for thin film growth, including DC diode, RF-diode, and magnetron diode**.**

3.2.5 PULSED LASER DEPOSITION (PLD)

This is a thin film deposition technique where a high power pulsed laser beam is focused inside a vacuum chamber to strike a target of the material so that the material can be deposited. This material is vaporized from the target which deposits it as a thin film on a substrate. This process is done in ultra-high vacuum or in the presence of a background gas, such as oxygen which is commonly used when depositing oxides to fully oxygenate the deposited films.

3.2.6 CATHODIC ARC DEPOSITION

This is a physical vapor deposition technique in which an electric are is used to vaporize material from a cathode target. The vaporized material then condenses on a substrate and forms a thin film. The technique is being done to deposit metallic, ceramic, and composite films.

3.2.7 ELECTRO HYDRONOMIC DEPOSITION

This is a relatively new process of thin film deposition. The liquid can be deposited either in the form of nanoparticle solution or simply a solution and it is fed to a small capillary nozzle (usually metallic) which is connected to a high power source. The substrate on which the film will be deposited is connected to the ground terminal of the power source. Through the influence of electric field the liquid comes out of the nozzle and takes a conical shape (Taylor cone) and at the apex of the cone a thin jet emanates which disintegrates into very fine and small positively charged droplets. The droplets keep getting smaller and smaller and finally get deposited on the substrate as a uniform thin layer.

3.3 SILAR METHOD

Here I chose the silar method because it is inexpensive. Simple and capable of deposition of optically smooth, uniform and homogeneous layers.

ZnO thin film were prepared by SILAR method using glass substrates. Before deposition, substrates were cleaned in acetone or ethanol. Later they were rinsed with distilled water**.**

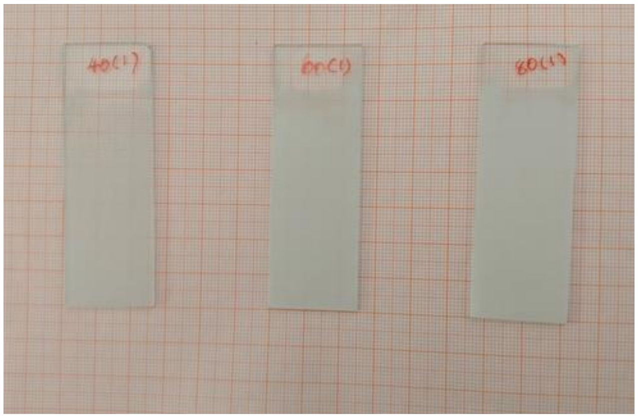

.

Fig 3.1 ZnO Thin film

For this deposition, cationic precursor was prepared by dissolving 0.1M of Zinc Chloride and 4g of Sodium Hydroxide in 100ml of distilled water. The precursor solution was stirred thoroughly using magnetic stirrer .The anionic precursor was made of 100ml of Hot distilled water maintained at 70-80°C. Well cleaned glass substrates were dipped into solution of Zinc Chloride for 10s. It was then immersed in the hot distilled water for 10s. This formed one SILAR deposition cycle. Films were deposited by repeating SILAR cycles for 40,60 and 80 times.

CHAPTER 4

RESULT AND DISCUSSION

4.1 INTRODUCTION

The thin film can be characterized using various techniques such as XRD, UV, SEM, TEM, FTIR, THICKNESS, PL, etc, The ZnO thin films were subjected to XRD, PL, THICKNESS, FTIR, in the present work**.**

4.2 X- RAY DIFFRACTION (XRD)

X-Ray diffraction is one of the important non-destructive tools to analyze all kinds of matter ranging from fluids, to powder and crystals. From research to production and engineering, XRD is an indispensable method for materials characterization and quality control. X-Ray diffraction techniques are used for the identification of crystalline phase analysis subsequent to the identification. X-Ray diffraction techniques are superior in elucidating the three dimensional atomic structure of crystalline solids. The properties and function of materials largely depend on the crystal structure. X-Ray diffraction techniques have therefore, been widely used as an indispensable means in materials research development and production.

The Bragg equation, $\mathbf{n\lambda=2d\sin\theta}$, is one of the keynotes in understanding X-Ray diffraction.

Where,

n – Integer

λ – Wavelength of the X-Ray impinging on the crystallize sample

d – Interplanar spacing between rows of atoms

θ – Angle of the X-Ray beam with respect to these planes

When this equation is satisfied X-Ray scattered by the atoms in the plane of a periodic structure or in phase and diffraction occurs in the direction defined by the angle θ. In the simplest instance, an X-Ray diffraction experiment consists of a set of diffracted intensities and the angles can be thought of a chemical fingerprint and chemical identification can be performed by comparing this diffraction pattern to a data base of known patterns

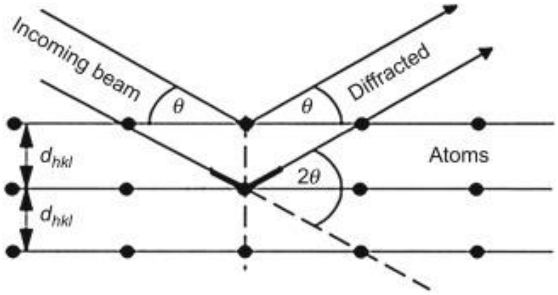

Fig 4.1 X-Ray diffraction pattern

4.3 PHOTOLUMINESCENCE

PL is a process in which the substance absorbs and re-radiates photons. In quantum mechanics, it can be described as an excitation to a higher energy state and then return to a lower energy state accompanied by the emission of a photon. This is one of many forms of luminescence (light emission). The period between absorption and emission is typically extremely short, in the order of 10 nanoseconds. Under special circumstances, however, this period can be extended into minutes or hours. PL spectroscopy can be used to identify surface, interface, and impurity levels and to gauge alloy disorder and interface roughness. The intensity of the PL signal provides information on the quality of surface and interfaces. PL measurements have proven to be a sensitive and non-destructive technique for examining the optical property of the material.

4.4 FOURIER TRANSFORM INFRARED (FTIR)

In infrared spectroscopy, IR radiation are passed through the sample. Some of the infrared radiation is absorbed by the sample and some of it is passed, transmitted. The resulting spectrum represents the molecular absorption and transmission creating a molecular fingerprint of the sample. Like the finger print no two unique molecular structures produce the same infrared spectrum. This makes infrared spectroscopy useful for several types of analysis. FTIR can identify unknown materials. It can determine the quality or consistency of a sample. It can determine the amount of components in a mixture. Infrared spectroscopy has been a workhorse technique for materials analysis in the laboratory for over seventy years. An infrared spectrum represents a fingerprint of a sample with absorption peaks which correspond to the frequencies of vibrations between the bonds of the atoms making up the material. Because each different material is a unique combination of atoms, no two compounds produce the exact same infrared spectrum. Therefore infrared spectroscopy can result in a positive identification of every different kind of material.

4.5 XRD PATTEREN OF ZnO PREPARED BY SILAR METHOD

To study the structural properties of the deposited ZnO thin films X-ray diffraction (XRD) study was carried out. Fig 4.2,4.3,and 4.4 show that XRD pattern of ZnO deposited by SILAR Method for different deposition cycles of 40, 60 and 80 respectively. The observed XRD pattern show the prominent peak (002) plane orientation for all the films prepared by different deposition cycles. However film deposited with 80 cycles show well defined peak with high intensity compared to films prepared at 40 and 60 deposition cycles. All diffraction Peaks of the ZnO thin film correspond to the characteristic hexagonal wurtzite structure of ZnO thin films. The observed ‘d’ values were compared with standard ‘d’ values using joint Committee on Powder Diffraction Standards (JCPDS card no 36-1451).

The crystallite size of thin film were calculated from XRD patterns by using Scherrer's formula given below

$$D=k\lambda/ \beta \cos \theta$$

Where,

D = Crystallite size

K = Constant

β = Corrected FWHM of the most intense peak

θ = Braggs angle Using these formula grain sizes can be determined.

The dislocation density has been calculated using crystallite size, by the equation

$$\text{Dislocation} = 1/D^2$$

The microstrain has been calculated by the given formula,

$$\text{Microstrain} = \beta \cos \theta/4$$

The lattice parameter calculated for ZnO by the given formula

$$1/D^2 = (4/3)\, [h^2+hk+k^2/a^2] + [l^2/c^2]$$

The lattice parameter has been calculated and reported. The grain size, dislocation density, micro strain and lattice spacing of ZnO thin film for various deposition cycles have been given below.

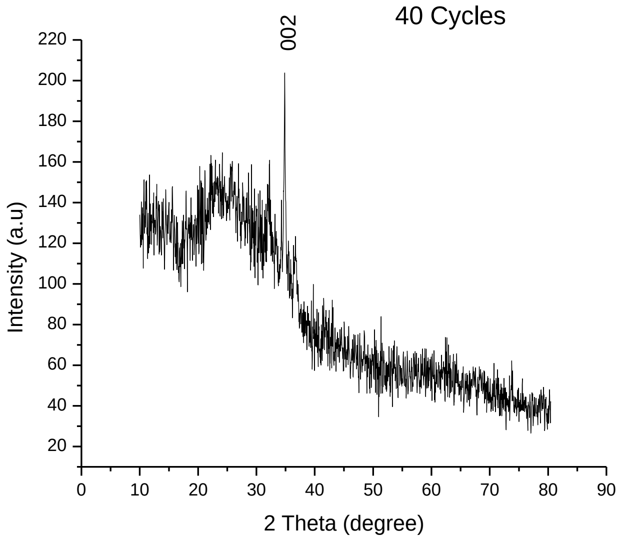

Fig 4.2 XRD pattern of ZnO thin film for 40 deposition cycle

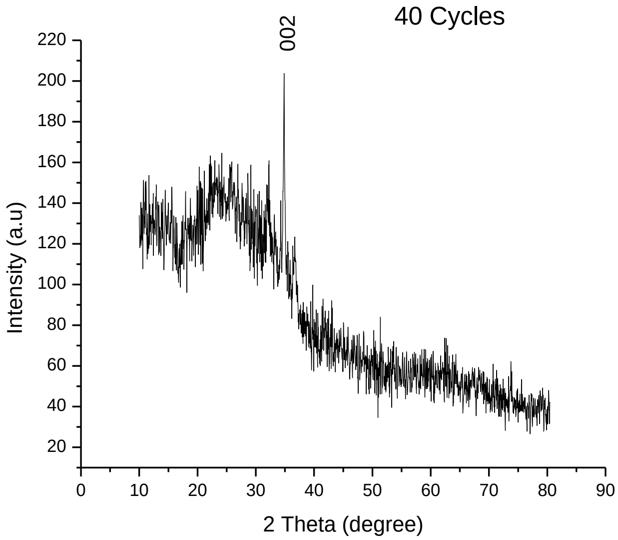

Fig 4.3 XRD pattern of ZnO thin film for 60 deposition cycle

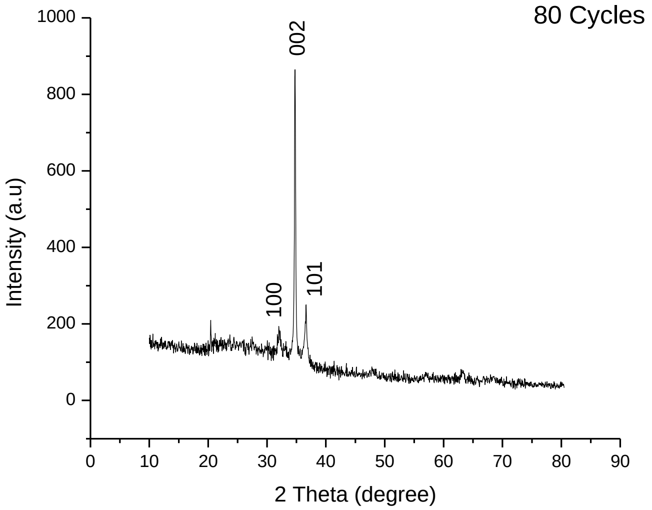

Fig 4.4 XRD pattern of ZnO thin film for 80 deposition cycle

Deposition cycle	h k l	2θ degree	Grain size($10^{-9}m$)	Dislocation density (line/m^2)	Micro strain (10^{-4})	Lattice constant
40	0 0 2	34.8439	52.9269	35.6982	6.5494	a= 2.973 c=5.5721
60	1 0 0	31.9868	70.0184	20.3974	4.9506	a= 3.230 c=5.1590
	0 0 2	34.7794	42.3263	55.8186	8.1895	
	1 0 1	36.6321	26.5882	1.4145	0.1303	

80	1 0 0	32.090	17.5119	3.2608	0.1979	a=3.2207 c=5.1622
	0 0 2	34.757	52.9158	35.7132	6,5506	
	1 0 1	36.652	53.2001	35.3322	6.5156	

Table 4.1 structural parameter for ZnO for various deposition cycles

4.6 RESULT FOR PHOTOLUMINESCENCE.

Photoluminescence is one of the important tools to study the structural defects and quality of crystalline structure which has been shown to play crucial role in the development of photocatalytic property. The PL emission spectra were observed in the range of 340-600nm with an excitation wavelength of 320nm. The strong UV emission were observed at 378 nm.

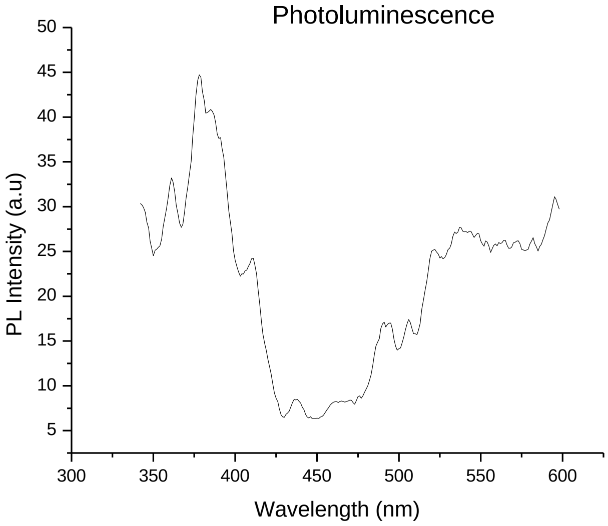

Fig 4.5 photoluminescence of ZnO

4.7 THICKNESS MEASUREMENT

In the present study thickness measurement were done by the weight gain method for different deposition cycles.

$$t = m / A\rho$$

where

m – mass of difference of the substrate before and after deposition give the mass of thin film

A – Area of the film coated

ρ – Density of film (Zinc oxide)

Deposition of cycles	Thickness (microns)
40	0.0475
60	0.0142
80	0.0142

Table 4.4 Thickness measurement for different deposition cycles

4.8 FTIR ANALYSIS

The functional group and chemical compound present in the prepared ZnO Were identified using FT- IR spectrum. The FT-IR spectrum of ZnO show broad absorption band between 400 to 4000cm^{-1} Spectrum for 40, 60, and 80 deposition cycles were shown in figure 4.6,4.7, and 4.9 respectively.

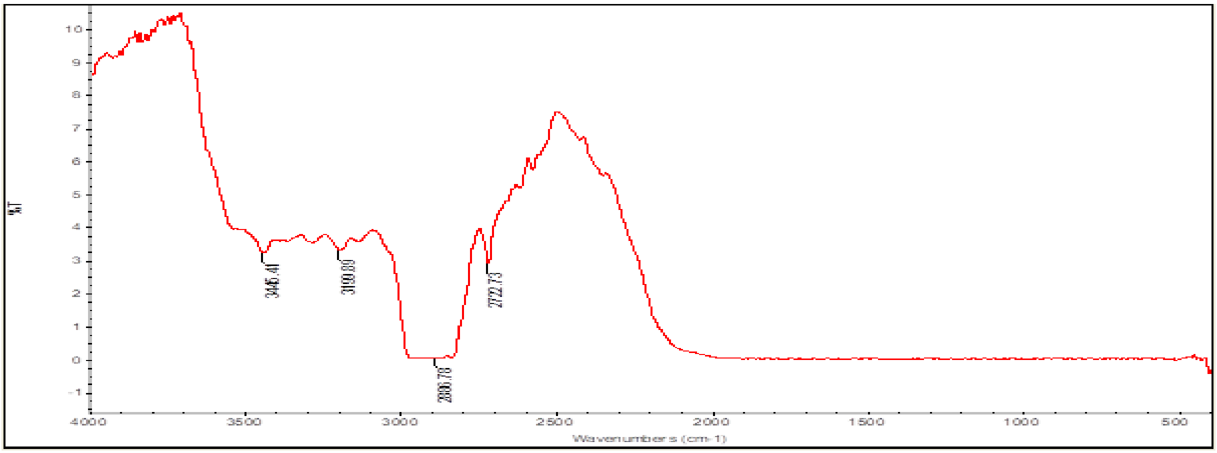

Fig 4.6 FTIR Spectrum for 40 Deposition Cycle

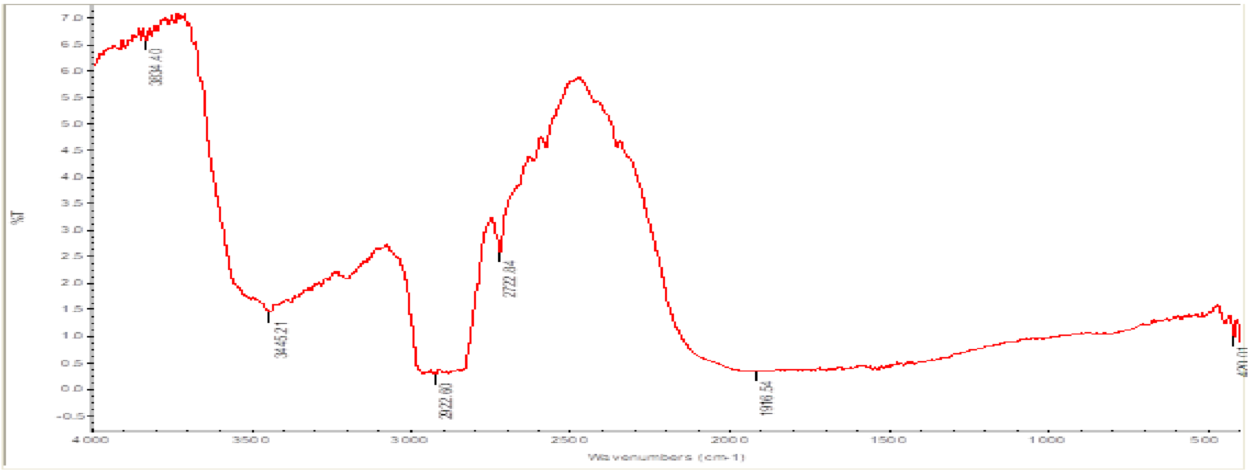

Fig 4.6 FTIR Spectrum for 60 Deposition Cycle

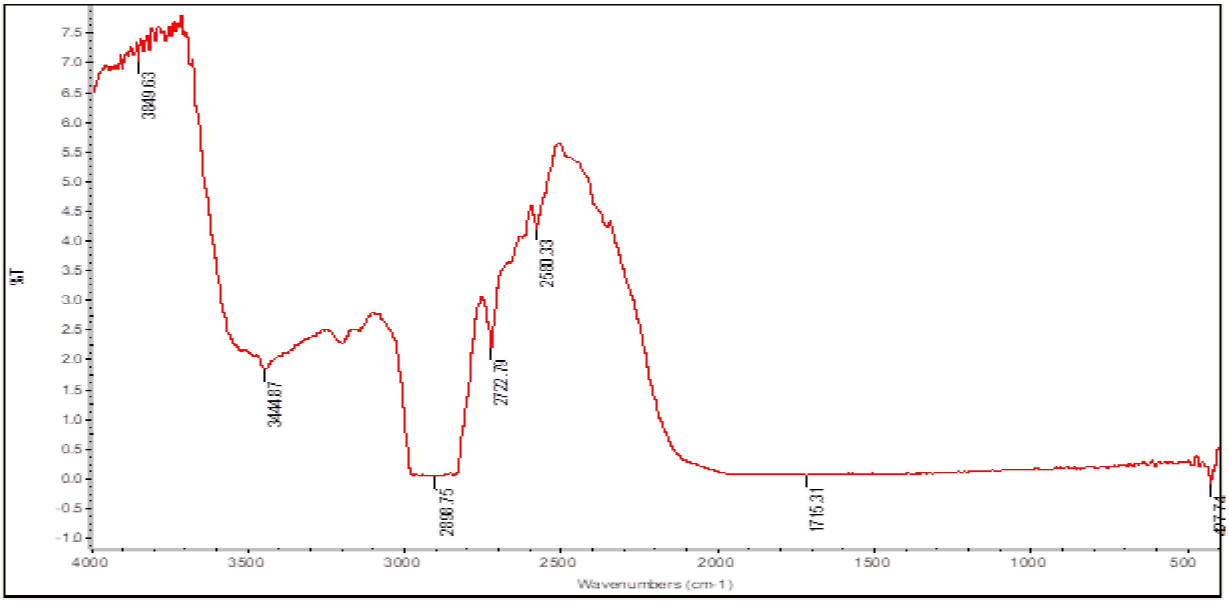

Fig 4.8 FTIR Spectrum for 80 Deposition Cycle

Deposition	Wavenumber (cm^{-1})	Types of Bond	Types of vibration
40	3444.87	O-H	Stretch
60	420.01	Zn-O	Stretch
	2992.60	C-H	
	3445.21	O-H	
80	427.4	Zn-O	Stretch
	3444.87	O-H	

Table 4.3 Bonding in FTIR Spetrum for various Deposition Cycles

4.9 UV-VIS SPECROSCOPY ANALYSIS

UV visible spectroscopy is most widely used technique for optical characterization of ZnO thin film. It was done by UV-VIS Spectrophotometer. The spectrum was recorded for a wavelength of 300-800 nm.

The absorbance and wavelength in ZnO Thin film were plotted for different deposition cycles of 40, 60 and 80 .

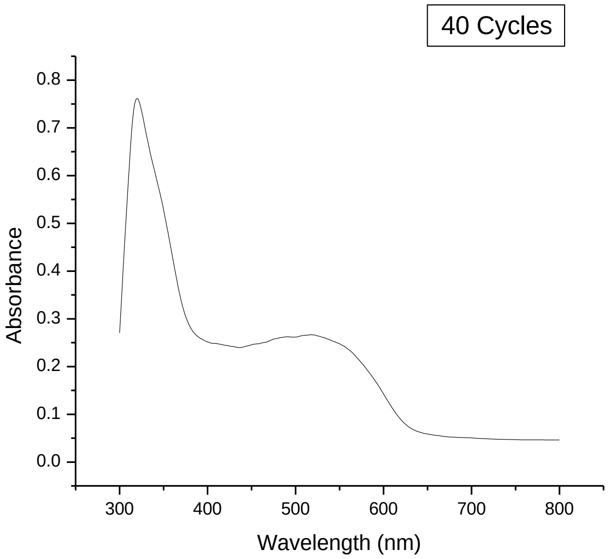

Fig 4.9 UV-Visible Spectrum of Absorbance for 40 Deposition Cycle

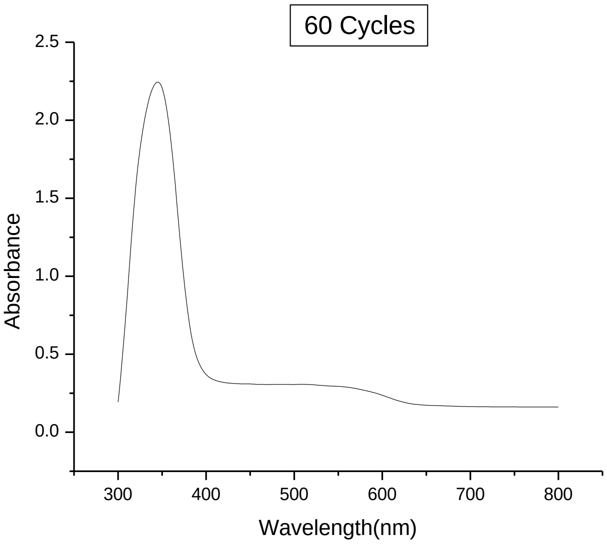

Fig 4.9 UV-Visible Spectrum of Absorbance for 60 Deposition Cycle

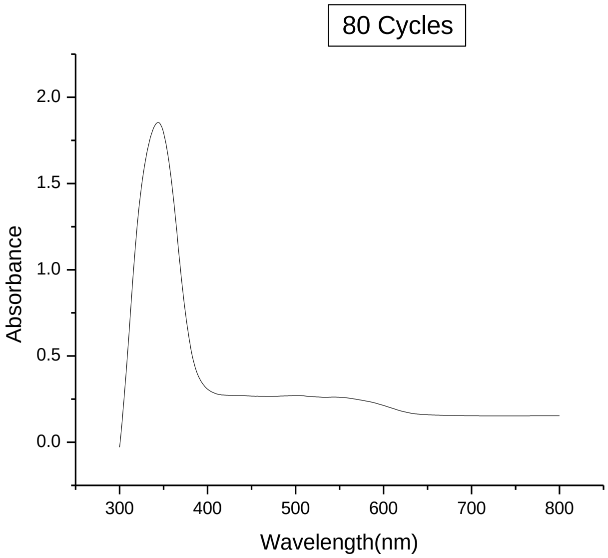

Fig 4.9 UV-Visible Spectrum of Absorbance for 80 Deposition Cycle

The Transmittance and wavelength in ZnO thin film is plotted for different cycles .

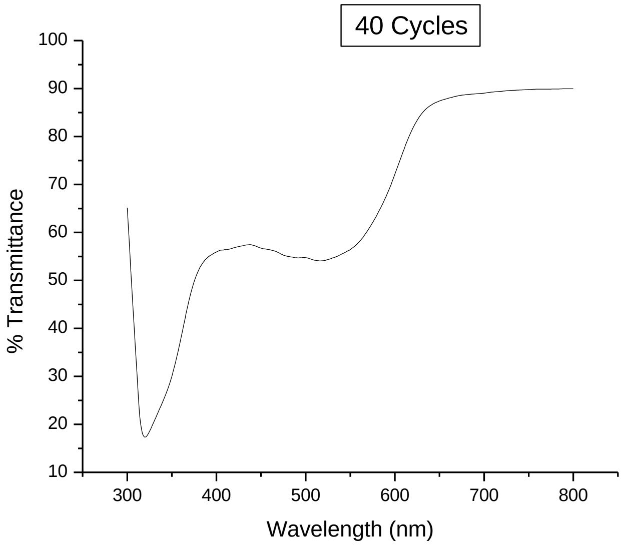

Fig 4.12 UV- Visible Spectrum of Transmittance for 40 Deposition cycle

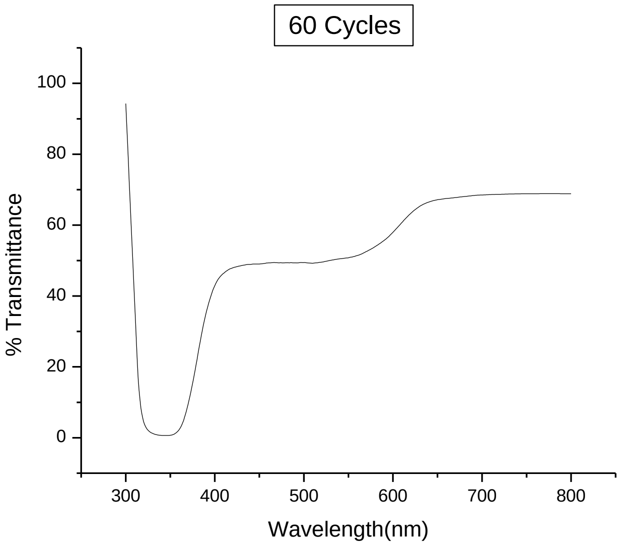

Fig 4.13 UV- Visible Spectrum of Transmittance for 60 Deposition Cycle

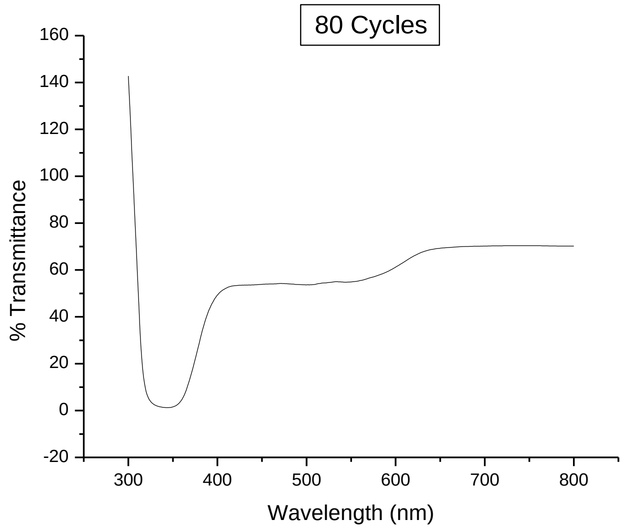

Fig 4.14 UV- Visible spectrum of Transmittance for 80 Deposition Cycle

CHAPTER 5

SUMMARY AND CONCLUSION

In this work, ZnO thin films were prepared by SILAR method and were subjected to various studies such as XRD, PL, Thickness, FTIR, and UV-VIS.

The synthesized films were characterized by XRD. The grain size of ZnO thin film for various deposition cycles were calculated by De-Scherrer's Formula and the result proves that ZnO thin film is a Hexagonal wurtzite structure.

PL showed strong UV emission at 378 nm.

FTIR Showed ZnO Stretching vibrational modes, which confirmed the synthesis of ZnO thin film.

Thickness of the prepared films were calculated by Weight gain method which showed that the coated films were thin in nature.

The absorbance and transmittance of ZnO thin films were analyzed by UV-VIS spectroscopy for optoelectronic applications.

Thus, the investigated surface properties of ZnO thin films varied with a number of deposition cycles .This film may pave the way for utilizing various optoelectronic application based on surface and electrical studies which will be carried out in future.

REFERENCE

[1] Ennaqoui, A., Weber, M., Scheer, R. and Lewerenz, H.J. (1992) ‘Chemical-Bath ZnO Buffer Layer for $\mathrm{CuIn}S_2$ Thin Film Solar Cells. Solar Energy material and solar cells’, vol. 54, pp.277-286.

[2] Chander, S. and Dhaka, M.S, (2015) ‘Physical properties of vacuum evaporated CdTe thin films with post-deposition thermal annealing’, J. Physica E, vol. 73, pp. 35-39.

[3] Kasuga, M. and Mochizuki, M. (1981) ‘Orientation Relationships of Zinc Oxide on Sapphire in Heteroepitaxial Chemical Vapor Deposition’, journal of crystal growth vol. 54, pp. 185-194.

[4] Wu, X. J., Zhang, Z. Z., Zhang, J. Y., et al.,(2008) ‘Growth of FeSe on general substrates by metal-organic chemical vapor deposition and the application in magnet tunnel junction devices’, Thin Solid Film, vol. 516, pp. 6116–6119.

[5] Kaidashev, E.M., Lorenz, M., Wenckstern, H.V., Rahm, A., Semmelhack, H.C., Han, K.H., Benndorf, G., et al., (2003) ‘High Electron Mobility of Epitaxial ZnO Thin Films on c-Plane Sapphire Grown by Multistep Pulsed-Laser Deposition. Applied Physics Letters’,vol. 82, pp.3901.

[6] Lee, J.H., and Park, B.O., (2004) ‘Characteristics of Al-Doped ZnO Thin Films Obtained by Ultrasonic Spray Pyrolysis: Effects of Al Doping and an Annealing Treatment. Materials Science and Engineering. B’, vol 106, pp. 242-245.

[7] Wei, A., Zhao, X., Liu, J., Zhao, Y., (2013) 'Investigation on the structure and optical properties of chemically deposited ZnSe nanocrystalline thin films', Physica B, vol. 410, pp. 120–125.

[8] Pathan, H., and Lokhande, C., (2004) 'Deposition of metal chalcogenide thin films by successive ionic layer adsorption and reaction (SILAR) method', Bulletin of Materials Science, vol. 27, 85.

[9] Ristov, M., Sinadinovski, G., and Grozdanov, I., (1985) 'Chemical deposition of CU_2O thin films', Thin Solid Films, vol.123, 63.

[10] https://en.wikipedia.org/wiki/Zinc oxide

[11] Jiménez-González, A., and Suarez-Parra, R., (1996) 'Effect of Heat Treatment on the Properties of ZnO Thin Films Prepared by Successive Ion Layer Adsorption and reaction(SILAR)', journal of crystal growth,vol.167,pp.649-655.

[12] http://www.azom.com/details.asp?Article ID= 2357

[13] Datta Roy, S., and Mitra, P., (2008) 'Preparation of ZnS thin film by SILAR method', Material Science Research India.

[14] http://en.wikipedia.org/wiki/sodium hydroxide

[15] www.wikipedia.distilled water

[16] GaniYergaliuly, Baktiyar Soltabayev, Sandugash Kalybekkyzy1(2022) 'Effect of thickness and reaction media on properties of ZnO thin films by SILAR.

[17] Sreedev, p., Malavika Sunil., et al., (2022) 'Optical,Structural and Surface analysis of ZnO thin films prepared by SILAR method', AIP Conf. Proc. 2222,pp. 020010-1–020010-6.

[18] Aishwaray santhamoorthy, parathasarathy Srinivasan,et.al.,(2021) ‘SILAR-deposited nanostructured ZnO thin films. effect of deposition cycles on surface properties.

[19] Kiran , Poonam , Arindam Ghosh, (2019) ‘Effect of Annealing on the Structural and Opto-electrical Properties of As-grown ZnO Thin Films by Successive Ionic Layer Adsorption and Reaction (SILAR) Technique’, AIP Conference Proceedings 2142,pp. 030009-1-030009-6.

[20] Sreedev, P., Rakhesh, V.,Roshima, N.,(2019) ‘Preparation of Zinc Oxide Thin films by SILAR method and its Optical analysis’, Journal of Physics, Conf. Series 1172(012024).

[21] Nilam, B., Amol, R., Nimbalkara,c. , Maruti, G.,(2018) ‘ZnO thin film prepared by a sol-gel spin coating technique for NO_2detection’, Materials Science and Engineering: B vol.227,pp.53-60.

[22] Nirmala1, M.,.Kavitha ,B., Iswarya,K., Firose Banu,A.,(2017) ‘Optical Analysis of ZnO Thin Films by SILAR Method’, Vol. 6, pp. 36-41.

[23] Sara Maroufa, Abdelkrim Beniaiche, (2017) ‘Morphological, Structural and Optical Properties of ZnO Thin Films Deposited by Dip Coating Method’, vol.20(1), pp. 88-95.

[24] Raidou1, A., Benmalek, F., Sall, T., et.al., (2014) ‘Characterization of ZnO Thin Films Grown by SILAR Method’, Open Access Library Journal, 1, 588.

[25] Nagarani, N., Vasu, V., (2013) ‘Structural and Optical Characterization of ZnO thin films by Sol- Gel Method’, Vol.2.

[26] Pay-Yu Lee1 , Sheng-Po Chang,et.al., (2013) ‘Highly Transparent Nanostructured Zinc Oxide Photodetector Prepared by Successive Ionic Layer Adsorption and Reaction’,vol. 8, pp. 6425 – 6432.

[27] Raidou, A., Benmalek,F., et,al., (2013) ‘The influence of rinsing period on the structural and optical properties of ZnO thin films’.

[28] Lehraki a,N., Aida,M.S.,et,al., (2012) ‘ZnO thin films deposition by spray pyrolysis Influence of precursor solution properties’, Current Applied Physics,pp. 1-5,

[29] Shih-Chang Shei , Pay-Yu Lee, Shoou-Jinn Chang,(2012) ‘Effect of temperature on the deposition of ZnO thin films by successive ionic layer adsorption and reaction’, Applied Surface Science Vol-258, pp- 8109-8116.

[30] Sakthivelu,A., Saravanan ,V.,(2011) ‘Structural,Morphological and optical study of molarity based ZnO thin films, Journal of Ovonic Research, Vol-7,pp.1-7.

[31] Ziaul Raza Khan, Mohd Shoeb Khan, et.al., (2011) ‘Optical and Structural Properties of ZnO Thin Films Fabricated by Sol-Gel Method’, Materials Sciences and Applications, Vol. 2, pp.340-345.

[32] Kathalingam, A., Ambika ,N.,et.al.,(2010) ‘Chemical bath deposition and characterization of nanocrystalline ZnO thin films’, Materials Science, Vol. 28,No,2.

[33] Raidoua, A., Aggoura, M.,et.al.,(2010) ‘Preparation And Characterisation Of Zno Thin Films Deposited By SILAR Method’,Vol. 12,No.2.

[34] Smirnov,M., Baban ,C., Rusu,G.I.,(2010) ‘Structural and optical characteristics of spin-coated ZnO thin film’, Applied Surface Science ,Vol. 256, pp.2405–2408.

[35] Ghosh ,A., Deshpande,N.G.,et.al.,(2009) ‘Effect of annealing on structural and optical properties of zinc oxide thin film deposited by successive ionic layer adsorption and reaction technique’, Journal of Alloys and Compounds,Vol. 469, pp. 56–60,

[36] Siti Nuurul Fatimah Hasim, Muhammad Azmi Abdul Hamid,et.al.,(2009) ‘Synthesis and characterization of ZnO thin films by thermal evaporation’, Journal of Physics and Chemistry of Solids,Vol. 70 . pp.1501–1504

[37] Bouderbala, M., Hamzaoui, S., et.al., (2008) ‘Thickness dependence of structural, electrical and optical behaviour of undoped ZnO thin films,’Vol.403, pp. 3326-3330,

[38] Shinde, V.R., Gujar, T.P., Lokhande,C.D.,(2007) ‘Studies on growth of ZnO thin films by a novel chemical method’, Solar Energy Materials & Solar Cells,Vol. 91, pp.1055–1061.

[39] Hong Seong Kang, Jeong Seok Kang,et.al.,(2003) ‘Variation of light emitting properties of ZnO thin films depending on post-annealing temperature’,Materials Science and Engineering ,Vol.102, pp. 313-316.

[40] Jae-Min Myoung,Wook-Hi Yoon,et.al.,(2002) ‘Effects of Thickness Variation on Properties of ZnO Thin Films Grown by Pulsed Laser Deposition’, Journal. Appl. Phys, Vol. 41, pp. 28–31.

[41] Purica. M., Budianu, E., (2002) ‘Optical and structural investigation of ZnO thin films prepared by chemical vapor deposition’, Thin Solid Films, Vol.403 – 404, pp. 485–488.